THE ROLE OF miR-196a AND HOXB9 IN HEAD AND NECK CANCER

LAV KISHOR DARDA

A thesis submitted in fulfillment of the requirements for the award of the degree of Doctor of Philosophy

School of Clinical Dentistry

December 2013

Abstract

Head and neck cancers are a heterogeneous group of cancers with 90% of them originating from the squamous epithelium. Only 50% of patients survive on being diagnosed with this cancer after five years and this statistic has not improved over the last few decades. The main risk factors for head and neck squamous cell carcinoma (HNSCC) are smoking and alcohol consumption. In recent years, there has been more interest in understanding the function of elements involved in gene expression such as transcription factors and non-coding RNA's and their role in oncogenesis.

HOX genes are transcription factors involved in oncogenesis and embryogenesis. In total, there are 39 HOX genes distributed in four clusters across the human genome. HOX genes have been observed to be aberrantly expressed in several cancers. MicroRNAs are non-coding short RNA transcripts which are approximately 21 nucleotides in length and lead to down-regulation of their target genes by acting on their 3'UTR. miR-196a is found in HOX gene cluster upstream of HOX9 paralogous group. Even miR-196a has been found to be aberrantly expressed in different cancers.

The expression pattern of 39 HOX genes in cancer cell lines showed that HOXB9 was highly over-expressed compared to normal cells, which was further confirmed by qPCR in wider cell panel consisting of four normal, four oral pre-malignant and five HNSCC cell lines ($p<0.05$). miR-196a was also found to be over-expressed in cancer cell lines compared to normal cells when similar sets of cell lines were used ($p<0.05$). This data was also found to be replicated in tissue samples and it was observed that HOXB9 and miR-196a were significantly over-expressed in cancer tissue samples compared to normal tissue samples ($p<0.05$). HOXB9 siRNA transfection into HNSCC cells showed significant decrease in invasion, migration and proliferation, whereas anti-miR-196a

transfection in HNSCC cells showed significant decrease in invasion, migration and adhesion compared to negative control transfected HNSCC cells ($p<0.05$).

HOXB9 and miR-196a-1 are spatially closely related to each other on chromosome 17. To check if these two are co-transcribed on same primary transcript, nested PCR was performed with appropriate controls consisting of RNaseA treated RNA and no reverse transcriptase control, which suggested that novel primary transcript for HOXB9 and miR-196a-1 co-expression might exist in HNSCC cells which was confirmed by DNA sequencing. Expression microarray analysis was performed using anti-miR-196a in oral pre-malignant and HNSCC cells and pre-miR-196a in immortalized normal cells to assess if there were any novel direct targets of miR-196a in HNSCC. Based on qPCR ($p<0.05$), dual luciferase reporter assay ($p<0.001$) and site-directed mutagenesis, MAMDC2 was found to be a direct target of miR-196a in HNSCC.

This is the first study in HNSCC looking at expression patterns of both miR-196a and HOXB9 and needs further work to validate them into biomarkers for early detection of HNSCC. miR-196a and HOXB9 could also be developed into potential therapeutic targets in HNSCC, particularly the novel primary transcript could be a novel therapeutic target. Further characterization of MAMDC2 is required but could turn into exciting therapeutic target as it is expressed as transmembrane receptor.

Acknowledgements

There are many whom I would like to thank and without them this PhD would not be possible. I am most grateful to my supervisor, Dr Keith Hunter, whose patience, guidance and answering all my trivial queries every time I knocked on his door made this day possible. Special thanks to my co-supervisor, Dr Daniel Lambert, for his input in my project, encouragement and assistance. I would also like to thank Dr Craig Murdoch for his help throughout this project anytime I needed it. To Brenka McCabe, without her help in molecular biology lab this PhD would not have finished in three years. Thank you to Kirsty Franklin and Jill Callaghan for their help down in tissue culture. I would like to thank everyone in postgraduate office, especially to Emma and Fahad for helping me with protocols and experiments.

Dr Paul Heath deserves a special mention for all his help with LCM and microarray. Here, I would also like to thank Jonathan Cooper-Knock for his help and input in analyzing microarray data. I would also like to acknowledge Dr Richard Morgan for his help with HOX gene expression analysis. The list of people goes on, who have encouraged or helped me during my PhD and I would like to thank one and all.

I am indebted to my family without their help, support and love I would have not reached here at the first place. Their presence in my life has helped me smile and kept me going even in worst days of my PhD. I would like to thank all my friends, not only here in Sheffield but also back home in India for their support and encouragement.

Lastly, I would like to thank The University of Sheffield and The British Society for Oral and Maxillofacial Pathology for funding my research.

Table of Contents

List of Figures

List of Tables

List of Abbreviations

APS- Ammonium per-sulphate

ASR- Age Standardized Rate

BCA- Bicinchoninic acid

BSA- Bovine Serum Albumin

DMEM- Dulbecco's Modified Eagle Medium

DMSO- Dimethyl Sulfoxide

DLRA- Dual Luciferase Reporter Assay

EMT- Epithelial-to-mesenchymal transition

FCS- Foetal Calf Serum

FFPE- Formalin-fixed Paraffin Embedded

FGF- Fibroblast Growth Factor

HNSCC- Head and Neck Squamous Cell Carcinoma

IHC- Immunohistochemistry

iNOK- Immortalised Normal Oral Keratinocytes

KGM- Keratinocyte Growth Media

LCM- Laser Capture Microdissection

MCS- Multiple Cloning Site

MM- Mastermix

MTS- 3-(4,5-dimethylthiazol-2-yl)-5-(3-carboxymethoxyphenyl)-2-(4-sulfophenyl)-2H-tetrazolium

NF-κβ- Nuclear factor kappa beta

NOK- Normal Oral Keratinocytes

OSCC- Oral Squamous Cell Carcinoma

OPL- Oral Pre-malignant Lesion

OPM- Oral Pre-Malignant

PAR-CLIP- Photoactivable-ribonucleoside Cross-linking and Immunoprecipitation

PBS- Phosphate Buffered Saline

PT primers- Primary transcript primers

pSILAC- Pulsed stable isotope labelling of amino acid in cell culture

RIN- RNA Integrity Number

RP- Random Primers

rt-PCR- Reverse transcription polymerase chain reaction

SDS- Sodium dodecyl sulfate

SDM- Site-directed mutagenesis

SEM- Standard Error Mean

TEMED- Tetramethylethylenediamine

TF- Transcription Factor

Tm- Melting Temperature

qPCR- Quantitative real-time polymerase chain reaction

wt- Wild type

The work described in this thesis is that of the author, unless otherwise stated.

Chapter 1: Statistics and Pathology of Head and Neck Squamous Cell Carcinoma (HNSCC)

Head and neck cancers mostly arise in squamous epithelium and are thus called squamous cell carcinoma. Head and neck cancer affects a number of subsites, including oral cavity, pharynx, larynx, paranasal sinuses and salivary glands. Oral cavity cancers are the most common type of head and neck cancer found. More than 90% of oral cavity cancer cases diagnosed are oral squamous cell carcinoma. Hence, this study concentrated on squamous cell carcinoma (Thakker and Hunter, 2011) (National Cancer Institute, 2013).

1.1 Statistics and Pathology

In 2008, the World Health Organisation (WHO) assessed that worldwide 12.7 million new cases of cancer and 7.6 million deaths due to cancer occurred (Johnson et al., 2011).

1.1.1 Incidence and mortality rates

Oral and pharyngeal cancer is ninth most common cancer worldwide, in men and women together. In 2008, eighth most frequent neoplasm was in oral and pharyngeal sites in the European Union (Johnson et al., 2011). In developing countries, cancer of oral cavity and pharynx is the sixth most frequent site in men and eighth in women. There were 399,642 new cases of oral and pharyngeal cancer worldwide according to GLOBOCAN 2008 (Ferlay J, GLOBOCAN 2008).

A.

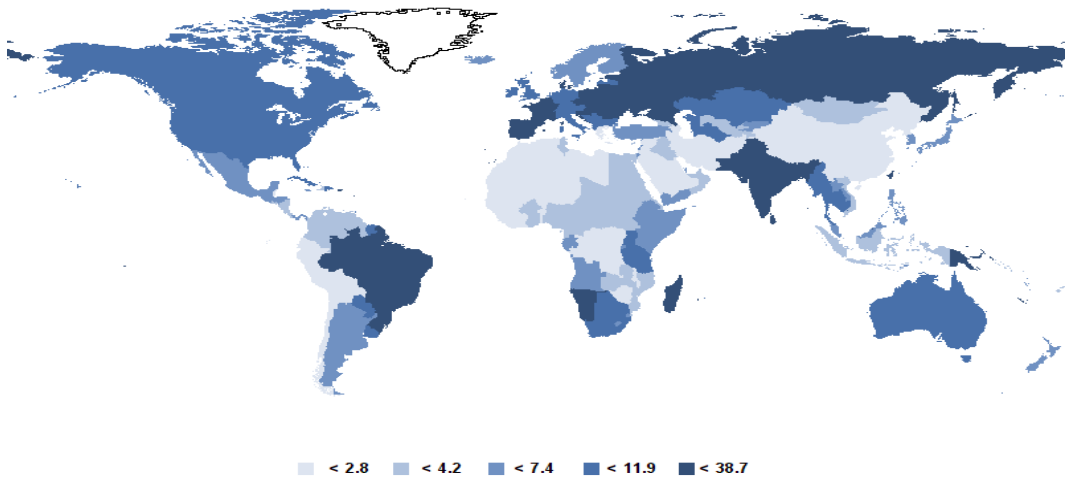

B.

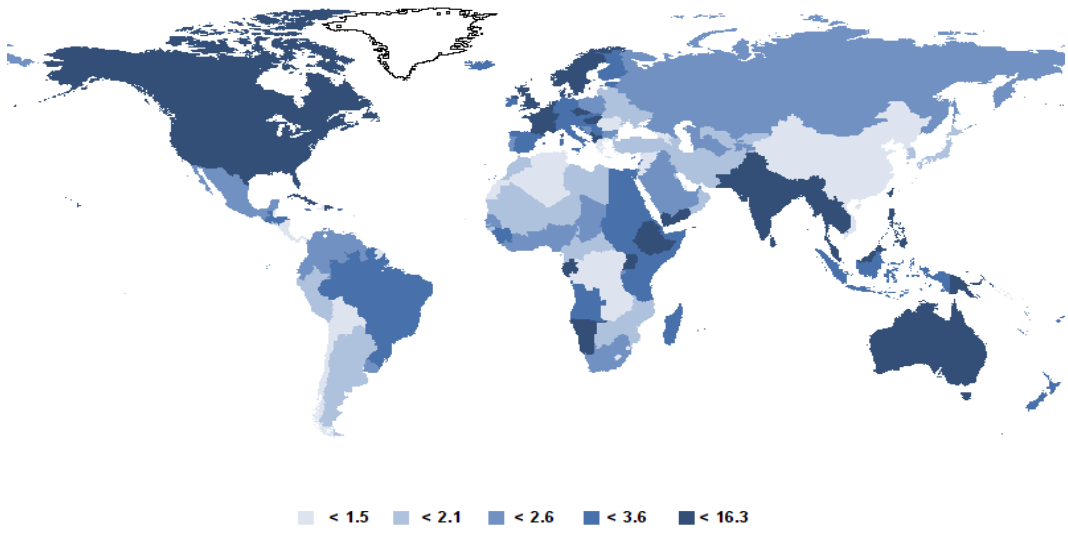

Figure 1.1. Age-standardized rates (ASR) for oral and pharyngeal cancer incidence per 100,000 worldwide for A. men and B. Women. Modified from (Ferlay J, GLOBOCAN 2008).

The highest oral cancer incidence in the world has been noted in Melanesia, Sri Lanka, France, Hungary and Croatia (Figure 1.1). Melanesia is a region with relatively small population, the oral cancer incidence rates are very high in this area which can be attributed to smoking and betel nut consumption (Johnson et al., 2011). In countries like India, Sri Lanka, Pakistan and Bangladesh approximately one-third of the total cancer diagnosed were oral cavity cancers (Sankaranarayanan, 1990), though it had been observed that the overall rates in India for tongue and mouth cancer in females and tongue cancer in males were decreasing (Satyanarayana and Asthana, 2008). In the USA, about 3% of all cancers accounted to head and neck cancer and close to twice the number of men were diagnosed with this cancer compared to women. In 2012, it was estimated by the researchers that nearly 52,000 men and women would be diagnosed with this cancer in the USA (National Cancer Institute, 2013). In Australia, for both sexes an upward trend was seen in terms of incidence (Moore et al., 2001). In Europe, the maximum incidence and mortality due to oral and pharyngeal cancer was seen in Hungary. In Italian and French men, it was observed that the mortality rate was highest in 1980s and decreased since then, though it has been noticed that there was continuous increase in incidence in Denmark, Belgium, Portugal, Greece and Scotland (Johnson et al., 2011).

In the UK, oral cancer ranked fifteenth in terms of its incidence in cancers and accounted for 2% of all new cancer cases in 2009. Oral cancer accounted for 6236 new cases in 2009 with 66% of them in men and rest of 34% in women. Based on the European ASR, the incidence rate in the Scotland was higher than Wales, England and Northern Ireland (Cancer Research UK, 2013). The major risk factors for the incidence of oral cancer in the UK are smoking and consumption of alcohol (Jerjes et al., 2012). The incidence of oral cancer is strongly related to the age of an individual, but it differs based on the gender. The incidence rate increases acutely from the age of 45 in men and

peaks between the age of 60-69, whereas in women the increase is gradual from 45 and peaks only at the age over 80 (Cancer Research UK, 2013).

Since mid-1970, the incidence of oral cancer has increased in the UK. Most growth in the incidence of oral cancer has been noted after late 1980s for both men and women (Figure 1.2). There has been increase in European ASR by 25% and 28% in men and women respectively over a period from 1998-2009 (Cancer Research UK, 2013).

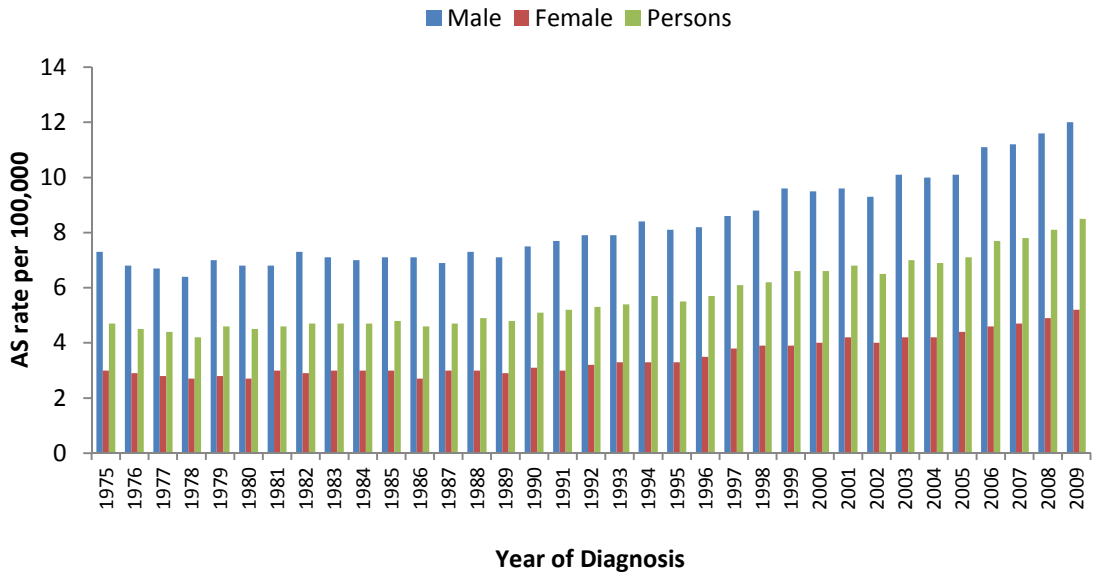

Figure 1.2. Graph showing European ASR per 100,000 population based on the gender over a period of 1975-2009 in the UK. Modified from (Cancer Research UK, 2013).

A.

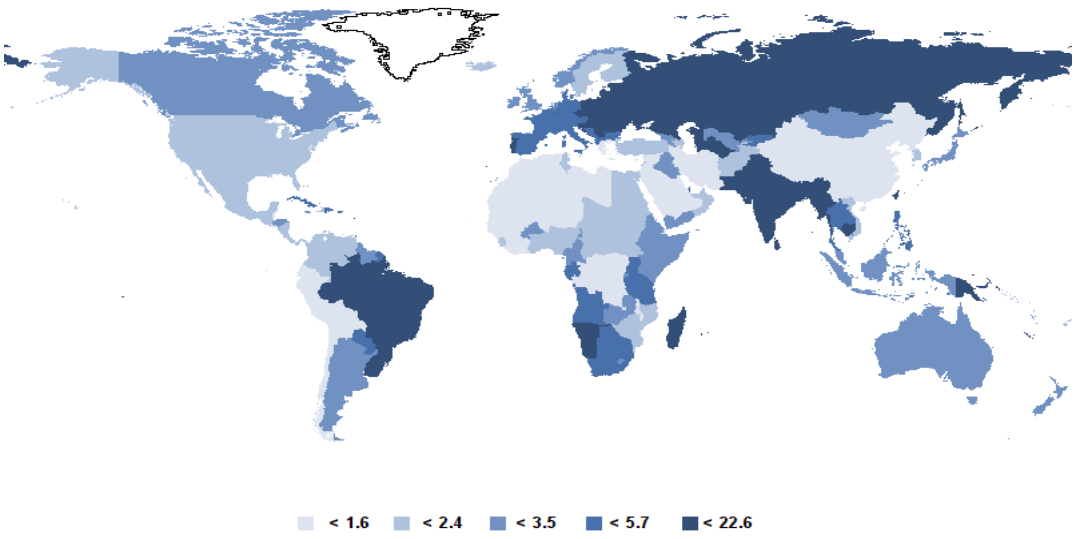

B.

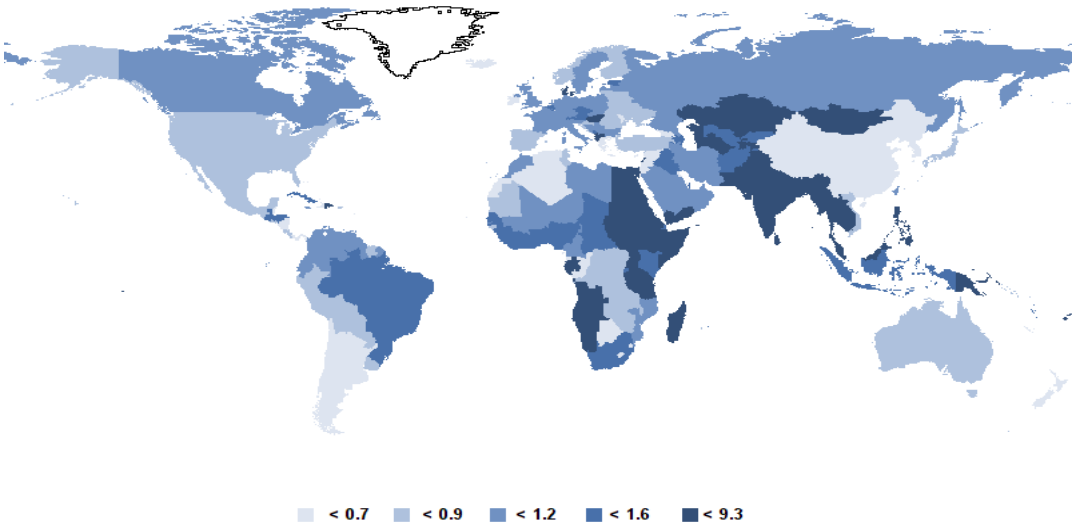

Figure 1.3. Age-standardized rates (ASR) for oral and pharyngeal cancer mortality per 100,000 worldwide for A. men and B. Women. Modified from (Ferlay J, GLOBOCAN 2008).

It was observed that Melanasia had the highest mortality rate in the world due to oral cancer (Figure 1.3). In the Western Europe, it was noted that there was steady growth in the oral cancer mortality from 1950s to late 1980s, but this rate has been in decline since. Oral cancer mortality had reached the highest rate in 1990s in central and Eastern European countries like Russia, Hungary, Slovenia and Slovakia. These rates are now showing decline as well, though the mortality rate in women was seen to be in upward trend in Hungary, Denmark, Belgium and Slovakia (Johnson et al., 2011). In the USA, it was noticed that between 2006-2010, the median age of death by oral and pharyngeal cancer was 67. The ASR for mortality between 2006-2010 was seen to be 2.5 per 100,000 men and women per year in the USA (National Institute of Health, 2013). A study carried out in Mumbai, India showed decline in the oral cancer mortality rate during the period of 1986-2000 (Sunny et al., 2004). There were 1822 deaths due to oral cancer in the UK in 2008. The mortality rate was seen to be highest in Scotland which is consistent with the high incidence rate. The ASR for mortality has been fairly stable with 3.3 and 1.4 per 100,000 male and female respectively, between 1971-2008 (Cancer Research UK, 2013).

1.1.2 Risk Factors

The pre-eminent causes have been long known for oral cancer and the most important risk factors are tobacco smoking or chewing and alcohol consumption, both of which can be curbed. These two factors put together account for about 75% of the cases of oral cancer and diet lacking in nutrition leads to another 10-15% oral cancer cases across Europe (La Vecchia et al., 1997).

1.1.2.1 Tobacco

The main forms of tobacco intake in UK are by pipe, cigarette and cigar smoking which can lead to oral cancer (Warnakulasuriya et al., 2005). It has been shown that a current

smoker has three times the risk of getting oral cancer than a non-smoker (Gandini et al., 2008). Dose and duration of smoking are both linked to development of oral cancer whereas stopping smoking can reduce the risk (Rodriguez et al., 2004). In one of the studies done in Cuba, it was observed that smoking 30 cigarettes or more in a day are comparable to smoking 4 cigars or more (Cancer Research UK, 2013). It has also been noted that smoking bidi (tobacco hand-rolled in a tendu leaf) raises the risk of oral cancer (Rahman et al., 2003). There is also evidence that passive smoking can also lead to oral cancer, with 63% raise in the risk for non-smokers who are exposed to passive smoking at work or at home (Lee et al., 2009).

An analysis carried out recently showed that the use of smokeless tobacco (chewing tobacco, plug or snuff) had more than double the risk of causing oral cancer in the USA, around five times more risk in India and Asian countries and seven times more risk in Sudan when compared to non-smokers (Boffetta et al., 2008). It has been seen that the high incidence rate of oral cancer in the Asian sub-continental countries is due to the extensive use of betel quid and also the use of areca nut in those leaves (Bedi, 1996). Areca nut is a carcinogenic substance and the risk is increased by chewing betel quid with tobacco, though it is less when taken without tobacco (Vanwyk et al., 1993).

1.1.2.2 Alcohol

One of the major risk factors for oral cancer is alcohol consumption. Based on a study, 14 grams/day intake of alcohol could double the risk of oral cancer (Castellsague et al., 2004). Drinking alcohol and smoking together has much higher risk than drinking alcohol or smoking alone (Ferreira Antunes et al., 2013).

The result in the non-smokers but drinkers differs by the site of the effect, it has been noted from a study that there is no rise in the risk of oral cavity cancer but could lead to cancer of the hypopharynx or oropharynx (Hashibe et al., 2007). The risk of oral cancer

depends on the amount of ethanol taken rather than the type of the beverage (Altieri et al., 2004). The rising number of cases diagnosed with oral cancer in Europe is being attributed to the increase in the alcohol consumption throughout Europe (Hindle et al., 2000). In the UK, the alcohol consumption has increased by double since middle of the 19th century and risen from 3.9 litres to 8.6 litres of pure alcohol/year/head. The percentage of the people who surpass the recommended weekly level of 14 units for women and 21 units for men has decreased, with 26% of men and 18% of women exceeding recommended limit in 2009. Presently, the drinking level (8.6 litres/year/head) in the UK is lower than what is seen in most European countries like Portugal (11 litres/ year), France (10.7 litres/ year), Germany (10.6 litres/ year) and Spain (9.9 litres/ year), but the level of alcohol consumption is rising sharply in the UK and could reach nearly the top of the table in next ten years (Cancer Research UK, 2013).

1.1.2.3 Sun Exposure

Exposure to radiation can lead to lip cancer. It has been seen that lip cancer is three folds more common in men than women, which could be due to smoking, sun exposure and occupation (Lopez et al., 2003).

1.1.2.4 Nutrition and Diet

It was shown in an analysis that there is 50% reduction of risk of oral cancer if the intake of vegetable and fruit is increased (Pavia et al., 2006). In another case-control study, it was seen that the status of smoking, higher intake of vegetable and fruits reduced the risk of oral cancer in alcohol consumers and smokers, whereas it did not make any difference in non-drinkers or smokers (Kreimer et al., 2006). It has also been observed that risk reduces with higher Body Mass Index (BMI) (Nieto et al., 2003).

1.1.2.5 Human Papillomavirus (HPV)

HNSCC caused by HPV is considered a different clinical entity with HPV 16 being the most common subtype in HNSCC. It is also observed that the prognosis of HPV-associated HNSCC is better than the HNSCC associated with alcohol and smoking. E6 and E7 protein from the HPV target p53 and Rb, respectively, which leads to carcinogenesis in head and neck. HPV positive HNSCC have been found to have wild type p53, which goes with the fact that E6 inactivates it. E6 and E7 protein have been observed to interact with other proteins like hTERT, c-myc, p21, p27 and others (Rautava et al., 2012, Leemans et al., 2011). Based on International Agency for Research on Cancer (IARC) data it is suggested that HPV 16 has role in causing oral and pharyngeal cancer. It was also shown that 14% of oropharyngeal cancers and 8% oral cancers are HPV related (Parkin, 2011). The risk of oropharyngeal cancer also increases with the number of sex and oral sex partners indicating involvement of sexually transmitted HPV (Heck et al., 2010). It has also been noted in general that the risk of head and neck cancer increases in people exposed to HPV (Gillison, 2007).

1.1.2.6 Potentially Malignant Oral Lesions

Erythroplakia and leukoplakia are the two most common oral lesions which might lead to oral cancer. Other conditions include oral submucous fibrosis, sideropenic dysphagia, lichen planus and syphilitic glossitis. Generally, leukoplakia is less likely to turn into a cancerous lesion when compared to erythroplakia (Rodrigues et al., 1998). It has been assessed that the rate at which transformation of leukoplakia into oral cancer takes place is around 1% every year (Scheifele and Reichart, 2003). These lesions will be discussed later in detail.

1.1.3 Symptoms, Diagnosis and Treatment

Oral cancer might show following symptoms: an ulcer that does not heal, persistent pain in the mouth, red and/or white patches in the mouth, weight loss, problem swallowing food and lump in the neck. It is not always necessary that these symptoms always lead to diagnosis of cancer but could be related to some other disease process. In terms of diagnosis, the current methods involve collecting a tissue biopsy from the patient and sometimes fine needle aspiration to collect cells from neck lumps (Cancer Research UK, 2013). The future of diagnosis might involve using molecular biomarkers and brush biopsy cytology samples for early detection which could lead to higher specificity of diagnosis of HNSCC and reduced number of unwanted referrals (Brocklehurst et al., 2010). The treatment options available for head and neck cancer can range from surgery, radiotherapy, chemotherapy and targeted therapy depending on the stage of cancer and position of the cancer. Surgery depends on the size and position of the cancer and is mainly used when cancer is detected early (Nixon et al., 2013). Radiotherapy maybe used alone when the cancer has not spread too much, but it might also be used with chemotherapy if the cancer has spread locally. Radiotherapy is also used after surgery to kill off any cancer cells left. Chemotherapy is used in instances when the cancer has spread locally or after remission when the cancer recurs after surgery and radiotherapy (Denaro et al., 2013). In terms of targeted therapy, cetuximab (anti-EGFR-mAb) is the only targeted therapy drug which has been approved to be used in head and neck cancer treatment. Cetuximab can be used with chemotherapy or radiotherapy and has shown to improve overall survival rate (Bonner et al., 2006). Other targeted drugs such as panitumumab, zalutumumab and lapatinib are in clinical trials to assess their efficacy in head and neck cancer (Bonner et al., 2006, Markovic and Chung, 2012, Vermorken et al., 2008). Recently, there have been proteins identified which target tumour cells and led to their death or apoptosis. These proteins have been isolated

from human or viruses such as melanoma differentiation associated-7 (MDA-7) or apoptin (VP3) respectively (Argiris et al., 2011).

1.1.4 Clinical Pathology

1.1.4.1 Normal Oral Mucosa:

The oral mucosa is a lining mucous membrane which covers the entire oral cavity and also contains several sensory receptors which include the taste buds in the tongue. Stratified squamous type epithelium is seen in the oral mucosa which is likely to be keratinised in places which are subjected to friction, like palate and the dorsum of the tongue (Figure 1.4). Lamina propria is the dense collagenous tissue which sustains the oral epithelium (Wheater et al., 2000).

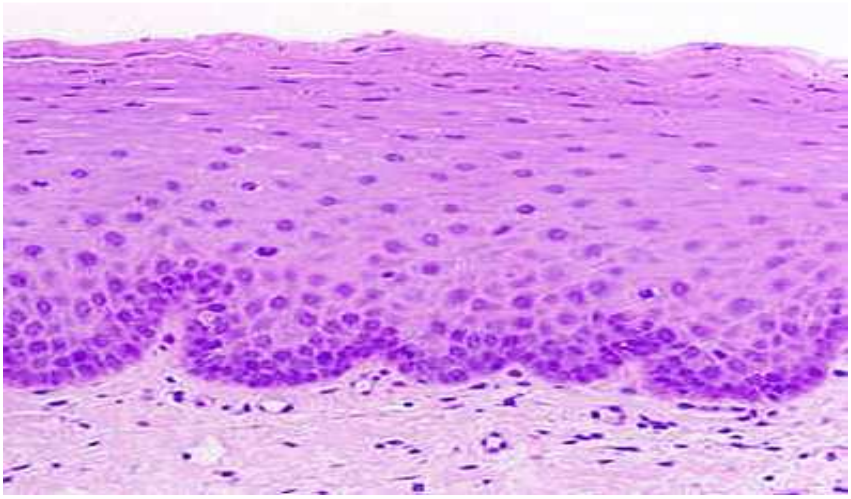

Figure 1.4. Non-keratinised normal oral mucosa (Courtesy of Dr. Keith Hunter).

Sub-mucosal supporting tissue attaches the lamina propria to the underlying muscle in highly mobile places like floor of the mouth and soft palate. Dense fibrous sub-mucosa firmly binds the lamina propria to the periosteum in the places where the bone is underneath the oral mucosa like the tooth-bearing ridges and hard palate. In the sub-mucosa, a number of accessory salivary glands of both mucous and serous types are present (Wheater et al., 2000).

1.1.4.2 Leukoplakia and Erythroplakia:

Leukoplakia is a white lesion on the mucous membrane of the oral cavity that cannot be defined as any other characterised lesion (Axell et al., 1996). Even though leukoplakia has no defined histological behaviour or change, it is possible that few of them present as invasive carcinoma or potentially malignant lesion but most are benign hyperkeratoses. It has been observed that the incidence of leukoplakia around the world varies from being less than 1% to over 10% (Soames and Southam, 2005).

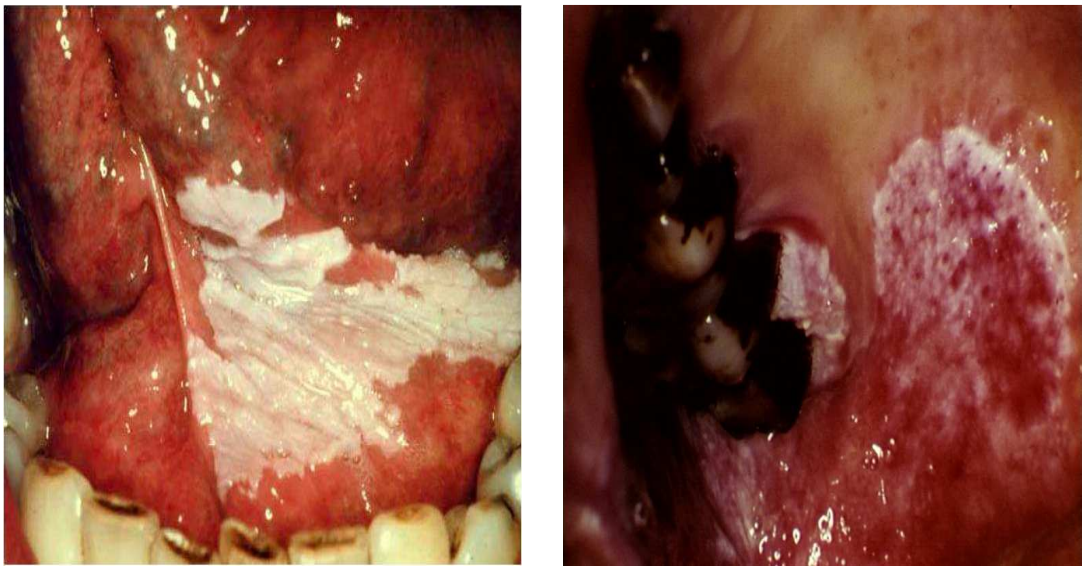

Figure 1.5. Homogenous and Non-Homogenous Leukoplakia (Courtesy of Dr. Keith Hunter).

Leukoplakia could present as homogenous or non-homogenous surface (Figure 1.5). Homogenous Leukoplakia is defined as a white lesion which appears thin and flat and may show shallow cracks and has a wrinkled, corrugated or smooth surface with constant texture all over. Non-Homogenous Leukoplakia can be defined as a white/ white-red lesion that may be unequally nodular, exophytic or flat. Slightly rounded, raised, white and/or red outgrowth are seen in the nodular lesions, whereas sharp protrusion or uneven bluntness might be seen in exophytic lesions (Axell et al., 1996). Prognosis for Non-Homogenous Leukoplakia is noted to be worse than Homogenous Leukoplakia as they are more known to show epithelial dysplasia (Napier and Speight, 2008).

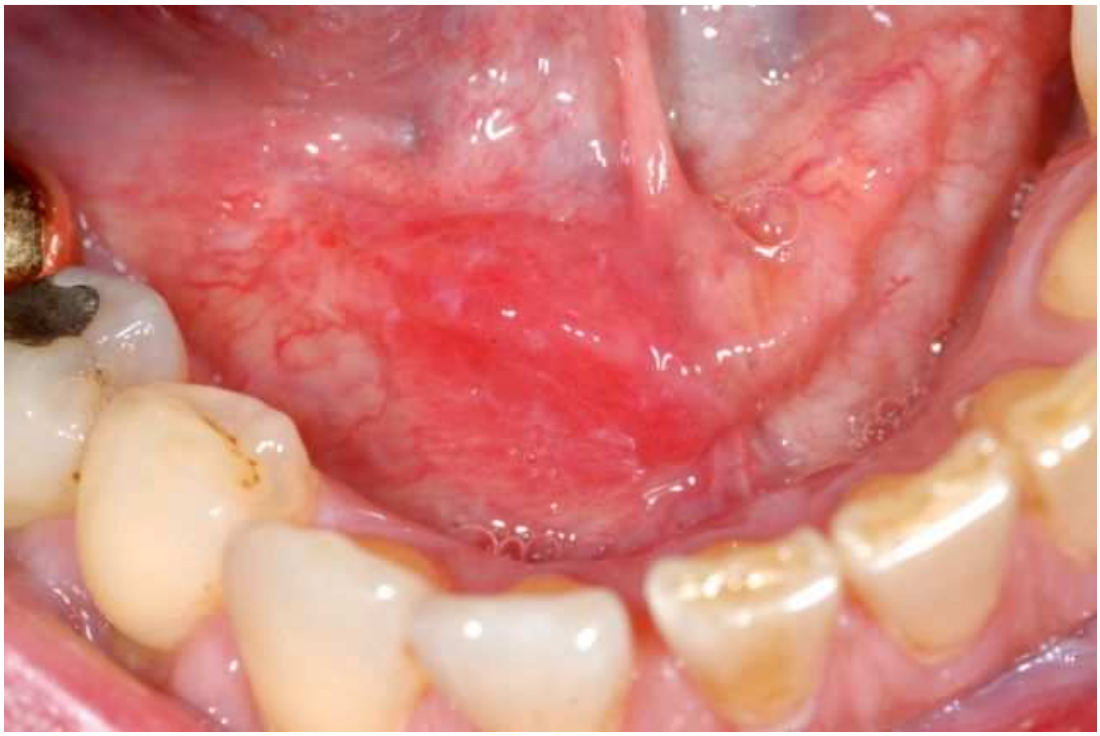

Figure 1.6. Erythroplakia (Courtesy of Dr. Keith Hunter/ Dr. Anne Hegarty).

A lesion which cannot be characterised pathologically or clinically as being any other condition and which is red in colour and presents as a velvety plaque on the oral mucosa can be defined as Erythroplakia (Figure 1.6). Erythroplakia may present itself as invasive carcinoma or carcinoma in-situ, hence its appearance in the previously white lesion could be alarming histologically. Induration, fixation, lymphadenopathy and ulceration are other signs which might be of concern (Soames and Southam, 2005).

1.1.4.3 Potentially Malignant Oral Lesions

Potentially malignant oral lesions are defined as mucosal lesions which have high risk of developing into squamous cell carcinoma compared to normal oral mucosa. This terminology is more preferred by the WHO. Mucosal lesions considered as potentially malignant includes leukoplakia, erythroplakia, oral lichen planus, oral submucous fibrosis and proliferative verrucous leukoplakia (Diajil et al., 2013).

1.1.4.4 Epithelial Dysplasia

Epithelial Dysplasia is defined as the sum of architectural and cytological changes seen histopathologically in the oral mucosa. It may present itself in normal oral mucosa as erythroplakia, leukoplakia or leukoerythroplakia clinically (Lumerman et al., 1995). The maturation, differentiation and proliferation of epithelial cells undergoes changes in the dysplastic epithelium (Soames and Southam, 2005). The histopathological changes which might be observed in epithelial dysplasia could range from basal cell hyperplasia, abnormal polarization and cell adhesion, abnormal mitosis, loss of normal cell keratinisation, enlargement of nucleus and hyperchromaticity, cell anaplasia, loss of epithelial stratification, rete ridges which are drop-shaped, surface pattern change and the epithelium thickness involved in dysplasia. All of these features are not noticed in one single case of epithelial dysplasia but most of them are seen (Lumerman et al., 1995). Dysplasia is graded as mild, moderate or severe. It has been noticed that severe

dysplasia has higher chance of transforming into cancer with age, sex, pre-cancerous conditions and diagnosis as other limiting factors (Warnakulasuriya et al., 2011). Non-homogenous leukoplakia and erythroplakia have a higher rate of epithelial dysplasia or also invasive carcinoma when compared to homogenous leukoplakia even though it is difficult to predict clinically its severity or presence (Mashberg, 1977). Through several studies it has been observed that homogenous leukoplakia shows dysplasia only in 10% cases while non-homogenous leukoplakia shows dysplasia in 50% of the cases (Soames and Southam, 2005). A very high incidence is seen in speckled leukoplakia for causing dysplasia especially when it clinically starts showing characteristics of erythroplakia (Mehta et al., 1981).

1.1.4.5 Squamous Cell Carcinoma

Of all the malignant neoplasms in the oral mucosa, 90% are squamous cell carcinoma. There are huge variations seen in the incidence of cancer throughout the world. In the UK and USA the rates are seen to be 4% of all types of tumours whereas it rises to almost 40% of all tumours in the south-east Asian countries (Soames and Southam, 2005).

There are many clinical forms in which squamous cell carcinoma can present. The key is to diagnose it early as this is a major factor influencing the clinical outcome of the patient and hence suspicion and vigilance are considered the key factors in the detection of cancer (Graveland et al., 2013). There are generally no symptoms seen for early lesions, though they might present themselves as a small exophytic growth with no erythema or ulceration, white patch, erythroplakia or a small ulcer (Neville, 2009). Clinically, features like induration, ulceration and tissue fixation to structures should stimulate the suspicion of an early carcinoma. A late stage lesion mostly presents itself as wide based outgrowth with a nodular, rough, haemorrhagic, warty or necrotic surface

or it can also be present as crater-like ulcer with rolled, raised everted edges which is destructive (Soames and Southam, 2005).

Oral squamous cell carcinoma shows various forms in its histology (Figure 1.7). Though, all the forms show destruction of tissue and invasion. The grading of squamous cell carcinoma is done on the basis of the histopathology of the carcinoma into well, moderately or poorly differentiated categories (Neville, 2009). Often, there is infiltration of the plasma cells and lymphocytic cells in the stroma which is supporting the invading epithelium. Some carcinomas invade with the broad front whereas others consist of small islands or even single invasive cells. The carcinoma with wide invasive front is referred to as cohesive whereas when small islands or single cells invade it is called non-cohesive. It has been noticed that non-cohesive form of invasion has worse prognosis. Vascular, neural and bone invasion can also take place (Jerjes et al., 2010). Metastatic spread of the carcinoma in the regional lymph nodes can be divided into two classes: Intracapsular spread, which is when the spread is confined to the capsule of the node and Extracapsular spread, which is when carcinoma spreads to the adjacent tissue close to the capsule. The prognosis of the carcinoma is worse when it has extracapsular spread (Okuyemi et al., 2013).

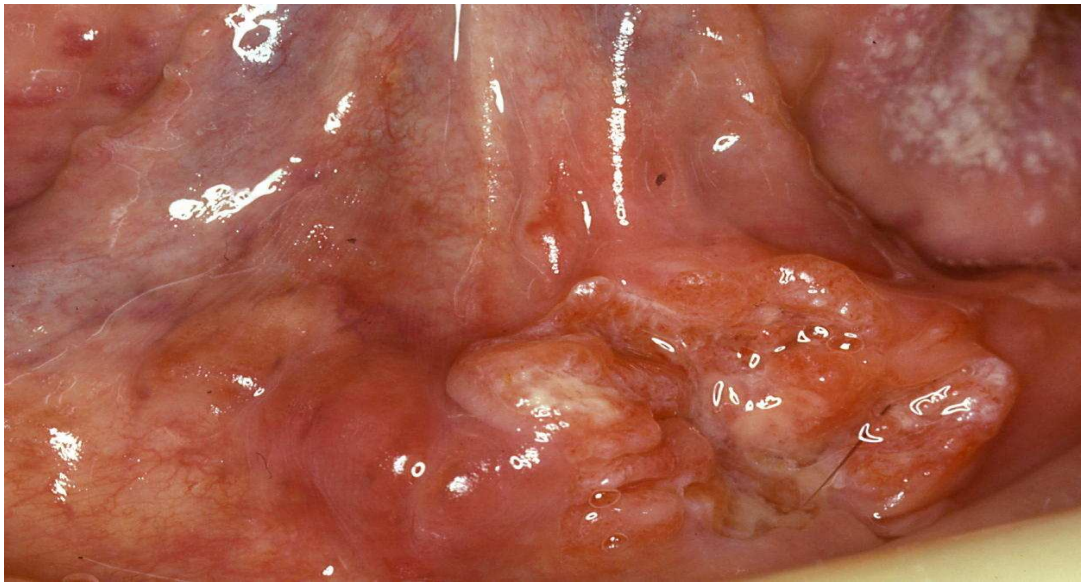

Figure 1.7. Oral Squamous Cell Carcinoma (Courtesy of Dr. Keith Hunter).

1.1.5 Molecular Pathology

It is a well-known fact that normal cells undergo dramatic changes genetically and epigenetically to transform into cancer cells. It is also known that there are cytogenetic changes as well in the cells, where there is either loss or gain of DNA segments or whole chromosomes in few cases (Delbaldo et al., 2008). Genomic instability arises due to large cytogenetic changes in the cells which could be either loss or gain of genomic DNA or chromosomes, like tetraploidy or aneuploidy (Ai et al., 2001). Many genetic alterations have been described not only in specific genes but also at specific chromosomal loci especially at gain of 3q and loss of 9p loci leading to loss of heterozygosity in HNSCC (Partridge et al., 1999, Graveland et al., 2011, Ha et al., 2009, Walter et al., 2013). In cancer, genes can also be rendered inactive by DNA methylation of the promoter region of the gene which is involved in gene expression leading to transcriptional silencing of the genes. DNA methylation generally occurs in the CpG islands (cytosine-guanine) (Ha and Califano, 2006). Recently it has been noted that there is widespread demethylation of the DNA as well in the cancer cells but its impact has still not been assessed completely (De Smet and Loriot, 2010).

1.1.5.1 Oncogenes

Generally, cell division begins and maintains itself based on cellular stimuli. These stimuli can either be autocrine or paracrine in nature which are mediated from receptors to the cell nucleus via complex signalling pathways. When these pathways are aberrantly activated it leads to cancer and these genes are then called ‘oncogenes’. In tumours, the most oncogenic changes are found in the receptors and their growth factors. They may produce surplus of growth factor which could act in autocrine or paracrine manner on the cancer cells (Myoken et al., 1994), they could also over-express or contain a mutation which increases the expression of growth factor receptors (Cheng et al., 2002) or increase the transduction of signal in the cell (Downward, 2003).

Epidermal Growth Factor Receptor was first isolated in 1980 and it is a receptor tyrosine kinase situated on the plasma membrane. EGFR is overexpressed in several cancers and can lead to tumour growth, survival and progression. EGFR exerts its effect in cancers either by cytoplasmic or nuclear mode. In cytoplasmic mode, EGFR is activated when it binds to its ligand which leads to recruitment, phosphorylisation and activation of several pathways such as Ras-Raf, PI-3K-Akt, PLC-γ and Jak-Stat pathway leading to proliferation, tumourigenesis, resistance and progression (Han and Lo, 2012). The nuclear mode is activated when EGFR binds its ligand in presence of vitamin D, hydrogen peroxide, cisplatin, heat or radiation. On translocation to nucleus, EGFR interacts with transcription factors such as STAT3 and E2F1 and activates expression of iNOS and B-Myb. It is also involved in increased expression of cyclin D1 and can promote G1/S progression, proliferation, metastasis or radioresistance (Lo and Hung, 2006). Cetuximab is the only approved targeted therapy in HNSCC against EGFR (Markovic and Chung, 2012). EGFR over-expression, based on meta-analysis of 37 studies in HNSCC, was found to have negative effect on overall survival in patients and was shown to reduce disease free survival rate only in oropharyngeal cancers (Keren et al., 2013). EGFR is over-expressed in >95% of HNSCC cases and also is an independent poor prognostic factor in HNSCC. A mutant version of EGFR, EGFRvIII is found in 42% of HNSCC cases alongside EGFR and can lead to treatment failure with targeted therapy (Sok et al., 2006).

Phosphatidylinositol-3-kinase (PI-3K) is activated in several cancers including HNSCC based on different molecular alterations. PI-3K is primarily activated by receptor tyrosine kinases in cancers. p85, regulatory subunit, is useful in binding to the tyrosine residues whereas p110 catalytic subunit is involved in phosphorylation of PIP2 to generate PIP3. PTEN, tumour suppressor gene, is involved in reverse reaction of de-phosphorylating PIP3 to PIP2. PIP3 binds 3-phopshoinositide dependent protein kinase

(PDK1) which helps in phosphorylation of protein kinase B (PKB or Akt). PI-3K is involved in tumourigenesis, metastasis, recurrence and progression (Du et al., 2012). PIK3CA, p110α subunit of PI-3K, is found to be mutated in 11% HNSCC cases (Qiu et al., 2006). PIK3CA has also been found to be associated with lymph node metastasis in HNSCC (Fenic et al., 2007). It was also seen that PIK3CA is involved in progression of dysplasia to invasive HNSCC (Woenckhaus et al., 2002). It has also been observed that PTEN expression is reduced in 30% HNSCC cases (Squarize et al., 2013).

Many oncogenes exert their effect by modulating the cell cycle. The cell cycle consists of four stages namely G1, S, G2 and M by which a cell undergoes cell division which involves DNA duplication which is followed by division of cytoplasm to give rise to two daughter cells (Loyer et al., 1996). Cyclin D1 is a protein which is engaged in the G1/S phase transition of the cell (Schuuring, 1995). It has been observed that cyclin D1 is deregulated or amplified in 30-50% of the HNSCC cases and many cell lines as well (Okami et al., 1999). Though, cyclin D1 is amplified in many cases it is not the only cause for development of HNSCC, there are other proteins which inhibit the cell cycle at different check points and could work in suppressing the tumour, hence these are called Tumour Suppressor Genes.

1.1.5.2 Tumour Suppressor Genes

Retinoblastoma protein in its unphosphorylated form allows G1/S phase transition in cell cycle (Adams, 2001). This protein can be deregulated either due to mutation or interaction with E7 protein of HPV. This protein is not commonly mutated in HNSCC (Ambrosch et al., 2001). Other class of proteins which inhibit cell cycle are called Cyclin-dependent Kinase (CDK) Inhibitors which consist of mainly two types, ink4 and Cip/Kip. CDK4 and 6 both are inhibited specifically by $p16^{ink4a}$ (Serrano et al., 1993). This protein has been observed to be deregulated in many cancers including HNSCC

(Cairns et al., 1995) and it is seen that its function can be silenced due to deletion, mutation or epigenetic silencing (McGregor et al., 2002). In HNSCC, it is present in 60-80% of the cases and silencing is generally due to epigenetic or genetic factors (Reed et al., 1996). Cip/kip family proteins inhibit wider range of CDK and only p27 has been shown to be involved in the development of HNSCC (Slingerland and Pagano, 2000). In HNSCC, loss of expression of p27 has been linked to poor prognosis of the disease and p27 expression might be lost in dysplastic epithelium (Jordan et al., 1998).

An important role of response by the cell to DNA damage is carried out by the transcription factor p53 (Tumour Protein p53). MDM2 is an E3 ubiquitin ligase and works as negative regulator of p53 in normal conditions. On DNA damage, there is activation of Ataxia telangiectasia mutated (ATM) and Ataxia telangiectasia related (ATR) leading to activation of CHK1 and CHK2. p53 is then phosphorylated by CHK1 and CHK2 which prevents MDM2 from degrading p53 (England et al., 2013).This acts to either arrest the cell cycle or initiate apoptosis. p53 has a short half-life and its activity is regulated at post-translational level. p53 phosphorylation leads to its activation and stabilisation which is carried out by signal transduction pathways (Hirao et al., 2000). Loss of p53 function can be due to mutation in the gene but also can be due to action of E6 protein from HPV (Shay et al., 1993). It has been observed that 75% of HNSCC cases carry p53 mutation (Balz et al., 2003).

1.1.5.3 Lifespan Control

The ends of the chromosomes consist of repetitive sequences of DNA which are called Telomeres. When a cell undergoes division a few of the repeats are lost (Levy et al., 1992) and hence it could be considered to be a mechanism by which to count the number of cell divisions (Allsopp et al., 1995). Telomerase enzyme consists of two components, TERT (reverse transcriptase part) and TERC (template of RNA) (Kim et

al., 1994). It has been observed that expression of hTERT can lead to immortality due to addition of telomere sequence. Its activity is repressed by p53, hence it leads to immortality in the p53 mutants (McGregor et al., 2002). It has been observed that TERC and TERT both are deregulated in the HNSCC with an increase in their expression which leads to immortalisation (Downey et al., 2001).

The development of HNSCC is not only due to the deregulation of cell cycle regulatory genes but also could be attributed to different transcription factors and more recently to micro-RNA.

1.1.5.4 Transcription Factors (TF)

Transcription factors as the name suggests are proteins that are involved in the control of transcription of their target genes. In terms of cancer, transcription factors can either be oncogenes or tumour suppressor genes. Hanahan and Weinberg in their review explained six hallmarks of cancer as proliferation, evading apoptosis, angiogenesis, immortality, invasion and migration and evading growth suppressors. In this review they also explained two emerging hallmarks as avoiding immune destruction and energy metabolism reprogramming and two enabling characteristics as genome instability and mutation and tumour-promoting inflammation. All of these hallmarks are largely governed by the transcription factors which are activated due to signal transduction and target genes they transcribe (Hanahan and Weinberg, 2011) (Figure 1.8).

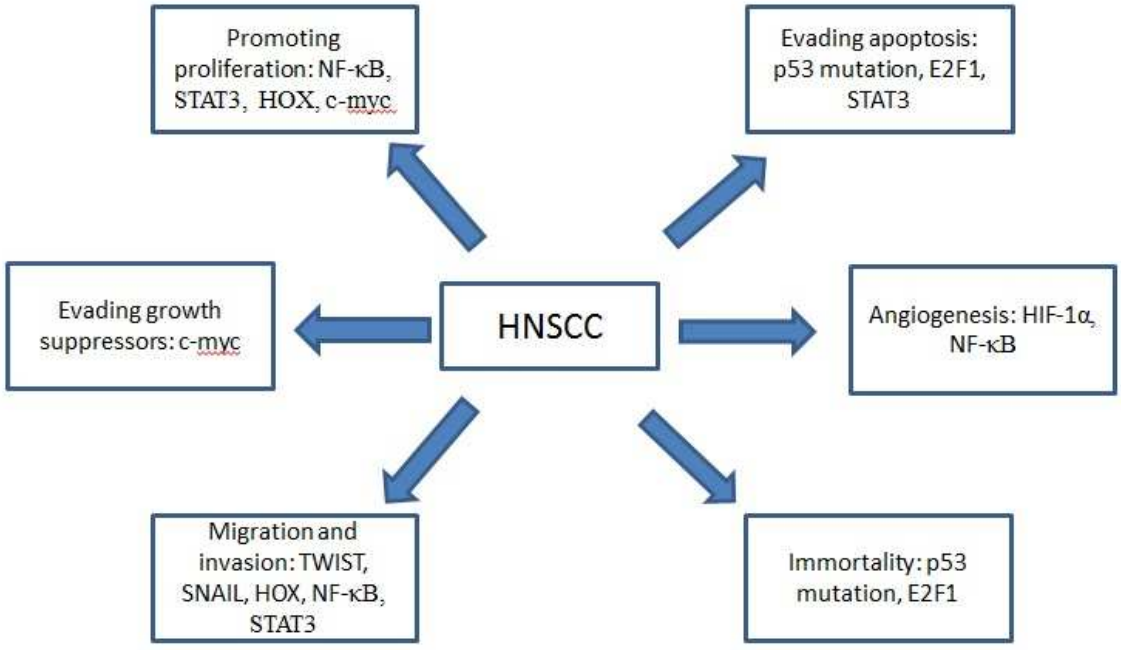

Figure 1.8. Transcription factors promoting different hallmarks of cancer.

NF-κB (Nuclear Factor Of Kappa Light Polypeptide Gene Enhancer In B-Cells) is a transcription factor which is not only involved in development of adaptive and innate immune system but also plays central role in cell survival and proliferation (Karin and Greten, 2005, Bhave et al., 2011). NF-κB consists of five subunits as follows: p52, p50, c-Rel, p65 and RelB (Karin, 2006). p65 is the DNA binding subunit of NF-κB (Wilhelmsen et al., 1984). NF-κB is upregulated in HNSCC which could lead to development of invasive cancer from premalignant lesions (Ondrey et al., 1999). Deregulated expression of NF-κB can also lead to angiogenesis and metastasis in cancer (Nakanishi and Toi, 2005). Signal Transducer and Activator of Transcription (STAT) genes are involved in the transcription of the genes related to immune responses, cell fate decision and growth. In total, the STAT family consists of seven genes called STAT1, 2, 3, 4, 5a, 5b and 6 (Darnell, 2002). It has been noted that the level of phosphorylated STAT3 is very high in HNSCC when EGFR is activated (Grandis et al., 1998) which may contribute to cell survival and proliferation (Leeman et al., 2006). It is also understood that STAT3 deregulation might be an early event in HNSCC (Grandis et al., 2000) and this elevation can also lead to poor prognosis and lymph node metastasis (Grandis et al., 1998).

SNAILs are transcription factors that are involved in promoting EMT (Epithelial-mesenchymal transition) by increasing expression of mesenchymal markers and decreasing epithelial markers (Scanlon et al., 2013). SNAIL has been implicated in promoting regional metastasis and lymphovascular invasion and is predictive of poorly differentiated HNSCC (Mendelsohn et al., 2012). TWIST (basic helix-loop-helix transcription factor) changes expression of its target genes based on E-box responsive elements (Scanlon et al., 2013). TWIST is activated during EMT and its expression is higher in cancers which metastasize (Zeisberg and Neilson, 2009). Lymph node metastasis is directly correlated with TWIST up-regulation and E-cadherin expression is

down-regulated by BMI1 and TWIST which leads to poor prognosis (Ou et al., 2008, Scanlon et al., 2013). LEF (Lymphoid Enhancer Factor) facilitates Wnt signalling with TCF (T-cell factor) as a co-transcriptional activator. LEF/TCF promotes EMT in oral squamous cell carcinoma (OSCC) and up-regulate MMP-7 expression when β-catenin is mutated (Iwai et al., 2010). NOTCH1 consists of intracellular and extracellular region and when this receptor is activated due to ligand binding, it leads to cleavage of NOTCH1 intracellular domain (NICD) and it translocates to nucleus and leads to transcriptional activation by forming transcription factor complex with Recombination Signal Binding Protein for Immunoglobulin Kappa J Region (CBF1) and coactivator Mastermind-like family (MAML). In leukemias, NOTCH1 has been found to have oncogenic mutations but in HNSCC it has also been observed that NOTCH1 mutation might have tumour suppressor functions which can be due to mutation in EGF-like region or NICD and hence in HNSCC, NOTCH1 can also act as tumour suppressor gene (Loyo et al., 2013, Agrawal et al., 2011). NOTCH1 mutations are found in 10 to 15% of HNSCC cases and it was observed that there is copy number increase for JAG1 which is NOTCH1 ligand or activation of HES1/HEY1 which are downstream effectors of NOTCH pathway. Hence, NOTCH1 can have oncogenic or tumour suppressor effects in HNSCC (Sun et al., 2014). NOTCH1 overexpression is also involved in cisplatin resistance in HNSCC (Gu et al., 2010).

Table 1.1 Other Transcription factors (TF) deregulated in HNSCC

TF	Effects	Reference
Runt-related transcription factor-3 (RUNX3)	Promotes cell growth and prevents apoptosis	(Kudo et al., 2011)
Avian myelocytomatosis viral oncogene homolog	Induces growth and avoids apoptosis	(Khan and Bisen, 2013)

(C-Myc)		
Forkhead box O3a (FOXO3a)	Growth inhibition	(Fang et al., 2011)
Activator protein-1 (AP-1)	Promotes expression of pro-inflammatory and pro-angiogenic cytokines	(Ondrey et al., 1999)

Another group of important TF's are HOX transcription factors, a family comprising of 39 HOX genes which are present on four different chromosomes. These transcription factors are involved in the embryogenesis and organogenesis in vertebrates. It has been observed that several HOX genes in different cancers are deregulated and these are involved in cell proliferation, apoptosis, metastasis and differentiation (Shah and Sukumar, 2010). HOXA1, A2, A3, B3, B7, B9, C8, D10 were noted to be up-regulated in OSCC when compared to normal tissue. HOXC6 expression was seen to be higher in lymph node metastatic cancer compared to primary cancer in this cancer type (Hassan et al., 2006).

1.1.5.5 Micro-RNA

Lin-4 and let-7 were the first two microRNA to be discovered in 1993 and 2000, respectively, in Caenorhabditis elegans (Lee et al., 1993, Reinhart et al., 2000). MicroRNA's are non-coding RNA transcripts which are generally approximately 22 nucleotides in length and function in post-transcriptional gene regulation (Popovic et al., 2009). RNA polymerase II generally transcribes most of the miRNAs, either from the intronic region or from the polycistronic region forming the primary RNA transcript (pri-miRNA) (van Rooij and Olson, 2007). This pri-miRNA transcript is cleaved by Drosha to give a 60-70 nucleotides pre-miRNA hairpin transcript (Lee et al., 2003).

This pre-miRNA transcript is transported to cytoplasm with the help of Exportin5 (Yi et al., 2003). Once in cytoplasm, pre-miRNA transcript is further cleaved to give duplex of ~22 nucleotide in length by Dicer (Zhang et al., 2002). This duplex binds with Argonaute protein and here single stranded miRNA carries out its function of either mRNA degradation or translational repression (Hammond et al., 2001) (Figure 1.9).

Around 30% of the genes which code for different proteins are targeted by the miRNA which have been discovered to date in humans (Filipowicz et al., 2008). miRNA are redundant in terms of binding to target genes which means they can bind to more than one mRNA transcripts (Chen et al., 2011a). miRNAs can also produce multiple miRNA isoforms (Isomirs) which can be generated due to trimming of 5’ or 3’end, change in internal miRNA sequence due to incorporation of wrong base in sequence or tailing where additional non-templated nucleotide are added to miRNA can produce Isomirs (Ameres and Zamore, 2013). Recently, another form of miRNA biogenesis has been described. Mirtrons are splicing dependent short pre-miRNA, which give rise to active mature miRNA which show physiological effects in vertebrates. Mirtrons are produced from the splicing of the intron and are drosha independent (Sibley et al., 2012).

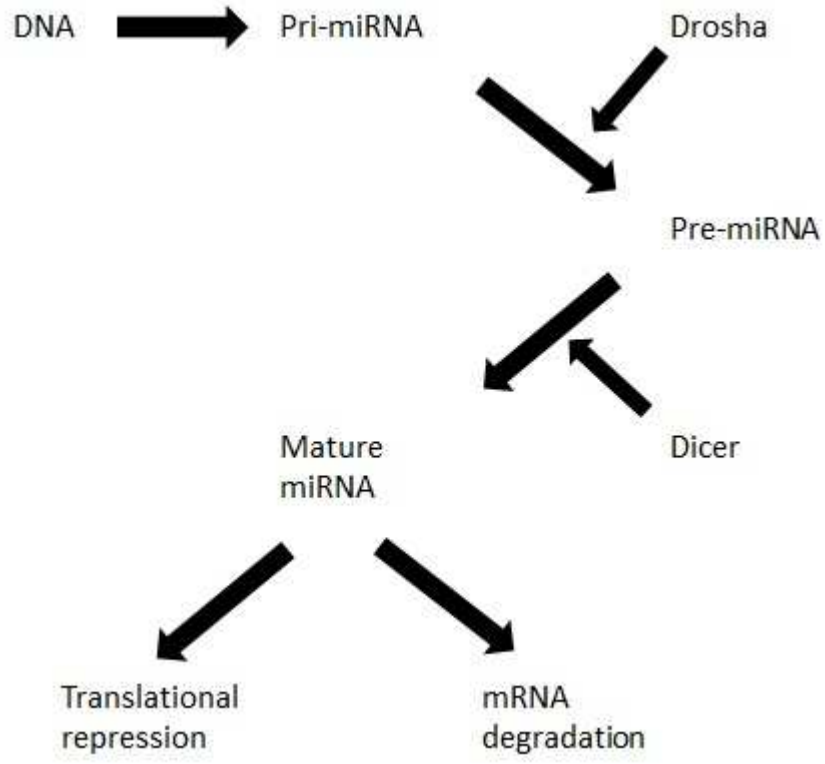

Figure 1.9. Basic depiction of miRNA biogenesis.

It has been shown that micro-RNA can have two classes: one which works as oncomir (oncogene) and others which act as tumour suppressor genes. Oncomir generally supports the development of cancer whereas tumour suppressor micro-RNAs act to inhibit oncogenesis (Lotterman et al., 2008). In different types of cancer, different micro-RNAs are deregulated. For HNSCC, it was noted that the level of miR-10a and miR-375 was reduced whereas miR-21, miR-106b, miR-423, miR-20a and miR-16 were over-expressed. In same study it was observed that knockdown of miR-106b led to arrest in G1 phase of cell cycle (Hui et al., 2010). miR-106b has also been shown to directly target p21 gene which reflects its phenotypic effects (Ivanovska et al., 2008). miR-21 was shown to directly target PTEN gene which is a tumour suppressor gene and was also shown to increase cell proliferation, migration and invasion in hepatocellular carcinoma. PTEN acts as inhibitor of Akt/mTOR pathway (Meng et al., 2007). miR-21 was shown to be one of the early deregulated microRNA in progression of leukoplakia to OSCC (Cervigne et al., 2009). It could mean that miR-21 shows its phenotypic effects by targeting tumour suppressor genes which leads to oncogenesis in HNSCC. miR-363 was shown to be down-regulated in HNSCC with lymph node metastasis and was shown to target podoplanin (PDPN). It was shown that increased PDPN expression due to down-regulation of miR-363 led to increased migration and invasion in HNSCC (Sun et al., 2013). Podoplanin is a platelet aggregation factor and is present as type I transmembrane glycoprotein. Podoplanin is also believed to be involved in lymphangiogenesis (Seki et al., 2013). miR-200a expression in OSCC was down-regulated and it was shown that miR-200 directly targets ZEB1 and ZEB2 which are transcriptional repressors of E-cadherin in murine mammary epithelial cells (Park et al., 2009, Korpal et al., 2008).

Table 1.2 List of aberrantly expressed miRNA in different cancers.

Cancer type	Aberrantly expressed miRNA	References
HNSCC	miR-10a, miR-375, miR-21, miR-106b, miR-423, miR-20a, miR-16, miR-196a	(Hui et al., 2010, Liu et al., 2012a)
Lung	let-7, miR-21, miR-34	(Takamizawa et al., 2004, Nana-Sinkam and Croce, 2013)
Breast	miR-145, miR-125b, miR-155, miR-21	(Iorio et al., 2005)
Colorectal	miR-143, miR-145	(Michael et al., 2003)
Pancreatic	miR-21, miR-196a, miR-190, miR-186, miR-221, miR-210, miR-222, miR-200b	(Bhat et al., 2012)

Early detection of cancer leads to better prognosis for the patients and hence there is need for more specific and sensitive biomarkers. In a study it was identified that miR-21, miR-181b and miR-345 could be potential biomarkers for progression of leukoplakia to oral squamous cell carcinoma (OSCC) (Cervigne et al., 2009). In another study it was observed that low expression of miR-205 and let-7d in HNSCC was indicative of poor prognosis for the patient (Childs et al., 2009). It has also been reported that expression of miR-125a and miR-200a was noted to be down-regulated in saliva of OSCC patients compared to healthy individuals (Park et al., 2009).

Another interesting micro-RNA is miR-196, which was found to be present in HOX gene clusters and has recently been seen to be deregulated in multiple cancers like

oesophageal adenocarcinoma, malignant melanoma, pancreatic cancer, leukaemia and breast cancer (Chen et al., 2011a). Recently, it was also observed miR-196a was highly expressed in oral carcinoma and was also increased in plasma of cancer patients compared to healthy individuals (Liu et al., 2012a). For this project, there was particular interest in the genomic location of miR-196a in HOXB cluster.

Chapter 2: HOXB9 and miR-196a

2.1 HOX genes:

The discovery of the homeotic genes, which are involved in organogenesis and embryogenesis, was possible due to observation of two major mutations in the Drosophila melanogaster. It was seen in Drosophila, that when there was mutation in the bithorax complex it led to change of haltere into wings and in the other one, it was seen that mutation in the antennapedia complex led to change of antenna into legs (Garciabellido, 1977). Later, it was discovered that the bithorax mutant seen in 1915 was actually part of a cluster called bithorax complex which consisted of Abd-B, Abd-A and Ubx whereas, antennapedia contains Antp, Scr, Dfd, Pb and Lab (Grier et al., 2005). This whole cluster was named HOM-C complex which were drosophila's homeotic genes. The counterpart of this complex in almost every vertebrate and in human was discovered in 1980's by sequence similarity and was called Homeobox genes (Abate-Shen, 2002) (Figure 2.1). Homeobox genes are present in two classes: Clustered and Non-clustered Homeobox genes. In total there are 200 Homeobox genes, out of which 39 HOX genes come under clustered Homeobox genes (Nagel et al., 2007). Most homeobox genes which are not present in HOX cluster do not play part in homeotic transformations. Most of these homeobox genes have been assigned to different families based on their sequence similarity for homeodomain and other domains present in protein form (Tupler et al., 2001).

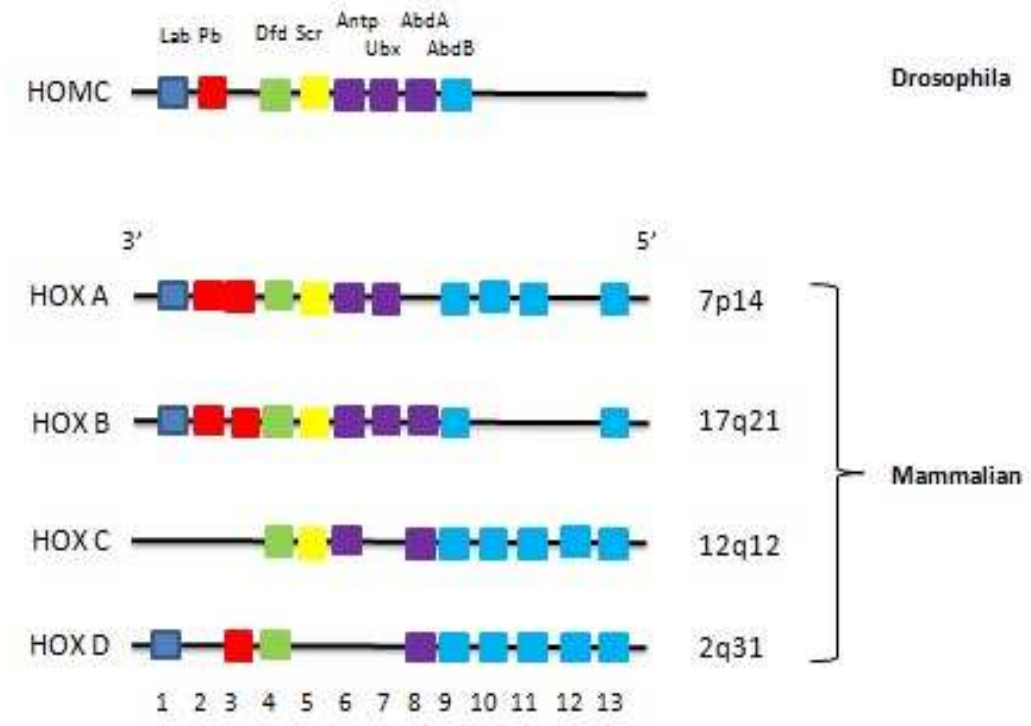

Figure 2.1. Drosophila HOMC genes and Mammlian HOX genes homology. Modified from (Eklund, 2011).

In humans, there are four clusters of HOX genes which have formed due to divergence and duplication from primitive HOX genes. These four clusters in human are found as follows, HOX A at chromosome 7p15, HOX B at 17p21, HOX C at 12q13 and HOX D at 2q31. In total, there are 39 HOX genes between these four clusters, divided into 13 paralogous groups with each cluster consisting of 9-11 genes (Duboule, 1992). HOX genes consist of two exons and one intron and homeodomain is situated in the exon 2 (Figure 2.2). Homeodomain is made up of 61 amino acids and has a helix-loop-helix structure which facilitates binding of HOX Transcription factor to DNA (Grier et al., 2005). There is presence of hexapeptide motif towards N-terminal side of Homeodomain which facilitates the binding of co-factor, PBX, to HOX protein and they also facilitate the binding site selection. MEIS is also an important co-factor for HOX proteins, but the motif involved in its interaction with HOX protein is not well understood (Eklund, 2011). The HOX-PBX heterodimer binds to bipartite sequence 5’ ATGATTNATNN 3’ which consists of two halves, with PBX binding the 5’ ATGAT 3’ sequence and HOX protein binding more variable 5’ TNATNN 3’ sequence. The preference for binding sequence differed from HOXB1 through to HOXB9 for HOX half of the HOX-PBX binding sequence (TTAT to TGAT) (Chang et al., 1996). Abd-B homolog HOX proteins interacted with Meis1 as co-factor, with Meis1 using 5’ TGACAG 3’ sequence as its binding site (Shen et al., 1997).

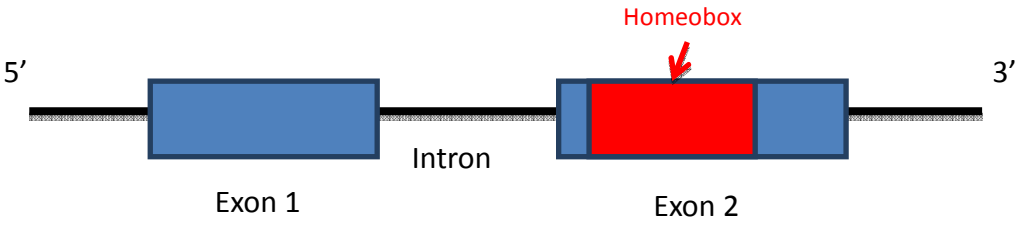

Figure 2.2. Structure of HOX genes. Modified from (Abate-Shen, 2002).

2.1.1 Relation to Development:

At the time of embryogenesis, structures like organs and limbs are formed when set of cells become committed for their formation. With time it has become apparent that group of HOX genes might be involved in the development of these structures along the AP axis in the body (Kmita and Duboule, 2003). Gap genes are the first to be expressed in the zygote along the AP axis and consist of genes like Kruppel, Hunchback and knirps (Hulskamp and Tautz, 1991). Depending on the concentration gradient of Gap genes, Pair rule genes are expressed in bands to form 14 parasegments along the AP axis. Hence, each parasegment has a different concentration of the gap and pair genes expression which defines the expression pattern of the HOM-C genes (Small and Levine, 1991, Grier et al., 2005). Initiation of the HOM-C complex may be due to the presence of gap and pair genes but there are other modifying genes which also might be involved in its expression, like genes which encode for chromatin-associated proteins such as Polycomb group and trithorax group (Hanson et al., 1999).

Histone methyltransferase proteins consist of polycomb (PcG) and trithorax (TrgX) proteins which contain histone-lysine methyltransferases and histone-arginine methyltransferases respectively. Transcriptionally active or repressed condition of HOX genes is maintained by opposite action of TrgX or PcG respectively (Barber and Rastegar, 2010). Repression of HOX genes, in part, is due to PcG protein activity which was first identified in drosophila (Zink and Paro, 1989). PcG proteins impart their effect of silencing on their targets by two protein complexes: PRC1 (Polycomb group repressive complex 1) and PRC2. During development, it was observed that these two complexes were involved in silencing of several developmental genes in human embryonic stem cells (Lee et al., 2006). PRC1 contains several protein subunits such as B Lymphoma Mo-MLV Insertion Region 1 (BMI1), Really Interesting New Gene 1 (Ring1), Ring2 and Early Development Regulator 2 (HPH2) (Wang et al., 2004)

whereas PRC2 contains Suppressor of Zeste 12 Homolog (SUZ12), embryonic ectoderm development (Eed) and enhancer of zeste homolog 2 (Ezh2) (Barber and Rastegar, 2010). BMI1 has been shown to repress expression of HOXA9 in leukemic stem cells (Smith et al., 2011a). SUZ12 and H3K27me3 marks were detected in normal cells for HOXB7, HOXC10, HOXC13 and HOXD8 genes and in OSCC, SUZ12 and H3K27me3 marks were not detected which led to higher expression of these genes (Marcinkiewicz and Gudas, 2013). Utx is TrgX group regulator and in drosophila it keeps the HOX genes, which are repressed by PcG action, in active state where it is required (Copur and Muller, 2013).

At the time of embryogenesis, HOX genes are expressed from 3’ to 5’ end along the antero-posterior axis. The function of HOX genes is to give positional identity along anterior-posterior axis. The HOX genes towards 3’ end are expressed earlier and also more anteriorly when compared to 5’ end genes which are expressed late and more posteriorly, this pattern of expression is called spatial collinearity (Lewis, 1978) (Figure 2.3). Retinoic acid (RA) has been observed to regulate the timing of HOX genes expression in the vertebrates. RA signalling is effected by heterodimerization of nuclear receptors, retinoic X receptors (RXRs) and retinoic acid receptors (RARs), which in turn bind to retinoic acid response elements (RARE) which are specific DNA sequences (Soshnikova, 2013). On stimulus by RA, 3’ HOXB genes respond earlier based on their looping out from chromosome which is dependent on the higher-order chromatin structure based on the histone modifications (Chambeyron and Bickmore, 2004).

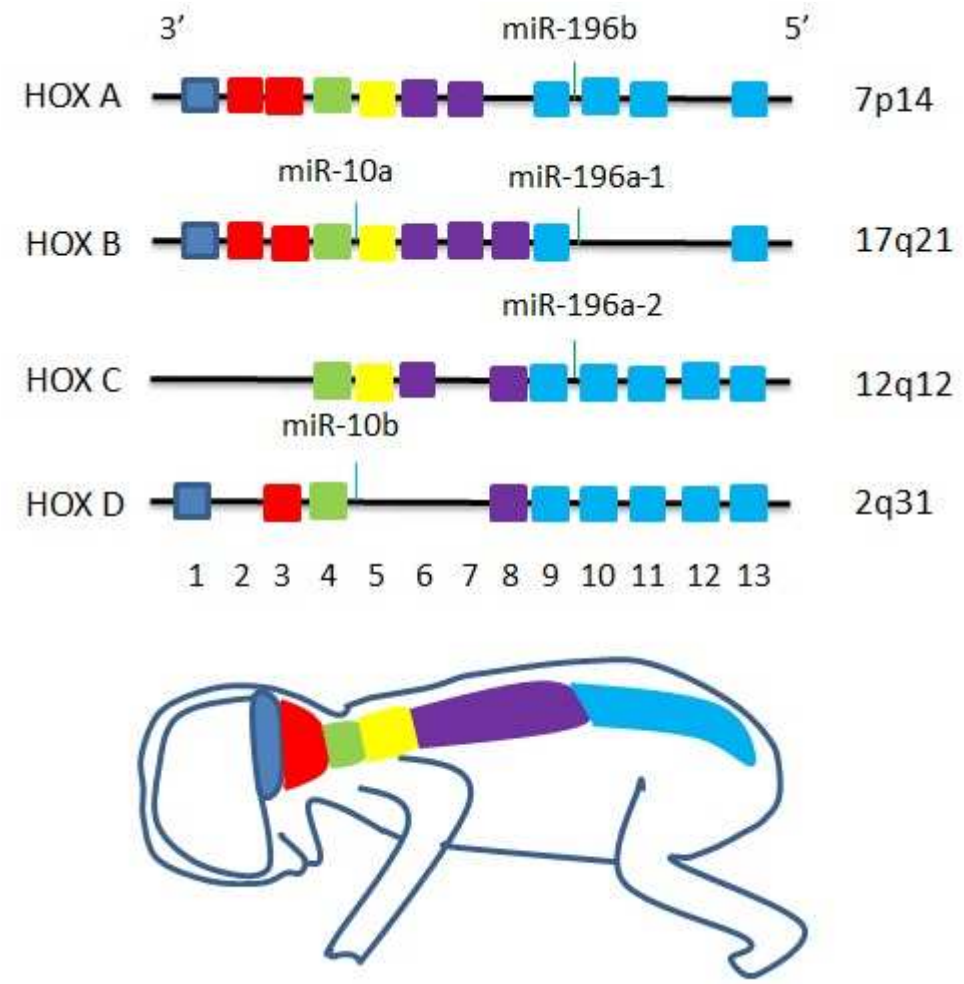

Figure 2.3. Positioning of HOX gene cluster at different chromosomes in human and showing spatial collinearity in expression of HOX genes. Modified from (Grier et al., 2005).

The HOM-C genes in drosophila and HOX genes in the vertebrates are responsible for patterning the development of the body. Ed Lewis in 1978 concluded that position of HOX genes within the cluster determined the effect, gain of function and loss of function, the two kinds of homeotic mutations. Formation of structures which are generally found more anteriorly are due to loss of function mutation, whereas development of structures which are formed posteriorly but are formed in anterior segments are due to gain of function mutation, and this consequence is called ‘posterior prevalence’. It has been observed that the function of 3’ end genes is inhibited by 5’ end genes which leads to ‘posterior prevalence’ (Lewis, 1978). It has also been noted that there are no severe changes in morphogenesis if there is mutation in single HOX gene. This could be due to the fact that HOX gene clusters were formed due to duplication and divergence and hence there is presence of redundancy in paralogous group members or its possible there are more effector genes in vertebrates which respond to quantitative effect of HOX protein (Suemori and Noguchi, 2000). Another pattern seen in expression of HOX gene is called ‘Temporal collinearity’ in which during embryonic development there is spatial expression of HOX gene, which is the expression of 3’ end genes first and as embryo develops, expression of 5’ genes progressively (Grier et al., 2005). In a study, mouse HOXD cluster was split into two clusters with HOXD11-HOXD13 isolated from rest of the HOXD cluster by 3 Mb insertion. This study showed that H3K27me3 pre-marked the transcription sites in the HOXD cluster but was not enough when remote enhancer sequences were absent for appropriate HOX gene activation, which showed that HOX clustering is important for HOX gene temporal activation (Soshnikova and Duboule, 2009).

2.1.2. HOX Cluster and Oncogenesis:

It has been observed that the expression pattern of the HOX genes in cancerous tissue seems to be dysregulated when compared to normal tissue. The expression pattern can

be contributed to the following three groups. The first group consist of the re-expression of the HOX genes in the oncogenic tissue which normally would only be expressed during development. Second contain the category of HOX genes which are expressed in tumour cells but are not expressed at all normally during development. Third is the group in which HOX gene expression is down-regulated when compared to normal expression in the completely differentiated cell (Abate-Shen, 2002). The deregulation of the HOX genes could be due to epigenetic deregulation, gene dominance or temporospatial deregulation (Shah and Sukumar, 2010).

One of the most important mechanisms of maintaining expression of any gene is epigenetic control which is true for HOX genes. Methylation is commonly seen in the CpG islands of the promoter of HOX genes which are silenced (Hershko et al., 2003). Polycomb and Trithorax group proteins have been seen to be involved with histone trimethylation. The methylation and demethylation in the CpG islands is carried out due to the changes caused in the chromatin structure by these proteins (Shah and Sukumar, 2010). For example in Mixed lineage leukemia (MLL) translocation containing lymphoblastic leukaemias, with MLL being a trithorax homologue, there is overexpression seen of HOX genes such as HOXA9 and HOXA10 which leads to poor prognosis (Golub et al., 1999, Ferrando et al., 2003).

Micro-RNAs like miR-196 and miR-10 are expressed within the HOX gene clusters. Through computational analysis and experimental results it has been seen that these microRNAs target different HOX genes. It has also been noted that in colon carcinoma cell line, at least 10% of all micro-RNA are methylated. This leads us to believe that promoter methylation of micro-RNAs involved in HOX gene expression, might be another mechanism of control in cancers (Han et al., 2007). It has also been noted that large intervening non-coding RNA (lincRNA) such as HOX transcript antisense RNA

(HOTAIR) are also involved in the expression of the HOX genes, which adds another mechanism of control of expression of HOX genes (Sessa et al., 2007, Rinn et al., 2007).

For normal organogenesis, it is important that the HOX gene follow their normal spatial and temporal regulation. Perturbed organogenesis has been associated with the oncogenesis and hence deregulation of temporospatial collinearity has been thought to be another reason for oncogenesis. It was seen in oesophageal carcinoma that when compared to normal expression of HOX gene, there were more 5' end HOX genes expressed at a higher level unlike normal oesophagus where more 3' HOX genes were expressed at higher levels (Takahashi et al., 2007). The other reason seen for oncogenesis is dominance of HOX genes expression. It has been seen that HOX genes have dose-dependent effect, where if one dose is important for normal development another could lead to cancer development (Lawrence et al., 1997). For example, it was seen that HOXA9 was overexpressed in the Acute Myeloid Leukaemia (AML) (Ghannam et al., 2004). When HOXA9 was knocked out in the cell culture models it was seen it not only limited oncogenesis but also hindered normal haematopoiesis whereas model with only one allele knocked out showed normal haematopoiesis (Lawrence et al., 1997).

Table 2.1 HOX genes aberrantly expressed in different cancers.

Cancer type	HOX genes deregulated	References
Oral cancer	HOXA1, HOXA2, HOXD10, HOXB3, HOXA3, HOXC8, HOXB9, HOXB7, HOXC6	(Hassan et al., 2006)
Breast cancer	HOXA6, HOXA13, HOXB2, HOXB4, HOXB5, HOXB6,	(Hur et al., 2013)

	HOXB7, HOXB8, HOXB9, HOXC5, HOXC9, HOXC13, HOXD1, HOXD8	
Acute myeloid leukemia	HOXB3, HOXB4, HOXA9, HOXA10, HOXA11	(Shah et al., 2012)
Colorectal cancer	HOXA9, HOXB3, HOXB8, HOXB9, HOXB2, HOXB13, HOXD1, HOXD3, HOXD4, HOXD8, HOXD12	(Kanai et al., 2010)
Hepatocellular cancer	HOXA3, HOXA5, HOXA6, HOXA7, HOXA9, HOXA10, HOXA11, HOXA13, HOXB1, HOXB6, HOXB7, HOXB8, HOXB9, HOXB13, HOXC5, HOXC6, HOXC8, HOXC9, HOXC10, HOXC11, HOXC12, HOXC13, HOXD1, HOXD3, HOXD4, HOXD8, HOXD9, HOXD10	(Kanai et al., 2010)
Non-small cell lung cancer	HOXA3, HOXA5, HOXC4, HOXC8, HOXC9, HOXC13, HOXD8, HOXD10	(Plowright et al., 2009)
Small cell lung cancer	HOXD13, HOXD11, HOXD10, HOXC10, HOXC8, HOXB9, HOXB8, HOXA11, HOXA10	(Tiberio et al., 1994)

2.2 HOXB9

HOXB9 is the ninth gene in HOXB cluster present on chromosome 17 in humans. It is also part of HOX9 paralogous group (Figure 2.2). Like other HOX genes, HOXB9 contains homeodomain which has a helix-loop-helix structure and facilitates DNA binding. Expression of HOXB9 was increased relatively in bovine and mouse embryos between oocyte and morula stage of development (Paul et al., 2011). HOXB9 has been implicated in the development of the forelimb, as HOX9 paralogous group mutant mice had severely deformed forelimbs. Early forelimb field anteroposterior polarisation required function of HOX9 paralogs. This was seen due to requirement of HOX9 paralogs in the posterior forelimb for expression of Heart and neural crest derivatives expressed 2 (HAND2), repression of Gli family zinc protein 3 (Gli3), Sonic hedgehog (Shh) expression and collinear expression of HOXA/D 10-13. In the same study, HOX9 mutants had no phenotypic effects in hindlimb development raising the possibility of differences in patterning (Xu and Wellik, 2011). In another study, HOXB9 homozygous mutant mice showed irregular attachment of the rib to sternum, intercostal segments showed irregular growth and sternum showed decrease in the number of intercostal segments. This revealed that HOXB9 played important role in thoracic skeletal development. Synergistic effects were observed in the mice which carried homozygous mutation for HOXA9 and HOXB9 genes and showed further defects of the rib and sternum (Chen and Capecchi, 1997).

Xcad3, a Xenopus caudal family member (Cdx), was the early target of fibroblast growth factor (FGF) signalling pathway and was important to posterior development of embryo. Xcad3 led to activation of different HOX genes in posterior development among which was HOXB9 (Isaacs et al., 1998) (Figure 2.4). FGF, retinoic acid receptors (RARs) and HOX genes interaction was studied in anteroposterior patterning for neurogenesis. It was observed that on blockage of FGF pathway it led to reduced

expression of members of RAR pathway such as RARα. Over-expression of RARα2 led to rescue of expression of Xcad3 and HOXB9 which meant that RARα2 was required to mediate the effects of FGF signalling for posterior development through expression of Xcad3 and HOXB9 (Shiotsugu et al., 2004) (Figure 2.4). In another study, it was seen that Deleted in azoospermia associated protein 2 (DAZAP2) was downstream target of FGF signalling and was involved in posterior development of neural plate. It was also studied that DAZAP2 led to induction of HOXB9 in FGF-dependent posterior patterning. Induction of HOXB9 by DAZAP2 was independent of Cdx activity and was thought to work in parallel or downstream of DAZAP2 (Roche et al., 2009) (Figure 2.4).

Neural stem cells from mice showed expression of HOXB4 and HOXB9 in the neural stem cells derived from spinal cord which helped these cells maintain their distinct positional identity and was also seen to be dependent on developmental stage (Onorati et al., 2011). Most work on HOXB9 has been done in terms of its involvement in development but it was also shown that HOXB9 plays a significant role post pregnancy in the differentiation of epithelial ductal system of mammary tissue in adult mice. During pregnancy and post child birth, triple mutant (HOXA9, HOXB9 and HOXD9) female mice showed hypoplasia of mammary gland and also these females failed to produce milk for their offspring (Chen and Capecchi, 1999).

Polycomb and trithorax group of proteins control the activity of different HOX genes in drosophila and vertebrates. Ring1B (Component of PRC1) was associated in the pathogenesis of Angelman syndrome and directly regulated the activity of HOXB9 in mice (Zaaroor-Regev et al., 2010) (Figure 2.4). BMI1, also a component of PRC1, regulated the activity of HOXB9 in Hodgkin lymphoma. It was studied here that constitutively active Extracellular signal-related kinase 5 (ERK5) pathway led to

repression of BMI1 in these cells and over-expression of HOXB9. FGF2 might also be one of the several growth factors involved in the activation of MAPK ERK5 pathway which leads to repression of BMI1 in these cells (Nagel et al., 2007) (Figure 2.4). F-Box and Leucine-Rich Repeat Protein 10 (FBXL10) was observed to regulate the binding of Ring1b to its target genes in mouse embryonic stem cells (Wu et al., 2013). HOXB9 promoter activity was affected by the secondary structure of DNA in the promoter region. HOXB9 promoter activity was linked to FBXL10 protein and silencing of this protein led to increased expression of HOXB9 promoter construct (Yamagishi et al., 2008) (Figure 2.4). HOXB9 also interacts with B-cell translocation gene 1 (BTG1) and BTG2 as its transcriptional co-factors and its binding to DNA is facilitated by this interaction (Prevot et al., 2000).

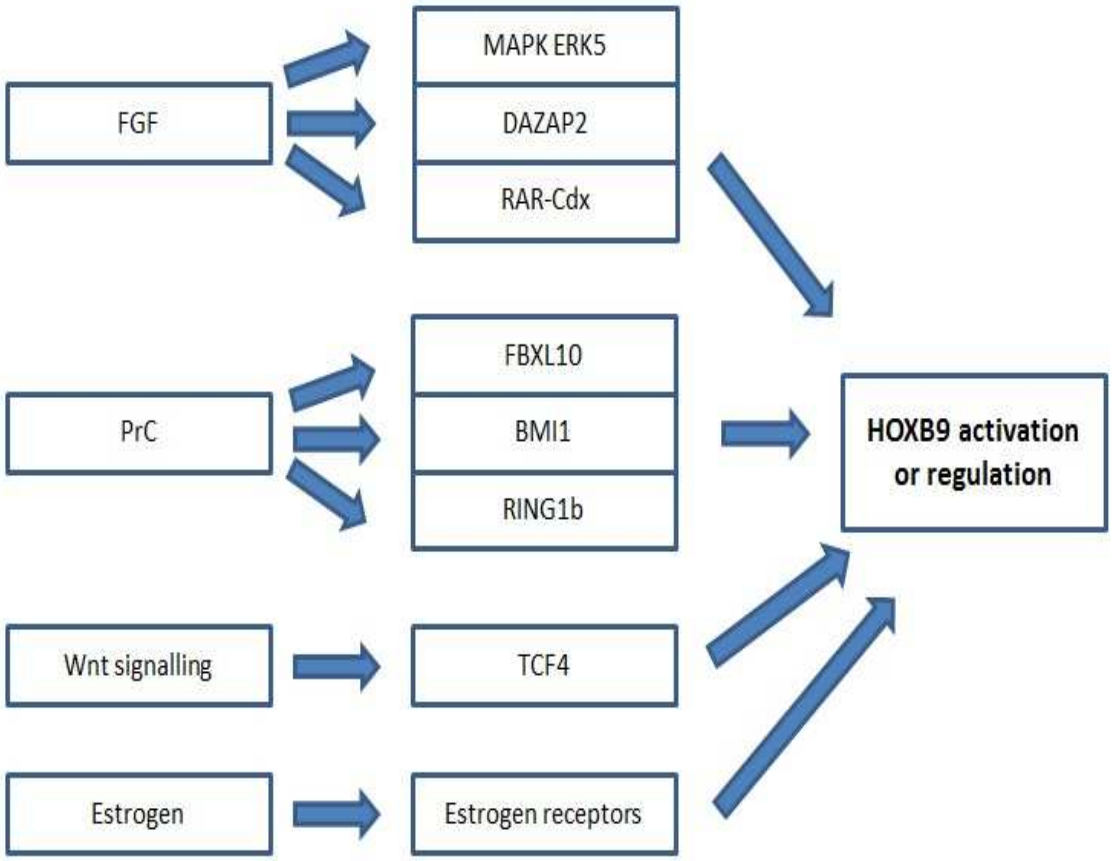

Figure 2.4. Different pathway and proteins involved in activation and regulation of HOXB9.

2.2.1 HOXB9 and Cancer

HOXB9 has been noted to be over-expressed in breast cancer (Seki et al., 2012, Hayashida et al., 2010). It has also been observed to regulate the expression of angiogenic factors such as Vascular endothelial growth factor (VEGF), Interleukin-8 (IL-8), Angiopoietin-like 2 (ANGPTL-2) and FGF2 in breast cancer. Erythroblastic leukemia viral oncogene (ErbB) ligands such as neuregulin-1 and 2, epiregulin and amphiregulin and Transforming growth factor- β (TGF-β) were also induced by HOXB9 which leads to increased cell motility and gain of mesenchymal features by the cells. It was seen that epiregulin and amphiregulin were transcriptional targets of HOXB9 as based on ChIP assay putative binding sites of HOXB9 were observed in promoter of these genes. It was also shown that HOXB9 promoted metastasis to the lung in the mouse (Hayashida et al., 2010). In another study HOXB9 promoted cell proliferation and angiogenesis in breast cancer and also was an important prognostic factor in the outcome of breast cancer (Seki et al., 2012). HOXB9 also confers radio-resistance in breast cancer cells by inducing the DNA damage response. HOXB9 led to increased baseline level of ataxia telangiectasia (ATM) in non-irradiated cells and upon radiating these cells it led to hyperactivation of ATM which in-turn increases DNA repair. It was also shown that TGF-β was a direct target of HOXB9 and induced epithelial-mesenchymal transition (EMT) in breast cancer cells. The HOXB9-TGF- β-ATM axis has an impact on DNA repair in breast cancer cells (Chiba et al., 2012). HOXB9 was also noted to be expressed as fusion protein of Breast carcinoma amplified sequence 3 (BCAS3)-HOXB9 in the breast cancer cell line (Schulte et al., 2012). HOXB9 expression was seen to be regulated by estrogen. There was presence of estrogen-responsive elements (ERE) in the promoter of HOXB9 and estrogen receptors α and β were seen to be important for HOXB9 activation. These receptors bind to ERE and so do Mixed-lineage leukemia 1 and 3 (histone methylase) which were observed to

be significant for estrogen-mediated HOXB9 activation (Ansari et al., 2011) (Figure 2.4).

HOXB9 was over-expressed at RNA and protein level in lung cancer cell lines and tumour samples (Calvo et al., 2000), with a suggested role in metastasis of lung adenocarcinoma to bone and brain. In this context, HOXB9 expression was regulated by Wnt/TCF pathway in lung adenocarcinoma cells. On treating cells with Wnt3a, TCF4 (T-cell factor 4) regulated expression of HOXB9 which led to enhanced metastasis of lung adenocarcinoma to bone and brain (Nguyen et al., 2009) (Figure 2.4). HOXB9 is also over-expressed in hepatocellular carcinoma, leukemia and colorectal carcinoma (Kanai et al., 2010, Ohnishi et al., 1998). HOXB9 expression was down-regulated in gastric cancer and was related to being a biomarker of poor prognostic outcome in patients (Sha et al., 2013). HOXB9 has also been shown to be over-expressed in oral cancer tissue compared to normal tissue (Hassan et al., 2006) but there is no research done to observe if over-expression of HOXB9 mRNA translates into over-expression of HOXB9 protein in cell lines and tissue samples in HNSCC. Also, there is no literature on what effects HOXB9 over-expression has on HNSCC cells.

2.3 miR-196a

Silencing and activation of HOX genes needs conservation of its original order in each of the clusters, miR-10 and miR-196 have similar evolutionary order as HOX genes. There are three miR-196 loci found on three different chromosomes in humans. miR-196a-1 is found to be present on chromosome 17 between HOXB9 and HOXB13, miR-196a-2 is located between HOXC9 and HOXC10 on chromosome 12 whereas miR-196b is present on chromosome 7 in the region flanked by HOXA9 and HOXA10 (Popovic et al., 2009, Tanzer et al., 2005). Though present on different chromosomes, miR-196a-1 and miR-196a-2 produce same mature miRNA sequence on processing,

whereas miR-196b produces a mature sequence which has one base pair different than miR-196a (Figure 2.5). miRNA carry a lot of evolutionary information with them even though they are small, and miR-196 homologues can be identified in many vertebrates (Tanzer et al., 2005).

The putative targets for miRNA are identified on the basis of bioinformatics analysis. This analysis depends on looking for complementarity regions in 3' UTR of the genes. Generally, it is based on whether 2 to 8 base pairs from the 5' end of the miRNA (which is called the seed region) match with the 3' UTR of the putative target gene. Putative target genes could show good match, but it can also depend on other factors such as whether there is high complementarity in 3' end of miRNA and mRNA of the gene then it can act to stabilise the binding even if seed region is not a perfect match (Filipowicz et al., 2008). Based on *in-silico* analysis, miR-196a could target HOXB8, HOXC8, HOXD8 and HOXA7.

Based on published literature, miR-196a did target multiple HOX genes. miR-196a was over-expressed in NSCLC and increased cell proliferation, invasion and migration in this cancer. It also targeted HOXA5 and this partially led to effects observed in NSCLC cells (Liu et al., 2012d). miR-196a was down-regulated in both breast cancer and melanoma. miR-196a was found to target HOXC8 in both the cancers. Ectopic over-expression of miR-196a in melanoma cells led to direct down-regulation of HOXC8 expression and it was shown to regulate progression of malignant melanoma and cell transformation (Mueller and Bosserhoff, 2011). In breast cancer, ectopic over-expression of miR-196a also led to direct targeting of HOXC8. It was also shown that miR-196a is a potent metastasis inhibitor in breast cancer and ratio of miR-196a to HOXC8 mRNA was an indicator of metastatic potential of these cells (Li et al., 2010). miR-196a was also observed to target HOXB8 in mouse embryos and play role in

development of vertebrates (Yekta et al., 2004). HOXB8 was also targeted by miR-196a in neural tube and affected motor neuron genesis. miR-196a targeting helped in restricting HOXB8 expression to thoracic-lumbar overlap (Asli and Kessel, 2010). miR-196 also targeted HOXB8 in hindlimb development of mouse (Hornstein et al., 2005). miR-196a targeted HOXB7 in malignant melanoma. It was also observed that down-regulation of miR-196a expression in melanoma leads to over-expression of HOXB7, which in-turn leads to induction of BMP4 in malignant melanoma and acts as major factor in migration of melanoma (Braig et al., 2010).

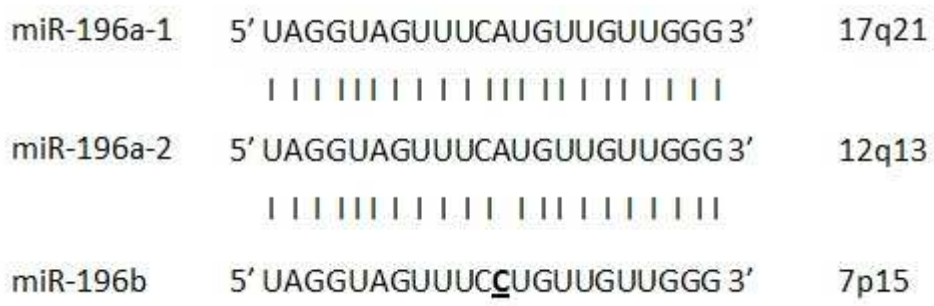

Figure 2.5. Position and mature miRNA sequence for all three miR-196.

Table 2.2 Some Other targets of miR-196a.

Condition or Disease	Target gene	References
Oesophageal cancer	AnnexinA1 (ANXA1), S100 calcium binding protein A9 (S100A9), Keratin5 (KRT5) and small proline-rich protein 2C (SPRR2C)	(Luthra et al., 2008, Maru et al., 2009a)
Gastric cancer	cyclin-dependent kinase inhibitor 1B (p27(kip1))	(Sun et al., 2012)
Keloid fibroblast	collagen type 1 A1 (COL1A1) and collagen type 3 A1 (COL3A1)	(Kashiyama et al., 2012)
Spinal and bulbar muscular atrophy	CUGBP, Elav-like family member 2 (CELF2)	(Miyazaki et al., 2012)

miR-196a was over-expressed in oesophageal cancer and led to increase in cell proliferation, reduced apoptosis and promoted anchorage-dependent growth (Luthra et al., 2008). miR-196a was over-expressed in gastric cancer compared to normal tissue. miR-196a promoted cell proliferation and was increased in the serum of gastric cancer patients and also this increase in expression could be used to predict recurrence of the cancer in the patients (Tsai et al., 2012, Sun et al., 2012). miR-196a over-expression in pancreatic cancer was associated with abnormal apoptosis, increased invasion and proliferation (Liu et al., 2013). miR-196a expression in serum of pancreatic cancer patients in combination with miR-16 and CA19-9 could be used for early diagnosis of pancreatic cancer (Liu et al., 2012b).

miR-196a was also noted to be over-expressed in oral squamous cell carcinoma. It was also observed to be associated with metastasis, recurrence and mortality. miR-196a expression was also detected in the plasma of the patients and could be used to distinguish from healthy individuals (Liu et al., 2012a). Based on unpublished data from miRNA microarray study, it was observed that miR-196a was over-expressed in HNSCC cell lines when compared to normal cell line (Lambert, Murdoch and Hunter, 2010, unpublished). Also, there are no known published targets of miR-196a in HNSCC.

2.4 Aims and Objectives

The hypothesis of the project was HOXB9 and miR-196a are highly expressed in HNSCC and contribute to the pro-tumourigenic phenotype. To test this hypothesis, following aims were outlined.

The aims and objectives of the project were:

1. To assess the expression of miR-196a in cell lines and tissue samples and assess the functional effects of miR-196a in HNSCC cells.

2. To evaluate the expression of HOXB9 gene in cell lines and tissue samples and assess the functional effects of HOXB9 in HNSCC cells.

3. To assess whether HOXB9 and miR-196a-1 were co-transcribed on the same primary transcript.

4. To search for novel direct target of miR-196a in HNSCC.

Chapter 3: Materials and Methods

3.1 Chemicals and Reagents:

List of all the suppliers and their location is available in appendix 9.1.

Unless stated otherwise, all the chemicals or reagents used were purchased from Sigma Aldrich.

For reverse-transcription and qPCR, unless stated otherwise, all the reagents were purchased from Applied Biosystems.

3.2 Cell lines Used:

The cell lines for the project were kindly provided by Dr. Keith Hunter and Dr. Craig Murdoch. Many cell lines listed below are well characterised HNSCC cell lines (McGregor et al., 2002, Stanton et al., 1994). All the cell lines tested HPV negative at the time of origin.

Table 3.1. The names, type and origin of all the cell lines used.

Cell line	Type	Site of Origin
OK21	Normal Oral Keratinocytes (NOK) (Primary)	Buccal Mucosa
OK102	NOK (Primary)	Buccal Mucosa
NOK2	NOK (Primary)	Buccal Mucosa
NOK319	NOK (Primary)	Buccal Mucosa
NOK320	NOK (Primary)	Buccal Mucosa
NOK329	NOK (Primary)	Buccal Mucosa
DEN8	NOK (Primary)	Buccal Mucosa
OK334	NOK (Primary)	Buccal Mucosa
OKF4-tert	Immortal Normal Oral Keratinocytes (iNOK)	Floor of Mouth (Dickson et al., 2000)
FNB6-tert	iNOK	Buccal Mucosa

OKF6-tert	iNOK	Floor of Mouth (Dickson et al., 2000)
D4	Oral Pre-Malignant (OPM)	Floor of Mouth
D19	OPM	Buccal Mucosa
D20	OPM	Tongue
D35	OPM	Floor of Mouth
B16	Primary head and neck squamous cell carcinoma (HNSCC)	Tongue
H357	Primary HNSCC	Tongue (Yeudall et al., 1993)
B56	Primary HNSCC	Tongue
T4	Primary HNSCC	Tongue
B22	Metastatic Cancer	Neck lymph node

3.3 Cell culture

The NOKs, iNOKs, OPM and HNSCC cell lines (Table 3.1) were maintained in KGM (Keratinocyte Growth Media) media. KGM media contained the following components:

Table 3.2. Components of KGM media.

Component	Volume or Final concentration
DMEM	Depends on final volume to be prepared
Ham's F-12	23% (v/v)
FCS (Foetal Calf Serum)	10% (v/v)
L-glutamine	2mM
Adenine	1.8 X 10^{-4} M
Hydrocortisone	0.5 µg/ml

Insulin	5 µg/ml
EGF (Epidermal Growth Factor)	10 ng/ml

The KGM media (Table 3.2) was removed and cells were washed with PBS (Phosphate Buffered Saline) and then incubated with trypsin (1mg/ml) - EDTA (0.4mg/ml) until the cells were detached from the flask. The trypsin was then neutralised by adding KGM media and centrifuged at 1000 rpm for 5 min. The cells were then re-suspended in the KGM media and counted on a Neubauer haemocytometer using trypan blue (Invitrogen) exclusion method (10 µl cell suspension in 10 µl trypan blue) by counting number of cells in four chambers around the central grid and then averaging the number and multiplying it by 10^6. The cells were then seeded into a new flask. The general seeding density used was 1:5 or 1:4 of the re-suspended cells depending on the cell count and doubling time of the cells. The cells were then incubated at 37^0C and 5% (v/v) CO_2. The cells were tested every two months for potential mycoplasma infection by performing PCR using EZ-PCR mycoplasma test kit (Geneflow).

3.3.1 Freezing and Thawing of the cells

The cells were initially adjusted to a million cells/ml in KGM. 10% (v/v) DMSO was added and cells were transferred into cryo-vials (Grenier Bio-one). The cells were then frozen down at a controlled rate of 1^0C/h in -80^0C freezer in a cryo-freezing container (Nalgene) before transferring it to liquid nitrogen for permanent storage.

When the cells were to be cultured from the frozen stock, the cryo-vial from the appropriate position was removed and thawed at 37^0C. The cells from vial were then transferred to a 25 ml universal tube (Sarstedt) to which fresh KGM was added and centrifuged at 1000 rpm for 5 min. The supernatant was discarded to remove any

dimethyl sulfoxide (DMSO). The cells were re-suspended in 5 ml of KGM and put in a T25 flask (Grenier Bio-one) and incubated at 37^0C with 5% (v/v) CO_2.

3.4 RNA isolation and PCR

The cells were washed with PBS, centrifuged to form a pellet and excess PBS was discarded. RNeasy mini kit (Qiagen) was used to extract the total RNA from the cell pellet. RNA was quantified using a Nanodrop spectrophotometer (Thermo Scientific) and quality was checked by noting the A260/280 ratio. Generally, RNA is considered of good quality if the ratio is >= 1.8. cDNA was synthesized from total RNA by using High capacity RNA-to-cDNA kit. The miRNA cDNA synthesis used 10ng of total RNA and miRNA specific reverse transcription primers. Following is the PCR cycle utilised: 16^0C for 30 min, 42^0C for 30 min and 85^0C for 5 min. The total cDNA synthesis used 200ng of total RNA and random primers (RP). Following is the PCR cycle utilised: 25^0C for 10 min, 37^0C for 2 h and 85^0C for 5 min. The other components for reverse transcription-Polymerase Chain Reaction (rt-PCR) such as reverse transcription buffer (10X), dNTP (100 mM), multiscribe and distilled water were used in the amounts specified by the manufacturer. The cDNA was then used to perform SYBR-green or Taqman quantitative PCR (qPCR) and SYBR-green Mastermix (MM) or Taqman MM was used respectively for the reaction. The other components such as forward and reverse primers for SYBR-green MM and Taqman primers for Taqman MM and distilled water were added based on the manufacturer's protocol. RNU48 for miRNA cDNA and U6 for total cDNA were used as the internal control for qPCR. Separate wells in a 96-well plate (Starlab) were used for target gene and internal control. SYBR-green qPCR detection of all 39 HOX genes was carried out in University of Surrey with the help of Dr. Richard Morgan on the Stratagene platform MX3005p, initially, and the internal control used was β-actin. β-actin was used as the internal control as it was part of pre-made grid for the experiment in Dr. Morgan's lab. The expression detection for

all the other qPCR was carried out on ABI 7900HT platform and the raw data was analysed using RQ manager 1.2.1 (Applied Biosystems). The absolute expression level for a gene was quantified by normalising the expression of the gene to the internal control gene expression level.

3.5 Laser Capture Microdissection (LCM)

Formalin-fixed paraffin embedded (FFPE) cancer and normal tissue sections (4 µm) were cut and placed onto twinfrost microscope slides (CellPath). In total, 16 cancer and normal tissue sections were used. These were dewaxed in xylene (Fisher) and graded ethanol (100% (v/v) and 70% (v/v)) (Fisher), stained with harris haematoxylin (CellPath) and dehydrated through 100% (v/v) ethanol and xylene with care taken to ensure complete dehydration. Pixcell II LCM system (Arcturus) was used to carry out LCM. The tissue section was viewed in the microscope and LCM cap (Applied Biosystems) adjusted to fit the tissue area to be collected. The normal and tumour cells were collected on the LCM caps (Figure 3.1) gathering as much material as possible on the cap. Extraction of RNA from LCM cap was carried out by using RNAqueous micro kit (Ambion) based on step-by-step protocol provided by the manufacturer.

A. B. C.

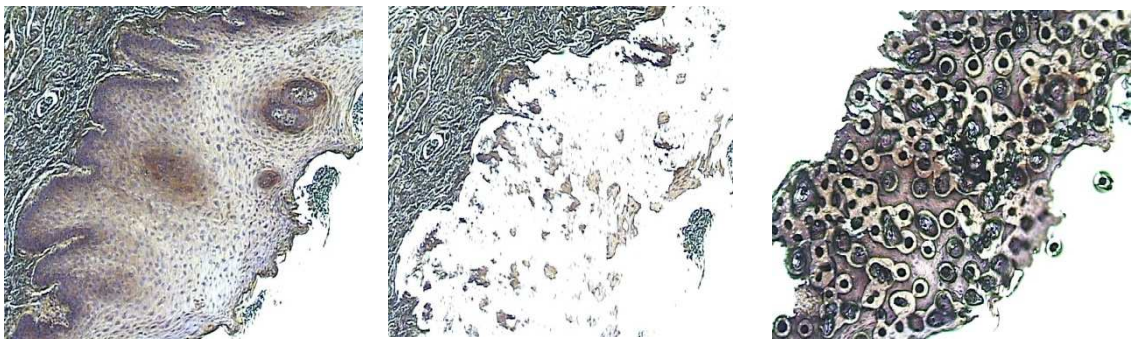

Figure 3.1.A. Photomicrograph of a normal tissue section as viewed under microscope before LCM was performed. B. The normal tissue as viewed under microscope after LCM was performed. C. The normal tissue cells collected on the LCM cap as viewed under microscope. The magnification used was 100X.

3.6 Primer Design

Homo sapiens referenced sequence of the appropriate target was retrieved from the NCBI website (http://www.ncbi.nlm.nih.gov/) (National Center for Biotechnology Information, 2011). The first and last nucleotide number of the coding sequence (CDS) was checked from the information on the page. The forward primer consisted of the first 21-27 nucleotides of the CDS and then 21-27 nucleotides were selected, 150-200 bp downstream of forward primer and run through programme called 'Reverse Complement' to give the reverse primer (Table 3.3) (http://www.bioinformatics.org/sms/rev_comp.html). Forward and reverse primers were checked using Primer Blast (http://www.ncbi.nlm.nih.gov/tools/primer-blast/) to assess their specificity, % GC content and melting temperature. It was considered best if the primer only detected the desired target sequence. The primers designed for the appropriate genes were ordered from Sigma Aldrich, whereas others were bought from Applied Biosystems.

Table 3.3. List of primers used, product length (bp) and primer sequence or ID. F: Forward primer; R: Reverse primer; ID: Applied Biosystems Taqman ID.

Primers Used	Product Length (bp)	Sequence or ID
hsa-miR-196a	-	241070
RNU48	-	001006
hsa-miR-196a-1	-	Hs03302792-pri
hsa-miR-196a-2	-	Hs03302912-pri

U6	94	F: 5’ CTCGCTTCGGCAGCACA R: 5’ AACGCTTCACGAATTTGCGT
KRT5	228	F: 5’ TCTCGCCAGTCAAGTGTGTCCTTC R: 5’ GCTGATGGATATCCTCTTGGAGCC
ANXA1	323	F: 5’ ATGGCAATGGTATCAGAATTCCTCAAG R: 5’ ACAACCTCCTCAAGGTGACCTGTAAGG
S100A9	202	F: 5’ ATGACTTGCAAAATGTCGCAGCTGG R: 5’ TGTCCAGGTCCTCCATGATGTGTTC
PSEN1	160	F: 5’ ATGACAGAGTTACCTGCACCGTTG R: 5’ GTCCATTAGATAATGGCTCAGGGT
LOXL4	133	F: 5’ ATGGCGTGGTCCCCACCAGCCACC R: 5’ GGCCCTCCTCTGGCTTGCTCTCTG
HOXC8	181	F: 5’ ATGAGCTCCTACTTCGTCAACCCC R: 5’ GGAAGAAGTCTTGAACGTGGTGCG
MAMDC2	187	F: 5’ ATGCTGTTAAGGGGCGTCCTCCTG R: 5’ CCTGCTTGCCAAAGGAGGTATCCA

The primer sequences for all the 39 HOX genes and β-actin were kindly provided by Dr. Richard Morgan (University of Surrey) (Appendix 9.2).

3.7 Protein Expression

3.7.1 Western Blotting

RIPA buffer (70-100 µL) (Sigma Aldrich) containing protease and phosphatase inhibitors (Roche) was added to the cell pellet. The cell pellet was then kept on ice for 20 min and centrifuged at 13,000 rpm for 5 min at 4^0C. The supernatant was transferred to a fresh eppendorf and protein quantification was done using BCA (Bicinchoninic acid) method (Thermo Scientific) (Smith et al., 1985) as per manufacturer's protocol. To the supernatant was added equal volume of 2X loading dye (0.5 M Tris-HCl (pH 6.8), 1 M Dithiothreitol (DTT), 20% (w/v) Sodium dodecyl sulphate (SDS), Glycerol, 0.02% (w/v) bromophenol blue, PI inhibitor tablet (Roche), water) and then heated for 5 min at 95^0C. SDS-PAGE (SDS-Polyacrylamide gel electrophoresis) (12%) was loaded with 40 µg of total protein. Following components were used for preparation of the gel (Table 3.4):

Table 3.4. Components and volume for resolving and stacking gel for SDS-PAGE gel.

Components	Resolving Gel	Stacking Gel (4%)
40% Acrylamide (Fisher)	2.4 ml	0.75 ml
1.5M Tris pH 8.8	2	-
0.5M Tris pH 6.8	-	1.25
10% APS	80 µl	50 µl
10% SDS	80 µl	50 µl
TEMED	8 µl	5 µl

Distilled water	3.4 ml	2.9 ml

To prepare the gel, 1mm gel cassette was used and placed on the clamps. Initially, the resolving gel was prepared and loaded in the gel cassette and water was added to make it even and allowed to set. Later, stacking gel was prepared and loaded on top of resolving gel and 10-well comb was inserted before the gel solidified. Then, the gel was placed into Mini-PROTEAN tetra system (Bio-Rad). The comb was removed after adding Running buffer (12g Tris base, 4g SDS, 57.5 glycine to 1L water) to the gel chamber and samples were loaded into the gel. It was then electrophoresed until the EZ-protein marker (Fisher) approached the bottom of the gel at 100 V supplied from PowerPac Basic (Bio-Rad). XCell SureLock system (Bio-Rad) was used for the wet transfer method which requires wet transfer buffer (24 mM Tris base, 192 mM glycine, 20% (v/v) methanol in distilled water). The filter pad, filter paper and nitrocellulose membrane (GE healthcare) were soaked in wet transfer buffer. The protein from the gel was transferred onto nitrocellulose membrane by electrotransfer for 1h at 30 V. The membrane was incubated for 1h in blocking buffer (TBST (Tris buffered saline tween-20) (10 mM Tris-Cl (pH 8.0), 150 mM NaCl, 0.05% (v/v) tween-20 in distilled water) with 5% (w/v) dried milk and 3% (w/v) BSA (Bovine Serum Albumin)) at room temperature on a shaker. The membrane was then washed with 0.1% TBST thrice with 15 min incubation. The membrane was then incubated overnight at 4^0C with anti-HOXB9 rabbit monoclonal primary antibody (1:500 in blocking buffer) (Abcam) or anti-β-actin mouse monoclonal primary antibody (1:10,000 in blocking buffer) (Sigma Aldrich). Following morning, the membrane was washed with TBST thrice to remove any excess antibody. The membrane was then incubated for 1 h at room temperature with horseradish peroxidase conjugated anti-rabbit IgG or anti-mouse IgG secondary

antibody (1:3000 in blocking buffer) (Sigma Aldrich). The membrane was washed with TBST thrice to remove any excess antibody. It was then treated with SuperSignal® west pico chemiluminescent substrate for a min (Thermo Scientific). The membrane was then put into Kodak cassette with CL-Xposure™ Film (Thermo Scientific) in the dark room and left for 15 min. The film was then developed using Compact X4 (Xograph). The membrane was stripped using Restore stripping buffer (Thermo Scientific) by incubating the membrane in the buffer between 5-15 min at room temperature. The membrane was then washed with TBST and primary antibody for β-actin was applied.

3.7.2 Immunohistochemistry (IHC)

Tissue microarray (TMA) sections for HNSCC were kindly provided by Mrs. Ibtisam Zargoun and few normal oral tissue sections were kindly provided by Dr. Abigail Pinnock. In total, 25 cancer tissue sections on TMA and 10 normal oral tissue sections were used for the study. The normal and cancer tissue sections were cut to 4µm thickness, de-waxed with 2 X 5 min wash of xylene (Fisher) and then dehydrated with 2 X 5 min wash of 100% ethanol (Fisher). The sections were then incubated for 20 min in methanol (Fisher) containing 30% (v/v) hydrogen peroxide (Fisher) to block the activity of endogenous peroxide. The antigen retrieval was carried out using pressure cooker method (Neves et al., 2005) and the sections were incubated for 20 min in 10 mM sodium citrate buffer (w/v) (pH 6) (Fisher). Antigen retrieval is performed so that any crosslinks formed between wax and protein and protein-protein can be broken so protein is more exposed on tissue section. The sections were washed with PBS twice for 5 min. The sections were blocked with 100% Normal Goat Serum (NGS) for 30 min. NGS was used as the blocking solution because the secondary antibody was raised in goat. The blocking serum was removed and sections were then incubated overnight at 4^0C with anti-HOXB9 rabbit polyclonal primary antibody (1:400) (Sigma Aldrich). Subsequently, the sections were washed with PBS twice for 5 min each next morning.

Anti-rabbit IgG secondary antibody from Vectastain Elite ABC rabbit IgG kit (Vector Laboratories Inc.) was applied to the sections and incubated for 30 min at room temperature. Excess antibody was removed by washing slides with PBS twice for 5 min each. Then, 2 drops of bottle A and 2 drops of bottle B were added in 5 ml PBS and left at room temperature for 30 min and later applied onto the slides. It is left at room temperature so that there is complex formation of avidin with biotinylated horseradish peroxidase enzyme. The sections were washed with PBS twice for 5 min each. The sections were then treated with DAB reagent (Vector Laboratories Inc.) for colour development and its reaction was neutralised by submerging slides into water. The slides were counter-stained with harris haematoxylin (CellPath) before covering the slide with cover slip (CellPath). The slides were viewed under Olympus light microscope at 200X magnification and photomicrograph were taken using Cell^D imaging software (Olympus).

3.8 Transfection of cells

Cells (B16, D19 and OKF4) were seeded in KGM media at a confluency of 50-70% and incubated at 37^0C and 5% (v/v) CO_2 overnight in 6-well plate (Corning Inc). These cells were transfected by using Oligofectamine reagent (Invitrogen) with anti-miR-196a or pre-miR-196a (Applied Biosystems) or HOXB9 siRNA (Sigma Aldrich) and negative control (random sequence) (Applied Biosystems) (50nM) in 500 µl Opti-mem media (Gibco). This transfection mix was incubated at room temperature for 30 min so that liposomes and oligonucleotides could form complexes. The cells were washed twice with opti-mem media before transfection mix was pipetted onto the wells. The cells were then incubated for 3-4 hours at 37^0C and 5% (v/v) CO_2. Next, 500 µl DMEM supplemented with 20% (v/v) FCS and containing 2 mM glutamine was added to the cells and incubated for 48 hours. qPCR was performed to assess the change in expression and later cells were used to perform functional assays.

3.9 Proliferation Assay

The transfected cells were trypsinised and re-suspended in DMEM with 10% (v/v) FCS and the cell number determined as described in section 3.3. In a 96-well plate, 5000 cells/well were seeded in 100 µl DMEM with 10% (v/v) FCS. The time points used for analysis were 0, 24, 48, 72 and 96h. Each sample was plated in triplicate for each time point. Media was pipetted in triplicate to be used as background when analysing. 20µl MTS (3-(4,5-dimethylthiazol-2-yl)-5-(3-carboxymetHOXyphenyl)-2-(4-sulfophenyl)-2H-tetrazolium) (Promega) solution was added to each well for appropriate time point and then incubated for 1 h at 37^0C and 5% (v/v) CO_2. MTS is reduced in the mitochondria by dehydrogenase enzyme to form formazan product which is soluble in media. Dehydrogenase enzyme is present in metabolically active cells and is a measure of metabolism of cells. The formazan product has absorbance at 490nm. The absorbance was calculated at 490 nm using Tecan infinite M200 and Magellan software (Tecan).

3.10 Adhesion Assay

The 96-well plate was coated with 0.1% (v/w) fibronectin (Sigma Aldrich) in PBS (1:100) and incubated at 4^0C overnight. The wells were then washed with PBS to remove any unbound fibronectin. Then, 100 µl of DMEM supplemented with 1% (v/w) BSA was added to the wells and kept in incubator at 37^0C and 5% (v/v) CO_2 for 1h. The transfected cells were counted and 30,000 cells/well were seeded in serum free medium (DMEM). These cells were then incubated for 1h at 37^0C and 5% (v/v) CO_2. The plate was washed with PBS to remove any cells which did not adhere and 100 µl of serum free DMEM was added to the wells before 20 µl of MTS. The plate was incubated for 1 h at 37^0C and 5% (v/v) CO_2. Then the plate was read at 490 nm with Tecan Infinite M200 using Magellan software.

3.11 Migration Assay

The transfected cells were trypsinised and re-suspended in DMEM supplemented with 0.1% (v/w) BSA medium after being washed with PBS and counted. The cells were seeded in transwell inserts (BD Biosciences) with membrane pore size of 8 µm and each sample was seeded in duplicate. DMEM supplemented with 2% (v/v) FCS or DMEM supplemented with 0.002% (v/v) fibronectin (0.1%) was added to the bottom of the wells. The cells were then incubated at 37^0C and 5% (v/v) CO_2 overnight. The following day, the medium was removed and the insert and well were washed with PBS. The membrane was cleaned with cotton swab to remove any remaining non-migrated cells to ensure that these cells were not counted. The cells in the insert were then fixed by adding 100% methanol (Fisher). The insert and well were again washed with PBS. The migrated cells were then stained with PBS with 0.1% (v/w) crystal violet. Then the count of the cells which migrated was taken in four different fields for each insert under Olympus light microscope at a magnification of 400X and the cell number for each field was averaged for an insert (Figure 3.2).

A.

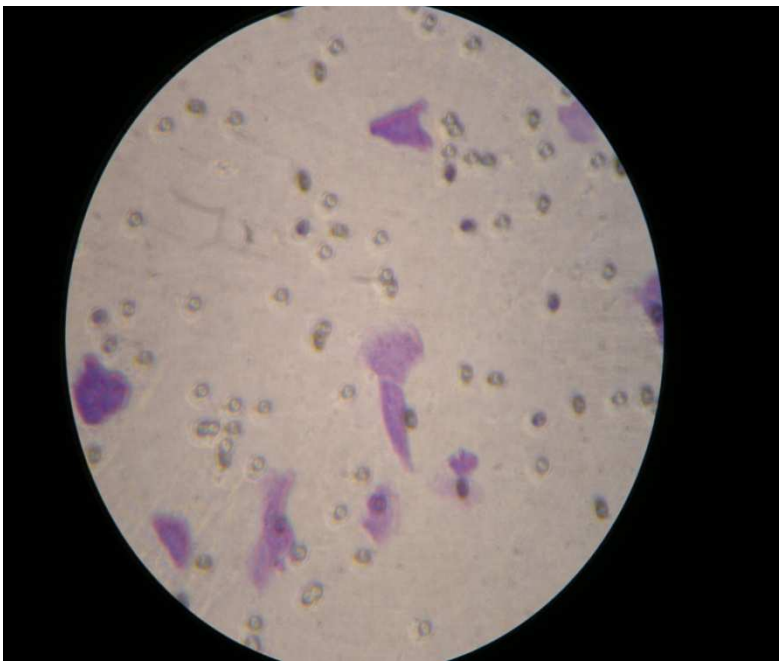

B.

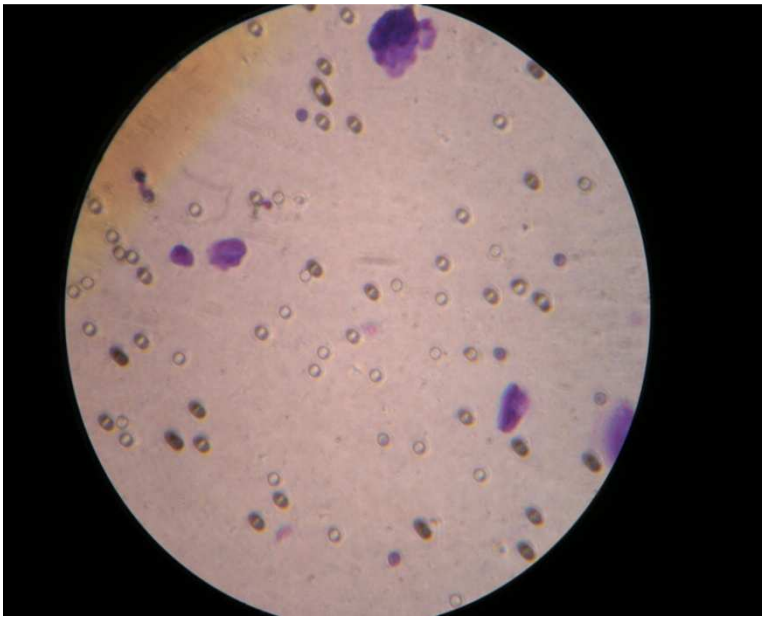

Figure 3.2. Photograph of a field in the insert showing cells that have migrated. A. D19 cells transfected with negative control. B. D19 cells transfected with anti-miR-196a.

3.12 Invasion Assay

Transwell inserts (BD Biosciences) were coated with 100µl growth factor reduced matrigel (BD Biosciences) in DMEM (1:45) and incubated overnight at 37^0C and 5% (v/v) CO_2. The transfected cells were trypsinised, washed with PBS and re-suspended in DMEM supplemented with 0.1% (v/w) BSA and counted. The bottom of the well was filled with DMEM supplemented with 2% (v/v) FCS and then cells were seeded in DMEM supplemented with 0.1% (v/w) BSA in the insert already coated with growth factor reduced matrigel. The plate was then incubated for 48 h. After 48 h, the insert and the well were washed with PBS. The membrane was cleaned with cotton swab to remove any remaining non-invading cells to ensure that these cells were not counted. The cells were fixed with 100% methanol (Fisher). The insert and the well were washed with PBS. Then the cells were stained in PBS with 0.1% (v/w) crystal violet. Invading cells were counted in four different fields for each insert under Olympus light microscope at a magnification of 400X and the cell number for each field was averaged for an insert.

3.13 Primary transcript HOXB9-miR-196a-1

The primer sequence for miR-196a-1 and HOXB9 primary transcript was as follows: PT forward: 5’ AAT TAG GTA GTT TCA TGT TGT TGG GCC 3’ and PT reverse: 5’ ATA ATA GCT GCT AAG CGT CCC AGA AAT 3’. B16 RNA was extracted with DNase step in the protocol. Initially, cDNA synthesis for primary transcript was carried out with B16 RNA using M-MLV RT (reverse transcriptase) (Promega) with RP or PT primers (Primary transcript primers) as per manufacturer’s protocol. The first PCR with cDNA was performed using Phusion (Thermo Scientific), Taq (Thermo Scientific) or Q5 (NEB) DNA polymerase with PT primers. The components and PCR cycles were set-up according to manufacturer’s protocol. Nested primers were designed within this

transcript to give a product of 295 bp, nested forward: 5’ AAA GTC AGG GCA GGA GAG GGA AGG GGA A 3’ and nested reverse: 5’ CAA TTT GCC AGC CCT ATG AAG TCT GCT 3’. Nested primers are primers which bind internally to an amplified transcript from first PCR reaction and generates PCR product of shorter length. As they bind internally in an amplified transcript it reduces chances of contamination, as there is little chance that a transcript other than the one to be amplified will consist of same two binding sites for first primers and nested primers. The nested PCR was run with Q5 DNA polymerase PCR product from the first round of PCR. Taq DNA polymerase was used for nested PCR with nested primers. The components were added and PCR cycle was set-up as per manufacturer’s protocol. For this reaction, two controls were used: RNase A and no-RT. For RNase A control, the RNA was treated with RNase A (100µg/ml) (Promega) for 1 h at 37^0C before start of rt-PCR step. For no-RT control, the rt-PCR step was carried out without addition of RT.

The 2% agarose gel was prepared by adding 1 g agarose to 50 ml of 1X TAE buffer (40 mM Tris, 20 mM acetic acid, 1 mM EDTA in 1 L distilled water) and after solubilising agarose in buffer by heating 1 µl of ethidium bromide was added. The PCR product and 100 bp ladder (NEB) was run on 2% (v/w) agarose gel at 80 V for 1 h and viewed under UV transilluminator. The PCR product was isolated from the gel by using Isolate PCR/Gel kit (Bioline). The PCR product was then cloned into pCR®2.1-TOPO® cloning vector (Invitrogen) by adding 2 µl of PCR product with 1 µl of vector, 1 µl of salt solution provided and made to 6 µl by addition of distilled water and incubated for 5 min at room temperature. The cloned vector was transformed into E.coli DH5α (NEB) by heat shock method following manufacturer’s protocol and then streaked on ampicillin (100 µg/ml) (Fisher) containing LB agar plate coated with 40 µl X-gal (5-bromo-4-chloro-3-indolyl-β-D-galactopyranoside) (Sigma Aldrich) in DMSO (20 mg/ml) solution. The positive colonies were selected based on blue/white screening the

following morning as the PCR product was cloned into lacZα gene in the pCR®2.1-TOPO® vector. When PCR product is cloned into lacZα then it cannot cleave X-gal giving white colonies. The positive colonies were added to LB broth (Fisher) to grow overnight at 37^0C. The plasmid from the broth was purified using Isolate plasmid mini-kit (Bioline) as per manufacturer's protocol. This vector was then sent for DNA sequencing.

3.14 Microarray

3.14.1 Microarray sample preparation

Microarray was performed using two 8-genome Oligonucleotide Microarray (Sureprint G3) chips (Agilent). Biological triplicates of B16 and D19 cells were transfected with negative control and anti-miR-196a. Biological duplicates of OKF4 cells were transfected with negative control and pre-miR-196a. In total, 16 independent RNA extractions were performed for transfected and negative control cells. The RNA was quantified with nanodrop spectrophotometer. The transfection efficiency was checked by performing qPCR for miR-196a expression for all transfected samples. The quality was assessed with Agilent Bioanalyzer 2100 using Agilent nanochip (Agilent). The RNA was considered of good quality if 28s:18s>= 2 and if RNA integrity number (RIN) was 10. Next the manufacturer's protocol was followed step-by-step for microarray sample preparation and hybridisation and scanning using Agilent microarray system (Figure 3.3). Briefly, 100ng of total RNA was used for reverse transcription with RNA spike In-one colour mix, T7 promoter primer mix and utilised AffinityScript cDNA synthesis mix and was incubated in water bath at 40^0C for 2hr. To each sample T7 RNA polymerase mix was added for formation of cRNA by incubating at 40^0C for 2hr in water bath. The cRNA was purified using Qiagen RNeasy kit. The cRNA was considered of good quality if yield (μg) was >= 0.825 and specific activity (pmol

Cy3/µg cRNA) was >= 6. The cRNA was then fragmented by using fragmentation mix. The hybridisation cocktail consisted of fragmented cRNA and GEx hybridisation buffer HI-RPM which was loaded onto Agilent SureHyb chamber base. Then, the active side of the array was lowered onto SureHyb chamber. The hybridisation was carried out in hybridisation chamber for 17 hrs at 65^0C. The following day the slides were washed and loaded into Agilent microarray scanner and raw data was later extracted.

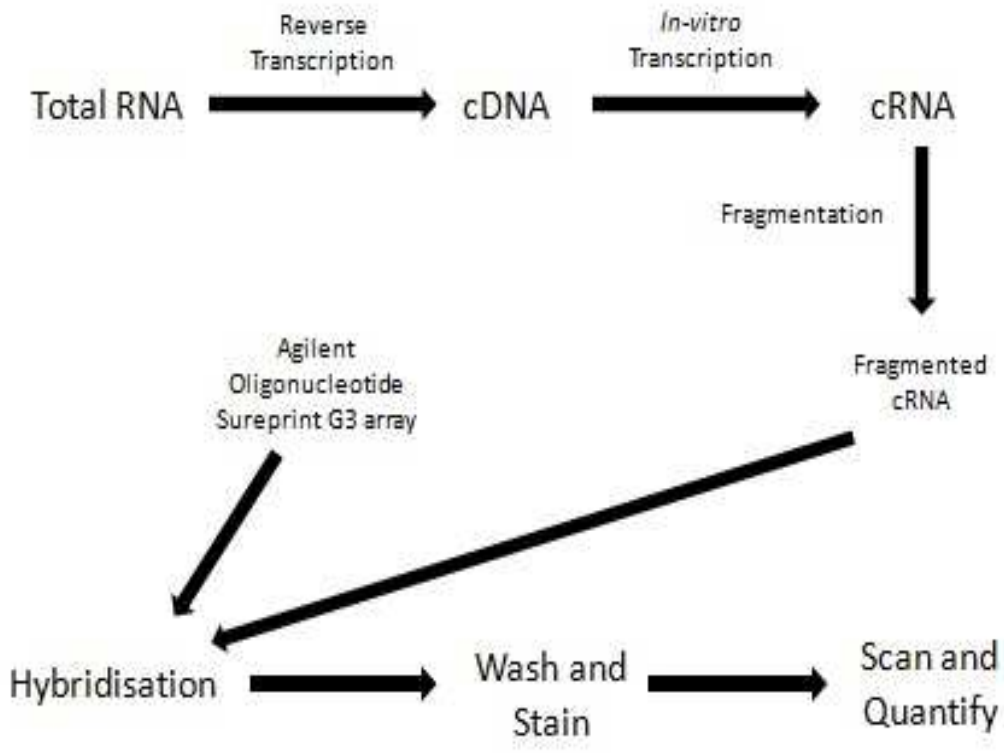

Figure 3.3. Flow chart depicting steps for microarray sample preparation and sample hybridisation.

3.14.2 Microarray Data analysis

3.14.2.1 Genespring

The microarray raw data in the format of .txt was loaded into microarray data analysis software Genespring 12 (Agilent). Each cell line data for negative control and anti-miR-196a or pre-miR-196a transfected cells was loaded as separate experiment into the experiment. The data was then normalised using 75th percentile shift normalization method and viewed in box plot. 75th percentile shift normalization is used as even the genes which are not expressed report intensity value, hence to get rid of these values higher percentile intensity values are taken and median for these are calculated. The data was then viewed in the three axes in principal component analysis (PCA) and the data which looked very different to other similar samples was eliminated from the analysis (one each of B16 anti-miR-196a, D19 anti-miR-196a and D19 negative control transfected were eliminated). These samples were then subjected to t-test statistical analysis with $p<0.05$ in which anti-miR-196a or pre-miR-196a samples were compared to negative control transfected samples. Each experiment was compared to each other for common genes being differentially expressed and common genes were selected for further analysis. Genes were also selected based on pathway analysis programme present in Genespring software. The selected genes were further subjected to qPCR for microarray samples to check for their expression.

3.14.2.2 Qlucore Omics Explorer

Dr. Paul Heath and Dr. Jonathan Cooper-Knock helped with analysis of microarray data with Qlucore Omics Explorer software (Qlucore). The raw data for all the samples was first loaded into the software and the data was subjected to normalization using 75th percentile shift method (The raw data files and normalised data file for all the samples were loaded onto public database http://www.ncbi.nlm.nih.gov/geo/ with accession no.

GSE52810). The samples were divided into two groups: low miR-196a expressing samples and high miR-196a expressing samples. Low miR-196a expressing group contained B16 and D19 anti-miR-196a and OKF4 negative control samples, whereas high miR-196a expressing group contained B16 and D19 negative control and OKF4 pre-miR-196a transfected samples. The samples were viewed in PCA in three axes to see the distribution of the samples. Parameters used for data analysis was as follows: t-test $p<0.01$ and cell-type eliminated. This gave in total 353 genes which were differentially expressed (Appendix 9.3) and then the top 100 genes which had highest variance were selected for further analysis. The genes which were predicted as direct targets of miR-196a in target prediction sites miRWalk (http://www.umm.uni-heidelberg.de/apps/zmf/mirwalk/) and microRNA (www.microrna.org) were subjected to qPCR analysis using microarray samples.

3.15 *In-silico* target prediction

The target prediction for miR-196a was initially carried out by checking for published miR-196a targets and then cross-referencing them with target prediction database 'TargetScan' (http://www.targetscan.org/) to check for their score which depends on the complementarity of the target gene 3'UTR and miRNA seed sequence. miRWalk is a database which gives option of looking at targets of particular miRNA in several different databases in one place. TargetScan, miRWalk and microRNA database uses miRNA:mRNA complementarity of the sequence, energy of binding, evolutionary conservation of the miRNA site and its position in homologous genes to predict its gene targets.

3.16 3'UTR Vector Cloning

The B16 cDNA was used to amplify the 3'UTR of MAMDC2. The MAMDC2 3'UTR amplified was called wild type (wt). The following primers were used for amplification:

wt forward 5’ AAA AAA AA**A CGC GT**A AAT GAT CTG CAT TGG ATT TAC T 3’ and wt reverse 5’ AAA AAA AA**G TTT AAA C**AA GAT TTT CAA ATT ATT TTT ATT AGG TAA TTT TAT AAT TTC 3’. wt forward primer consisted of MluI restriction digestion site (Sticky end), whereas wt reverse primer consisted of PmeI restriction digestion site (Blunt end); these are shown here in bold and underlined. The amplified product (1 µg) was then cloned into pMIR REPORT (1 µg) (Ambion) vector using serial digestion method with MluI (NEB) and PmeI (NEB) restriction digestion enzymes using 10 units of each and appropriate buffer based on manufacturer’s protocol. The only difference from the standard protocol was that the 3’UTR and vector were incubated overnight instead of 1h. The digested 3’UTR and vector were ligated using T4 DNA ligase (NEB) by incubating them overnight at 16^0C. The product was then transformed into E.coli DH5α chemically competent cells (NEB) using heat shock protocol as per manufacturer’s instructions. The transformed cells were plated on LB agar plate supplemented with ampicillin (v/w) (100 µg/ml) and incubated overnight at 37^0C. The positive colonies were selected and vector was extracted using Isolate Plasmid mini-kit (Bioline). The isolated vector was sent for DNA sequencing to confirm presence of MAMDC2 3’UTR, its exact sequence and its directionality. On confirmation, the remainder of transformed E.coli cells for vector sent for DNA sequencing were inoculated in 200 ml LB agar supplemented with ampicillin (v/w) (100 µg/ml) and incubated overnight at 37^0C. Following morning, the vector was extracted using Isolate plasmid maxi-kit (Bioline) to give cleaner vector.

3.16.1 Site-Directed Mutagenesis (SDM)

Site-directed mutagenesis is used for changing the nucleotide at specific place in a DNA sequence by using PCR. This can be achieved by designing primers which are complementary for a length of sequence with mutated nucleotides in the middle of the primer. SDM can be used to alter the DNA sequence to change the amino acid

expressed at that position and can also be used to confirm whether a miRNA is complementary to 3'UTR of a gene or not. PCR- based SDM was used to mutate the miR-196a binding site in MAMDC2 3'UTR. The MAMDC2 3'UTR wt vector was used as the template for the PCR. The following primers were used for SDM of miR-196a binding site, the mutated bases are shown in bold and underlined, mutated forward: 5' CCT TCT TTA TTC CCC CTT TGA **GAC GCT** TTT GAA GTC ACT ATG AGC 3' and mutated reverse: 5' GCT CAT AGT GAC TTC AAA **AGC GTC** TCA AAG GGG GAA TAA AGA AGG 3' (Figure 3.4).

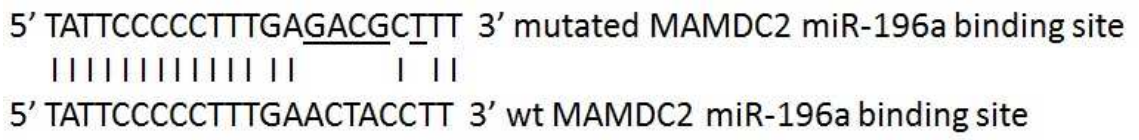

Figure 3.4. Point mutations made in miR-196a binding site in 3’UTR of MAMDC2.

The Tm (melting temperature) for the primers was >=78^{0}C. Phusion DNA polymerase (Thermo Scientific) was used for amplifying wt vector and reaction was set-up based on manufacturer's protocol. The following PCR cycle was used: 95^{0}C for 30 s, 18 cycles of 95^{0}C for 30 s, 55^{0}C for 1 min and 72^{0}C for 8 min (1 min/Kb), 72^{0}C for 10 min (final extension). The PCR product was then incubated for 1 h with DpnI (NEB) at 37^{0}C, to degrade methylated template DNA. The transformation, selection, isolation and DNA sequencing for mutated vector was carried out as described in section 3.16.

3.17 Dual Luciferase Reporter Assay (DLRA)

In Dual luciferase reporter assay, vector is used which consists of luciferase gene in which 3'UTR of target gene is cloned downstream of ORF of luciferase gene using multiple cloning sites. This vector and miRNA of interest are co-transfected, if miRNA binds and degrades the transcript from vector for luciferase gene, less luciferase protein will be produced leading to lesser luminescence compared to negative control transfected cells. DLRA was used to determine if miR-196a directly bound to MAMDC2 3'UTR or not. B16 cells were seeded in 6-well plate at a confluency of 50-70% and incubated overnight at 37^{0}C. They were transfected with pMIR REPORT (wt or mutated) (500ng), pRL-TK (renilla luciferase control vector) (50ng) (Promega) and negative control (random sequence) or pre-miR-196a (50nM) in Opti-mem media with the help of Fugene HD transfection reagent (Promega) as per manufacturer's protocol. The cells were incubated for 3-4 h before addition of DMEM containing 20% (v/v) FCS and then the cells were incubated for 48 h. On completion of 48 h, DLRA system (Promega) was used for the measurement of firefly (*Photinus pyralis*) and renilla (*Renilla reniformis*) luciferase activity as per manufacturer's protocol. The firefly luminescence was measured by addition of Luciferase Assay Reagent II (LAR II) (Promega) and then renilla luciferase was measured by addition of stop & glo reagent (Promega). For this reaction Nunc F96 Microwell white plate (Nalgene) was used to

minimise the loss of luminescence. The measurement of luminescence and analysis was done using GloMax 96 Microplate Luminometer (Promega). The relative luminescence was calculated by calculating ratio of firefly/renilla luminescence for each well.

3.18 Statistics

Non-parametric Mann-Whitney U test was performed on the absolute value from qPCR on LCM tissue sample for miR-196a and tissue sample scoring from IHC for HOXB9. For all other experiments student's t-test was used as the method of statistical analysis. Student's T-test was used as it is a parametric test and can be used for normally distributed samples. Normal distribution was determined using Graphpad prism software. Bonferroni correction was not utilised while using this test. Data was considered significant only if $p<0.05$.

3.19 Ethical Approval

Ethical approval was obtained from The West Glasgow LREC (ref: 08/S0709/70) for the use of biopsy samples in the study. Ethical approval was obtained from Sheffield Research Ethics Committee 09/H1308/66 for NOK primary culture.

Chapter 4: Effects of miR-196a in HNSCC

MicroRNAs are short non-coding RNA transcripts which lead to post-transcriptional changes in the expression of the genes by binding to a complementary sequence in their 3' UTR. The sequence does not have to be a perfect match with the 3' UTR of the gene and hence miRNA can have multiple targets. Binding of miRNAs leads to silencing of the gene by translational repression or mRNA degradation (Braig et al., 2010, Schimanski et al., 2009). miR-196 is present within the HOX gene clusters in vertebrates and well conserved evolutionarily. There are, in total, three miR-196 sequences distributed in HOXA, HOXB and HOXC clusters. miR-196a-1 and miR-196a-2 have been observed to be present upstream of HOXB9 and HOXC9 (Tanzer et al., 2005), whereas, miR-196b is seen to be present upstream of HOXA9 (Popovic et al., 2009) (Figure 2.3). There is only a single nucleotide difference between miR-196a and miR-196b and there is no difference in the mature sequence of miR-196a-1 and miR-196a-2 (Tanzer et al., 2005).

The aim of this chapter was to look at the expression of miR-196a in HNSCC cell lines and tissue samples compared to normal cell lines and tissue samples and effects of miR-196a in HNSCC. For this, qPCR technique was utilised with taqman primers for miR-196a detection in cell lines and LCM tissue based RNA extracted. iNOK cells were transfected with pre-miR-196a and OPM and HNSCC cells were transfected with anti-miR-196a to increase or decrease the expression of miR-196a in respective cells and to utilise these transfected cells for functional assays. Functional assays such as MTS proliferation, adhesion to fibronectin, migration and invasion were performed to look at the functional effects of miR-196a in iNOK, OPM and HNSCC cells. MTS reagent was used for both proliferation and adhesion absorbance calculation whereas transwell membrane was used for migration and invasion with matrigel.

4.1 Expression of miR-196a in HNSCC

Prior to commencement of the project, a miRNA affymetrix microarray was performed which indicated that the expression of miR-196a was higher in HNSCC cell lines when compared to normal cells (Lambert, Murdoch and Hunter, Unpublished data). This was intriguing as it had been reported earlier that miR-196a levels are increased in a number of other cancers (Tsai et al., 2012, Maru et al., 2009b) and also subsequently in oral cancer (Liu et al., 2012a). Hence, to assess the levels of miR-196a more closely qPCR was performed in the NOKs, iNOKs, OPM and HNSCC cell lines. qPCR was also performed to check expression of pri-miR-196a-1 and pri-miR-196a-2 in these cell lines as these are two loci which produce miR-196a mature sequence. It was observed that miR-196a expression was significantly higher in OPM and HNSCC cell lines compared to NOKs (Figure 4.1). Both pri-miR-196a-1 and pri-miR-196a-2 showed significant increase in expression in OPM and HNSCC cell lines compared to NOKs (Figure 4.2). LCM was performed on the cancer and normal FFPE tissue samples to determine the expression level of miR-196a in normal and cancer tissues. It was observed that quality of RNA from LCM was acceptable for length of miRNAs (Figure 4.3) and miR-196a was significantly over-expressed in cancer tissue compared to normal tissue (Figure 4.4). As miR-196a expression was seen to be significantly higher in OPM and HNSCC cells next functional effects of miR-196a in HNSCC were checked.

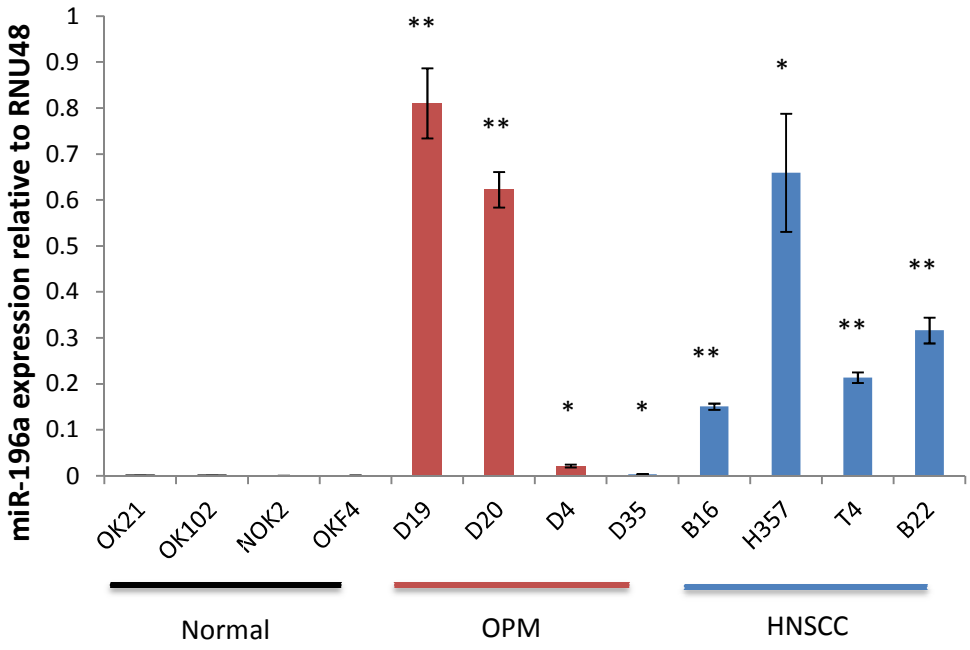

Figure 4.1. miR-196a was highly expressed in HNSCC and OPM cells compared to normal. miR-196a expression was assessed in Normal oral keratinocytes (NOKs), iNOK, OPM and HNSCC cells. miR-196a expression was higher in some OPM cells (D19) compared to cancer cells (B16). The data was normalised to internal control RNU48. The experiment was performed in triplicate. Error bars are representative of SEM. Student's t-test was applied to calculate p-value relative to OK21. *, p<0.05; **, p<0.01.

4.1.1 Expression of pri-miR-196a-1 and pri-miR-196a-2 in HNSCC

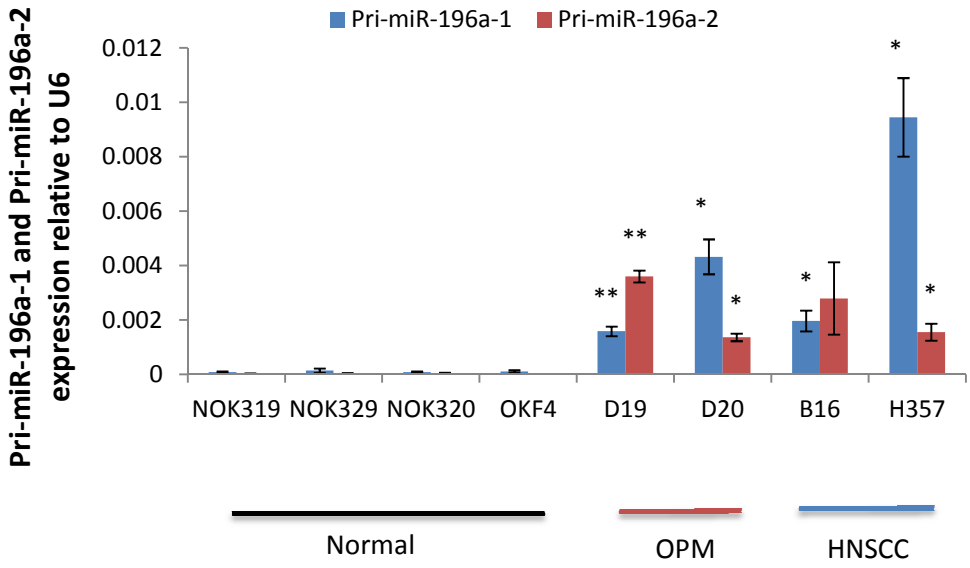

Figure 4.2. Pri-miR-196a-1 and pri-miR-196a-2 were significantly over-expressed in OPM and HNSCC cells compared to normal. Pri-miR-196a-1 and pri-miR-196a-2 expression was assessed in NOKs, iNOK, OPM and HNSCC cells. There was no set pattern of one locus being over-expressed compared to the other. The data was normalised to internal control U6. The experiment was performed in triplicate. Error bars are representative of SEM. Student's t-test was applied to calculate p-value relative to NOK319. *, $p<0.05$; **, $p<0.01$.

4.1.2 Expression of miR-196a in HNSCC tissue based on LCM (Laser Capture Microdissection)

Agilent RNA pico-chip was used to analyse the quality of RNA that was extracted by LCM from tissue samples on Agilent Bioanalyser 2100. Even though the RIN and 28s/18s ratio is not detected, there is good detection of RNA of ~25 nucleotides which approximately is the length of miRNA (Figure 4.3). The overall poor quality of the RNA can be attributed to the fact that these are FFPE tissue samples and RNA undergoes cross-linking and degradation. As miRNA are ~21-25 nucleotides in length, it meant that the RNA extracted was of good quality for the length of miR-196a.

A.

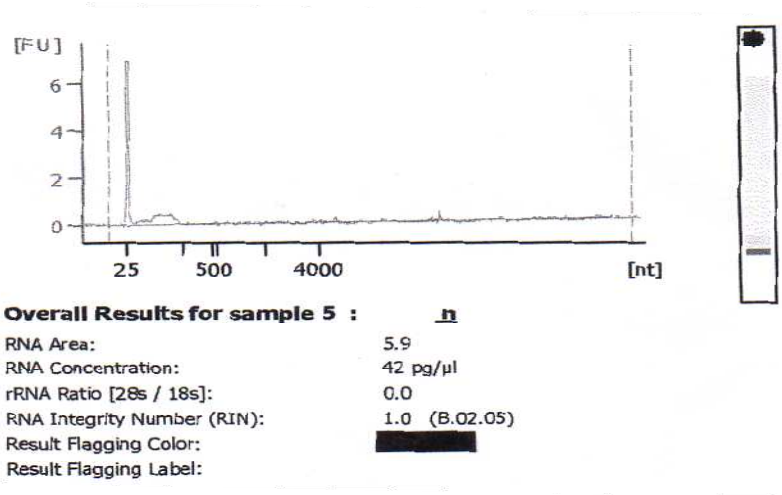

Overall Results for sample 5 : n

RNA Area:	5.9
RNA Concentration:	42 pg/µl
rRNA Ratio [28s / 18s]:	0.0
RNA Integrity Number (RIN):	1.0 (B.02.05)
Result Flagging Color:	
Result Flagging Label:	

B.

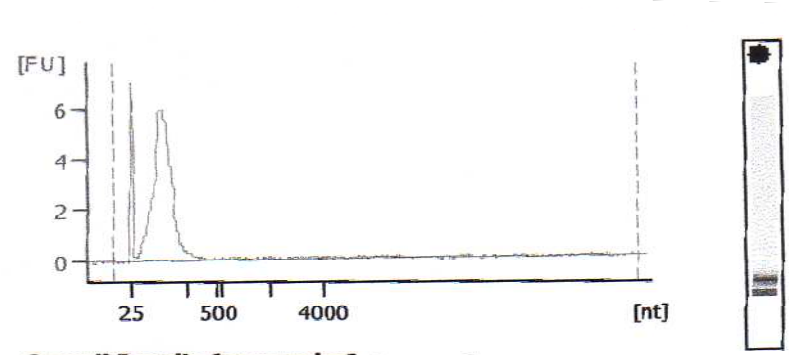

Overall Results for sample 6 : c

RNA Area:	52.6
RNA Concentration:	372 pg/µl
rRNA Ratio [28s / 18s]:	0.0
RNA Integrity Number (RIN):	2.6 (B.02.05)
Result Flagging Color:	
Result Flagging Label:	

Figure 4.3. Agilent Bioanalyser graph showing integrity of the RNA extracted from LCM of A. normal and B. cancer tissue.

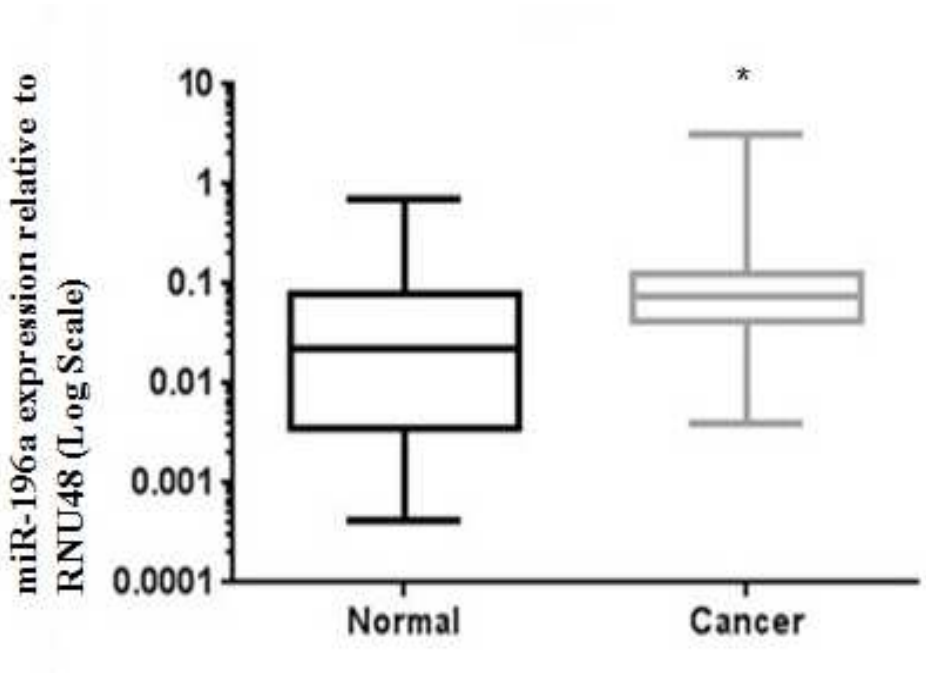

Figure 4.4. miR-196a expression was significantly increased in cancer tissue compared to normal tissue. miR-196a expression was assessed in FFPE normal tissue and cancer tissue. RNU48 was used as the internal control. The experiment was repeated in 16 unmatched normal and cancer tissues. The data was normalised to internal control RNU48. The experiment was performed in triplicate. Non-parametric Mann-Whitney U Test was applied to calculate p-value. *, $p<0.05$.

4.2 Functional effects of miR-196a in HNSCC

To assess the effect of the observed high expression of miR-196a on four basic characteristics of cancer cells, functional assays were performed. Based on the paper from Tsai et al., 2012, in gastric cancer it was seen that higher expression of miR-196a led to increased cell migration and invasion (Tsai et al., 2012). The oral cancer cells were assessed to see if they showed any of the similar effects and in addition to evaluate the effects on adhesion and proliferation. Performing both knockdown and over-expression of miR-196a experiment would increase the confidence in the specificity of the effects seen.

The B16 (HNSCC) and D19 (OPM) cells were transfected with anti-miR-196a or negative control. Down-regulation in the expression of miR-196a was confirmed by qPCR (Figure 4.5). These transfected cells were then used to perform different functional assays. There was no significant difference in proliferation (Figure 4.6) or migration towards fibronectin (Figure 4.9) between anti-miR-196a and negative control transfected cells. Only B16 anti-miR-196a transfected cells showed significant down-regulation in adhesion to fibronectin compared to negative control cells (Figure 4.7). Both B16 and D19 anti-miR-196a transfected cells showed significant decrease in migration (Figure 4.8) and invasion (Figure 4.10) compared to negative control cells.

The OKF4 (iNOK) cells were transfected with pre-miR-196a or negative control. Over-expression was observed in the expression of miR-196a by qPCR (Figure 4.11). There was no significant difference seen between pre-miR-196a and negative control transfected cells for proliferation (Figure 4.12), adhesion to fibronectin (Figure 4.13) and invasion (Figure 4.15). Though there was a significant increase in migration (Figure 4.14) of pre-miR-196a transfected cells compared to negative control cells.

4.2.1 Anti-miR-196a transfection

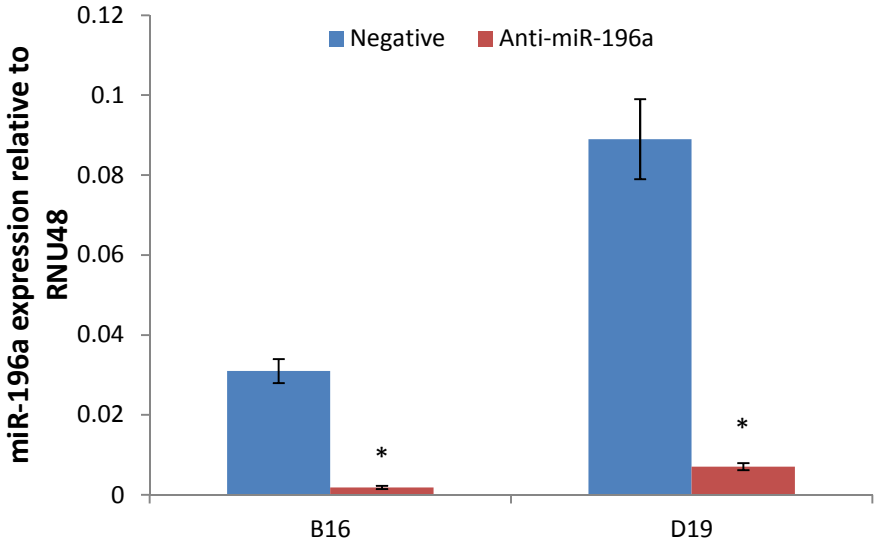

Figure 4.5. miR-196a expression significantly decreased in anti-miR-196a transfected cells compared to negative control cells. miR-196a expression was assessed in B16 (HNSCC) and D19 (OPM) anti-miR-196a transfected cells compared to negative control transfected. The transfected cells were incubated for 48 hr. There was 95% and 92% down-regulation observed in miR-196a expression in B16 and D19 anti-miR-196a transfected cells compared to negative control transfected cells, respectively. The data was normalised to internal control RNU48. The experiment was performed in triplicate. Error bars are representative of SEM. Student's t-test was applied to calculate p-value. *, $p<0.05$.

4.2.2 Proliferation assay

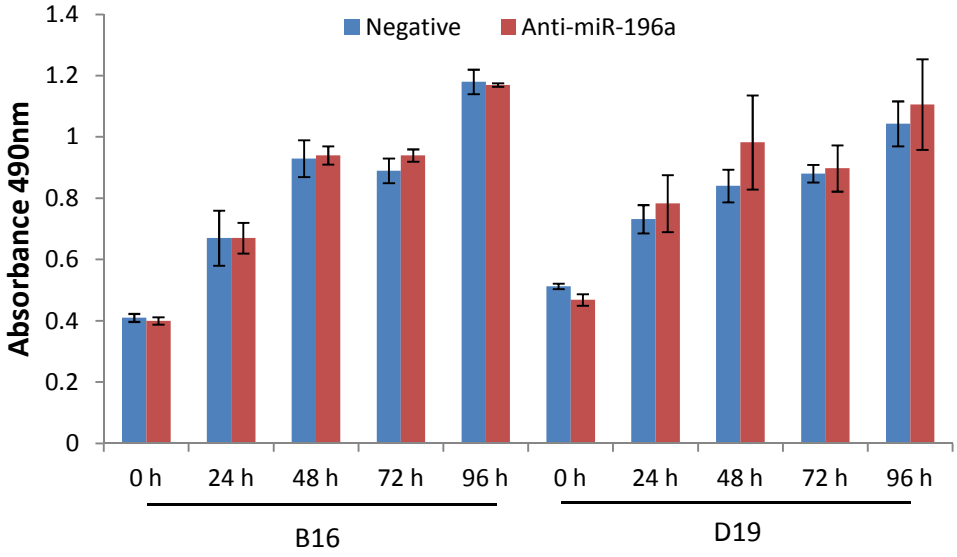

Figure 4.6. MTS proliferation assay showed no significant difference in absorbance for B16 and D19 anti-miR-196a and negative control transfected cells. Absorbance was checked at 490nm. The time points used for MTS proliferation assay were 0h, 24h, 48h, 72h and 96h. The experiment was performed in triplicate and repeated thrice. Error bars are representative of SEM. Student's t-test was applied to calculate p-value.

4.2.3 Fibronectin Adhesion assay

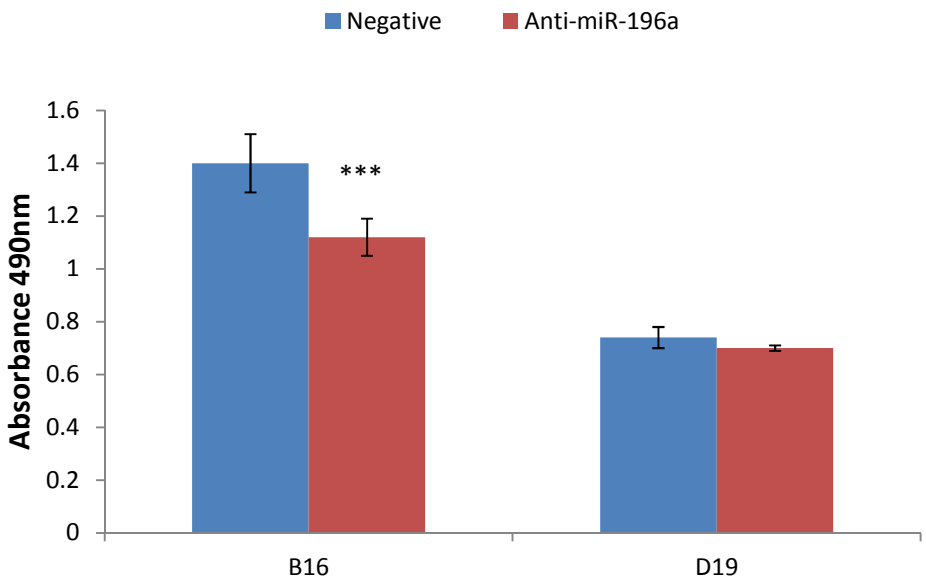

Figure 4.7. MTS adhesion assay showed significant decrease in B16 and no effect in D19 anti-miR-196a transfected cells compared to negative control cells. Absorbance was checked at 490nm after 1h incubation with MTS reagent. The experiment was performed in triplicate and repeated thrice. Error bars are representative of SEM. Student's t-test was applied to calculate p-value. ***, $p<0.001$.

4.2.4 Migration towards FCS (Fetal Calf Serum)

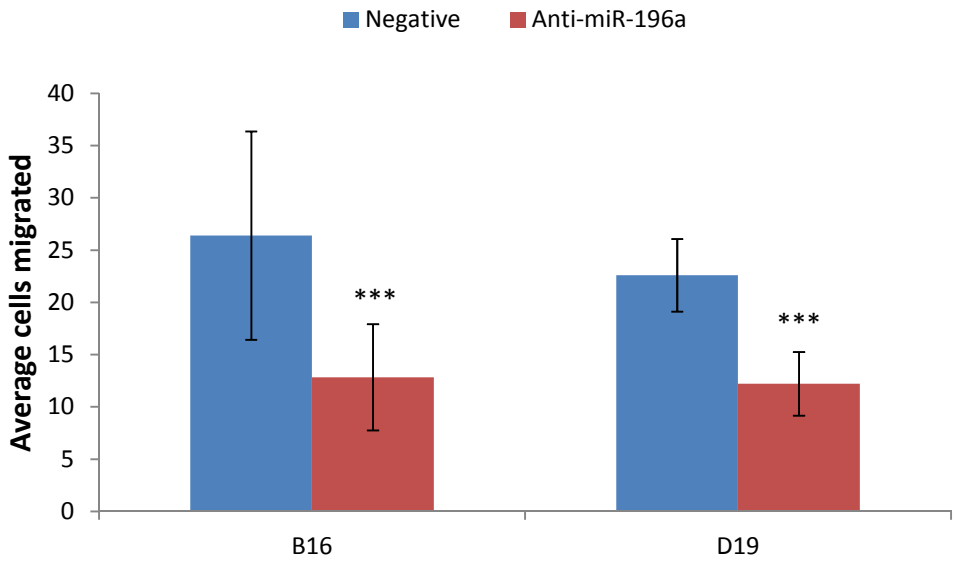

Figure 4.8. Transwell migration assay showed significant decrease in B16 and D19 anti-miR-196a transfected cells which migrated towards FCS compared to negative control cells. The cells were allowed to migrate for 24 hr. The experiment was performed in duplicate and repeated thrice. Error bars are representative of SEM. Student's t-test was applied to calculate p-value. ***, p<0.001.

4.2.5 Migration towards fibronectin

Migration towards fibronectin was performed to check the effect of fibronectin in migration as we had seen reduced adhesion to fibronectin in B16 anti-miR-196a cells compared to negative control cells.

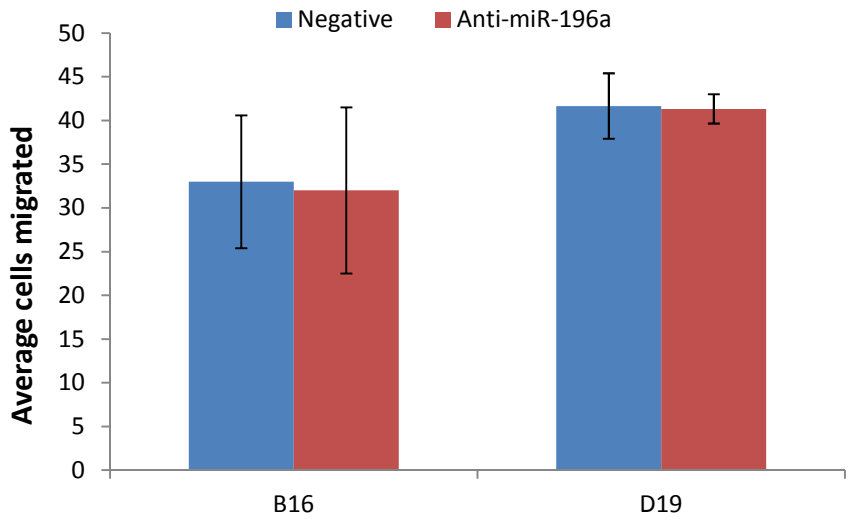

Figure 4.9. Transwell migration assay showed no effect in B16 and D19 anti-miR-196a cells which migrated towards fibronectin compared to negative control cells. The cells were allowed to migrate for 24 hr. The experiment was performed in duplicate and repeated thrice. Error bars are representative of SEM. Student's t-test was applied to calculate p-value.

4.2.6 Invasion assay

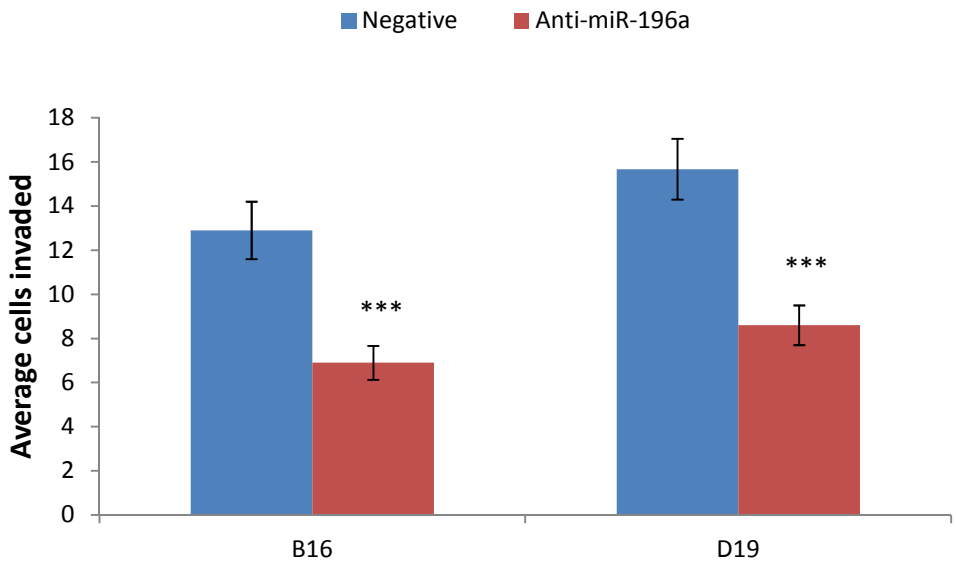

Figure 4.10. Transwell invasion assay showed significant decrease in B16 and D19 anti-miR-196a cells which invaded growth factor reduced matrigel compared to negative control cells. Growth factor reduced matrigel was used so that cells invasive potential is not over-shadowed by their affinity for other growth factors. The cells were allowed to invade through matrigel for 48 hr. The experiment was performed in duplicate and repeated thrice. Error bars are representative of SEM. Student's t-test was applied to calculate p-value. ***, p<0.001.

4.2.7 Pre-miR-196a transfection

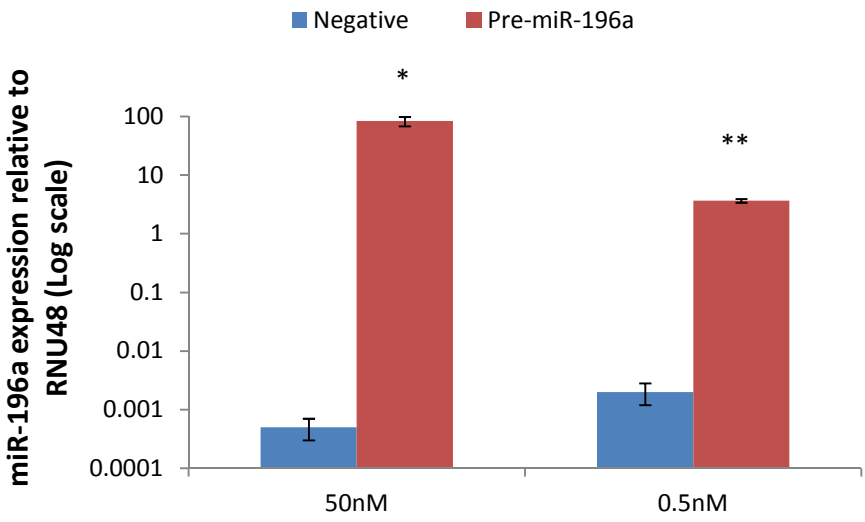

Figure 4.11. miR-196a expression was significantly increased in OKF4 pre-miR-196a cells compared to negative control cells. The transfected cells were incubated for 48 hr. The data was normalised to internal control RNU48. OKF4 showed 158,189 folds over-expression for miR-196a with 50nM pre-miR-196a transfection compared to negative control and hence to get expression to the same level as HNSCC and OPM cell lines, the pre-miR-196a was serially diluted to 0.5nM, where it showed 1800 folds over-expression. The experiment was performed in triplicate. Error bars are representative of SEM. Student's t-test was applied to calculate the p-value. *, $p<0.05$; **, $p<0.01$.

4.2.8 Proliferation assay

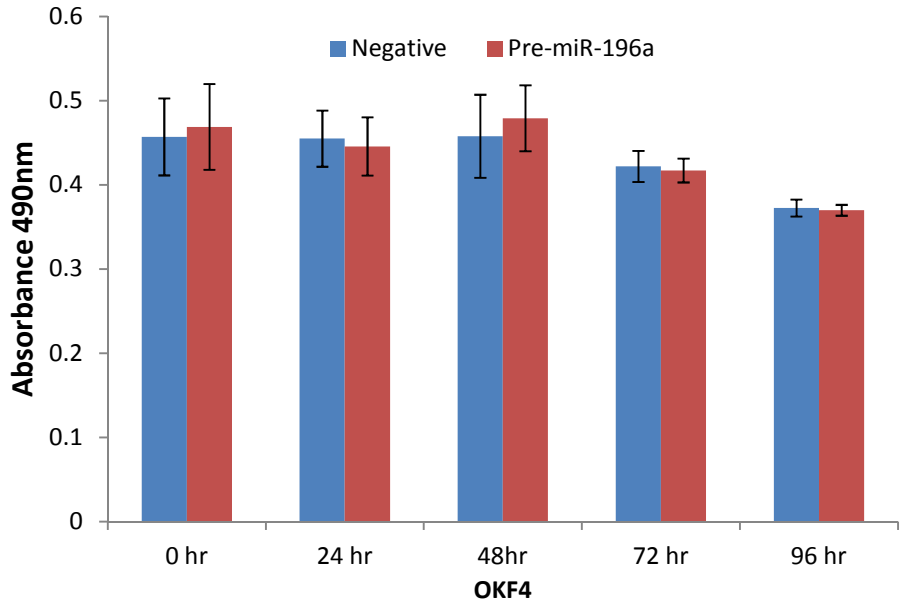

Figure 4.12. MTS proliferation assay showed no significant difference in absorbance between OKF4 pre-miR-196a and negative control cells. Absorbance was checked at 490nm. The time points used for MTS proliferation assay were 0h, 24h, 48h, 72h and 96h. The experiment was performed in triplicate and repeated thrice. Error bars are representative of SEM. Student's t-test was applied to calculate p-value.

4.2.9 Fibronectin Adhesion assay

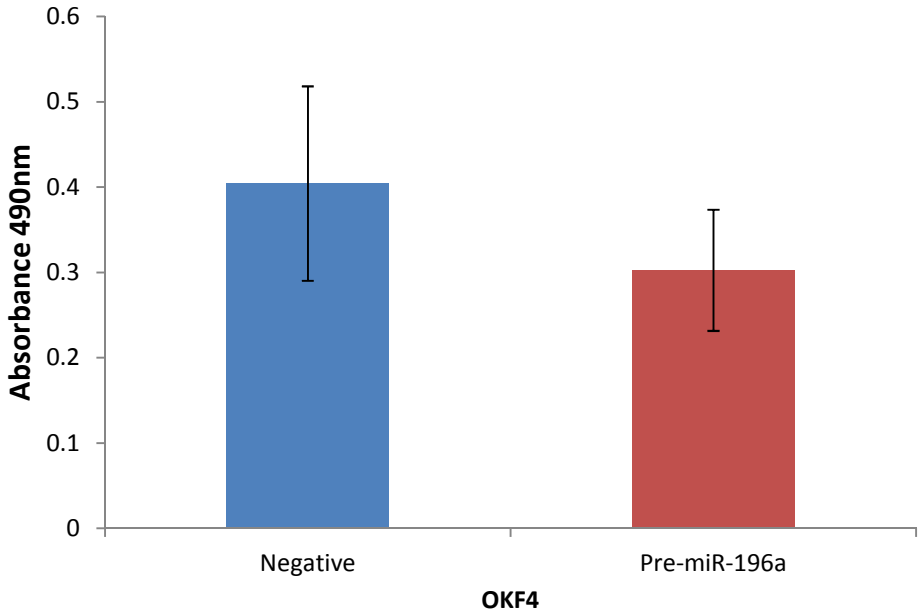

Figure 4.13. MTS adhesion assay showed no significant difference in adhesion to fibronectin between OKF4 pre-miR-196a and negative control cells. Absorbance was checked at 490nm after 1 hr incubation with MTS reagent. The experiment was performed in triplicate and repeated thrice. Error bars are representative of SEM. Student's t-test was applied to calculate p-value.

4.2.10 Migration assay

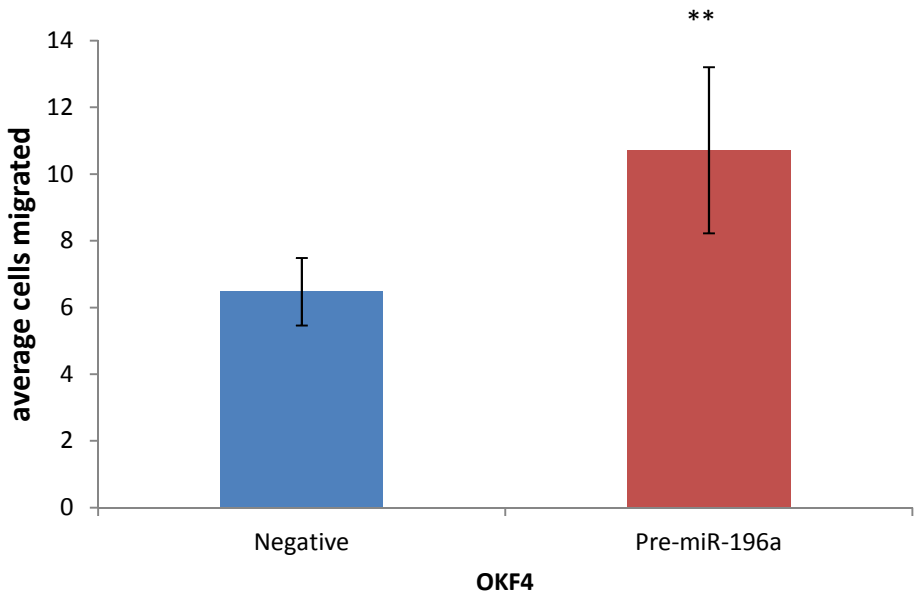

Figure 4.14. Transwell migration assay showed significant increase in OKF4 pre-miR-196a cells which migrated towards FCS compared to negative control cells. The cells were allowed to migrate for 24 hr. The experiment was performed in duplicate and repeated thrice. Error bars are representative of SEM. Student's t-test was applied to calculate p-value. **, $p<0.01$.

4.2.11 Invasion assay

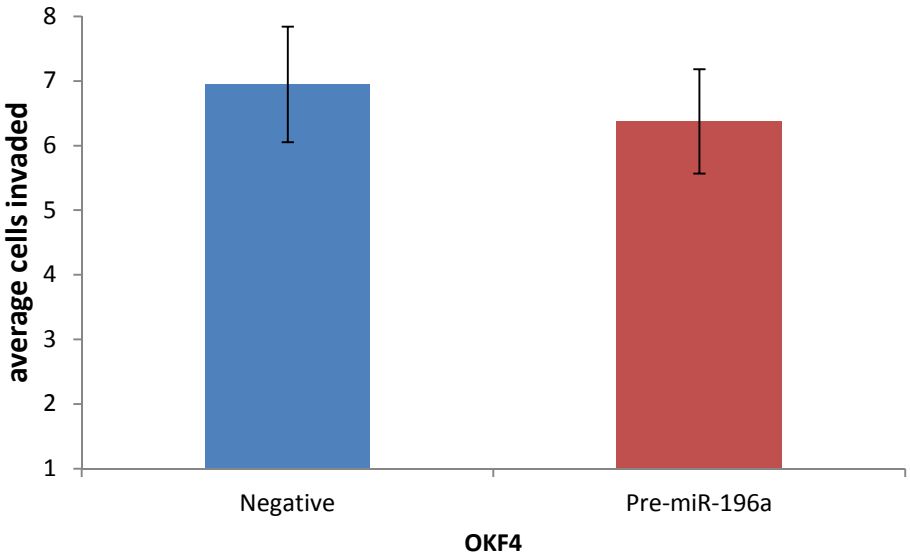

Figure 4.15. Transwell invasion assay showed no significant difference in OKF4 pre-miR-196a cells which invaded growth factor reduced matrigel compared to negative control cells. The cells were allowed to invade for 48 hr. The experiment was performed in duplicate and repeated thrice. Error bars are representative of SEM. Student's t-test was applied to calculate p-value.

4.3 Discussion:

miRNA-196 is present in the HOX gene cluster across different chromosomes. miR-196a expression was seen to be increased in OPM and HNSCC cells which correlates well with the data generated through affymetrix microarray (Lambert, Murdoch and Hunter, unpublished data) and seen by another group (Liu et al., 2012a) who also showed that miR-196a expression was higher in the oral squamous carcinoma cells compared to normal cells. miR-196a did not get detected in NOK's and probably testing another known miRNA, such as miR-375 (Chen et al., 2013), which is expressed in NOK's as control would have been good to show that there was no issue with cells or procedure. As discussed earlier, miR-196a has been observed to be up-regulated in several other cancers such as oesophageal, gastric and colorectal cancer (Tsai et al., 2012, Schimanski et al., 2009, Luthra et al., 2008). High levels of miR-196a suggest that it might play a role in either promoting HNSCC or could even be one of the early changes that take place in the cell based on the observation of higher miR-196a expression in some OPM cell lines compared to cancer cell lines. Hence, it would be interesting to assess miR-196a expression in OPL (Oral Pre-malignant Lesion) tissue samples. miR-196a expression has also been shown to be up-regulated in the serum of OSCC patients pre-operative (Liu et al., 2012a), and similarly, it would be very interesting to assess serum miR-196a level in OPL patients. This could lead to use of miR-196a as early diagnostic marker for HNSCC.

Pri-miR-196a-1 and pri-miR-196a-2 showed higher expression in OPM and HNSCC cells and as it might be recalled, miR-196a-1 and miR-196a-2 have identical mature sequence of miR-196a. Mature miR-196a expression in OPM and HNSCC compared to NOK was much higher than pri-miR-196a-1 or a-2. There is still much to be understood about miRNA biogenesis but it is suggested that SMAD protein might play a role in miRNA biogenesis (Davis et al., 2008). Recently, it was also observed that basic

pathways like Akt, ERK and TGF-β can also modulate the Drosha function and in turn modulate miRNA biogenesis (Blahna and Hata, 2013). Several growth factor pathways are dysregulated in HNSCC like Akt (Abrahao et al., 2013), ERK (Hehlgans et al., 2012) and TGF-β (Smith et al., 2013) and these in turn could play role in modulation of mature miR-196a expression. It has been shown that pre-miRNA transcript can also be made independent of Drosha activity from the splicing event of intron and these were called mirtrons (Sibley et al., 2012). The higher mature miR-196a expression that is seen in OPM and HNSCC could be attributed to any of these factors. In terms of miR-196a expression in the FFPE tissue samples, we observed similar results to those observed *in-vitro.*

The level of miR-196a expression in the cancer tissue was significantly higher than normal tissue and this result illustrates we observe the same outcome in the cell lines and tissue samples. Even though the magnitude of the change seen in tissue samples is much smaller than cell lines this could be due to the heterogeneous cell population present in tissue samples while cell lines have pure epithelial cell population. Hence, it was thought that miR-196a might be playing the same role *in-vivo* as observed *in-vitro*.

Transfection of anti-miR-196a and negative control into B16 (HNSCC) and D19 (OPM) cells led to reduced miR-196a expression. There was notable decrease in migration and invasion seen in HNSCC cells transfected with anti-miR-196a which sits well with the data published in a gastric cancer study (Tsai et al., 2012), where they found miR-196a promoted migration and invasion. In another study carried out in oral squamous cell carcinoma (OSCC) and non-small cell lung carcinoma (NSCLC) there was evidence that miR-196a promoted migration and invasion (Liu et al., 2012a, Liu et al., 2012d). Even though migration assay showed significant effect with 24 hr incubation, it could have been left for longer incubation to see even more migration of transfected cells. There was decrease in adhesion to fibronectin observed in B16 cells whereas there was

no significant change in adhesion in D19 cells. This result may be attributed to the fact that even though miR-196a expression is reduced by 92% in D19 cells, miR-196a expression in these cells is as high as B16 cells without transfection. It is possible that effect in adhesion is only noted after miR-196a expression is reduced below a critical level. miR-196a showed no effect on proliferation of HNSCC cells which was also observed in another study carried out in OSCC (Liu et al., 2012a). Migration towards fibronectin showed no effect in HNSCC cells even though based on *in-silico* analysis it has been observed that miR-196a targets both integrin α5 and β1. But fibronectin can bind multiple integrins on the cell surface and not only to its described primary integrin ligands integrin α5 and β1. Hence, there could be other integrins and pathways activated due to which no effect in migration to fibronectin was observed.

OKF4 (Immortalised NOK) cells were then transfected with pre-miR-196a and negative control to assess if increasing the miR-196a level in normal cells would show the opposite effect to that in cancer cells. miR-196a expression increased in OKF4 cells when transfected with pre-miR-196a and these cells were later used for functional assays. There was increase in migration observed for pre-miR-196a transfected OKF4 cells but no change in proliferation, adhesion or invasion was observed which may be ascribed to the fact that OKF4 cells are ‘normal’ and we are changing only one factor in these cells compared to dysplastic or cancer cells where there are several genetic changes already present. The other way of looking at it can also be that even though only one factor is being changed in normal cells, functional effect in terms of change in migratory potential of the cells is observed, thus emphasising the role miR-196a may play in this ability of the cells. This, like earlier, points to the direction that miR-196a de-regulation can be an early event in the progression of HNSCC.

Hence, from the data presented here it can be concluded that miR-196a is over-expressed in HNSCC cell lines and tissue samples. miR-196a also increases the

migratory, invasive and adhesive properties of HNSCC cells. miR-196a also increases the migratory property of iNOK cells. Next, the expression of all 39 HOX genes was checked in HNSCC and effects of HOXB9 were studied in HNSCC. This was studied as miR-196a is present in HOX gene cluster and has been found to target certain HOX genes. Based on all 39 HOX genes expression, if any HOX gene expression was down-regulated then it could be a potential target of miR-196a.

Chapter 5: Effects of HOXB9 in HNSCC

HOX genes are transcription factors which are involved in embryogenesis and organogenesis. HOX genes contain a 61 amino acid homeodomain. There are 39 class I HOX genes which are present in 13 paralogous groups and divided into four clusters present on different chromosomes (Sha et al., 2013, Ansari et al., 2011, Calvo et al., 2000). The HOX paralogous groups are closely related to each other in terms of their functional effects (Hayashida et al., 2010, Xu and Wellik, 2011). HOXB9 is part of the HOX9 paralogous group (towards 3' end) and it is part of HOXB cluster (Chen and Capecchi, 1999, Grier et al., 2005). HOXB9 and miR-196a-1 are present spatially closely to each other on chr 17. HOXB9 is over-expressed in several cancers like lung, breast, colorectal, hepatocellular and oral cancer (Calvo et al., 2000, Hassan et al., 2006, Kanai et al., 2010, Hayashida et al., 2010). Conversely, it has also been shown to be down-regulated in gastric cancer and this is related to poor prognosis (Sha et al., 2013). HOXB9 expression is regulated by several different factors and pathways in different cancers. In lung adenocarcinoma, HOXB9 expression is controlled by Wnt signalling and it is also a target of TCF4 (Nguyen et al., 2009). HOXB9 has several estrogen responsive elements (EREs) in its promoter and its expression has been shown to be regulated by estrogen in breast cancer (Ansari et al., 2011).

In terms of previous work on HOX genes in oral cancer, HOX genes including HOXB9 were shown to be up-regulated in oral squamous cell carcinoma compared to normal mucosa (Hassan et al., 2006). Hunter et al. in a previous expression microarray project, showed several HOX genes were up-regulated in oral squamous cell carcinoma cells (Hunter et al., 2006) (http://bioinformatics.picr.man.ac.uk/vice/PublicProjects.vice?pager.offset=15). The aim of this chapter was to check expression of all 39 HOX genes in HNSCC cells compared to normal cells. To check the expression of HOXB9 based on qPCR and

protein expression in HNSCC cell lines and tissue samples compared to normal cells and tissue samples and to check its effect in HNSCC. To assess whether HOXB9 and miR-196a-1 primary transcript was present in HNSCC cells or not. Thus, careful validation of these observations in our cell lines was necessary in addition to assessment of the expression of all 39 HOX genes across cell line panel consisting of NOKs, iNOK, OPM and HNSCC cells, to confirm which HOX genes had dysregulated expression in HNSCC. Based on the qPCR, HOXB9 was noted to be highly over-expressed in both OPM and HNSCC cells compared to normal. The protein expression levels of HOXB9 in cell lines and tissue samples were assessed by utilising techniques like western blotting and Immunohistochemistry (IHC) respectively. Like miR-196a, HNSCC and OPM cells were transfected with HOXB9 siRNA to reduce the expression of HOXB9 and then use these cells for functional assays. Functional assays such as MTS proliferation, adhesion to fibronectin, migration and invasion were performed to look at the functional effects of miR-196a in iNOK, OPM and HNSCC cells. MTS reagent was used for both proliferation and adhesion absorbance calculation whereas transwell membrane was used for migration and invasion with matrigel. The presence of primary transcript consisting of HOXB9 and miR-196a-1 was shown with the help of nested PCR and DNA sequencing.

5.1 Expression of HOX genes in HNSCC

The expression of all 39 HOX genes was assessed by qPCR in NOK, iNOK, OPM and HNSCC cells. The experiment was performed in 12 different cell lines which consisted of normal cells (OK21, OK102, NOK2), iNOK cell lines (FNB6 and OKF6), OPM cell lines (D19, D20, D4 and D35) and HNSCC cell lines (B16, T4 and B22). This experiment was carried out in the lab of Dr. Richard Morgan in the University of Surrey. The expression of each HOX gene in each cell line was initially normalised to internal control B-actin. Then, the absolute expression of all normal cells used was averaged and similarly expression of all OPM and HNSCC cell lines was averaged to plot in the graph. Based on the data generated, none of the HOX genes were down-regulated compared to the normal in the HNSCC. There was marked over-expression of HOXA4, HOXA5, HOXA9, HOXA10, HOXB9 and HOXC9 observed in OPM and HNSCC cells compared to normal (Figure 5.1, 5.2, 5.3, 5.4, 5.5, 5.6 and 5.7). It was observed that OKF6 and FNB6 showed significant expression compared to NOKs for certain genes. This can be attributed to them as they were immortalised normals with P16 knocked out and hTERT activated. HOXD10 was also noted to be over-expressed and its study was undertaken by my colleague, Mr. Fahad Hakami. Hence, the expression of all 6 HOX genes was re-assessed by qPCR. The primers for all 39 HOX genes and β-actin are listed in Appendix 9.2. As, HOXB9 expression was seen to be highly over-expressed in HNSCC cells compared to normal cells based on qPCR, it was decided to check the expression of HOXB9 protein by western blotting for cell lines and immunohistochemistry for tissue samples.

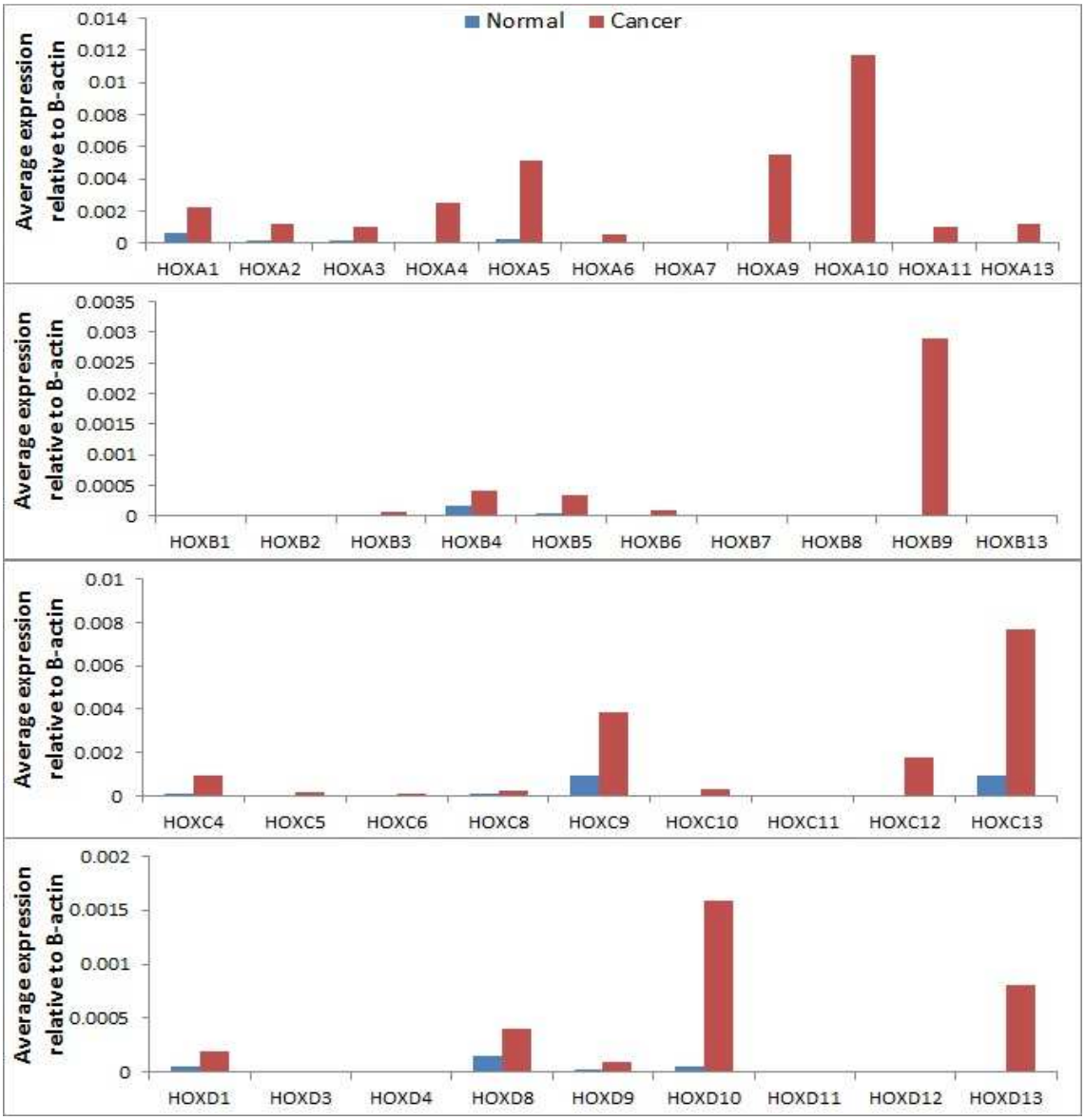

Figure 5.1. All 39 HOX genes expression shown for normal and cancer cells. The average of all normals (NOK+iNOK) and cancer (OPM+HNSCC) cell lines absolute expression for each HOX gene was used to represent in the graph. The data was normalised to internal control β-actin. The experiment was performed in single well for each HOX gene in each cell line.

5.1.1 HOXA4 expression in HNSCC

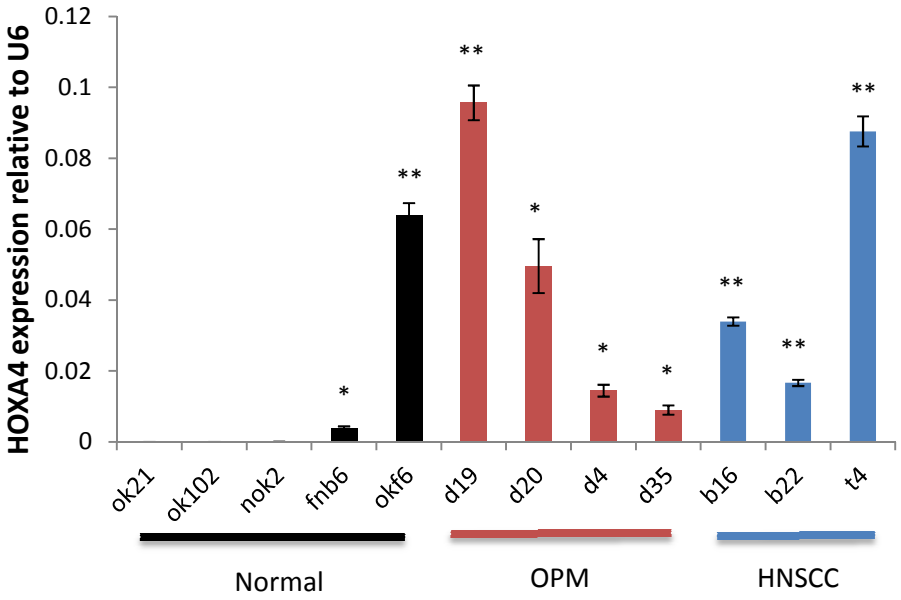

Figure 5.2. HOXA4 was seen to be significantly over-expressed in OPM and HNSCC cells compared to normal. The data was normalised to internal control U6. The experiment was performed in triplicate. Error bars are representative of SEM. Student's t-test was applied to calculate p-value relative to OK21. *, p<0.05; **, p<0.01.

5.1.2 HOXA5 expression in HNSCC

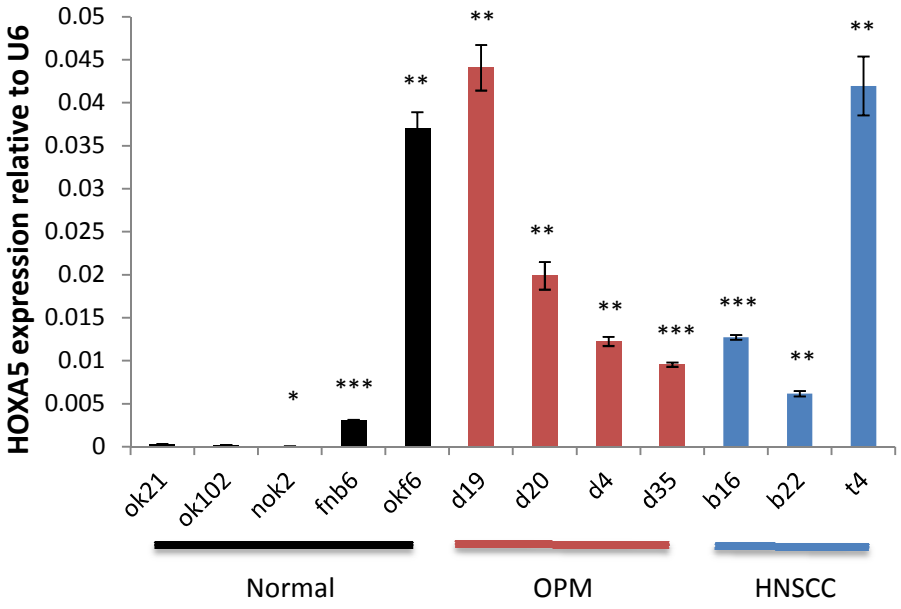

Figure 5.3. HOXA5 was seen to be significantly over-expressed in OPM and HNSCC cells compared to normal. The data was normalised to internal control U6. The experiment was performed in triplicate. Error bars are representative of SEM. Student's t-test was applied to calculate p-value relative to OK21. *, p<0.05; **, p<0.01; ***, p<0.001.

5.1.3 HOXA9 expression in HNSCC

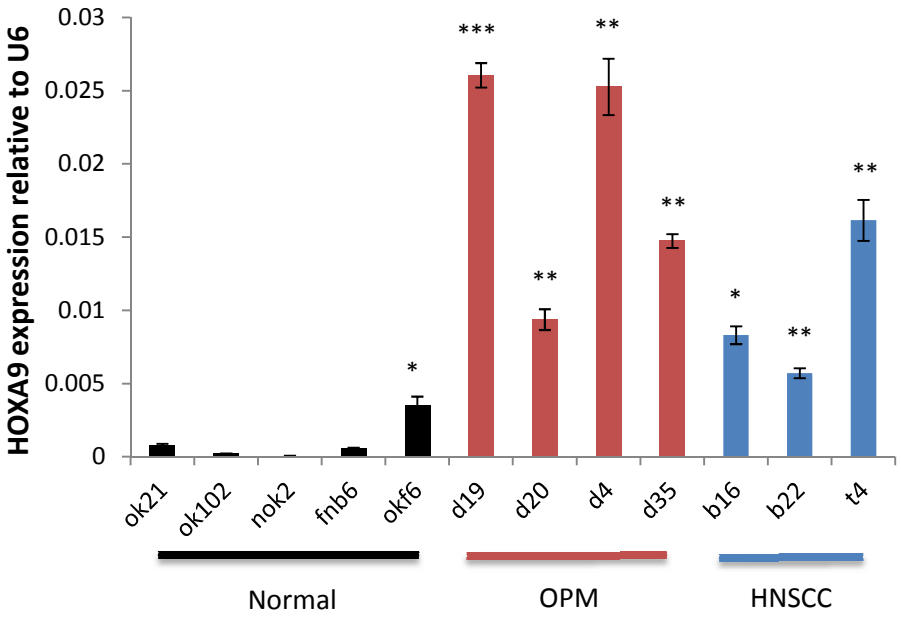

Figure 5.4. HOXA9 was seen to be significantly over-expressed in OPM and HNSCC cells compared to normal. The data was normalised to internal control U6. The experiment was performed in triplicate. Error bars are representative of SEM. Student's t-test was applied to calculate p-value relative to OK21. *, $p<0.05$; **, $p<0.01$; ***, $p<0.001$.

5.1.4 HOXA10 expression in HNSCC

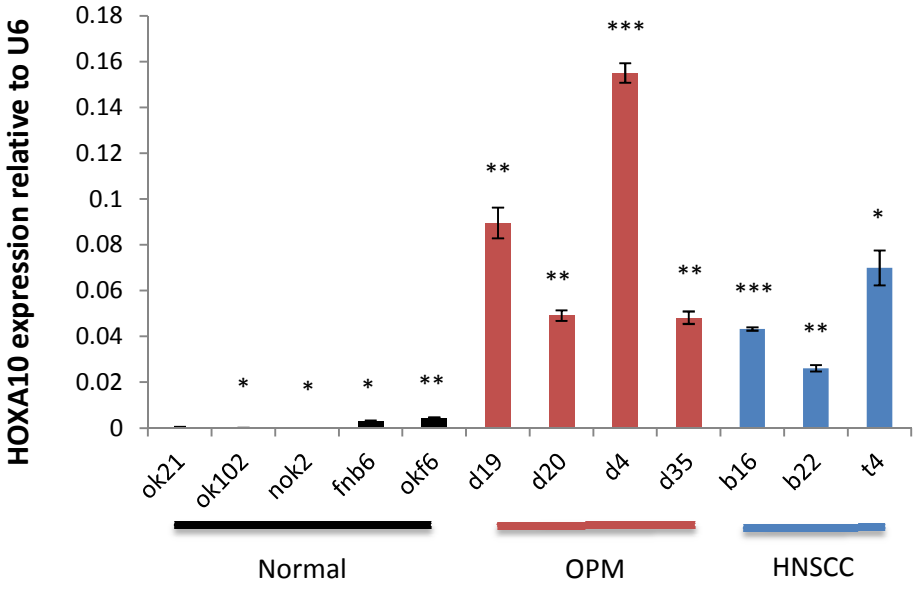

Figure 5.5. HOXA10 was seen to be significantly over-expressed in OPM and HNSCC cells compared to normal. The data was normalised to internal control U6. The experiment was performed in triplicate. Error bars are representative of SEM. Student's t-test was applied to calculate p-value relative to OK21. *, p<0.05; **, p<0.01; ***, p<0.001.

5.1.5 HOXB9 expression in HNSCC

It can be seen that OKF6 expresses HOXB9 at higher level compared to other normal (Figure 5.6.A). Expression of HOXB9 in OPM and HNSCC was similar. It can clearly be seen that HOXB9 is the most highly over-expressed HOX gene in HNSCC compared to normal cells. HOXB9 is also spatially closely related to miR-196a-1 on chromosome 17 and hence it was decided to study the effect of HOXB9 further in HNSCC. It was decided to use another iNOK cell line called OKF4 instead of OKF6 and cell panel was widened by including H357 and B56 cells (Figure 5.6.B). Note that in figure 5.6.B, HOXB9 expression is represented in Log scale unlike figure 5.6.A, indicating the large dynamic scale of change in expression seen. It can also be noted that HOXB9 expression in OPM and HNSCC cells is alike when compared to each other.

A.

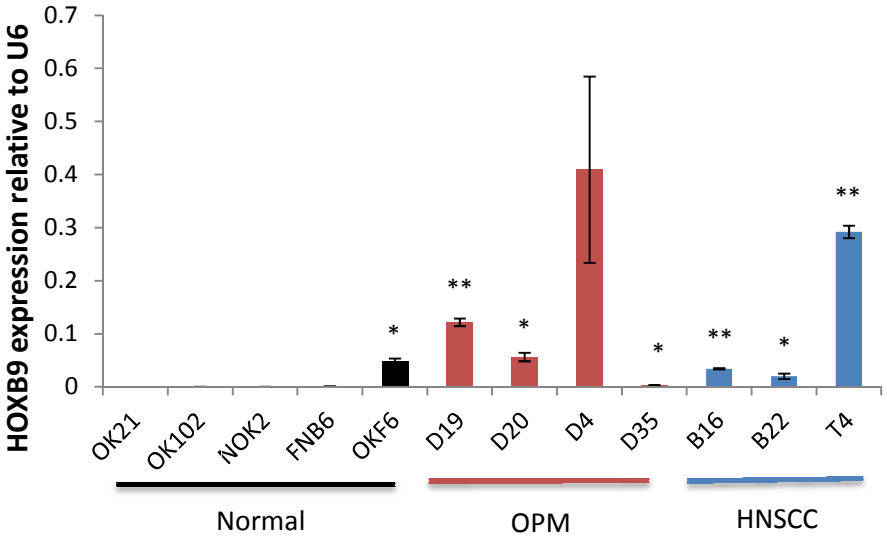

B.

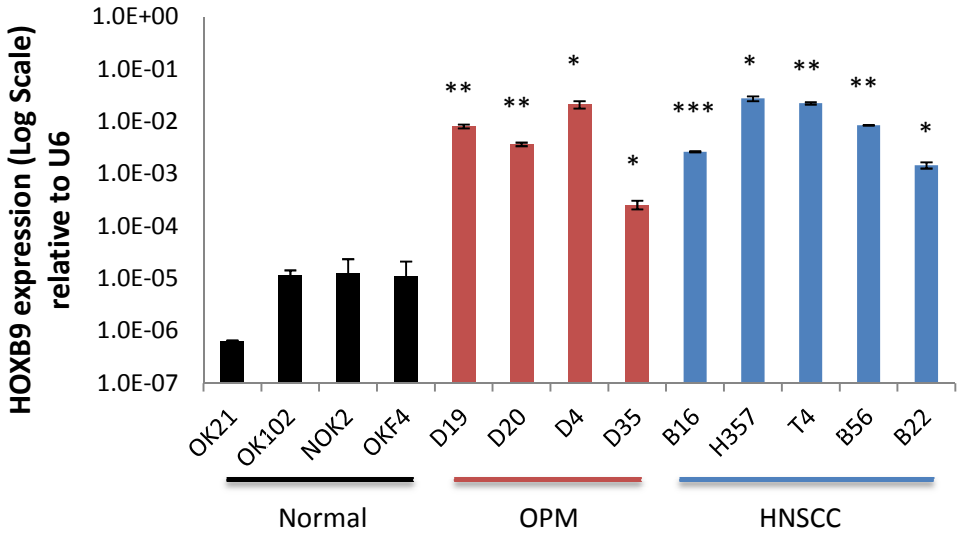

Figure 5.6.A HOXB9 was seen to be significantly over-expressed in OPM and HNSCC cells compared to normal. B. Cell line panel was extended. HOXB9 was seen to be significantly over-expressed in OPM and HNSCC cells compared to normal. The data was normalised to internal control U6. The experiment was performed in triplicate. Error bars are representative of SEM. B. Student's t-test was applied to calculate p-value relative to OK21. *, p<0.05; **, p<0.01; ***, p<0.001.

5.1.6 HOXC9 expression in HNSCC

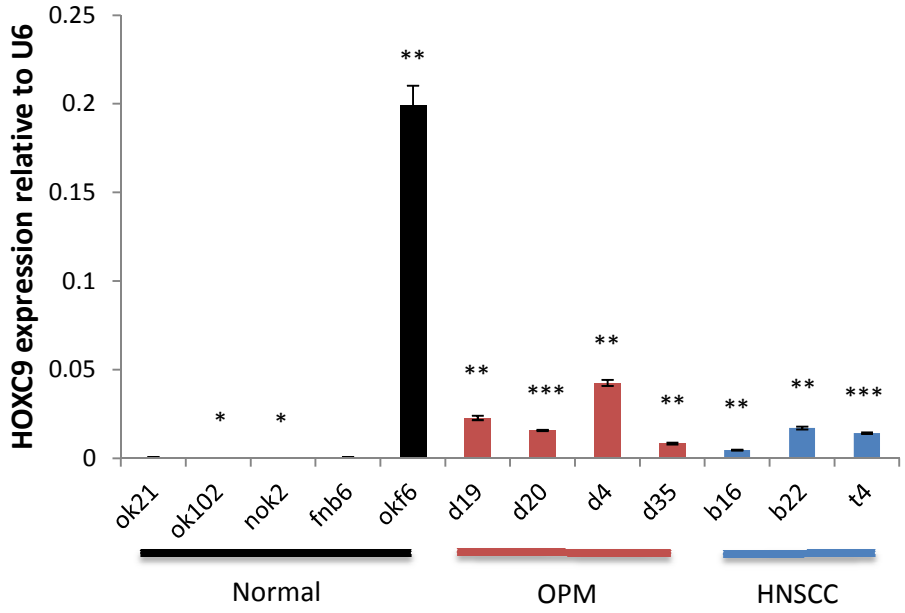

Figure 5.7. HOXC9 was seen to be significantly over-expressed in OPM and HNSCC cells compared to normal. The data was normalised to internal control U6. The experiment was performed in triplicate. Error bars are representative of SEM. Student's t-test was applied to calculate p-value relative to OK21. *, p<0.05; **, p<0.01; ***, p<0.001.

5.2 HOXB9 protein expression agrees with RNA data in HNSCC

The HOXB9 expression was increased in RNA level but it was needed to check if it translated to increase in the protein expression levels in cell lines and tissue samples. Anti-HOXB9 primary antibody (rabbit monoclonal) from Abcam was used to assess expression of HOXB9 protein in cell lines. Theoretical weight of HOXB9 was predicted to be 28Kd. The Abcam antibody produced a band at same molecular weight. The band was observed at 28Kd. β-actin was observed at 42Kd keeping with the predicted weight. It was observed that expression of HOXB9 protein was higher in B16, B22 and B56 cells when compared to normal (Figure 5.8).

The expression of HOXB9 was more extensive in the cancer tissue compared to normal tissue (Figure 5.10). There was faint staining in the normal tissue whereas in cancer tissue the intensity of staining was stronger. For normal tissue samples staining was seen in the nuclei of basal and some prickle cells in the epithelium (Figure 5.9.A). For some cancer tissue samples, the staining was not only seen in nucleus but also in the cytoplasm of the cells (Figure 5.9.B). The multiplicative quickscore method (semi-quantitative) (Detre et al., 1995) was used based on the intensity (1-3) and extent (1-3) of staining to score the tissue samples. These results point that the increase in HOXB9 seen in cancer cell lines and tissue samples might be having some effect in the HNSCC cells. As there was increase in RNA and protein level of HOXB9 in HNSCC cells, next it was checked what functional effects HOXB9 had in HNSCC.

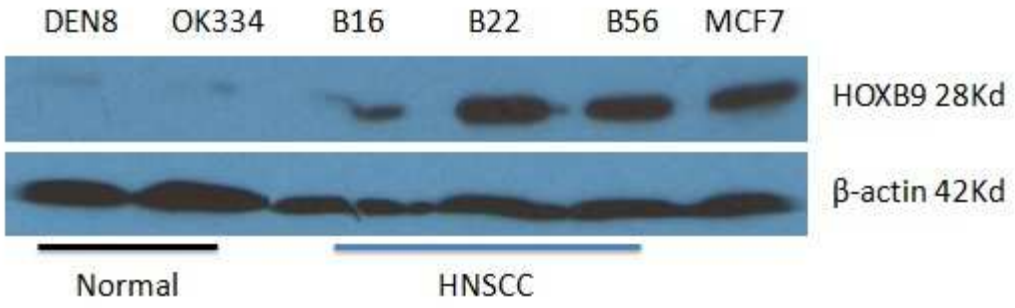

Figure 5.8. Western blotting representing the over-expression of HOXB9 protein in HNSCC cell lines compared to normal. β-actin was used as the internal and loading control. MCF7 was used as positive control based on manufacturer's specification sheet. This blot is representative of 4 repeats.

A.

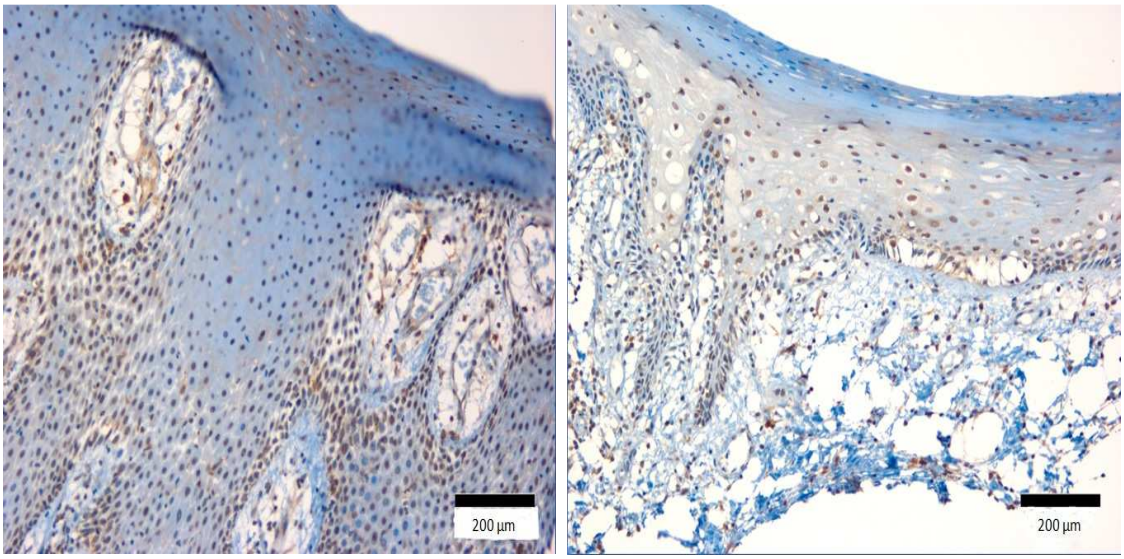

B.

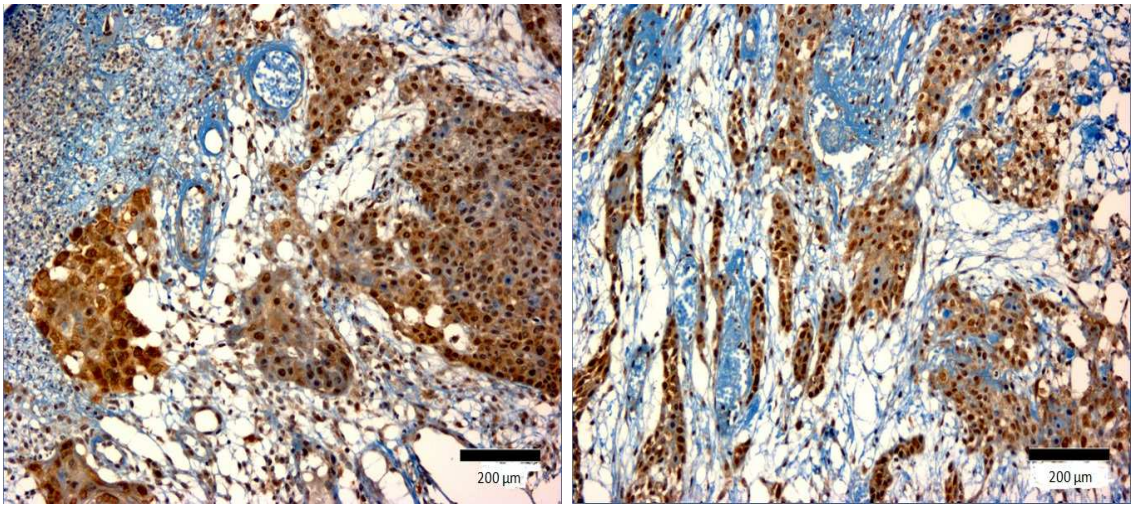

Figure 5.9. A. HOXB9 protein detection in normal tissue by IHC, as described in materials and methods. B. HOXB9 protein detection in cancer tissue based on IHC. Magnification used was 200X on Olympus light microscope.

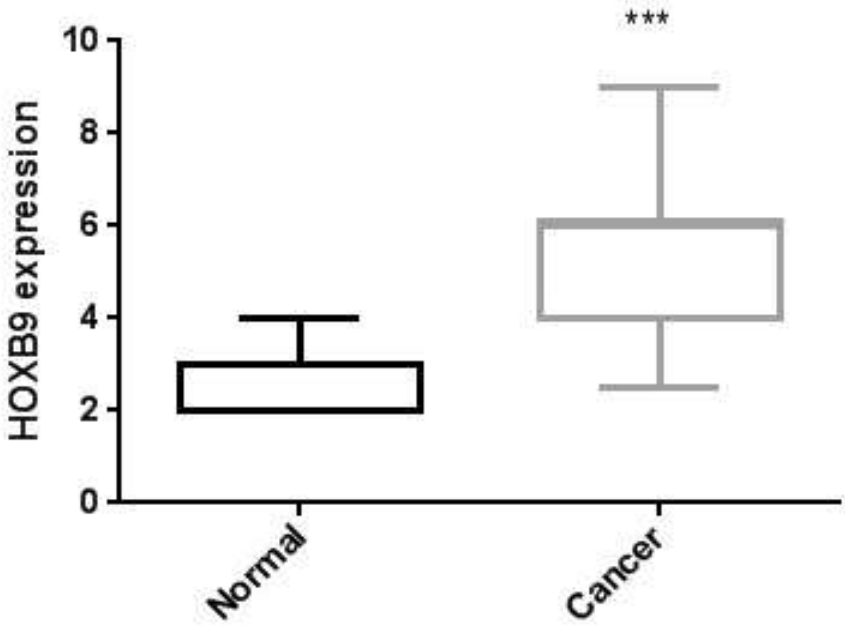

Figure 5.10. Box plot representing over-expression of HOXB9 in cancer tissue compared to normal tissue. 25 cancer tissues on TMA and 10 normal tissues were used for IHC. Mann-whitney U-test was applied to the data for statistical analysis. ***, p<0.001.

5.3 Functional effects of HOXB9 in HNSCC

To assess effects of HOXB9 in HNSCC, functional assays were performed in B16 (HNSCC) and D19 (OPM) cells. These cells were transfected with HOXB9 siRNA and negative control siRNA. The efficiency of silencing HOXB9 was assessed using qPCR and it was noted that HOXB9 siRNA significantly down-regulated the expression of HOXB9 compared to negative control (Figure 5.11). These transfected cells were then used for functional assays. It was observed that HOXB9 siRNA transfected cells showed significant decrease in proliferation (Figure 5.12), migration (Figure 5.14) and invasion (Figure 5.15) compared to negative control cells. There was no change noticed in adhesion to fibronectin between either cells (Figure 5.13).

5.3.1 HOXB9 siRNA transfection

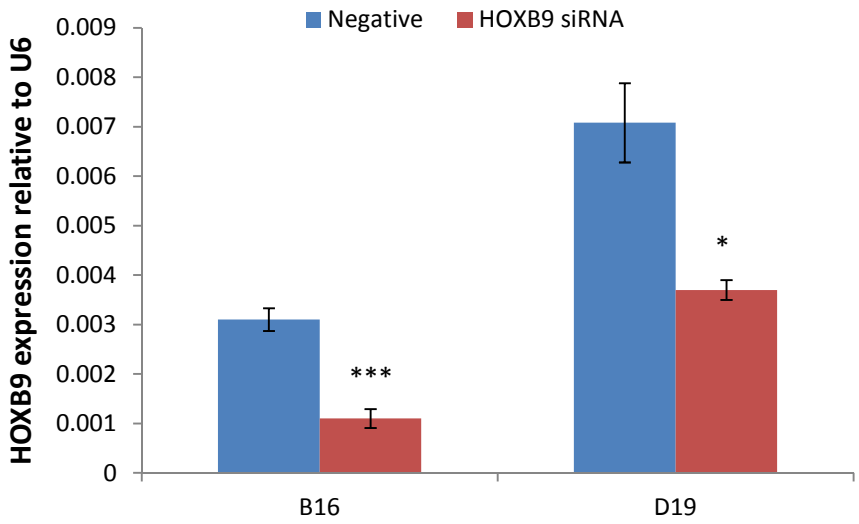

Figure 5.11. HOXB9 expression significantly decreased in B16 and D19 HOXB9 siRNA cells compared to negative control cells. The transfected cells were incubated for 48 hr. The data was normalised to internal control U6. There was 62% and 48% down-regulation observed in HOXB9 expression in B16 and D19 HOXB9 siRNA transfected cells compared to negative control transfected cells, respectively. The experiment was performed in triplicate. Error bars are representative of SEM. Student's t-test was applied to calculate p-value. *, $p<0.05$; ***, $p<0.001$.

5.3.2 Proliferation Assay

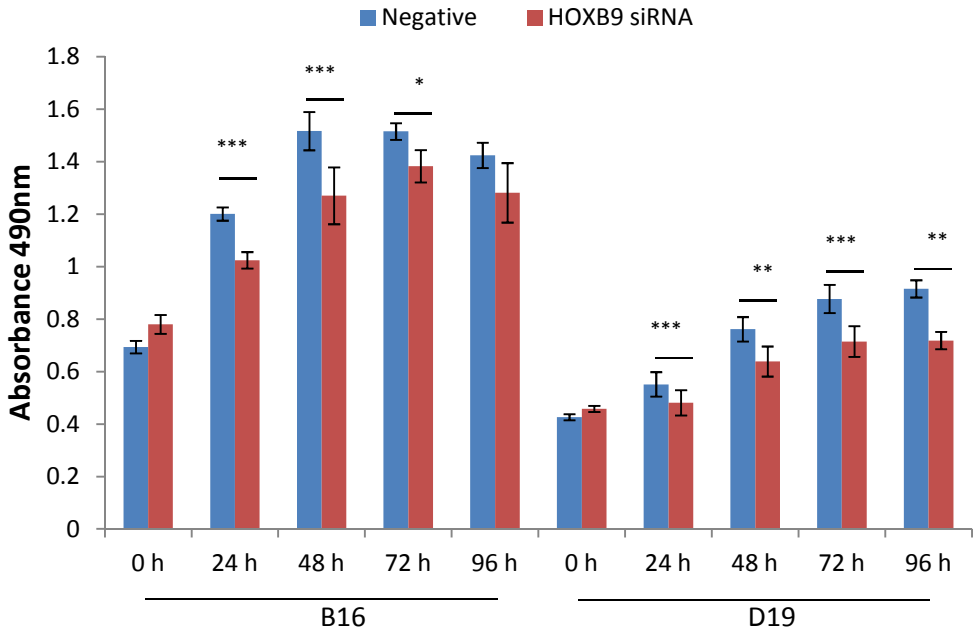

Figure 5.12. MTS proliferation assay showed significant decrease in proliferation of B16 and D19 HOXB9 siRNA cells compared to negative control cells. Absorbance was checked at 490nm. The time points used for proliferation assay were 0h, 24h, 48h, 72h and 96h. The experiment was performed in triplicate and repeated thrice. Error bars are representative of SEM. Student's t-test was applied to calculate p-value. *, p<0.05; **, p<0.01; ***, p<0.001.

5.3.3 Fibronectin Adhesion Assay

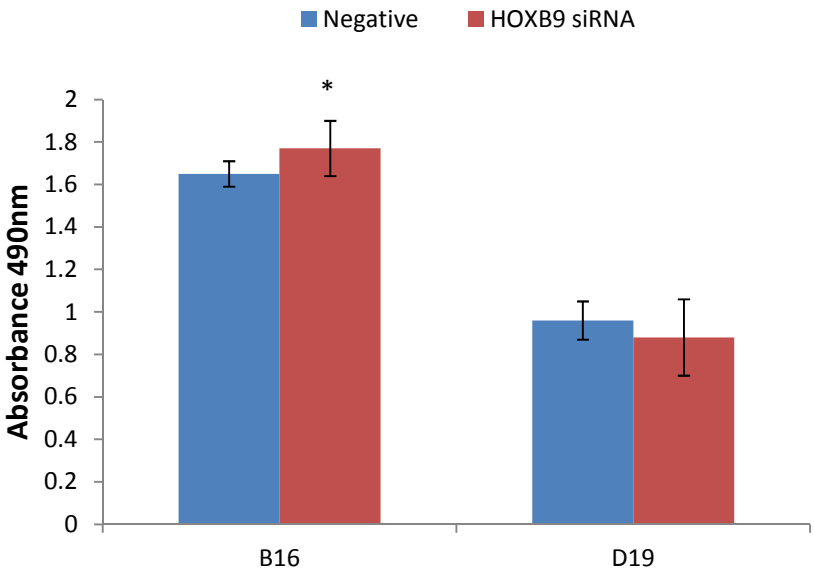

Figure 5.13. MTS adhesion assay showed significant increase in adhesion for B16 HOXB9 siRNA cells compared to negative control cells whereas there was no change noted for D19 cells. Absorbance was checked at 490nm after 1 hr incubation with MTS reagent. The experiment was performed in triplicate and repeated thrice. Error bars are representative of SEM. Student's t-test was applied to calculate p-value. *, $p<0.05$.

5.3.4 Migration towards FCS

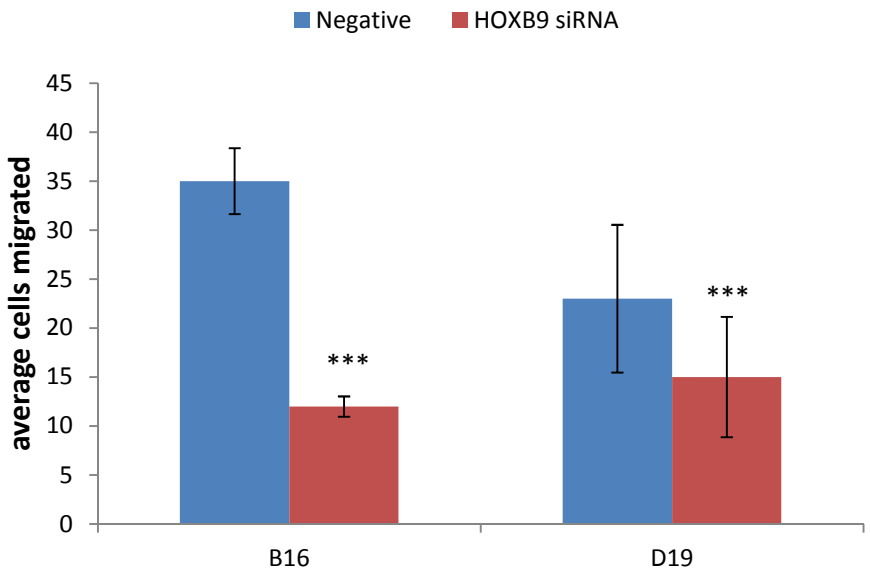

Figure 5.14. Transwell migration assay showed significant decrease in migration towards FCS of B16 and D19 HOXB9 siRNA cells compared to negative control cells. The cells were allowed to migrate for 24 hr. The experiment was performed in duplicate and repeated thrice. Error bars are representative of SEM. Student's t-test was applied to calculate p-value. ***, p<0.001.

5.3.5 Invasion Assay

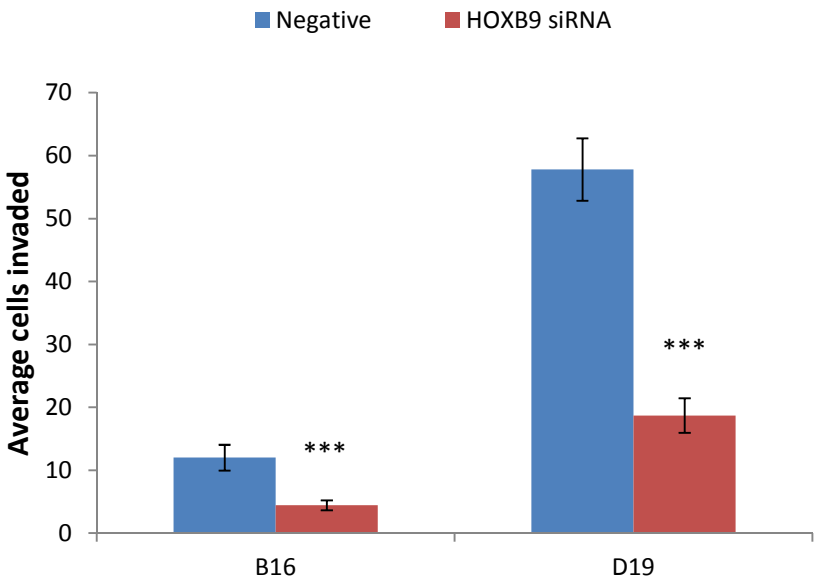

Figure 5.15. Transwell invasion assay showed significant decrease in B16 and D19 HOXB9 siRNA cells which invaded growth factor reduced matrigel compared to negative control cells. Growth factor reduced matrigel was used so that cell's invasive potential is not over-shadowed by their affinity for other growth factors. The cells were allowed to invade for 48 hr. The experiment was performed in duplicate and repeated thrice. Error bars are representative of SEM. Student's t-test was applied to calculate p-value. ***, $p<0.001$.

5.4 PCR for miR-196a-1 and HOXB9 primary transcript with different DNA polymerase

miR-196a-1 and HOXB9 are present in the HOXB cluster on chromosome 17. miR-196 is present upstream of HOX9 paralogous group (Yekta et al., 2004). Based on *in-silico* analysis, it has been suggested that HOX gene clusters produce multiple polycistronic mRNA transcripts (Mainguy et al., 2007). In the same paper it was also proposed that HOXB7, HOXB8, HOXB9 and miR-196a-1 are co-expressed on a single primary transcript. This proposed primary transcript has also been annotated in Ensembl (www.ensembl.org), spanning 32 Kb on chromosome 17 (Transcript: RP11-357H14.19-001), although these predictions have not been experimentally verified. Based on the data presented here, which shows over-expression for both miR-196a and HOXB9, this primary transcript could exist in HNSCC cells.

The primers for the PCR to assess for the presence of primary transcript co-expressing miR-196a-1 and HOXB9 were designed from precursor miR-196a-1 sequence (PT forward) and exon 1 of HOXB9 (PT reverse). The total length of the predicted amplicon using these primers was 6320 bp and the primers only amplified this particular transcript based on the analysis from Primer Blast (http://www.ncbi.nlm.nih.gov/tools/primer-blast/). The forward and reverse primer Tm (melting temperature) (PT primers) was calculated to 68.1^0C and 67.2^0C. B16 RNA was extracted and M-MLV reverse transcriptase was used for rt-PCR. cDNA from the reaction was used with Phusion and Taq DNA polymerase for PCR. Gradient PCR was used to assess for the presence of the transcript from 40^0C to 70^0C annealing temperature. Phusion DNA polymerase was used as it has got proof reading quality which would avoid the possibility of incorporation of wrong base, but there was no detection of the transcript at 6.3Kb. Hence, PCR was performed with Taq DNA polymerase even though it does not have exonuclease activity but has high efficiency.

But still there was no detection of a transcript of 6.3Kb. GAPDH was used as the internal control to assess for the integrity of the RNA and also to evaluate if M-MLV was reverse transcribing the RNA to cDNA. GAPDH was expressed in the B16 cells with an amplicon detected with the expected size of 240 bp.

5.5 miR-196a-1 and HOXB9 are co-expressed on same novel primary transcript

Inside the 6.3 Kb transcript the nested primers were designed to amplify an intergenic region and give a 295 bp transcript (nested forward, T_m 77^0C; nested reverse, T_m 75^0C) (Figure 5.16). The primers used for rt-PCR were changed, using random primers or PT primers with B16 RNA. The first PCR was done using another DNA polymerase Q5 (NEB) which has proof-reading quality due to the failure of the PCR before, as per manufacturer's protocol with PT primers at two different annealing temperature 55^0C and 60^0C. Then, nested PCR was run with the cDNA produced from first PCR (Table 5.1) based on manufacturer's protocol and used three different annealing temperatures 55^0C, 60^0C and 65^0C. A 300 bp product was produced as shown by the marker for nested PCR run at all three temperatures only for the samples which had PT primers in rt-PCR (Figure 5.17.A). To confirm this expression of primary transcript the experiment was repeated with two controls: (-) RT (reverse transcriptase) and +RNase A (Figure 5.17.B). As can be seen, a 300 bp product was produced as before. In control samples, no product was seen which suggested that there was no DNA contamination and the transcript was being produced from RNA. This reaction shows that there is a primary transcript co-expressing miR-196a-1 and HOXB9. GAPDH was used as an internal control for B16 RNA and RP was used for the reaction. It was expressed at 240 bp expected length (Figure 5.17.C).

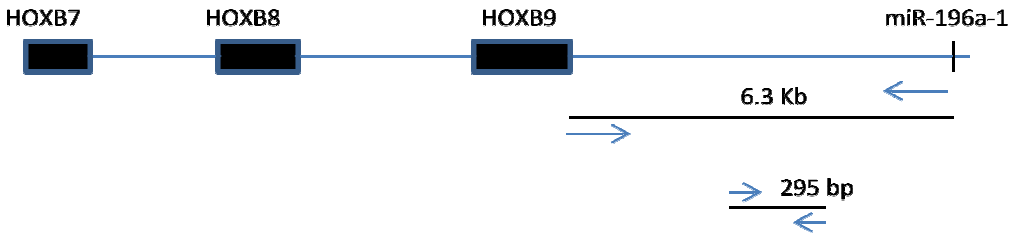

Figure 5.16. Schematic diagram of strategy applied to detect presence of HOXB9 and miR-196a-1 primary transcript.

A.

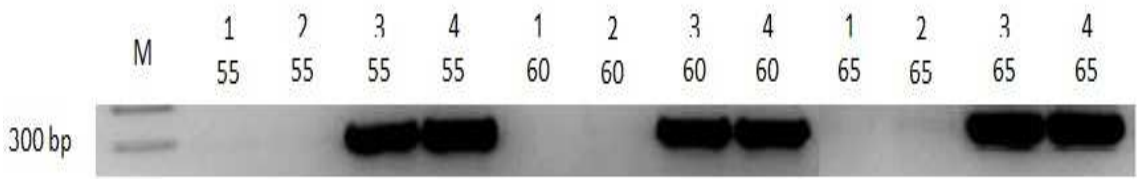

B.

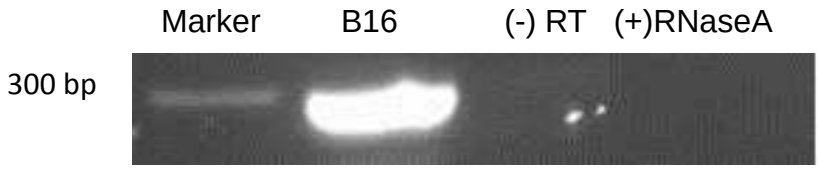

C.

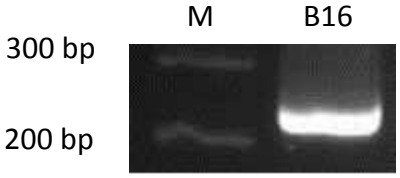

Figure 5.17. Co-transcription of miR-196a-1 and HOXB9 on same primary transcript. A. Initial Agarose gel run loaded with Marker (M) and PCR product showing presence of primary transcript at different conditions used in PCR (figure legend described in Table 5.1). The B16 RNA used was from previous experiment. B. Agarose gel run showing presence of primary transcript in B16 cells with newly extracted B16 RNA. We utilised two control conditions to show that expression was detected from RNA, (i) (–) RT and (ii) (+) RNase A. RT, reverse transcriptase. C. GAPDH was used as the internal control for newly extracted B16 RNA.

Table 5.1. Table describing symbol from Figure 5.17.A. B16 cells were used for total RNA extraction. Primers and temperatures used for PCR. RP, Random Primers; PT primers, Primary transcript primers.

Symbol on gel	Primer for rt-PCR	Primer and Temperature for first PCR	Primer and Temperature for second PCR
1, 55	RP	PT primers, 55^0C	Nested primers, 55^0C
2, 55	RP	PT primers, 60^0C	Nested primers, 55^0C
3, 55	PT	PT primers, 55^0C	Nested primers, 55^0C
4, 55	PT	PT primers, 60^0C	Nested primers, 55^0C
1, 60	RP	PT primers, 55^0C	Nested primers, 60^0C
2, 60	RP	PT primers, 60^0C	Nested primers, 60^0C
3, 60	PT	PT primers, 55^0C	Nested primers, 60^0C
4, 60	PT	PT primers, 60^0C	Nested primers, 60^0C
1, 65	RP	PT primers, 55^0C	Nested primers, 65^0C
2, 65	RP	PT primers, 60^0C	Nested primers, 65^0C
3, 65	PT	PT primers, 55^0C	Nested primers, 65^0C
4, 65	PT	PT primers, 60^0C	Nested primers, 65^0C

5.6 DNA sequencing to confirm the presence of transcript

B16 RNA was used for rt-PCR with PT primers, cDNA synthesized was used for first PCR with Q5 DNA polymerase with PT primers. The nested PCR was performed with PCR product from first PCR with Taq DNA polymerase with nested primers. To confirm that the PCR product observed on the gel was the 295 bp transcript which was expected, DNA sequencing was performed for the product. The DNA sequencing was perfect match for 295 bp transcript predicted using the nested primers (Figure 5.18). This result suggested that there was a novel primary transcript in B16 cells which contains miR-196a-1 and the coding sequence of HOXB9.

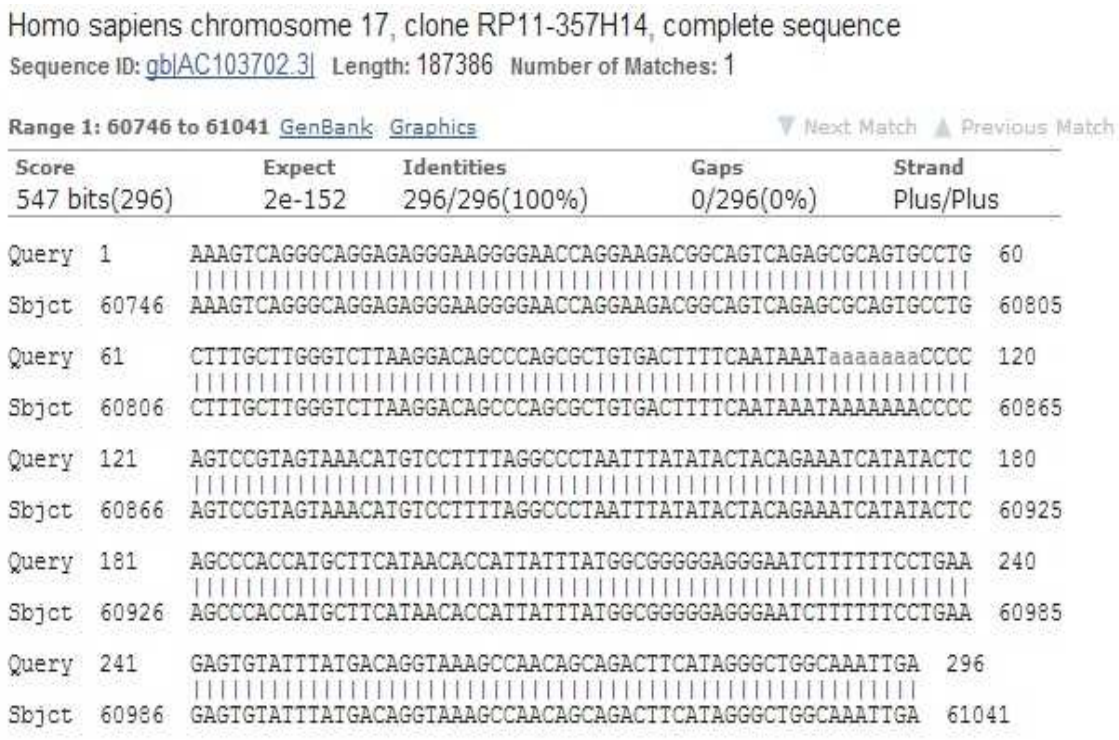

Figure 5.18. DNA sequencing of the PCR product confirms the presence of primary transcript.

5.7 Discussion

HOXB9 is present in the HOXB cluster on chromosome 17 and is a part of HOX9 paralogous group (Grier et al., 2005). HOXB9 expression was seen to be most highly increased between all 39 HOX gene panel and individual qPCR and this result agrees with the other publication which suggested that HOXB9 was over-expressed in oral squamous cell carcinoma (Hassan et al., 2006). HOXB9 has also been shown to be up-regulated in several other cancers as well like breast, lung, colorectal and hepatocellular carcinoma (Hayashida et al., 2010, Calvo et al., 2000, Kanai et al., 2010).

HOXB9 protein was observed to be over-expressed based on western blotting for cell lines and IHC for tissue samples. It was shown that expression of HOXB9 in HNSCC cell lines was higher compared to normal through western blotting. The band for HOXB9 protein was observed at the predicted molecular weight of 28Kd. This result proved that the over-expression that was observed in terms of RNA for HNSCC cell lines also translated into over-expression of HOXB9 protein in these cell lines compared to normal cells. The result for IHC staining was calculated based on the quickscore method which takes into account the extent and intensity of staining and is a semi-quantitative method. In normal tissue, staining was observed in the basal layer of the epithelium and also it was noted to be faint in intensity. In cancer tissue, staining was observed in higher extent covering whole epithelium and at much greater intensity. Nuclear staining was observed for both normal and cancer tissue but cytoplasmic staining was also seen in cancer tissue as observed in another study in gastric carcinoma and adjacent non-cancerous tissues (Sha et al., 2013).

B16 and D19 HOXB9 siRNA cells showed significantly decreased expression of HOXB9 compared to negative control cells and these cells were then used for functional assays. In terms of adhesion assay, we observed increase in adhesion to fibronectin in

B16 cells transfected with HOXB9 siRNA, but there is difference between being statistically significant and biologically significant. The increase seen in adhesion was marginal, it is not clear if this represents a significant biological effect in HNSCC.

There was reduced migration, invasion and proliferation observed in OPM and HNSCC cells transfected with HOXB9 siRNA, these three characteristics are very critical for cancer to progress. In breast cancer, it was observed that HOXB9, as in our experiments, increased migration and invasion. They also observed that HOXB9 expression lead to loss of cell-cell contact and also lead to epithelial-to-mesenchymal transition (EMT) (Hayashida et al., 2010). In another study carried out in breast cancer patient samples it was shown that HOXB9 promoted proliferation and angiogenesis (Seki et al., 2012). In a separate study, it was noted that expression of HOXB9 had anti-apoptotic effect in Hodgkin lymphoma and its expression increased the cell number (Nagel et al., 2007). Based on our observations and other studies there is strong evidence that HOXB9 plays a critical role in these important cancer characteristics. Hence, HOXB9 could be a novel therapeutic target in HNSCC.

The hypothesis that HOXB9 and miR-196a-1 were present on the same primary transcript was suggested by Mainguy et al. in 2007 based on *in-silico* analysis (Mainguy et al., 2007). Given high expression of HOXB9 and miR-196a in B16 cells, it was hypothesised that this transcript may be present in HNSCC cells. Initially, Phusion and Taq DNA polymerase were used for PCR and no product was observed at 6.3 Kb length in the agarose gel. There could be number of reasons why no product was seen. Firstly, it could be because the primary transcript was present in very low abundance and on single round of amplification there was not enough product to view on the gel. It could also be that the DNA polymerase was not able to transcribe such a long transcript.

In order to address these concerns, PT primers or RP were used in reverse transcription, along with Q5 DNA polymerase for first and nested PCR which has higher fidelity than

Phusion. This was done to see if using specific primers for the transcript could help in its reverse transcription. Nested primers were designed, which were present in the intergenic region of the transcript with length of 295 bp. The experiment was performed with appropriate controls. The product for B16 sample run with same protocol as earlier was present at 300 bp, with no product present for control amplification. This suggested that there was no DNA contamination and amplification was coming from RNA present, which proposed that primary transcript might be present. GAPDH was used as an internal control to assess for the integrity of the RNA. GAPDH was present at the expected length suggesting that the B16 RNA was intact.

The DNA sequencing showed us that the transcript had exact match to the sequence of 295 bp transcript present between nested primers. This experiment confirmed that the novel primary transcript co-transcribing miR-196a-1 and HOXB9 was present in B16 cells.

It is possible not all expression of HOXB9 or miR-196a in HNSCC comes from this primary transcript. It was observed in zebrafish that HOXB3a splv2 and miR-10c were co-transcribed on the same primary transcript too and authors suggested that the expression of HOXB3a might be under the control of global and local enhancers (Woltering and Durston, 2008). The other possibility of expression is amplification of this locus, but it is understood that HOXB9 and miR-196a-1 locus is not amplified in HNSCC cells (N Thakker, K Hunter, personal communication). HOXB9 expression has been shown to be under the control of Wnt signalling pathway in lung cancer (Nguyen et al., 2009), estrogen signalling in breast cancer (Ansari et al., 2011) and PRC1 in angelman syndrome (Zaaroor-Regev et al., 2010). Also, miR-196a expression has been suggested not to be under the control of only elements near HOX genes (Mansfield et al., 2004). However, this transcript could prove to be important therapeutic target as it

could lead to down-regulation in the expression of both HOXB9 and miR-196a in HNSCC.

In this chapter it was shown that HOXB9 is the most over-expressed gene in terms of fold change between all 39 HOX genes. The expression of HOXB9 protein was increased in HNSCC cell line and tissue samples. HOXB9 also increase the migratory, invasive and proliferative potential of HNSCC cells. As HOXB9 and miR-196a-1 are spatially closely related to each other, based on PCR and DNA sequencing it was suggested that this primary transcript exists in HNSCC cells.

Next, the search for novel direct target of miR-196a in HNSCC was undertaken. This was done as miR-196a was highly overexpressed in HNSCC and showed effect on adhesion, migration and invasion. To study how miR-196a was mediating these effects in HNSCC, it was decided to look for its target in this cancer.

Chapter 6: Search for novel miR-196a targets in HNSCC

It has been proposed that miR-196a targets several HOX genes such as HOXB8, HOXC8, HOXA5 and HOXB7 based on experimental and *in-silico* analyses (Yekta et al., 2004, Mueller and Bosserhoff, 2011, Braig et al., 2010, Liu et al., 2012d). However, miR-196a does not only target HOX genes but several other genes such as ANXA1, S100A9, KRT5, SPRR2C, p27 (Sun et al., 2012, Luthra et al., 2008, Maru et al., 2009b). miR-196a, as shown earlier, is over-expressed in HNSCC (Figure 4.1). Transfection with anti-miR-196a leads to decreased adhesion, migration and invasion in HNSCC (Figure 4.7, 4.8 and 4.10), illustrating the pro-tumourigenic phenotype elicited by miR-196a. With these properties in mind, a search for targets of miR-196a in HNSCC was carried out.

The aim of this chapter was to find a direct target for miR-196a in HNSCC. Initially, qPCR was utilised to check for expression of already published targets in other cancers in HNSCC transfected cells. Later, the technique of microarray was performed. Agilent microarray was used with iNOK pre-miR-196a transfected cells and OPM and HNSCC anti-miR-196a transfected cells. To analyse the raw data, Qlucore Omics Explorer was used. To confirm MAMDC2 was direct target of miR-196a in HNSCC, DLRA and SDM was performed.

6.1 Search for targets based on published miR-196a targets

Initially, the targets already published for miR-196a in other cancers were evaluated. This is an appropriate starting point as these were already shown to be targets and were assessed in target prediction database called TargetScan (http://www.targetscan.org/). Hence, they were good candidates to be direct targets of miR-196a in HNSCC. There was no attempt made to validate any published HOX genes as miR-196a targets as in the screening for 39 HOX genes expression (Figure 5.1), none of them were down-regulated compared to normal which suggested that none were being targeted by miR-196a. Hence, other published targets such as Keratin 5 (KRT5), Annexin A1 (ANXA1) and S100 calcium binding protein A9 (S100A9) were pursued in cells transfected with anti-miR-196a to assess if any of them could be validated as possible miR-196a targets in HNSCC. It was observed KRT5 (Figure 6.1), ANXA1 (Figure 6.2) and S100A9 (Figure 6.3) showed no significant difference of expression between anti-miR-196a transfected cells compared to negative control. Hence, to find novel miR-196a target in HNSCC it was decided to perform microarray in B16, D19 and OKF4 transfected cell lines.

6.1.1 Keratin 5 (KRT5)

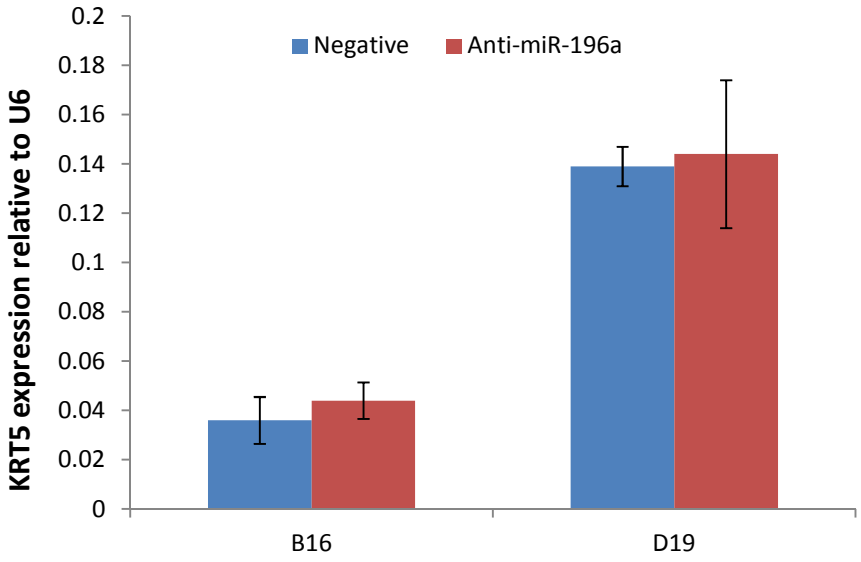

Figure 6.1. KRT5 expression showed no significant difference for B16 and D19 anti-miR-196a transfected cells compared to negative control cells. The data was normalised to internal control U6. The experiment was performed in triplicate. Error bars are representative of SEM. Student's t-test was applied to calculate p-value.

6.1.2 Annexin A1 (ANXA1)

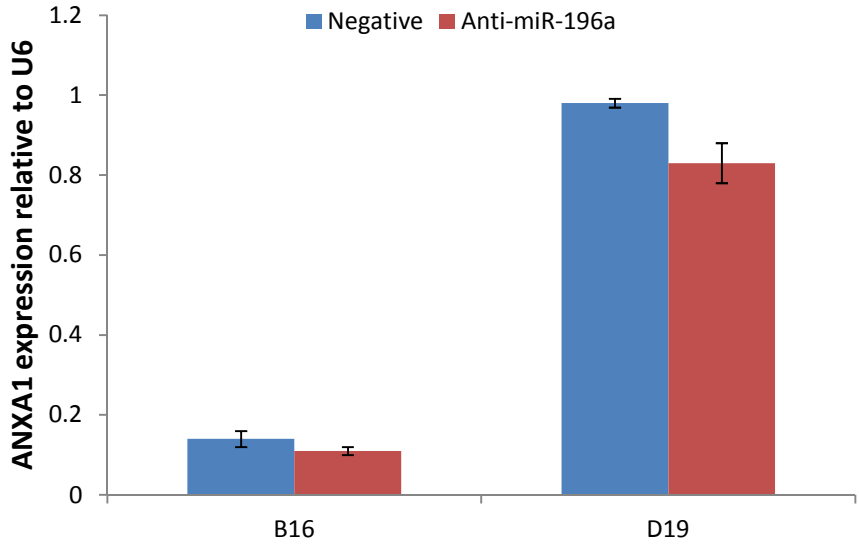

Figure 6.2. ANXA1 expression showed no significant difference for B16 and D19 (p=0.12) anti-miR-196a transfected cells compared to negative control cells. The data was normalised to internal control U6. The experiment was performed in triplicate. Error bars are representative of SEM. Student's t-test was applied to calculate p-value.

6.1.3 S100 calcium binding protein A9 (S100A9)

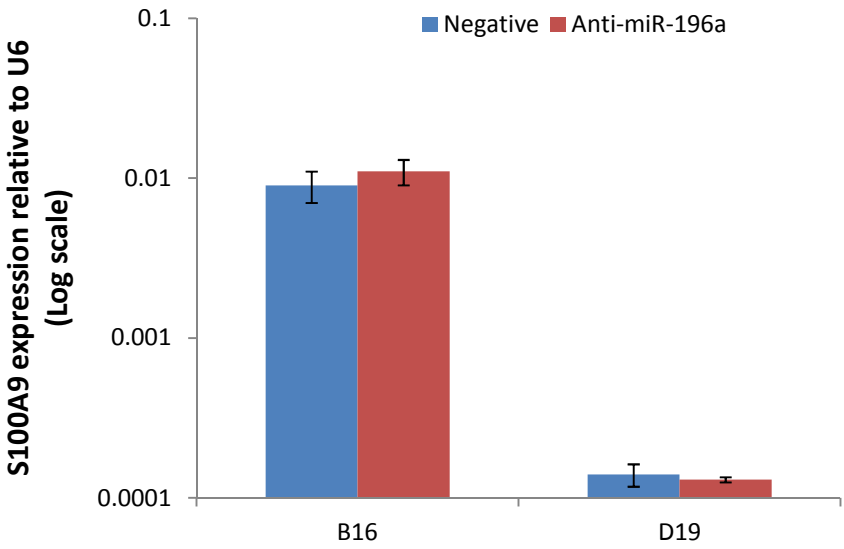

Figure 6.3. S100A9 expression showed no significant difference for B16 and D19 anti-miR-196a transfected cells compared to negative control cells. The data was normalised to internal control U6. The experiment was performed in triplicate. Error bars are representative of SEM. Student's t-test was applied to calculate p-value.

6.2 Agilent Oligonucleotide Microarray

There were few other published targets for miR-196a but after assessing the three best characterised targets in other systems with no success, a better method of finding a target was to look at overall transcriptome changes when miR-196a expression was altered. This approach would also allow for possible identification of novel targets of miR-196a rather than a published target. Hence, a number of different approaches were considered to search for a target of miR-196a. In terms of recent techniques, PAR-CLIP (photoactivable-ribonucleoside cross-linking and immunoprecipitation) (Ascano et al., 2012) and pSILAC (pulsed stable isotope labelling with amino acid in cell culture) (Selbach et al., 2008) were considered. PAR-CLIP had the advantage of assessing the mRNA transcript directly bound with target miRNA and pSILAC had the advantage that, changes at protein level caused by target miRNA could be directly observed, but both techniques were still in early stage of development. Even though the techniques have developed, the bioinformatics analytical techniques required were still lagging behind the technical experiment and due to this it would be difficult to differentiate signal from noise. Furthermore, these techniques are very expensive. Hence, the established technique of expression microarray was selected which would show the changes for whole transcriptome and also had reliable analytical software to analyse the raw data generated. For microarray B16, D19 and OKF4 transfected cells were used and raw data analysed using Qlucore Omics Explorer (Figure 6.7). Based on the data analysis and qPCR of microarray samples, it was observed that MAMDC2 might be a direct target of miR-196a in HNSCC (Figure 6.9). Next, to confirm whether MAMDC2 is a direct target of miR-196a or not in HNSCC, DLRA and SDM were performed.

6.2.1 Samples for microarray

Three different cell lines were used B16 (HNSCC), D19 (OPM) and OKF4 (iNOK) (Table 3.1). B16 and D19 had high expression of miR-196a compared to normal whereas OKF4 had expression similar to normal (Figure 4.1). B16 and D19 cells were transfected with anti-miR-196a and negative control in triplicates whereas OKF4 cells were transfected with pre-miR-196a and negative control in duplicates. This was done so that the opposite effect could be seen in target gene expression in B16 and D19 cells compared to OKF4 cells. The total RNA was then extracted from the transfected cells and analysed for their quality by using Agilent 2100 Bioanalyzer. The samples were then prepared as per the manufacturer's protocol to be mounted and hybridised onto the microarray. This experiment was carried out with the help of Dr. Paul Heath.

6.2.2 RNA quantity and quality

The RNA quantity for all the samples was checked with Nanodrop spectrophotometer and recorded. qPCR was performed to assess the decrease and increase in the expression of miR-196a in B16, D19 and OKF4 transfected cells. The quality of the RNA was based on the RIN (RNA Integrity Number) which is graded from 1-10, 10 being the best quality RNA, and 28s:18s ratio which if higher than 2 is considered good quality RNA. All samples had a RIN of 10 and 28s/18s ratios of more than two (Figure 6.4). This confirms that the total RNA extracted from the transfected cells was of very good quality and hence it could be used for microarray experiment. The samples for microarray were prepared according to manufacturer's protocol (Agilent), hybridised, scanned and raw data collected. This raw data was then loaded into software for data analysis.

A.

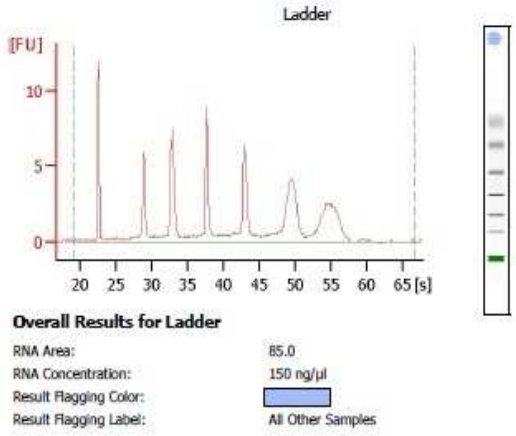

B.

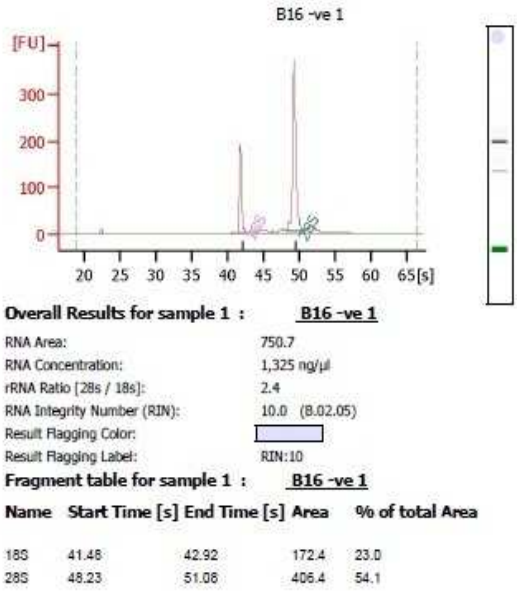

C.

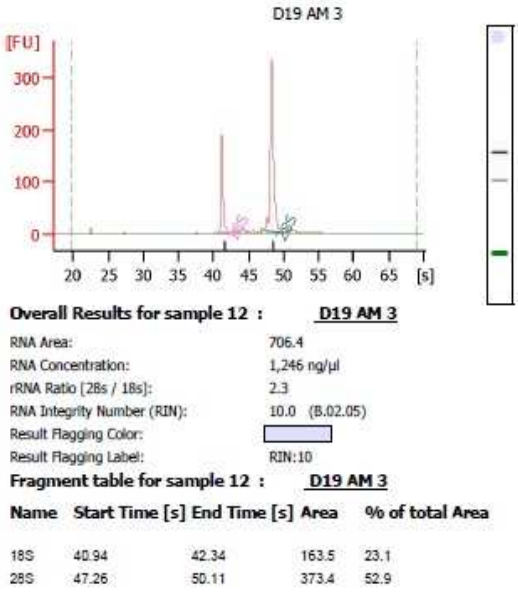

D.

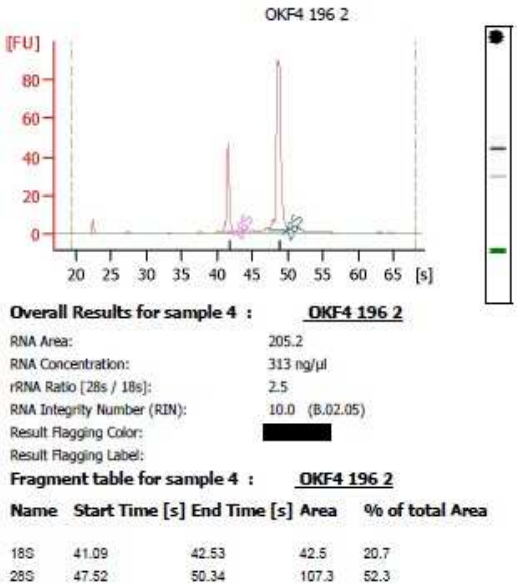

Figure 6.4. Data output from Agilent 2100 Bioanalyzer showing high quality of RNA for a few of the samples based on RIN and 28s/18s ratio. A. Ladder was used as a reference for analysis of data. B. B16 –ve 1 showing 28s/18s > 2 and RIN of 10. C. D19 AM 3 showing 28s/18s > 2 and RIN of 10. D. OKF4 196 2 showing 28s/18s > 2 and RIN of 10. –ve, negative control; AM, anti-miR-196a; 196, pre-miR-196a.

6.2.3 Genespring

Genespring 12 (Agilent) was initially used for microarray raw data analysis. For every cell line transfected, a new experiment was created. The control and transfected sample raw data for each cell line was uploaded in these experiments. Then the sample raw data was normalised based on 75^{th} percentile normalization method for inter-array normalization. Then all the samples were viewed on box plot to assess if all the array data was normalized around zero and to assess if any array data differed a lot from this value. The normalized data was viewed in principal component analysis in three-dimensions to see their clustering. The array data which differed significantly from the clustering for other similar condition arrays was rejected from further analysis, as the data from that array would differ and could lead to obscure results. The normalized data was then subjected to T-test analysis with no multiple hypothesis correction when transfected samples (anti-miR-196a or pre-miR-196a) were compared to negative control samples. There were >3000 genes with significant differential expression ($p<0.05$) in each experiment between transfected and negative control samples. The miR-196a expression in B16 and D19 was highly over-expressed compared to normal cells, whereas the miR-196a expression in OKF4 cells is similar to normal cells (Figure 4.1). Therefore, based on this knowledge search was initiated for genes which were differentially expressed in all three cell lines. There were only 15 genes seen to be differentially expressed, but all of them differed from expected orientation of their expression depending on the cell line (Table 6.1). Hence, only genes which were significantly up-regulated ($p<0.05$) in B16 and D19 cell lines (Table 6.2) were considered further. It was selected to look for genes in B16 and D19 as they are HNSCC and OPM cell lines and hence would have more similarity in their gene expression.

Table 6.1. Expression of 15 differentially expressed genes in B16, D19 and OKF4 cell lines based on Genespring analysis. P-value and fold change shown in appendix 9.4.

GeneSymbol	B16 Transfected v/s control	D19 Transfected v/s control	OKF4 Transfected v/s control
Expected expression directionality	up	up	down
KRTAP6-2	up	down	up
FBXW2	down	up	up
BMP7	down	up	down
AKAP9	up	down	up
AIFM2	down	up	down
IFITM10	down	up	up
PDPN	down	up	down
DIRC2	up	down	up
C6orf154	down	up	down
UNG	down	up	up
ZNF470	down	up	down
WDFY3	up	down	up
TPM1	down	up	down
FMNL3	down	up	down
KCNH5	down	down	down

Table 6.2. List of all the genes over-expressed in B16 and D19 anti-miR-196 transfected cells compared to negative control cells based on Genespring analysis. Highlighted genes are illustrated as examples later in the chapter.

Gene symbol	B16 transfected v/s control	p-value	Absolute fold change	D19 transfected v/s control	p-value	Absolute fold change
GPER	up	0.039	1.465	up	0.029	1.285
LOXL4	up	0.042	1.311	up	0.037	1.091
ERVMER34-	up	0.009	1.259	up	0.008	1.147

1						
TRAPPC9	up	0.008	1.208	up	0.045	1.163
BBS5	up	0.029	1.201	up	0.012	1.147
SMOX	up	0.034	1.193	up	0.025	1.138
ABI3BP	up	0.031	1.192	up	0.014	1.337
HIST1H1C	up	0.014	1.186	up	0.026	1.051
ANKRD33B	up	0.038	1.179	up	0.019	1.117
MMP7	up	0.029	1.177	up	0.011	1.179
EVI5L	up	0.020	1.167	up	0.041	1.225
NSFL1C	up	0.003	1.166	up	0.011	1.146
FBXO42	up	0.044	1.165	up	0.040	1.023
SLCO2B1	up	0.023	1.156	up	0.028	2.414
PSEN1	up	0.021	1.154	up	0.033	1.117
OR7E156P	up	0.008	1.124	up	0.048	1.347
PTPRM	up	0.025	1.120	up	0.044	1.156
PAFAH1B1	up	0.019	1.116	up	0.027	1.242
PIEZO1	up	0.044	1.099	up	0.005	1.215
MED25	up	0.049	1.089	up	0.027	1.104
DBP	up	0.036	1.078	up	0.013	1.306
LOXL1	up	0.040	1.067	up	0.021	1.318
SPECC1L	up	0.010	1.063	up	0.032	1.186
CNDP2	up	0.016	1.053	up	0.027	1.111
ZNF346	up	0.034	1.051	up	0.013	1.198
CCDC50	up	0.036	1.045	up	0.017	1.157
ABCF3	up	0.024	1.039	up	0.028	1.117

6.2.3.1 PSEN1 (Presenilin-1)

This is an example of one of the many genes selected based on the initial parameters to be the putative target of miR-196a. This gene was predicted to be over-expressed in B16 and D19 anti-miR-196a transfected samples compared to negative control samples in Genespring 12 analysis. Based on the pathway analysis, PSEN1 was seen to be part of Notch signalling pathway which was found to be one of the pathways significantly activated ($p<0.05$) when B16 and D19 gene list were compared. The raw data value in B16 was less for anti-miR-196a samples compared to negative control and in D19 it was observed to be similar (Figure 6.5.A and B). PSEN1 was down-regulated in B16 microarray sample and not significantly up-regulated in D19 microarray sample when qPCR was performed on anti-miR-196a and negative control cells (Figure 6.6). Hence, it was decided not to pursue with PSEN1 as a target for miR-196a.

A.

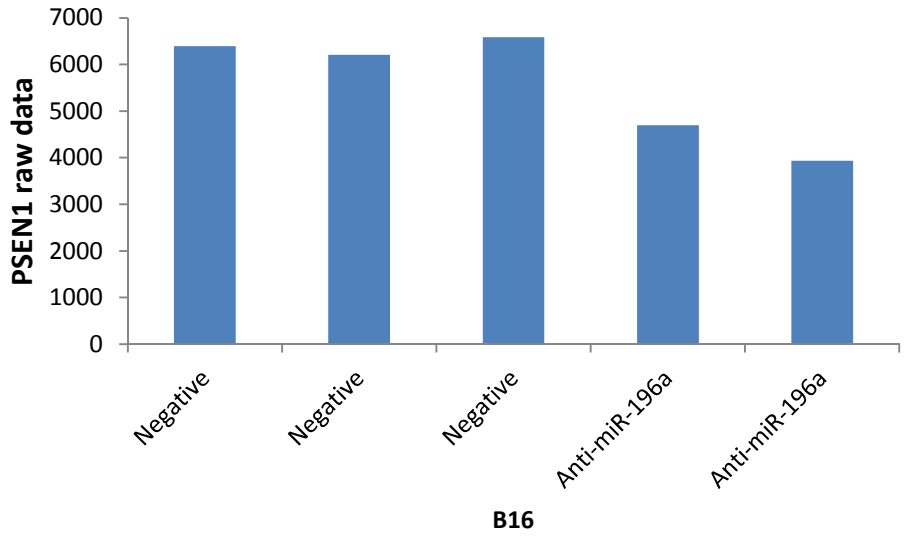

B.

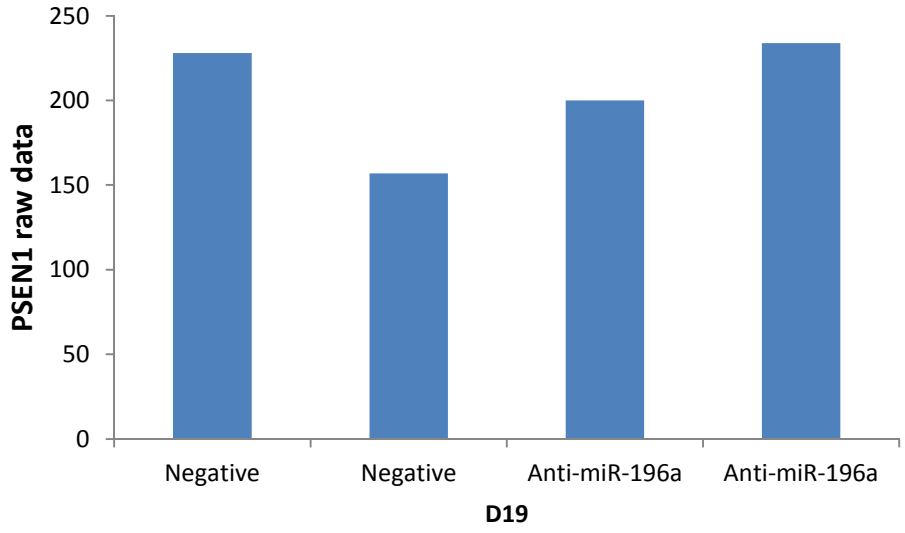

Figure 6.5.A. PSEN1 raw data of B16 microarray samples showing down-regulation for anti-miR-196a samples compared to negative control. B. PSEN1 raw data of D19 microarray samples showing no change for anti-miR-196a samples compared to negative control.

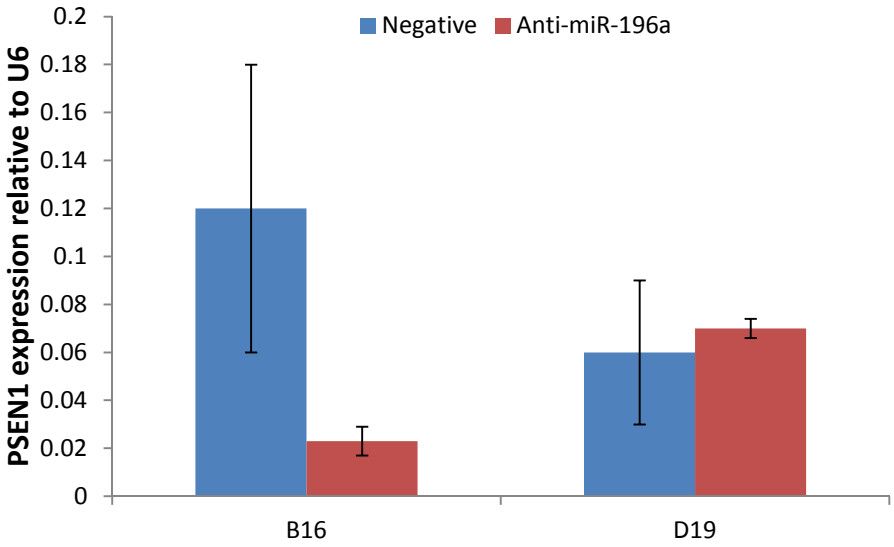

Figure 6.6. PSEN1 expression in microarray samples. PSEN1 expression showed no significant difference in B16 and D19 anti-miR-196a cells compared to negative control cells. The data was normalised to internal control U6. The experiment was performed in triplicate. Error bars are representative of SEM. Student's t-test was applied to calculate p-value.

6.2.3.2 LOXL4 (Lysyl Oxidase-like 4)

LOXL4 is another example of a gene thought to be putative target of miR-196a based on the analysis. The microarray data indicated that LOXL4 was up-regulated ($p<0.05$) in B16 and D19 anti-miR-196a transfected sample compared to negative control based on the Genespring 12 analysis. The raw data for B16 showed that value for anti-miR-196a was lower than negative control samples. The raw data for D19 showed similar value for both anti-miR-196a and negative control samples in microarray samples (Figure 6.7.A and B). The expression of LOXL4 was down-regulated in B16 and D19 anti-miR-196a transfected microarray samples compared to negative control when qPCR was performed on them (Figure 6.8). Hence, LOXL4 was not pursued further as miR-196a target. Similar contradictions were seen for many other putative targets.

The selection criterion was changed and raw data value for each putative target was assessed before performing qPCR. But even then it was observed for genes up-regulated in analysis and in value for raw data for anti-miR-196a transfected samples, when qPCR was performed the expression of the gene was down-regulated or had no difference in anti-miR-196a transfected sample compared to negative control. There was lack of control on the data and its manipulation was difficult due to stringency of each step in Genespring. Due to use of different cell lines, the effect of miR-196a was being over-shadowed by the differences in cell types. This led to not finding right targets based on Genespring analysis as demonstrated. Hence, different software was decided to be used for data analysis.

A.

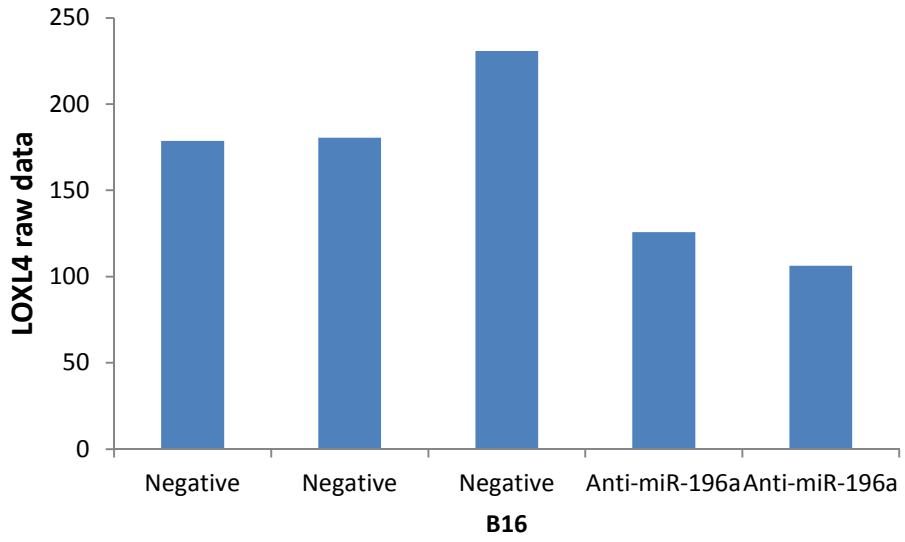

B.

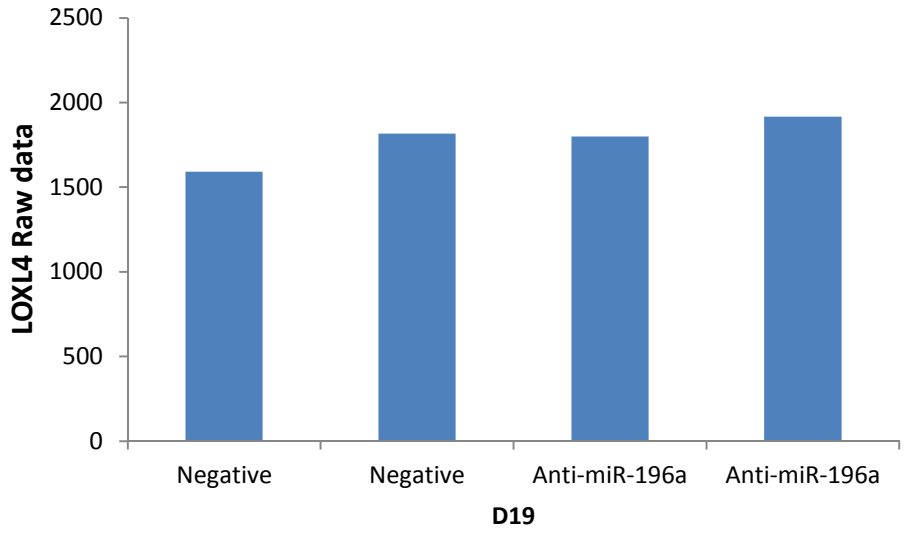

Figure 6.7.A. LOXL4 raw data of B16 microarray samples showing down-regulation for anti-miR-196a samples compared to negative control. B. LOXL4 raw data of D19 microarray samples showing no change for anti-miR-196a samples compared to negative control.

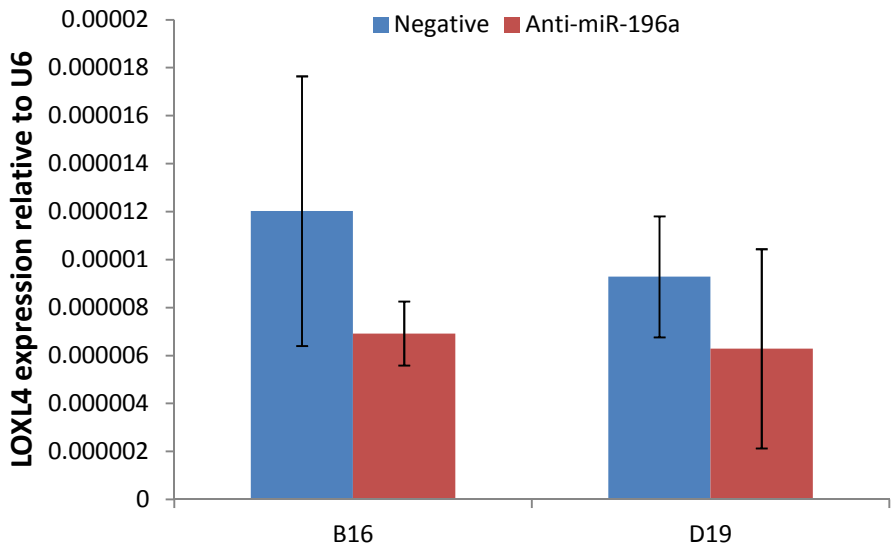

Figure 6.8. LOXL4 expression in microarray samples. LOXL4 expression showed no significant difference in B16 and D19 anti-miR-196a cells compared to negative control cells. The data was normalised to internal control U6. The experiment was performed in triplicate. Error bars are representative of SEM. Student's t-test was applied to calculate p-value.

6.2.4 Qlucore Omics Explorer

The difficulties faced with Genespring led to meeting with Dr. Paul Heath and Dr. Jonathan Cooper-knock. Based on their suggestions, the data was re-analysed using Qlucore Omics Explorer (Qlucore, Lund, Sweden), a software for microarray data analysis. Dr. Jonathan Cooper-knock helped with the analysis of the data with Qlucore Omics Explorer.

The raw data from all the three cell lines for negative control and transfected samples was loaded into the software. There were two groups made to compare the data against each other. B16 and D19 anti-miR-196a transfected samples and OKF4 negative control samples were grouped together (Group 1), whereas B16 and D19 negative control samples and OKF4 pre-miR-196a transfected samples were grouped together (Group 2). The raw data was then normalised using 75^{th} percentile shift method. The normalised data for all the samples was viewed on PCA to check for the clustering of different samples in each group. Then to analyse this data, T-test was applied and the p-value was set to $p<0.01$. The cell-type was eliminated to mean-centre each sample over each sub-group defined by its cell type. Based on this analysis, there were 353 genes found which varied significantly between the two groups (Appendix 9.3). Then top 100 genes were selected by setting the standard deviation to 0.44 and it contained 50 up-regulated and down-regulated genes (Figure 6.9). Then each gene from this list was assessed if they had putative miR-196a binding site in their 3'UTR and to do this we utilised online software called miRWalk (http://www.umm.uni-heidelberg.de/apps/zmf/mirwalk/). The up-regulated genes from the list were first assessed and the genes which had putative binding site were selected to perform further qPCR based analysis on microarray samples.

6.2.4.1 Raw data analysis

In terms of treatment, yellow boxes represent the group of B16 and D19 negative control samples and OKF4 pre-miR-196a samples, whereas blue boxes represents group of B16 and D19 anti-miR-196a samples and OKF4 negative control samples. There is good segregation of the gene expression signature based on the treatment they belong to. It can be observed that MAMDC2, HOXC8, ZFHX4 and RFC3 were not only part of top 20 up-regulated targets but also were predicted to be putative targets of miR-196a based on *in-silico* analysis in miRWalk software. Though, when 3'UTR of these genes were checked for putative miR-196a binding site in www.microrna.org it was found that ZFHX4 and RFC3 had no binding sites but MAMDC2 and HOXC8 had 1 and 3 respectively (Table 6.3). Based on this analysis, qPCR was performed on microarray samples to check the orientation and extent of change in expression of these two genes in all three cell lines. It was observed that both HOXC8 (Figure 6.10) and MAMDC2 (Figure 6.11) showed expected orientation and significant change in expression in transfected cells compared to negative control.

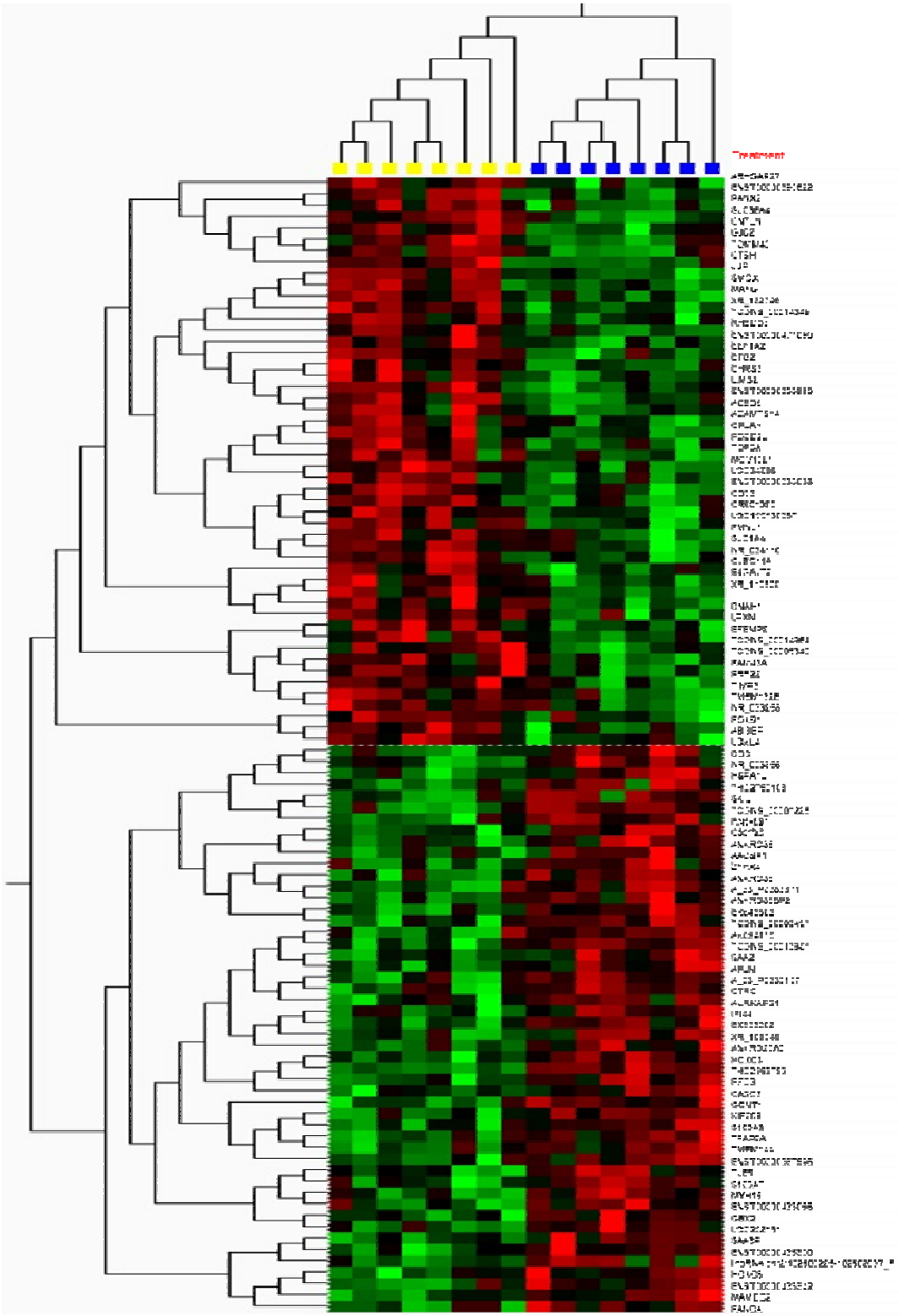

Figure 6.9. Heat Map representing Top 100 (up-regulated and down-regulated) variable genes between two groups.

Table 6.3. List of top 20 up-regulated putative targets between two groups. It also represents the hits in miRWalk and number of miR-196a binding sites in the 3'UTR of the genes based on prediction from www.microrna.org. Variance value for each gene shown in Appendix 9.5.

Top 20 putative targets (up-regulated)	Hits in miRWalk	No. of miR-196a sites
CASC5	0	0
S100A7	0	0
APLN	0	0
DDC	0	0
MAMDC2	3	1
IFI44	0	0
CTRC	0	0
SKIL	0	0
ZFHX4	1	0
S100A8	0	0
C5orf23	0	0
HSPA1L	0	0
KIF20B	0	0
HOXC8	5	3
ANKRD36BP2	0	0
SAA3P	0	0
LOC202181	0	0
RFC3	1	0
ANKRD36	0	0
AURKAPS1	0	0

6.2.4.2 HOXC8 (Homeobox C8)

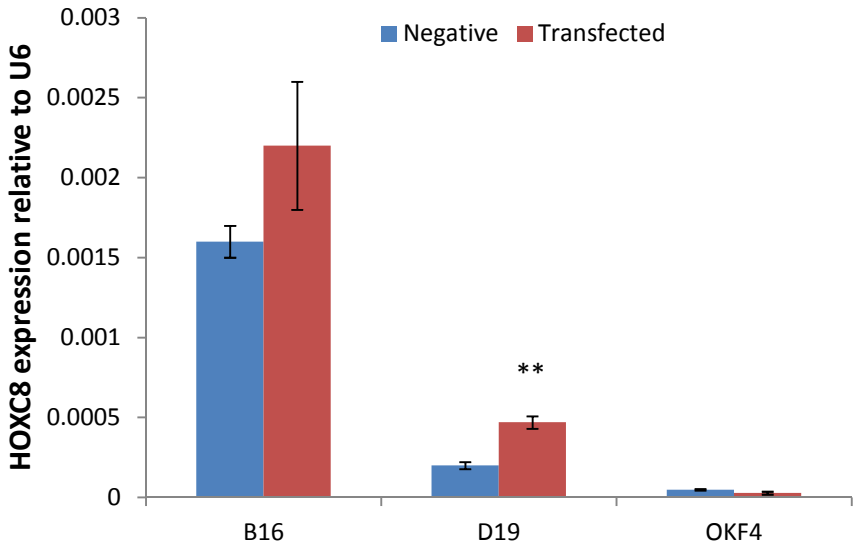

Figure 6.10. HOXC8 expression showed significant up-regulation in D19 anti-miR-196a cells compared to negative control cells, with no significant effect in B16 and OKF4 cells. The expression observed in three cell lines was as expected to be seen. The data was normalised to internal control U6. The experiment was performed in triplicate. Error bars are representative of SEM. Student's T-test was applied to calculate p-value. **, $p<0.01$.

6.2.4.3 MAMDC2 (MAM containing Domain 2)

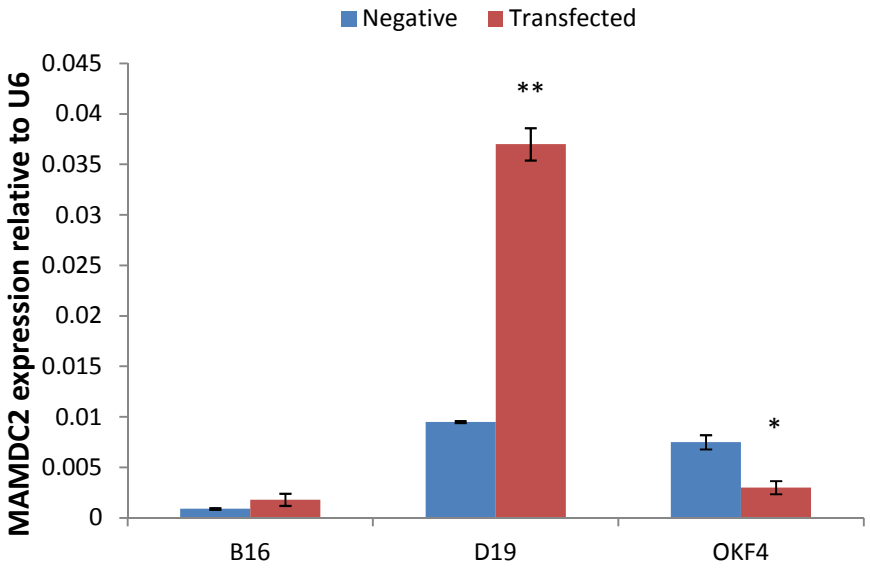

Figure 6.11. MAMDC2 expression showed significant up-regulation in D19 anti-miR-196a cells and down-regulation in OKF4 pre-miR-196a transfected cells compared to negative control cells with no significant effect in B16 cells. The expression observed in three cell lines was as expected to be seen. The data was normalised to internal control U6. The experiment was performed in triplicate. Error bars are representative of SEM. Student's T-test was applied to calculate p-value. *, p<0.05; **, p<0.01.

6.3 DLRA (Dual Luciferase Reporter Assay)

Initially, for this experiment only MAMDC2 was pursued as HOXC8 has already been shown to be direct target of miR-196a in melanoma and breast cancer (Li et al., 2010, Mueller and Bosserhoff, 2011) and MAMDC2 was a novel putative target. Based on DLRA and SDM data, it was confirmed that MAMDC2 was a direct target of miR-196a in HNSCC (Figure 6.13). Based on the data analysis and qPCR of microarray samples, it was hypothesized that MAMDC2 and HOXC8 were direct targets of miR-196a in HNSCC. DLRA was utilised to address this hypothesis only for MAMDC2. In DLRA, a vector containing luciferase gene with multiple cloning sites (MCS) in its 3'UTR is cloned with putative target 3'UTR and this construct with mature miRNA or negative control is transfected into cells. If the luminescence value is significantly lower for mature miRNA transfected cells compared to negative control transfected cells then it would mean the miRNA directly degrades or represses the target gene.

6.3.1 Vector Construction

pMIR REPORT vector was selected for cloning of 3'UTR of the target gene as it was a validated miRNA expression reporter system vector (Figure 6.12.A). It contains firefly luciferase gene, which is under the control of a mammalian promoter and terminator. Downstream of luciferase translation sequence there were multiple cloning sites (MCS) for insertion of target gene 3'UTR. Also, pMIR REPORT vector has been published for use of miRNA target validation in several papers (Liu et al., 2012c, Hunt et al., 2011, Chen et al., 2011b). pMIR REPORT vector also contained an ampicillin resistance cassette.

The wild-type MAMDC2 3'UTR (wt) was cloned into pMIR REPORT vector as per the strategy (Figure 6.12.B) and cloning method described in section 3.16. The miR-196a binding site in the MAMDC2 3'UTR was mutated using site-directed mutagenesis to give mutated MAMDC2 3'UTR (mutated) and cloned into pMIR REPORT vector as described in section 3.16.1. Based on DLRA, it was observed that the relative luminescence of wt vector co-transfected with pre-miR-196a was significantly decreased compared to wt vector co-transfected with negative control. There was no significant difference in relative luminescence of mutated vector co-transfected with pre-miR-196a and mutated vector co-transfected with negative control (Figure 6.13).

A.

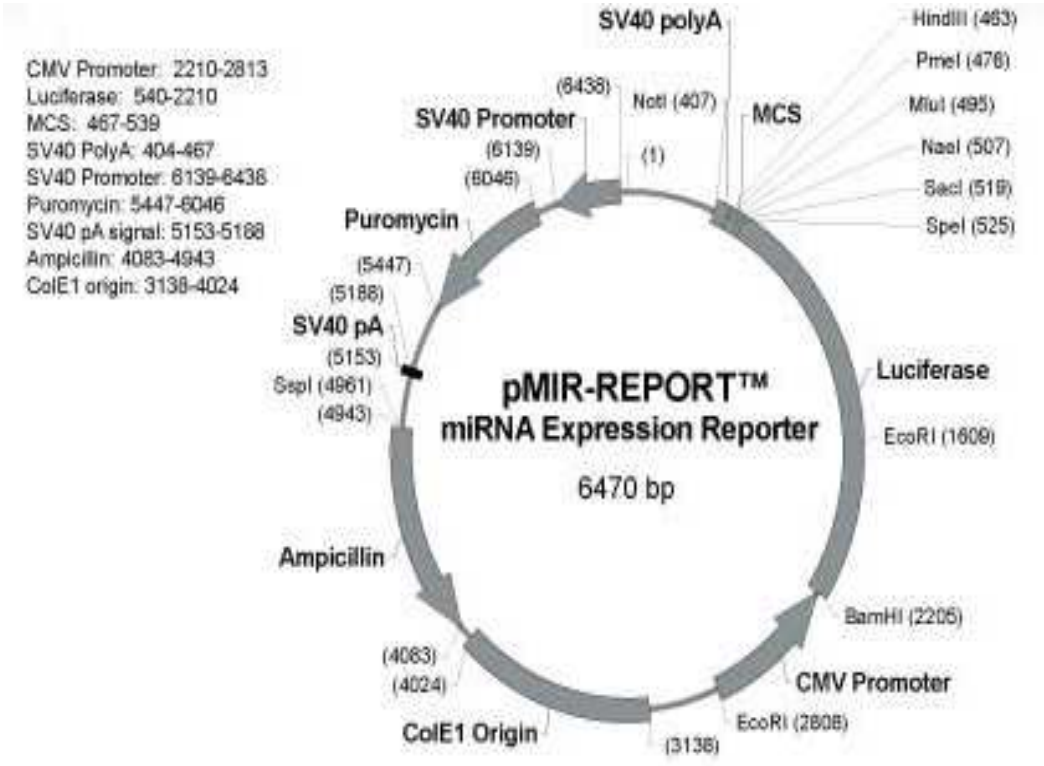

B.

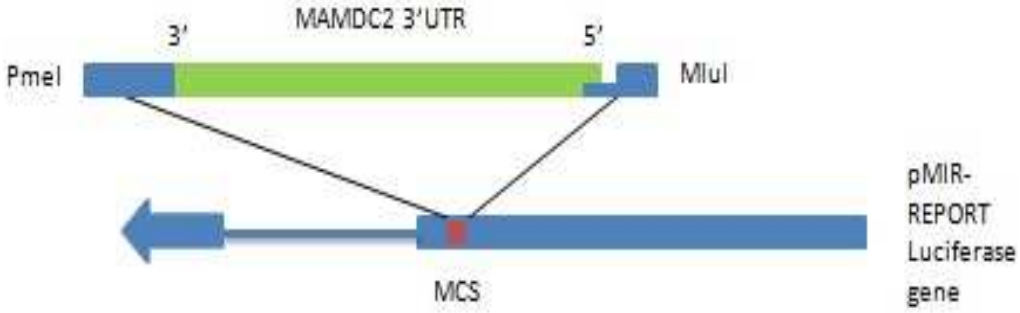

Figure 6.12.A. figure representing backbone of pMIR REPORT vector (http://products.invitrogen.com/ivgn/product/AM5795**). B. Strategy for cloning of MAMDC2 3'UTR in the MCS of pMIR REPORT vector.**

6.3.2 Wild type (wt) and site-directed mutagenesis (SDM)

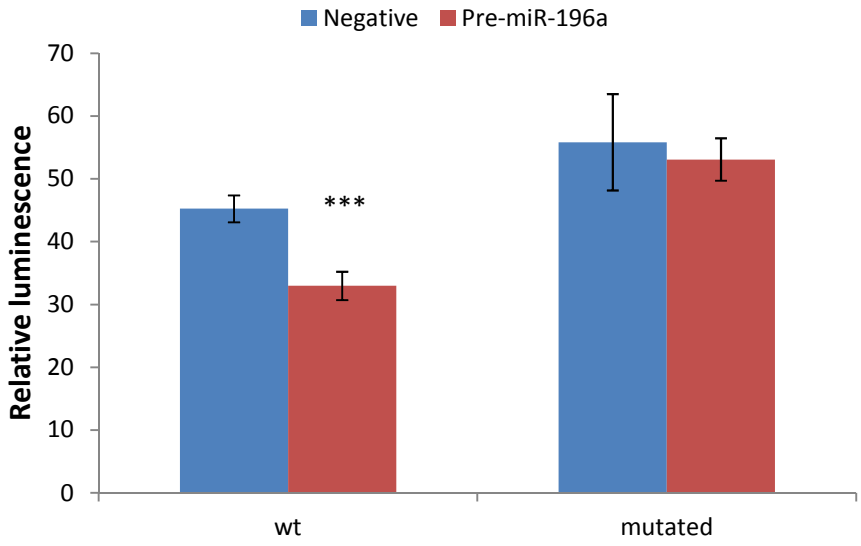

Figure 6.13. Relative luminescence (firefly/renilla) showed significant decrease in B16 cells transfected with wt MAMDC2 3'UTR, pRL-TK (renilla luciferase control vector) and pre-miR-196a compared to negative control transfected whereas B16 cells transfected with mutated MAMDC2 3'UTR showed no effect. The transfected cells were incubated for 48 hr. pRL-TK was used as an internal control for luminescence. The experiment was performed in triplicates and repeated thrice. Error bars are representative of SEM. Student's T-test was applied to calculate p-value. ***, $p<0.001$.

6.4 Discussion

miR-196a is highly expressed in HNSCC when compared to NOK. In most cancers where miR-196a was observed to be over-expressed, a target gene was also identified. In, NSCLC (non-small cell lung carcinoma) high miR-196a expression leads to down-regulation of HOXA5 (Liu et al., 2012d), in oesophageal adenocarcinoma miR-196a targets KRT5, S100A9 and SPRR2C (Maru et al., 2009b) and also in gastric cancer where miR-196a expression is increased, it targets p27(kip1) (Sun et al., 2012). Hence, it was thought that due to high expression of miR-196a in HNSCC that it might be targeting a gene or genes. The search for miR-196a targets in HNSCC was initially based on the published targets and for this expression of KRT5, S100A9 and ANXA1 were assessed in anti-miR-196a and negative control samples, but it was found that in HNSCC, miR-196a did not target these genes as there was no consistent change in expression. These genes were observed to be targets of miR-196a in oesophageal adenocarcinoma, which is different cancer than HNSCC with different genetic changes happening and hence showed differential effect on these targets by miR-196a. This illustrates the heterogeneity between different cancers. For most of these genes in the paper they were suggested to be targets of miR-196a, they were assessed using qPCR. Hence, to be more effective in our approach, qPCR data was used to check for difference in expression and if there was no significant change then the gene was not pursued further. Though, it would have been a good positive control to use an esophageal cancer cell line or breast cancer cell line used in these papers (Luthra et al., 2008, Maru et al., 2009a). Hence, it was decided that a look at whole transcriptome for change in gene expression signature was better way of finding targets for miR-196a than assessing every published target.

Different techniques were considered for search of miR-196a target in HNSCC. Even though PAR-CLIP (Ascano et al., 2012) and pSILAC (Selbach et al., 2008) are up-

coming methods of identifying the targets of microRNA, still they have drawbacks of being difficult to analyse, having high noise or not covering entire proteome in case of pSILAC. Briefly, PAR-CLIP works by incorporation of photoactivable thioribonucleoside and then by inducing crosslinks by using UV-365 which is then precipitated using immunoprecipitation. It is further purified by SDS-PAGE and finally analysed using next-generation sequencing (Ascano et al., 2012). It is known that miRNA exerts its effect either by mRNA degradation or translational repression. It is thought that miRNA binding site architecture relates to whether miRNA leads to mRNA degradation or translational repression. Hence, miRNA can regulate gene expression by direct effect on translation process. In pSILAC, two samples are labelled with two different heavy isotope of essential amino acid which leads to proteins with medium-heavy or heavy isotope. These can then be differentiated using Mass spectrometry for different amount of protein present in the samples (Selbach et al., 2008). Hence, it was decided to use the widely accepted technique of microarray. Microarray also has drawback that miRNA related translation repression changes cannot be detected and changes in protein expression for particular target gene cannot be noted, but it has advantage that it covers whole transcriptome and has reliable analytical software for search of targets (Selcuklu et al., 2012, Gregersen et al., 2012, Chuang et al., 2012). Agilent oligonucleotide microarray (Sureprint G3) was utilised for identification of miR-196a targets. High miR-196a expressing cell lines B16 and D19 were transfected with anti-miR-196a and low miR-196a expressing cell line OKF4 was transfected with pre-miR-196a.

The raw data generated from the microarray experiment was then loaded onto Genespring 12 software for data analysis. The data was normalised, statistical test applied and analysed. The identification of targets turned out to be more difficult based on this approach. PSEN1 and LOXL4 were seen to be over-expressed in B16 and D19

anti-miR-196a samples based on analysis but when qPCR was performed in microarray samples, they were observed to be down-regulated or with no change in expression. Based on their raw data from microarray, it was seen that they were down-regulated. Some other genes which were up-regulated in analysis based on Genespring, did not even reach threshold florescence level to be detected in terms of their raw data when checked (data not shown). One of the biggest setbacks with Genespring software is that cell type cannot be eliminated and as three different cell lines were used it influences the data analysis and possibility of false positive results increases. As there was no way of eliminating cell type, it was not possible to group different cell types together to get more dynamic analysis. Hence, it was decided to source different software for data analysis of microarray.

Qlucore Omics Explorer was utilised next to analyse the microarray data. The transfected and negative control samples were separated into two groups as described earlier for data analysis. The data was normalised and then viewed on 3d-axis by principal component analysis (PCA) to check for segregation of the samples on the axis. T-test was used as the statistical test with $p<0.01$. T-test like all other statistical tests have drawback of generating false positive results and hence certain correction methods like Bonferroni correction can be used to reduce the number of false positives. Bonferroni corrections in the analysis was not used as it is a very stringent correction and after the experience with Genespring, it was decided to go without correction method but to validate putative targets by performing qPCR on microarray samples. Also instead of using $p<0.05$, it was decided to use $p<0.01$ which would also reduce the number of false positives. During analysis, cell-type eliminate function was used which was the major difference between the two analyses from Genespring and Qlucore which was the principal component in Genespring and hence did not give accurate data. But in Qlucore because cell type was eliminated, the principal component was shifted to just

difference in expression of genes. Cell-type eliminate function allowed the expression across different cell lines to be averaged and then to look at real difference in expression of different genes in the two groups. HOXC8 and MAMDC2 were recognised to be putative targets with miR-196a binding sites in their 3'UTR. Hence, qPCR was performed on the microarray samples to assess for expression of HOXC8 and MAMDC2. The orientation and significant change in expression of transfected cells compared to negative control cells for HOXC8 and MAMDC2 was what was expected to be seen, even though not all samples showed significant difference and hence it was thought they both could be direct targets of miR-196a in HNSCC. As HOXC8 was already shown to be target of miR-196a in melanoma and breast cancer (Mueller and Bosserhoff, 2011, Li et al., 2010), it was decided to first pursue MAMDC2.

Dual luciferase reporter assay have the advantage of being rapid, accurate and easy to interpret. Their short-coming is that these are based on artificial system and transient in nature, hence long term effect cannot be studied (Alcaraz-Perez et al., 2008). Based on the DLRA experiment, MAMDC2 was shown to be a direct and novel target of miR-196a in HNSCC. Western blots for MAMDC2 with normal, OPM and HNSCC cell lines was attempted but did not give any bands on the blot which can be more attributed to the quality of antibody. The protein from the gel had transferred onto membrane based on the β-actin bands being detected on the same blot (Data not shown). MAMDC2 is a gene which has not been studied to any extent in any disease. Based on the information from the family members, MDGA1 (MAMDC3) and MDGA2 (MAMDC1), it contains MAM domain (Meprin, A5 protein, receptor protein-tyrosine phosphatase μ) and immunoglobulin domains which are structural features of cell adhesion molecules. It is well known that alterations in adhesion to extracellular matrix plays important role in the outcome of cancer. It was shown that increased expression of integrin β1 was related to increased lymph node and lung metastasis in HNSCC (Wang

et al., 2012). miR-124 targets Integrin β1 in OSCC which leads to reduced adherence and motility in OSCC cells (Hunt et al., 2011). In oral squamous cell carcinoma it was noted that as cancer became less differentiated the expression of collagen IV was reduced (Agarwal and Ballabh, 2013). MDGA1 has been implicated in decreasing the adhesion with extracellular matrix proteins in kidney cells (Diaz-Lopez et al., 2010). When anti-miR-196a was transfected into HNSCC cells, there was reduction in adhesion to fibronectin. Though not conclusive, miR-196a might be mirroring its effect of reducing adhesion through MAMDC2 regulation. MDGA1 plays role in migration of cortical neurons to upper cortical layer (Ishikawa et al., 2011). Even though here MDGA1 was involved in migration of cells, it has to be considered that it was in neural cells and during developmental phase. MDGA1 or MDGA2 have not been studied in cancer cells or in developed cells and hence it is difficult to judge what effect MAMDC2 will have in terms of migration.

In this chapter, initially, search for target of miR-196a was undertaken based on published targets but to no avail. Hence, it was decided to search for novel target by use of microarray technique. Based on analysis of raw data, MAMDC2 was narrowed down as one of the putative targets of miR-196a. It was later confirmed by DLRA and SDM that MAMDC2 was a novel direct target of miR-196a in HNSCC.

Chapter 7: Discussion

The aims set out for this project were:

1. To assess the expression of miR-196a in cell lines and tissue samples and to observe the functional effects it had in HNSCC.

2. To assess the expression of HOXB9 in cell lines and tissue samples and to note the functional effects it had in HNSCC.

3. To show that miR-196a-1 and HOXB9 were co-transcribed on same primary transcript in HNSCC.

4. To search for novel direct target of miR-196a in HNSCC.

7.1 miR-196a is over-expressed and MAMDC2 is a novel direct target of miR-196a in HNSCC

Based on the unpublished preliminary data from affymetrix miRNA microarray, it was observed that miR-196a was over-expressed in HNSCC cell lines compared to NOKs. It was noted based on qPCR data that miR-196a was over-expressed in HNSCC cell lines and tissue samples compared to NOKs and normal tissue samples respectively (Chapter 4). It was also observed that miR-196a increased migration, invasion and adhesion in HNSCC cells with no effect in proliferation (Chapter 4). By using Agilent oligonucleotide microarray, it was shown that MAMDC2 was a putative target of miR-196a in HNSCC based on raw data and *in-silico* analysis, which was confirmed to be direct target based on dual luciferase reporter assay data using wild-type and mutated 3'UTR (Chapter 6).

7.2 HOXB9 is over-expressed in HNSCC

Based on the microarray data from paper published in 2006, it was observed several HOX genes were over-expressed in HNSCC cell lines (Hunter et al., 2006) (http://bioinformatics.picr.man.ac.uk/vice/PublicProjects.vice?pager.offset=15).

Initially, qPCR was performed for all 39 HOX genes in HNSCC cell lines and NOKs and it was observed that HOXB9 was most aberrantly expressed. It was noted that HOXB9 was over-expressed in HNSCC cell lines compared to NOKs. HOXB9 protein was also over-expressed in HNSCC cell lines and tissue samples compared to NOKs and normal tissue samples, respectively. HOXB9 was shown to increase the migration, invasion and proliferation of HNSCC cells. Adhesion showed statistical significance but was probably not biologically significant (Chapter 5).

7.3 HOXB9 and miR-196a-1 are co-transcribed on same novel primary transcript

HOXB9 and miR-196a-1 are spatially closely related to each other on chromosome 17 and were hypothesised to be co-transcribed on same primary transcript based on *in-silico* analysis in a paper published in 2007 (Mainguy et al., 2007). It was shown that miR-196a-1 and HOXB9 were indeed co-transcribed on same novel primary transcript based on nested PCR (Chapter 5).

7.4 Implications and Future work

miR-196a has been observed to be over-expressed in gastric, oesophageal, lung and oral cancer (Sun et al., 2012, Luthra et al., 2008, Liu et al., 2012d, Liu et al., 2012a) but also was down-regulated in melanoma (Braig et al., 2010). HOXB9 was over-expressed in breast, lung, colorectal, hepatocellular and oral cancer (Hayashida et al., 2010, Calvo et al., 2000, Kanai et al., 2010, Hassan et al., 2006) but was also down-regulated in gastric cancer (Sha et al., 2013). This variation in expression of miR-196a and HOXB9 in

different cancers shows that each cancer and its expression of a gene and miRNA can differ between individuals and between different cancers. Hence, when looking at a gene or miRNA as a therapeutic option, it can be targeted towards only specific cancer and may not apply to all cancers in general. For miR-196a, it was observed based on expression in cell lines that its expression was higher in some OPM cell lines compared to HNSCC cell lines. The transcriptional profiles of all the OPM and HNSCC cell lines used in this project have been published and it was observed that the profile of OPM and HNSCC cells varied from each other (Hunter et al., 2006). But as there is no set transcriptional profile for HNSCC cells, it would be hard to say whether OPM cells were more dysplastic or had already assumed HNSCC characteristics genetically. It would be interesting to see if this over-expression of miR-196a is true for Oral Pre-malignant Lesions (OPL) samples, as it could mean that aberrant miR-196a expression in HNSCC is an early event and could mean miR-196a is involved in oncogenesis of HNSCC. miR-196a was also noted to be over-expressed in plasma of OSCC patients pre-operative (Liu et al., 2012a). It is always good to find non-invasive methods for diagnosis. Based on this, it will be useful to assess if miR-196a is secreted into saliva and whether it is over-expressed in potentially malignant oral lesions and HNSCC patients compared to healthy individual. Similarly it would be intriguing to note the expression of HOXB9 protein in OPL tissue samples even though there was not much difference seen in HOXB9 RNA expression between OPM and HNSCC cell lines. It will also be interesting to increase the cohort of patient tissue samples used for the study and to use matched cancer and normal tissue samples to study the expression of miR-196a and HOXB9 in HNSCC.

It is also important to study the clinical outcome of miR-196a and HOXB9 over-expression in terms of overall survival rate, disease-free survival rate and lymph node metastasis in HNSCC. It was observed that over-expression of miR-196a was correlated

to worse prognosis and survival in OSCC patients (Liu et al., 2012a). In NSCLC, higher miR-196a expression was related to advanced pathological stage and metastasis to lymph node (Liu et al., 2012d). HOXB9 in breast cancer was seen to be a prognostic factor for overall survival rate and disease-free progression, with HOXB9 positive tumour having worse prognosis (Seki et al., 2012). HOXB9 was observed to be an independent prognostic factor in gastric cancer and lower expression of HOXB9 in these tumours led to worse overall survival rate (Sha et al., 2013). It will also be useful to assess the effect of miR-196a and HOXB9 over-expression in patients undergoing therapy, whether it leads to any resistance to therapy or not. Based on these parameters, HOXB9 and miR-196a could be validated into biomarkers for early detection of HNSCC and also to predict the prognosis on diagnosis.

miR-196a when over-expressed in OSCC led to increased migration of these cells (Liu et al., 2012a). miR-196a was also seen to promote migration and invasion in gastric cancer where it was over-expressed (Tsai et al., 2012). At the same time, reduced miR-196a expression was also related to increased migration in melanoma, due to increased expression of HOXB7 and BMP4 (Braig et al., 2010). HOXB9 when over-expressed in breast cancer led to increase in proliferation, angiogenesis, migration and invasion. HOXB9 was also observed to increase EMT in breast cancer cells. HOXB9 over-expression was also shown to decrease the disease free survival in breast cancer patients based on multivariate analysis (Hayashida et al., 2010, Seki et al., 2012). HOXB9 was also noted to promote radio resistance in breast cancer cells (Chiba et al., 2012). On the other hand, HOXB9 down-regulation was related to decrease in overall survival in gastric cancer patients with reduced expression of HOXB9 linked to cancer progression and metastasis in gastric cancer (Sha et al., 2013). These examples of functional effects based on over-expression or down-regulation of miR-196a or HOXB9 re-iterate the point that care should be taken in administration of therapy in each cancer as each

cancer and patient might respond differently to the therapy, that is individualisation of therapy.

Transient transfection method was used for over-expression and down-regulation of miR-196a and HOXB9. Transient transfection leads to only transient down or up-regulation of miRNA or gene of interest as siRNA do not integrate into the genome. Also, transient transfection material can be lost due to environmental factors or cell doubling time (Kim and Eberwine, 2010, Dykxhoorn et al., 2003). As the transfection time in the experiments was 48 hr with further time depending on the assay it could be thought that the effect of siRNA might be lost by then. MTS proliferation assay has advantages such as ease in setting up and measuring and quantifying colorimetric data. But it has two major drawbacks such as giving false-positive result if there are any aspects that affect metabolic process and differentiating cell cycle inhibition or cell death (Smith et al., 2011b). Even though, migration and invasion both contribute towards metastasis in cancer, they both are separate features which may contribute to metastasis. Migration is defined as the cell movement along basal membrane with no obstruction and occurs on 2D surfaces. Invasion is defined as movement of cell through 3D extracellular matrix which involves change in cellular morphology, migration and proteolysis of extracellular matrix (ECM) by matrix metalloproteases (MMPs) (Kramer et al., 2013). Invasion needs activation of several different pathways which leads to changes in cells which help it to invade such as NF-κβ pathway (Rehman and Wang, 2008) and EGFR and MAPK pathway (Zhang et al., 2004). Similar pathways such as PI3K/Akt, EGFR and MAPK were also needed for induction of MMP9 in HNSCC (P et al., 2004). Similarly, migration needs activation of other pathways such as hedgehog signalling pathway and PI3K/Akt pathway (Fyffe and Falasca, 2013). Migration and invasion assays for anti-miR-196a and HOXB9 siRNA transfected cells were carried out in transwell membranes. There are several advantages to using these assays such as

ease of setting up these assays, short chemoattractant exposure and availability of different pore size membranes. However, there are disadvantages too such as the cells are migrating or invading without the use of adhesion or attachment which gives them rounded morphology, the chemoattractant and layer of ECM used are not necessarily distributed equally and also these assays only give 2D view, but these are most widely used migration and invasion assays (Kramer et al., 2013).

As it was observed for both HOXB9 and miR-196a that they promoted invasion *in-vitro*, it would have been good to look at known invasion markers such as expression of E-cadherin, β-catenin (Hayashida et al., 2010, Tanaka et al., 2002) and vimentin (Miao et al., 2014) in the tissue samples used for LCM and TMA used for HOXB9. It would be interesting to see when HNSCC cells are stably transfected with lentivirus expressing anti-miR-196a or HOXB9 siRNA, would the results be same in organotypic models (Jenei et al., 2011) or when xenografted onto mice as these experiments give more dynamic and similar results to what would happen *in-vivo* and may give an idea of metastasis too. It can also be used to analyse whether miR-196a or HOXB9 can cause tumourigenesis on their own. It would also be intriguing to note what would be the effect of adhesion on anti-miR-196a or HOXB9 siRNA transfected cells towards other extracellular matrix proteins.

The presence of HOXB9 and miR-196a-1 primary transcript meant that it might be contributing to expression of HOXB9 and mature miR-196a in HNSCC. It will be useful to disrupt this primary transcript with specific siRNA and assess the expression of HOXB9 and miR-196a to know how much of total expression of HOXB9 and miR-196a is contributed by this primary transcript in HNSCC. It will also be interesting to look at changes in functional effects such as migration, invasion, proliferation and adhesion when primary transcript is knocked-out using specific siRNA. It will

especially be intriguing to note whether knocking-out of this transcript shows similar functional effects as it showed when individual HOXB9 and miR-196a expression was knocked-out. It has already been shown that HOXB9 expression is driven by different promoter sequences and transcription factors such as RING1b in angelman syndrome (Zaaroor-Regev et al., 2010), Wnt/Tcf signalling in lung cancer (Nguyen et al., 2009), retinoic acid in embryonic stem cells (Chambeyron and Bickmore, 2004) and estrogen response elements in breast cancer (Ansari et al., 2011). But there is little known about promoter sequences or transcription factors involved in miRNA expression and even lesser in miR-196a expression. It will be interesting to study which promoter sequences or transcription factors might be involved in the expression of HOXB9, miR-196a and primary transcript in HNSCC.

MAMDC2 has not been studied in terms of its role in humans and its effect in any diseases. As MAMDC2 was shown to be novel direct target of miR-196a in HNSCC, it would be interesting to look at its effects. It will be useful to look at protein expression of MAMDC2 in high miR-196a expressing cell lines and tissue samples compared to low miR-196a expressing cell lines and tissue samples. It will also be interesting to stably transfect high and low miR-196a expressing cell lines with lentivirus expressing MAMDC2 RNA and to observe the changes it causes in functional effects in HNSCC and if it shows any effects opposite to those observed with miR-196a. It will be very interesting to assess which pathways MAMDC2 activates in HNSCC based on the functional assays data.

EGFR is over-expressed in almost all HNSCC when compared to normal but in varying intensity (Kearsley et al., 1990). EGFR based targeted therapy is the only approved personalised therapy in HNSCC (Markovic and Chung, 2012), but varying degree of EGFR expression poses a problem and also underlines the fact that cancers can be

heterogeneous in nature between different patients. Due to this varying degree sometimes the dose of cetuximab can be insufficient to bind all target receptor which leads to reduced efficacy. Also, it has been observed that mutant EGFRvIII expression present in 40% HNSCC cases and can lead to reduced sensitivity to cetuximab (Langer, 2012). The other mechanisms of resistance against cetuximab could be autocrine or paracrine production of ligand, activation of pathway downstream of the receptor or cancer switching to alternative pathway (Morgillo and Lee, 2005). Hence, there is need for other targets for development of personalised therapy in HNSCC. Initially, it was thought miRNAs are fine tuners for the expression of certain genes in the genome. With time more was understood about miRNA biogenesis and its deregulation in cancers. There are several miRNAs now identified which are dysregulated in different cancers such as miR-146a which is thought to be tumour suppressor and is aberrantly expressed in cancers like papillary thyroid, breast, gastric, pancreatic and other cancers (Labbaye and Testa, 2012). miR-196a as explained earlier is over-expressed in several cancers too. Based on our microarray data, it was also observed that putative targets of miR-196a in HNSCC were several transcription factors such as HOXC8, HOXC6, NFYB, GBX2, ZNF273 and others (Appendix 9.3). HOXC8 was already shown to be direct target of miR-196a in breast cancer and melanoma (Li et al., 2010, Mueller and Bosserhoff, 2011). These transcription factors in turn could lead to aberrant expression of several genes they transcribe. This makes miRNAs attractive therapeutic targets and not just to be used as biomarkers. Recently, it has been shown that extracellular vesicles called exosomes can carry miRNA, mRNA and proteins between cells. These exosomes are 30-200 nm in diameter and can lead to functional changes in recipient cells (Marcus and Leonard, 2013). These exosomes are being tested in clinical trials for their viability as therapeutic agents. Dendritic cells derived exosomes were loaded with melanoma-associated antigens and tested for safety, efficacy and feasibility in NSCLC patients. It

was seen that this therapy was well tolerated in the patients and some even showed activation of effectors of immune response (Morse et al., 2005). Hence, this delivery system could be used to deliver anti-miR-196a to HNSCC cells directly which could prove to be therapeutic target in HNSCC, as it already was seen in this study that miR-196a promoted migration, invasion and adhesion.

Depending on how much expression of HOXB9 and miR-196a comes from the primary transcript, it could be a very good target therapeutically as it would reduce the effects of both HOXB9 and miR-196a in HNSCC, simultaneously. The same exosome-based delivery system could be utilised to deliver primary transcript specific siRNA to HNSCC cells.

Due to the high expression of HOXB9 in HNSCC, it is likely, that silencing the expression could lead to therapeutic effects in HNSCC. It was shown that HXR9, a synthetic short peptide, could disrupt the dimerization of HOX/PBX in breast cancer and had therapeutic effects in this cancer as it led to apoptosis and its sensitivity could be determined based on average expression of HOXB1 through HOXB9 in each cancer sample, proving to be useful biomarker for HXR9 activity (Morgan et al., 2012). Similarly, it was also shown that HXR9 leads to apoptosis in ovarian cancer cell lines and tumour growth is retarded *in-vivo* (Morgan et al., 2010), though, it has also been observed that HOXB9 does not need PBX as co-factor to interact with binding sequence in mouse (Pan et al., 2001). Despite that example shows that interaction between HOXB9 and its co-factor can be disrupted with either a synthetic peptide or small molecule inhibitor in HNSCC. HOXB9 protein could also be directly targeted with small molecule inhibitors which interfere with homeodomain binding to DNA for example and could lead to therapeutic effects in HNSCC. HOXB9 RNA could also be

targeted with specific siRNA using exosomes-based therapy in HNSCC which would eventually lead to decreased HOXB9 protein expression.

This study has shown that MAMDC2 is a novel direct target of miR-196a in HNSCC and also re-iterated that miR-196a was over-expressed and promoted migration, invasion and adhesion. This is the first study in HNSCC to establish that HOXB9 protein is over-expressed and leads to increase in migration, invasion and proliferation. It also showed that HOXB9 and miR-196a-1 are co-transcribed on same novel primary transcript. Even though further work is still required based on this study, it opens the avenue to utilising miR-196a and HOXB9 as biomarker and therapeutic targets in HNSCC.

Chapter 8: References

1. ABATE-SHEN, C. 2002. Deregulated homeobox gene expression in cancer: cause or consequence? *Nat Rev Cancer,* 2**,** 777-85.
2. ABRAHAO, A. C., GIUDICE, F. S., SPERANDIO, F. F. & PINTO JUNIOR, D. D. 2013. Effects of celecoxib treatment over the AKT pathway in head and neck squamous cell carcinoma. *J Oral Pathol Med*.
3. ADAMS, P. D. 2001. Regulation of the retinoblastoma tumor suppressor protein by cyclin/cdks. *Biochim Biophys Acta,* 1471**,** M123-33.
4. AGARWAL, P. & BALLABH, R. 2013. Expression of type IV collagen in different histological grades of oral squamous cell carcinoma: an immunohistochemical study. *J Cancer Res Ther,* 9**,** 272-5.
5. AGRAWAL, N., FREDERICK, M. J., PICKERING, C. R., BETTEGOWDA, C., CHANG, K., LI, R. J., FAKHRY, C., XIE, T. X., ZHANG, J., WANG, J., ZHANG, N., EL-NAGGAR, A. K., JASSER, S. A., WEINSTEIN, J. N., TREVINO, L., DRUMMOND, J. A., MUZNY, D. M., WU, Y., WOOD, L. D., HRUBAN, R. H., WESTRA, W. H., KOCH, W. M., CALIFANO, J. A., GIBBS, R. A., SIDRANSKY, D., VOGELSTEIN, B., VELCULESCU, V. E., PAPADOPOULOS, N., WHEELER, D. A., KINZLER, K. W. & MYERS, J. N. 2011. Exome sequencing of head and neck squamous cell carcinoma reveals inactivating mutations in NOTCH1. *Science,* 333**,** 1154-7.
6. AI, H., BARRERA, J. E., MEYERS, A. D., SHROYER, K. R. & VARELLA-GARCIA, M. 2001. Chromosomal aneuploidy precedes morphological changes and supports multifocality in head and neck lesions. *Laryngoscope,* 111**,** 1853-8.

7. ALCARAZ-PEREZ, F., MULERO, V. & CAYUELA, M. L. 2008. Application of the dual-luciferase reporter assay to the analysis of promoter activity in Zebrafish embryos. *BMC Biotechnol,* 8**,** 81.

8. ALLSOPP, R. C., CHANG, E., KASHEFI-AAZAM, M., ROGAEV, E. I., PIATYSZEK, M. A., SHAY, J. W. & HARLEY, C. B. 1995. Telomere shortening is associated with cell division in vitro and in vivo. *Exp Cell Res,* 220**,** 194-200.

9. ALTIERI, A., BOSETTI, C., GALLUS, S., FRANCESCHI, S., DAL MASO, L., TALAMINI, R., LEVI, F., NEGRI, E., RODRIGUEZ, T. & LA VECCHIA, C. 2004. Wine, beer and spirits and risk of oral and pharyngeal cancer: a case-control study from Italy and Switzerland. *Oral Oncology,* 40**,** 904-909.

10. AMBROSCH, P., SCHLOTT, T., HILMES, D. & RUSCHENBURG, I. 2001. p16 alterations and retinoblastoma protein expression in squamous cell carcinoma and neighboring dysplasia from the upper aerodigestive tract. *Virchows Arch,* 438**,** 343-9.

11. AMERES, S. L. & ZAMORE, P. D. 2013. Diversifying microRNA sequence and function. *Nat Rev Mol Cell Biol,* 14**,** 475-88.

12. ANSARI, K. I., SHRESTHA, B., HUSSAIN, I., KASIRI, S. & MANDAL, S. S. 2011. Histone methylases MLL1 and MLL3 coordinate with estrogen receptors in estrogen-mediated HOXB9 expression. *Biochemistry,* 50**,** 3517-27.

13. ARGIRIS, K., PANETHYMITAKI, C. & TAVASSOLI, M. 2011. Naturally occurring, tumor-specific, therapeutic proteins. *Exp Biol Med (Maywood),* 236**,** 524-36.

14. ASCANO, M., HAFNER, M., CEKAN, P., GERSTBERGER, S. & TUSCHL, T. 2012. Identification of RNA-protein interaction networks using PAR-CLIP. *Wiley Interdiscip Rev RNA,* 3**,** 159-77.

15. ASLI, N. S. & KESSEL, M. 2010. Spatiotemporally restricted regulation of generic motor neuron programs by miR-196-mediated repression of Hoxb8. *Dev Biol,* 344**,** 857-68.

16. AXELL, T., PINDBORG, J. J., SMITH, C. J. & VAN DER WAAL, I. 1996. Oral white lesions with special reference to precancerous and tobacco- related lesions: conclusions of an international symposium held in Uppsala, Sweden, May 18-21 1994. International Collaborative Group on Oral White Lesions. *J Oral Pathol Med,* 25**,** 49-54.

17. BALZ, V., SCHECKENBACH, K., GOTTE, K., BOCKMUHL, U., PETERSEN, I. & BIER, H. 2003. Is the p53 inactivation frequency in squamous cell carcinomas of the head and neck underestimated? Analysis of p53 exons 2-11 and human papillomavirus 16/18 E6 transcripts in 123 unselected tumor specimens. *Cancer Res,* 63**,** 1188-91.

18. BARBER, B. A. & RASTEGAR, M. 2010. Epigenetic control of Hox genes during neurogenesis, development, and disease. *Ann Anat,* 192**,** 261-74.

19. BEDI, R. 1996. Betel-quid and tobacco chewing among the United Kingdom's Bangladeshi community. *Br J Cancer Suppl,* 29**,** S73-7.

20. BHAT, K., WANG, F., MA, Q., LI, Q., MALLIK, S., HSIEH, T. C. & WU, E. 2012. Advances in biomarker research for pancreatic cancer. *Curr Pharm Des,* 18**,** 2439-51.

21. BHAVE, S. L., TEKNOS, T. N. & PAN, Q. 2011. Molecular parameters of head and neck cancer metastasis. *Crit Rev Eukaryot Gene Expr,* 21**,** 143-53.

22. BLAHNA, M. T. & HATA, A. 2013. Regulation of miRNA biogenesis as an integrated component of growth factor signaling. *Curr Opin Cell Biol,* 25**,** 233-40.

23. BOFFETTA, P., HECHT, S., GRAY, N., GUPTA, P. & STRAIF, K. 2008. Smokeless tobacco and cancer. *Lancet Oncol,* 9**,** 667-75.

24. BONNER, J. A., HARARI, P. M., GIRALT, J., AZARNIA, N., SHIN, D. M., COHEN, R. B., JONES, C. U., SUR, R., RABEN, D., JASSEM, J., OVE, R., KIES, M. S., BASELGA, J., YOUSSOUFIAN, H., AMELLAL, N., ROWINSKY, E. K. & ANG, K. K. 2006. Radiotherapy plus cetuximab for squamous-cell carcinoma of the head and neck. *N Engl J Med,* 354**,** 567-78.

25. BRAIG, S., MUELLER, D. W., ROTHHAMMER, T. & BOSSERHOFF, A. K. 2010. MicroRNA miR-196a is a central regulator of HOX-B7 and BMP4 expression in malignant melanoma. *Cell Mol Life Sci,* 67**,** 3535-48.

26. BROCKLEHURST, P. R., BAKER, S. R. & SPEIGHT, P. M. 2010. Oral cancer screening: what have we learnt and what is there still to achieve? *Future Oncol,* 6**,** 299-304.

27. CAIRNS, P., POLASCIK, T. J., EBY, Y., TOKINO, K., CALIFANO, J., MERLO, A., MAO, L., HERATH, J., JENKINS, R., WESTRA, W. & ET AL. 1995. Frequency of homozygous deletion at p16/CDKN2 in primary human tumours. *Nat Genet,* 11**,** 210-2.

28. CALVO, R., WEST, J., FRANKLIN, W., ERICKSON, P., BEMIS, L., LI, E., HELFRICH, B., BUNN, P., ROCHE, J., BRAMBILLA, E., ROSELL, R., GEMMILL, R. M. & DRABKIN, H. A. 2000. Altered HOX and WNT7A expression in human lung cancer. *Proc Natl Acad Sci U S A,* 97**,** 12776-81.

29. CASTELLSAGUE, X., QUINTANA, M. J., MARTINEZ, M. C., NIETO, A., SANCHEZ, M. J., JUAN, A., MONNER, A., CARRERA, M., AGUDO, A., QUER, M., MUNOZ, N., HERRERO, R., FRANCESCHI, S. & BOSCH, F. X. 2004. The role of type of tobacco and type of alcoholic beverage in oral carcinogenesis. *International Journal of Cancer,* 108**,** 741-749.

30. CERVIGNE, N. K., REIS, P. P., MACHADO, J., SADIKOVIC, B., BRADLEY, G., GALLONI, N. N., PINTILIE, M., JURISICA, I., PEREZ-ORDONEZ, B., GILBERT, R., GULLANE, P., IRISH, J. & KAMEL-REID, S. 2009. Identification of a microRNA signature associated with progression of leukoplakia to oral carcinoma. *Hum Mol Genet,* 18**,** 4818-29.

31. CHAMBEYRON, S. & BICKMORE, W. A. 2004. Chromatin decondensation and nuclear reorganization of the HoxB locus upon induction of transcription. *Genes Dev,* 18**,** 1119-30.

32. CHANG, C. P., BROCCHIERI, L., SHEN, W. F., LARGMAN, C. & CLEARY, M. L. 1996. Pbx modulation of Hox homeodomain amino-terminal arms establishes different DNA-binding specificities across the Hox locus. *Mol Cell Biol,* 16**,** 1734-45.

33. CHEN, C. Y., ZHANG, Y. Q., ZHANG, L. D., WEAKLEY, S. M. & YAO, Q. Z. 2011a. MicroRNA-196: critical roles and clinical applications in development and cancer. *Journal of Cellular and Molecular Medicine,* 15**,** 14-23.

34. CHEN, D., CABAY, R. J., JIN, Y., WANG, A., LU, Y., SHAH-KHAN, M. & ZHOU, X. 2013. MicroRNA Deregulations in Head and Neck Squamous Cell Carcinomas. *J Oral Maxillofac Res,* 4**,** e2.

35. CHEN, F. & CAPECCHI, M. R. 1997. Targeted mutations in hoxa-9 and hoxb-9 reveal synergistic interactions. *Dev Biol,* 181**,** 186-96.

36. CHEN, F. & CAPECCHI, M. R. 1999. Paralogous mouse Hox genes, Hoxa9, Hoxb9, and Hoxd9, function together to control development of the mammary gland in response to pregnancy. *Proc Natl Acad Sci U S A,* 96**,** 541-6.

37. CHEN, Y., ZAMAN, M. S., DENG, G., MAJID, S., SAINI, S., LIU, J., TANAKA, Y. & DAHIYA, R. 2011b. MicroRNAs 221/222 and genistein-

mediated regulation of ARHI tumor suppressor gene in prostate cancer. *Cancer Prev Res (Phila),* 4**,** 76-86.

38. CHENG, B., FU, X., SUN, T., SUN, X. & SHENG, Z. 2002. Expression of epidermal growth factor receptor and related phosphorylation proteins in hypertrophic scars and normal skin. *Chin Med J (Engl),* 115**,** 1525-8.

39. CHIBA, N., COMAILLS, V., SHIOTANI, B., TAKAHASHI, F., SHIMADA, T., TAJIMA, K., WINOKUR, D., HAYASHIDA, T., WILLERS, H., BRACHTEL, E., VIVANCO, M. D., HABER, D. A., ZOU, L. & MAHESWARAN, S. 2012. Homeobox B9 induces epithelial-to-mesenchymal transition-associated radioresistance by accelerating DNA damage responses. *Proc Natl Acad Sci U S A,* 109**,** 2760-5.

40. CHILDS, G., FAZZARI, M., KUNG, G., KAWACHI, N., BRANDWEIN-GENSLER, M., MCLEMORE, M., CHEN, Q., BURK, R. D., SMITH, R. V., PRYSTOWSKY, M. B., BELBIN, T. J. & SCHLECHT, N. F. 2009. Low-level expression of microRNAs let-7d and miR-205 are prognostic markers of head and neck squamous cell carcinoma. *Am J Pathol,* 174**,** 736-45.

41. CHUANG, T. D., PANDA, H., LUO, X. & CHEGINI, N. 2012. miR-200c is aberrantly expressed in leiomyomas in an ethnic-dependent manner and targets ZEBs, VEGFA, TIMP2, and FBLN5. *Endocr Relat Cancer,* 19**,** 541-56.

42. COPUR, O. & MULLER, J. 2013. The histone H3-K27 demethylase Utx regulates HOX gene expression in Drosophila in a temporally restricted manner. *Development,* 140**,** 3478-85.

43. DARNELL, J. E., JR. 2002. Transcription factors as targets for cancer therapy. *Nat Rev Cancer,* 2**,** 740-9.

44. DAVIS, B. N., HILYARD, A. C., LAGNA, G. & HATA, A. 2008. SMAD proteins control DROSHA-mediated microRNA maturation. *Nature,* 454**,** 56-61.

45. DE SMET, C. & LORIOT, A. 2010. DNA hypomethylation in cancer: Epigenetic scars of a neoplastic journey. *Epigenetics,* 5.

46. DELBALDO, C., RAYMOND, E., VERA, K., HAMMERSHAIMB, L., KAUCIC, K., LOZAHIC, S., MARTY, M. & FAIVRE, S. 2008. Phase I and pharmacokinetic study of etaracizumab (Abegrin), a humanized monoclonal antibody against alphavbeta3 integrin receptor, in patients with advanced solid tumors. *Invest New Drugs,* 26**,** 35-43.

47. DENARO, N., RUSSI, E. G. & MERLANO, M. C. 2013. Strategies for Non-Resectable Head and Neck Cancer. *Curr Treat Options Oncol*.

48. DETRE, S., SACLANI JOTTI, G. & DOWSETT, M. 1995. A "quickscore" method for immunohistochemical semiquantitation: validation for oestrogen receptor in breast carcinomas. *J Clin Pathol,* 48**,** 876-8.

49. DIAJIL, A., ROBINSON, C. M., SLOAN, P. & THOMSON, P. J. 2013. Clinical outcome following oral potentially malignant disorder treatment: a 100 patient cohort study. *Int J Dent,* 2013**,** 809248.

50. DIAZ-LOPEZ, A., INIESTA, P., MORAN, A., ORTEGA, P., FERNANDEZ-MARCELO, T., SANCHEZ-PERNAUTE, A., TORRES, A. J., BENITO, M. & DE JUAN, C. 2010. Expression of Human MDGA1 Increases Cell Motility and Cell-Cell Adhesion and Reduces Adhesion to Extracellular Matrix Proteins in MDCK Cells. *Cancer Microenviron,* 4**,** 23-32.

51. DICKSON, M. A., HAHN, W. C., INO, Y., RONFARD, V., WU, J. Y., WEINBERG, R. A., LOUIS, D. N., LI, F. P. & RHEINWALD, J. G. 2000. Human keratinocytes that express hTERT and also bypass a p16(INK4a)-enforced mechanism that limits life span become immortal yet retain normal growth and differentiation characteristics. *Mol Cell Biol,* 20**,** 1436-47.

52. DOWNEY, M. G., GOING, J. J., STUART, R. C. & KEITH, W. N. 2001. Expression of telomerase RNA in oesophageal and oral cancer. *J Oral Pathol Med,* 30**,** 577-81.

53. DOWNWARD, J. 2003. Targeting RAS signalling pathways in cancer therapy. *Nature Reviews Cancer,* 3**,** 11-22.

54. DU, L., SHEN, J., WEEMS, A. & LU, S. L. 2012. Role of phosphatidylinositol-3-kinase pathway in head and neck squamous cell carcinoma. *J Oncol,* 2012**,** 450179.

55. DUBOULE, D. 1992. The vertebrate limb: a model system to study the Hox/HOM gene network during development and evolution. *Bioessays,* 14**,** 375-84.

56. DYKXHOORN, D. M., NOVINA, C. D. & SHARP, P. A. 2003. Killing the messenger: short RNAs that silence gene expression. *Nat Rev Mol Cell Biol,* 4**,** 457-67.

57. EKLUND, E. 2011. The role of Hox proteins in leukemogenesis: insights into key regulatory events in hematopoiesis. *Crit Rev Oncog,* 16**,** 65-76.

58. ENGLAND, B., HUANG, T. & KARSY, M. 2013. Current understanding of the role and targeting of tumor suppressor p53 in glioblastoma multiforme. *Tumour Biol,* 34**,** 2063-74.

59. FANG, L., WANG, H., ZHOU, L. & YU, D. 2011. Akt-FOXO3a signaling axis dysregulation in human oral squamous cell carcinoma and potent efficacy of FOXO3a-targeted gene therapy. *Oral Oncol,* 47**,** 16-21.

60. FENIC, I., STEGER, K., GRUBER, C., ARENS, C. & WOENCKHAUS, J. 2007. Analysis of PIK3CA and Akt/protein kinase B in head and neck squamous cell carcinoma. *Oncol Rep,* 18**,** 253-9.

61. FERLAY J, S. H., BRAY F, FORMAN D, MATHERS C AND PARKIN DM. GLOBOCAN 2008. *Cancer Incidence and Mortality Worldwide* [Online]. Lyon, France: International Agency for Research on Cancer, 2010. Available: http://globocan.iarc.fr [Accessed 31 July 2013].

62. FERRANDO, A. A., ARMSTRONG, S. A., NEUBERG, D. S., SALLAN, S. E., SILVERMAN, L. B., KORSMEYER, S. J. & LOOK, A. T. 2003. Gene expression signatures in MLL-rearranged T-lineage and B-precursor acute leukemias: dominance of HOX dysregulation. *Blood,* 102**,** 262-8.

63. FERREIRA ANTUNES, J. L., TOPORCOV, T. N., BIAZEVIC, M. G., BOING, A. F., SCULLY, C. & PETTI, S. 2013. Joint and independent effects of alcohol drinking and tobacco smoking on oral cancer: a large case-control study. *PLoS One,* 8**,** e68132.

64. FILIPOWICZ, W., BHATTACHARYYA, S. N. & SONENBERG, N. 2008. Mechanisms of post-transcriptional regulation by microRNAs: are the answers in sight? *Nat Rev Genet,* 9**,** 102-14.

65. FYFFE, C. & FALASCA, M. 2013. 3-Phosphoinositide-dependent protein kinase-1 as an emerging target in the management of breast cancer. *Cancer Manag Res,* 5**,** 271-80.

66. GANDINI, S., BOTTERI, E., IODICE, S., BONIOL, M., LOWENFELS, A. B., MAISONNEUVE, P. & BOYLE, P. 2008. Tobacco smoking and cancer: a meta-analysis. *Int J Cancer,* 122**,** 155-64.

67. GARCIABELLIDO, A. 1977. HOMOEOTIC AND ATAVIC MUTATIONS IN INSECTS. *American Zoologist,* 17**,** 613-629.

68. GHANNAM, G., TAKEDA, A., CAMARATA, T., MOORE, M. A., VIALE, A. & YASEEN, N. R. 2004. The oncogene Nup98-HOXA9 induces gene transcription in myeloid cells. *J Biol Chem,* 279**,** 866-75.

69. GILLISON, M. L. 2007. Current topics in the epidemiology of oral cavity and oropharyngeal cancers. *Head Neck,* 29**,** 779-92.

70. GOLUB, T. R., SLONIM, D. K., TAMAYO, P., HUARD, C., GAASENBEEK, M., MESIROV, J. P., COLLER, H., LOH, M. L., DOWNING, J. R., CALIGIURI, M. A., BLOOMFIELD, C. D. & LANDER, E. S. 1999. Molecular classification of cancer: class discovery and class prediction by gene expression monitoring. *Science,* 286**,** 531-7.

71. GRANDIS, J. R., DRENNING, S. D., CHAKRABORTY, A., ZHOU, M. Y., ZENG, Q., PITT, A. S. & TWEARDY, D. J. 1998. Requirement of Stat3 but not Stat1 activation for epidermal growth factor receptor- mediated cell growth In vitro. *J Clin Invest,* 102**,** 1385-92.

72. GRANDIS, J. R., DRENNING, S. D., ZENG, Q., WATKINS, S. C., MELHEM, M. F., ENDO, S., JOHNSON, D. E., HUANG, L., HE, Y. & KIM, J. D. 2000. Constitutive activation of Stat3 signaling abrogates apoptosis in squamous cell carcinogenesis in vivo. *Proc Natl Acad Sci U S A,* 97**,** 4227-32.

73. GRAVELAND, A. P., BREMMER, J. F., DE MAAKER, M., BRINK, A., COBUSSEN, P., ZWART, M., BRAAKHUIS, B. J., BLOEMENA, E., VAN DER WAAL, I., LEEMANS, C. R. & BRAKENHOFF, R. H. 2013. Molecular screening of oral precancer. *Oral Oncol*.

74. GRAVELAND, A. P., GOLUSINSKI, P. J., BUIJZE, M., DOUMA, R., SONS, N., KUIK, D. J., BLOEMENA, E., LEEMANS, C. R., BRAKENHOFF, R. H. & BRAAKHUIS, B. J. 2011. Loss of heterozygosity at 9p and p53 immunopositivity in surgical margins predict local relapse in head and neck squamous cell carcinoma. *Int J Cancer,* 128**,** 1852-9.

75. GREGERSEN, L. H., JACOBSEN, A., FRANKEL, L. B., WEN, J., KROGH, A. & LUND, A. H. 2012. MicroRNA-143 down-regulates Hexokinase 2 in colon cancer cells. *BMC Cancer,* 12**,** 232.

76. GRIER, D. G., THOMPSON, A., KWASNIEWSKA, A., MCGONIGLE, G. J., HALLIDAY, H. L. & LAPPIN, T. R. 2005. The pathophysiology of HOX genes and their role in cancer. *J Pathol,* 205**,** 154-71.

77. GU, F., MA, Y., ZHANG, Z., ZHAO, J., KOBAYASHI, H., ZHANG, L. & FU, L. 2010. Expression of Stat3 and Notch1 is associated with cisplatin resistance in head and neck squamous cell carcinoma. *Oncol Rep,* 23**,** 671-6.

78. HA, P. K. & CALIFANO, J. A. 2006. Promoter methylation and inactivation of tumour-suppressor genes in oral squamous-cell carcinoma. *Lancet Oncol,* 7**,** 77-82.

79. HA, P. K., CHANG, S. S., GLAZER, C. A., CALIFANO, J. A. & SIDRANSKY, D. 2009. Molecular techniques and genetic alterations in head and neck cancer. *Oral Oncol,* 45**,** 335-9.

80. HAMMOND, S. M., BOETTCHER, S., CAUDY, A. A., KOBAYASHI, R. & HANNON, G. J. 2001. Argonaute2, a link between genetic and biochemical analyses of RNAi. *Science,* 293**,** 1146-50.

81. HAN, L., WITMER, P. D., CASEY, E., VALLE, D. & SUKUMAR, S. 2007. DNA methylation regulates MicroRNA expression. *Cancer Biol Ther,* 6**,** 1284-8.

82. HAN, W. & LO, H. W. 2012. Landscape of EGFR signaling network in human cancers: biology and therapeutic response in relation to receptor subcellular locations. *Cancer Lett,* 318**,** 124-34.

83. HANAHAN, D. & WEINBERG, R. A. 2011. Hallmarks of cancer: the next generation. *Cell,* 144**,** 646-74.

84. HANSON, R. D., HESS, J. L., YU, B. D., ERNST, P., VAN LOHUIZEN, M., BERNS, A., VAN DER LUGT, N. M., SHASHIKANT, C. S., RUDDLE, F. H., SETO, M. & KORSMEYER, S. J. 1999. Mammalian Trithorax and polycomb-group homologues are antagonistic regulators of homeotic development. *Proc Natl Acad Sci U S A,* 96**,** 14372-7.

85. HASHIBE, M., BRENNAN, P., BENHAMOU, S., CASTELLSAGUE, X., CHU, C., CURADO, M. P., DAL MASO, L., DAUCT, A. W., FABIANOVA, E., WUNSCH, V., FRANCESCHI, S., HAYES, R. B., HERRERO, R., KOIFMAN, S., LA VECCHIA, C., LAZARUS, P., LEVI, F., MATES, D., MATOS, E., MENEZES, A., MUSCAT, J., ELUF, J., OLSHAN, A. F., RUDNAI, P., SCHWARTZ, S. M., SMITH, E., STURGIS, E. M., SZESZENIA-DABROWSKA, N., TALAMINI, R., WEI, Q. Y., WINN, D. M., ZARIDZE, D., ZATONSKI, W., ZHANG, Z. F., BERTHILLER, J. & BOFFETTA, P. 2007. Alcohol drinking in never users of tobacco, cigarette smoking in never drinkers, and the risk of head and neck cancer: Pooled analysis in the international head and neck cancer epidemiology consortium. *Journal of the National Cancer Institute,* 99**,** 777-789.

86. HASSAN, N. M., HAMADA, J., MURAI, T., SEINO, A., TAKAHASHI, Y., TADA, M., ZHANG, X., KASHIWAZAKI, H., YAMAZAKI, Y., INOUE, N. & MORIUCHI, T. 2006. Aberrant expression of HOX genes in oral dysplasia and squamous cell carcinoma tissues. *Oncol Res,* 16**,** 217-24.

87. HAYASHIDA, T., TAKAHASHI, F., CHIBA, N., BRACHTEL, E., TAKAHASHI, M., GODIN-HEYMANN, N., GROSS, K. W., VIVANCO, M., WIJENDRAN, V., SHIODA, T., SGROI, D., DONAHOE, P. K. & MAHESWARAN, S. 2010. HOXB9, a gene overexpressed in breast cancer,

promotes tumorigenicity and lung metastasis. *Proc Natl Acad Sci U S A,* 107**,** 1100-5.

88. HECK, J. E., BERTHILLER, J., VACCARELLA, S., WINN, D. M., SMITH, E. M., SHAN'GINA, O., SCHWARTZ, S. M., PURDUE, M. P., PILARSKA, A., ELUF-NETO, J., MENEZES, A., MCCLEAN, M. D., MATOS, E., KOIFMAN, S., KELSEY, K. T., HERRERO, R., HAYES, R. B., FRANCESCHI, S., WUNSCH-FILHO, V., FERNANDEZ, L., DAUDT, A. W., CURADO, M. P., CHEN, C., CASTELLSAGUE, X., FERRO, G., BRENNAN, P., BOFFETTA, P. & HASHIBE, M. 2010. Sexual behaviours and the risk of head and neck cancers: a pooled analysis in the International Head and Neck Cancer Epidemiology (INHANCE) consortium. *Int J Epidemiol,* 39**,** 166-81.

89. HEHLGANS, S., EKE, I. & CORDES, N. 2012. Targeting FAK radiosensitizes 3-dimensional grown human HNSCC cells through reduced Akt1 and MEK1/2 signaling. *Int J Radiat Oncol Biol Phys,* 83**,** e669-76.

90. HERSHKO, A. Y., KAFRI, T., FAINSOD, A. & RAZIN, A. 2003. Methylation of HoxA5 and HoxB5 and its relevance to expression during mouse development. *Gene,* 302**,** 65-72.

91. HINDLE, I., DOWNER, M. C., MOLES, D. R. & SPEIGHT, P. M. 2000. Is alcohol responsible for more intra-oral cancer? *Oral Oncol,* 36**,** 328-33.

92. HIRAO, A., KONG, Y. Y., MATSUOKA, S., WAKEHAM, A., RULAND, J., YOSHIDA, H., LIU, D., ELLEDGE, S. J. & MAK, T. W. 2000. DNA damage-induced activation of p53 by the checkpoint kinase Chk2. *Science,* 287**,** 1824-7.

93. HORNSTEIN, E., MANSFIELD, J. H., YEKTA, S., HU, J. K. H., HARFE, B. D., MCMANUS, M. T., BASKERVILLE, S., BARTEL, D. P. & TABIN, C. J. 2005. The microRNA miR-196 acts upstream of Hoxb8 and Shh in limb development. *Nature,* 438**,** 671-674.

94. HUI, A. B., LENARDUZZI, M., KRUSHEL, T., WALDRON, L., PINTILIE, M., SHI, W., PEREZ-ORDONEZ, B., JURISICA, I., O'SULLIVAN, B., WALDRON, J., GULLANE, P., CUMMINGS, B. & LIU, F. F. 2010. Comprehensive MicroRNA profiling for head and neck squamous cell carcinomas. *Clin Cancer Res,* 16**,** 1129-39.

95. HULSKAMP, M. & TAUTZ, D. 1991. Gap genes and gradients--the logic behind the gaps. *Bioessays,* 13**,** 261-8.

96. HUNT, S., JONES, A. V., HINSLEY, E. E., WHAWELL, S. A. & LAMBERT, D. W. 2011. MicroRNA-124 suppresses oral squamous cell carcinoma motility by targeting ITGB1. *FEBS Lett,* 585**,** 187-92.

97. HUNTER, K. D., THURLOW, J. K., FLEMING, J., DRAKE, P. J., VASS, J. K., KALNA, G., HIGHAM, D. J., HERZYK, P., MACDONALD, D. G., PARKINSON, E. K. & HARRISON, P. R. 2006. Divergent routes to oral cancer. *Cancer Res,* 66**,** 7405-13.

98. HUR, H., LEE, J. Y., YUN, H. J., PARK, B. W. & KIM, M. H. 2013. Analysis of HOX Gene Expression Patterns in Human Breast Cancer. *Mol Biotechnol*.

99. IORIO, M. V., FERRACIN, M., LIU, C. G., VERONESE, A., SPIZZO, R., SABBIONI, S., MAGRI, E., PEDRIALI, M., FABBRI, M., CAMPIGLIO, M., MENARD, S., PALAZZO, J. P., ROSENBERG, A., MUSIANI, P., VOLINIA, S., NENCI, I., CALIN, G. A., QUERZOLI, P., NEGRINI, M. & CROCE, C. M. 2005. MicroRNA gene expression deregulation in human breast cancer. *Cancer Res,* 65**,** 7065-70.

100. ISAACS, H. V., POWNALL, M. E. & SLACK, J. M. 1998. Regulation of Hox gene expression and posterior development by the Xenopus caudal homologue Xcad3. *EMBO J,* 17**,** 3413-27.

101. ISHIKAWA, T., GOTOH, N., MURAYAMA, C., ABE, T., IWASHITA, M., MATSUZAKI, F., SUZUKI, T. & YAMAMOTO, T. 2011. IgSF molecule MDGA1 is involved in radial migration and positioning of a subset of cortical upper-layer neurons. *Dev Dyn,* 240**,** 96-107.

102. IVANOVSKA, I., BALL, A. S., DIAZ, R. L., MAGNUS, J. F., KIBUKAWA, M., SCHELTER, J. M., KOBAYASHI, S. V., LIM, L., BURCHARD, J., JACKSON, A. L., LINSLEY, P. S. & CLEARY, M. A. 2008. MicroRNAs in the miR-106b family regulate p21/CDKN1A and promote cell cycle progression. *Mol Cell Biol,* 28**,** 2167-74.

103. IWAI, S., YONEKAWA, A., HARADA, C., HAMADA, M., KATAGIRI, W., NAKAZAWA, M. & YURA, Y. 2010. Involvement of the Wnt-beta-catenin pathway in invasion and migration of oral squamous carcinoma cells. *Int J Oncol,* 37**,** 1095-103.

104. JENEI, V., NYSTROM, M. L. & THOMAS, G. J. 2011. Measuring invasion in an organotypic model. *Methods Mol Biol,* 769**,** 223-32.

105. JERJES, W., UPILE, T., PETRIE, A., RISKALLA, A., HAMDOON, Z., VOURVACHIS, M., KARAVIDAS, K., JAY, A., SANDISON, A., THOMAS, G. J., KALAVREZOS, N. & HOPPER, C. 2010. Clinicopathological parameters, recurrence, locoregional and distant metastasis in 115 T1-T2 oral squamous cell carcinoma patients. *Head Neck Oncol,* 2**,** 9.

106. JERJES, W., UPILE, T., RADHI, H., PETRIE, A., ABIOLA, J., ADAMS, A., KAFAS, P., CALLEAR, J., CARBINER, R., RAJARAM, K. & HOPPER, C. 2012. The effect of tobacco and alcohol and their reduction/cessation on mortality in oral cancer patients: short communication. *Head Neck Oncol,* 4**,** 6.

107. JOHNSON, N. W., JAYASEKARA, P. & AMARASINGHE, A. A. 2011. Squamous cell carcinoma and precursor lesions of the oral cavity: epidemiology and aetiology. *Periodontol 2000,* 57**,** 19-37.

108. JORDAN, R. C., BRADLEY, G. & SLINGERLAND, J. 1998. Reduced levels of the cell-cycle inhibitor p27Kip1 in epithelial dysplasia and carcinoma of the oral cavity. *Am J Pathol,* 152**,** 585-90.

109. KANAI, M., HAMADA, J., TAKADA, M., ASANO, T., MURAKAWA, K., TAKAHASHI, Y., MURAI, T., TADA, M., MIYAMOTO, M., KONDO, S. & MORIUCHI, T. 2010. Aberrant expressions of HOX genes in colorectal and hepatocellular carcinomas. *Oncol Rep,* 23**,** 843-51.

110. KARIN, M. 2006. Nuclear factor-kappaB in cancer development and progression. *Nature,* 441**,** 431-6.

111. KARIN, M. & GRETEN, F. R. 2005. NF-kappaB: linking inflammation and immunity to cancer development and progression. *Nat Rev Immunol,* 5**,** 749-59.

112. KASHIYAMA, K., MITSUTAKE, N., MATSUSE, M., OGI, T., SAENKO, V. A., UJIFUKU, K., UTANI, A., HIRANO, A. & YAMASHITA, S. 2012. miR-196a downregulation increases the expression of type I and III collagens in keloid fibroblasts. *J Invest Dermatol,* 132**,** 1597-604.

113. KEARSLEY, J. H., FURLONG, K. L., COOKE, R. A. & WATERS, M. J. 1990. An immunohistochemical assessment of cellular proliferation markers in head and neck squamous cell cancers. *Br J Cancer,* 61**,** 821-7.

114. KEREN, S., SHOUDE, Z., LU, Z. & BEIBEI, Y. 2013. Role of EGFR as a prognostic factor for survival in head and neck cancer: a meta-analysis. *Tumour Biol*.

115. KHAN, Z. & BISEN, P. S. 2013. Oncoapoptotic signaling and deregulated target genes in cancers: special reference to oral cancer. *Biochim Biophys Acta,* 1836**,** 123-45.

116. KIM, N. W., PIATYSZEK, M. A., PROWSE, K. R., HARLEY, C. B., WEST, M. D., HO, P. L., COVIELLO, G. M., WRIGHT, W. E., WEINRICH, S. L. & SHAY, J. W. 1994. Specific association of human telomerase activity with immortal cells and cancer. *Science,* 266**,** 2011-5.

117. KIM, T. K. & EBERWINE, J. H. 2010. Mammalian cell transfection: the present and the future. *Anal Bioanal Chem,* 397**,** 3173-8.

118. KMITA, M. & DUBOULE, D. 2003. Organizing axes in time and space; 25 years of colinear tinkering. *Science,* 301**,** 331-3.

119. KORPAL, M., LEE, E. S., HU, G. & KANG, Y. 2008. The miR-200 family inhibits epithelial-mesenchymal transition and cancer cell migration by direct targeting of E-cadherin transcriptional repressors ZEB1 and ZEB2. *J Biol Chem,* 283**,** 14910-4.

120. KRAMER, N., WALZL, A., UNGER, C., ROSNER, M., KRUPITZA, G., HENGSTSCHLAGER, M. & DOLZNIG, H. 2013. In vitro cell migration and invasion assays. *Mutat Res,* 752**,** 10-24.

121. KREIMER, A. R., RANDI, G., HERRERO, R., CASTELLSAGUE, X., LA VECCHIA, C., FRANCESCHI, S. & STUDY, I. M. O. C. 2006. Diet and body mass, and oral and oropharyngeal squamous cell carcinomas: Analysis from the IARC multinational case-control study. *International Journal of Cancer,* 118**,** 2293-2297.

122. KUDO, Y., TSUNEMATSU, T. & TAKATA, T. 2011. Oncogenic role of RUNX3 in head and neck cancer. *J Cell Biochem,* 112**,** 387-93.

123. LA VECCHIA, C., TAVANI, A., FRANCESCHI, S., LEVI, F., CORRAO, G. & NEGRI, E. 1997. Epidemiology and prevention of oral cancer. *Oral Oncol,* 33**,** 302-12.

124. LABBAYE, C. & TESTA, U. 2012. The emerging role of MIR-146A in the control of hematopoiesis, immune function and cancer. *J Hematol Oncol,* 5**,** 13.

125. LANGER, C. J. 2012. Exploring biomarkers in head and neck cancer. *Cancer,* 118**,** 3882-92.

126. LAWRENCE, H. J., HELGASON, C. D., SAUVAGEAU, G., FONG, S., IZON, D. J., HUMPHRIES, R. K. & LARGMAN, C. 1997. Mice bearing a targeted interruption of the homeobox gene HOXA9 have defects in myeloid, erythroid, and lymphoid hematopoiesis. *Blood,* 89**,** 1922-30.

127. LEE, R. C., FEINBAUM, R. L. & AMBROS, V. 1993. The C. elegans heterochronic gene lin-4 encodes small RNAs with antisense complementarity to lin-14. *Cell,* 75**,** 843-54.

128. LEE, T. I., JENNER, R. G., BOYER, L. A., GUENTHER, M. G., LEVINE, S. S., KUMAR, R. M., CHEVALIER, B., JOHNSTONE, S. E., COLE, M. F., ISONO, K., KOSEKI, H., FUCHIKAMI, T., ABE, K., MURRAY, H. L., ZUCKER, J. P., YUAN, B., BELL, G. W., HERBOLSHEIMER, E., HANNETT, N. M., SUN, K., ODOM, D. T., OTTE, A. P., VOLKERT, T. L., BARTEL, D. P., MELTON, D. A., GIFFORD, D. K., JAENISCH, R. & YOUNG, R. A. 2006. Control of developmental regulators by Polycomb in human embryonic stem cells. *Cell,* 125**,** 301-13.

129. LEE, Y., AHN, C., HAN, J., CHOI, H., KIM, J., YIM, J., LEE, J., PROVOST, P., RADMARK, O., KIM, S. & KIM, V. N. 2003. The nuclear RNase III Drosha initiates microRNA processing. *Nature,* 425**,** 415-9.

130. LEE, Y. C., MARRON, M., BENHAMOU, S., BOUCHARDY, C., AHRENS, W., POHLABELN, H., LAGIOU, P., TRICHOPOULOS, D., AGUDO, A., CASTELLSAGUE, X., BENCKO, V., HOLCATOVA, I., KJAERHEIM, K., MERLETTI, F., RICHIARDI, L., MACFARLANE, G. J., MACFARLANE, T. V., TALAMINI, R., BARZAN, L., CANOVA, C., SIMONATO, L., CONWAY, D. I., MCKINNEY, P. A., LOWRY, R. J., SNEDDON, L., ZNAOR, A., HEALY, C. M., MCCARTAN, B. E., BRENNAN, P. & HASHIBE, M. 2009. Active and involuntary tobacco smoking and upper aerodigestive tract cancer risks in a multicenter case-control study. *Cancer Epidemiol Biomarkers Prev,* 18**,** 3353-61.

131. LEEMAN, R. J., LUI, V. W. & GRANDIS, J. R. 2006. STAT3 as a therapeutic target in head and neck cancer. *Expert Opin Biol Ther,* 6**,** 231-41.

132. LEEMANS, C. R., BRAAKHUIS, B. J. & BRAKENHOFF, R. H. 2011. The molecular biology of head and neck cancer. *Nat Rev Cancer,* 11**,** 9-22.

133. LEVY, M. Z., ALLSOPP, R. C., FUTCHER, A. B., GREIDER, C. W. & HARLEY, C. B. 1992. Telomere end-replication problem and cell aging. *J Mol Biol,* 225**,** 951-60.

134. LEWIS, E. B. 1978. A gene complex controlling segmentation in Drosophila. *Nature,* 276**,** 565-70.

135. LI, Y., ZHANG, M., CHEN, H., DONG, Z., GANAPATHY, V., THANGARAJU, M. & HUANG, S. 2010. Ratio of miR-196s to HOXC8 messenger RNA correlates with breast cancer cell migration and metastasis. *Cancer Res,* 70**,** 7894-904.

136. LIU, C. J., TSAI, M. M., TU, H. F., LUI, M. T., CHENG, H. W. & LIN, S. C. 2012a. miR-196a Overexpression and miR-196a2 Gene Polymorphism Are Prognostic Predictors of Oral Carcinomas. *Ann Surg Oncol*.

137. LIU, J., GAO, J., DU, Y., LI, Z., REN, Y., GU, J., WANG, X., GONG, Y., WANG, W. & KONG, X. 2012b. Combination of plasma microRNAs with serum CA19-9 for early detection of pancreatic cancer. *Int J Cancer,* 131**,** 683-91.

138. LIU, J., VAN MIL, A., AGUOR, E. N., SIDDIQI, S., VRIJSEN, K., JAKSANI, S., METZ, C., ZHAO, J., STRIJKERS, G. J., DOEVENDANS, P. A. & SLUIJTER, J. P. 2012c. MiR-155 inhibits cell migration of human cardiomyocyte progenitor cells (hCMPCs) via targeting of MMP-16. *J Cell Mol Med,* 16**,** 2379-86.

139. LIU, M., DU, Y., GAO, J., LIU, J., KONG, X., GONG, Y., LI, Z., WU, H. & CHEN, H. 2013. Aberrant Expression miR-196a Is Associated With Abnormal Apoptosis, Invasion, and Proliferation of Pancreatic Cancer Cells. *Pancreas,* 42**,** 1169-81.

140. LIU, X. H., LU, K. H., WANG, K. M., SUN, M., ZHANG, E. B., YANG, J. S., YIN, D. D., LIU, Z. L., ZHOU, J., LIU, Z. J., DE, W. & WANG, Z. X. 2012d. MicroRNA-196a promotes non-small cell lung cancer cell proliferation and invasion through targeting HOXA5. *BMC Cancer,* 12**,** 348.

141. LO, H. W. & HUNG, M. C. 2006. Nuclear EGFR signalling network in cancers: linking EGFR pathway to cell cycle progression, nitric oxide pathway and patient survival. *Br J Cancer,* 94**,** 184-8.

142. LOPEZ, E. P. M., MINARRO-DEL MORAL, R. M., MARTINEZ-GARCIA, C., ZANETTI, R., ROSSO, S., SERRANO, S., ANEIROS, J. F., JIMENEZ-PUENTE, A. & REDONDO, M. 2003. Lifestyles, environmental and phenotypic factors associated with lip cancer: a case-control study in southern Spain. *British Journal of Cancer,* 88**,** 1702-1707.

143. LOTTERMAN, C. D., KENT, O. A. & MENDELL, J. T. 2008. Functional integration of microRNAs into oncogenic and tumor suppressor pathways. *Cell Cycle,* 7**,** 2493-9.

144. LOYER, P., CARIOU, S., GLAISE, D., BILODEAU, M., BAFFET, G. & GUGUEN-GUILLOUZO, C. 1996. Growth factor dependence of progression through G1 and S phases of adult rat hepatocytes in vitro. Evidence of a mitogen restriction point in mid-late G1. *J Biol Chem,* 271**,** 11484-92.

145. LOYO, M., LI, R. J., BETTEGOWDA, C., PICKERING, C. R., FREDERICK, M. J., MYERS, J. N. & AGRAWAL, N. 2013. Lessons learned from next-generation sequencing in head and neck cancer. *Head Neck,* 35**,** 454-63.

146. LUMERMAN, H., FREEDMAN, P. & KERPEL, S. 1995. Oral Epithelial Dysplasia and the Development of Invasive Squamous-Cell Carcinoma. *Oral Surgery Oral Medicine Oral Pathology Oral Radiology and Endodontics,* 79**,** 321-329.

147. LUTHRA, R., SINGH, R. R., LUTHRA, M. G., LI, Y. X., HANNAH, C., ROMANS, A. M., BARKOH, B. A., CHEN, S. S., ENSOR, J., MARU, D. M., BROADDUS, R. R., RASHID, A. & ALBARRACIN, C. T. 2008. MicroRNA-196a targets annexin A1: a microRNA-mediated mechanism of annexin A1 downregulation in cancers. *Oncogene,* 27**,** 6667-78.

148. MAINGUY, G., KOSTER, J., WOLTERING, J., JANSEN, H. & DURSTON, A. 2007. Extensive polycistronism and antisense transcription in the mammalian Hox clusters. *PLoS One,* 2**,** e356.

149. MANSFIELD, J. H., HARFE, B. D., NISSEN, R., OBENAUER, J., SRINEEL, J., CHAUDHURI, A., FARZAN-KASHANI, R., ZUKER, M., PASQUINELLI, A. E., RUVKUN, G., SHARP, P. A., TABIN, C. J. & MCMANUS, M. T. 2004. MicroRNA-responsive 'sensor' transgenes uncover Hox-like and other

developmentally regulated patterns of vertebrate microRNA expression. *Nat Genet,* 36**,** 1079-83.

150. MARCINKIEWICZ, K. M. & GUDAS, L. J. 2013. Altered epigenetic regulation of homeobox genes in human oral squamous cell carcinoma cells. *Exp Cell Res.*

151. MARCUS, M. E. & LEONARD, J. N. 2013. FedExosomes: Engineering Therapeutic Biological Nanoparticles that Truly Deliver. *Pharmaceuticals (Basel),* 6**,** 659-680.

152. MARKOVIC, A. & CHUNG, C. H. 2012. Current role of EGF receptor monoclonal antibodies and tyrosine kinase inhibitors in the management of head and neck squamous cell carcinoma. *Expert Rev Anticancer Ther,* 12**,** 1149-59.

153. MARU, D. M., SINGH, R. R., HANNAH, C., ALBARRACIN, C. T., LI, Y. X., ABRAHAM, R., ROMANS, A. M., YAO, H., LUTHRA, M. G., ANANDASABAPATHY, S., SWISHER, S. G., HOFSTEFTER, W. L., RASHID, A. & LUTHRA, R. 2009a. MicroRNA-196a Is a Potential Marker of Progression during Barrett's Metaplasia-Dysplasia-Invasive Adenocarcinoma Sequence in Esophagus. *American Journal of Pathology,* 174**,** 1940-1948.

154. MARU, D. M., SINGH, R. R., HANNAH, C., ALBARRACIN, C. T., LI, Y. X., ABRAHAM, R., ROMANS, A. M., YAO, H., LUTHRA, M. G., ANANDASABAPATHY, S., SWISHER, S. G., HOFSTETTER, W. L., RASHID, A. & LUTHRA, R. 2009b. MicroRNA-196a is a potential marker of progression during Barrett's metaplasia-dysplasia-invasive adenocarcinoma sequence in esophagus. *Am J Pathol,* 174**,** 1940-8.

155. MASHBERG, A. 1977. Erythroplasia vs. leukoplasia in the diagnosis of early asymptomatic oral squamous carcinoma. *N Engl J Med,* 297**,** 109-10.

156. MCGREGOR, F., MUNTONI, A., FLEMING, J., BROWN, J., FELIX, D. H., MACDONALD, D. G., PARKINSON, E. K. & HARRISON, P. R. 2002. Molecular changes associated with oral dysplasia progression and acquisition of immortality: potential for its reversal by 5-azacytidine. *Cancer Res,* 62**,** 4757-66.

157. MEHTA, F. S., GUPTA, P. C. & PINDBORG, J. J. 1981. Chewing and smoking habits in relation to precancer and oral cancer. *J Cancer Res Clin Oncol,* 99**,** 35-9.

158. MENDELSOHN, A. H., LAI, C. K., SHINTAKU, I. P., FISHBEIN, M. C., BRUGMAN, K., ELASHOFF, D. A., ABEMAYOR, E., DUBINETT, S. M. & ST JOHN, M. A. 2012. Snail as a novel marker for regional metastasis in head and neck squamous cell carcinoma. *Am J Otolaryngol,* 33**,** 6-13.

159. MENG, F., HENSON, R., WEHBE-JANEK, H., GHOSHAL, K., JACOB, S. T. & PATEL, T. 2007. MicroRNA-21 regulates expression of the PTEN tumor suppressor gene in human hepatocellular cancer. *Gastroenterology,* 133**,** 647-58.

160. MIAO, L., XIONG, X., LIN, Y., CHENG, Y., LU, J., ZHANG, J. & CHENG, N. 2014. miR-203 inhibits tumor cell migration and invasion via caveolin-1 in pancreatic cancer cells. *Oncol Lett,* 7**,** 658-662.

161. MICHAEL, M. Z., SM, O. C., VAN HOLST PELLEKAAN, N. G., YOUNG, G. P. & JAMES, R. J. 2003. Reduced accumulation of specific microRNAs in colorectal neoplasia. *Mol Cancer Res,* 1**,** 882-91.

162. MIYAZAKI, Y., ADACHI, H., KATSUNO, M., MINAMIYAMA, M., JIANG, Y. M., HUANG, Z., DOI, H., MATSUMOTO, S., KONDO, N., IIDA, M., TOHNAI, G., TANAKA, F., MURAMATSU, S. & SOBUE, G. 2012. Viral delivery of miR-196a ameliorates the SBMA phenotype via the silencing of CELF2. *Nat Med,* 18**,** 1136-41.

163. MOORE, S. R., ALLISTER, J., RODER, D., PIERCE, A. M. & WILSON, D. F. 2001. Lip cancer in South Australia, 1977-1996. *Pathology,* 33**,** 167-71.

164. MORGAN, R., BOXALL, A., HARRINGTON, K. J., SIMPSON, G. R., GILLETT, C., MICHAEL, A. & PANDHA, H. S. 2012. Targeting the HOX/PBX dimer in breast cancer. *Breast Cancer Res Treat,* 136**,** 389-98.

165. MORGAN, R., PLOWRIGHT, L., HARRINGTON, K. J., MICHAEL, A. & PANDHA, H. S. 2010. Targeting HOX and PBX transcription factors in ovarian cancer. *BMC Cancer,* 10**,** 89.

166. MORGILLO, F. & LEE, H. Y. 2005. Resistance to epidermal growth factor receptor-targeted therapy. *Drug Resist Updat,* 8**,** 298-310.

167. MORSE, M. A., GARST, J., OSADA, T., KHAN, S., HOBEIKA, A., CLAY, T. M., VALENTE, N., SHREENIWAS, R., SUTTON, M. A., DELCAYRE, A., HSU, D. H., LE PECQ, J. B. & LYERLY, H. K. 2005. A phase I study of dexosome immunotherapy in patients with advanced non-small cell lung cancer. *J Transl Med,* 3**,** 9.

168. MUELLER, D. W. & BOSSERHOFF, A. K. 2011. MicroRNA miR-196a controls melanoma-associated genes by regulating HOX-C8 expression. *Int J Cancer,* 129**,** 1064-74.

169. MYOKEN, Y., OKAMOTO, T., KAN, M., SATO, J. D. & TAKADA, K. 1994. Release of Fibroblast Growth-Factor-I by Human Squamous-Cell Carcinoma Correlates with Autocrine Cell-Growth. *In Vitro Cellular & Developmental Biology-Animal,* 30A**,** 790-795.

170. NAGEL, S., BUREK, C., VENTURINI, L., SCHERR, M., QUENTMEIER, H., MEYER, C., ROSENWALD, A., DREXLER, H. G. & MACLEOD, R. A. 2007. Comprehensive analysis of homeobox genes in Hodgkin lymphoma cell lines

identifies dysregulated expression of HOXB9 mediated via ERK5 signaling and BMI1. *Blood,* 109**,** 3015-23.

171. NAKANISHI, C. & TOI, M. 2005. Nuclear factor-kappaB inhibitors as sensitizers to anticancer drugs. *Nat Rev Cancer,* 5**,** 297-309.

172. NANA-SINKAM, S. P. & CROCE, C. M. 2013. Clinical applications for microRNAs in cancer. *Clin Pharmacol Ther,* 93**,** 98-104.

173. NAPIER, S. S. & SPEIGHT, P. M. 2008. Natural history of potentially malignant oral lesions and conditions: an overview of the literature. *J Oral Pathol Med,* 37**,** 1-10.

174. NEVES, J. I., BEGNAMI, M. D., ARIAS, V. & SANTOS, G. C. 2005. Antigen retrieval methods and estrogen receptor immunoexpression using 1D5 antibody: a comparative study. *Int J Surg Pathol,* 13**,** 353-7.

175. NEVILLE, B. W. 2009. *Oral and maxillofacial pathology,* St. Louis, Mo, Saunders/Elsevier.

176. NGUYEN, D. X., CHIANG, A. C., ZHANG, X. H., KIM, J. Y., KRIS, M. G., LADANYI, M., GERALD, W. L. & MASSAGUE, J. 2009. WNT/TCF signaling through LEF1 and HOXB9 mediates lung adenocarcinoma metastasis. *Cell,* 138**,** 51-62.

177. NIETO, A., SANCHEZ, M. J., MARTINEZ, C., CASTELLSAGUE, X., QUINTANA, M. J., BOSCH, X., CONDE, M., MUNOZ, N., HERRERO, R. & FRANCESCHI, S. 2003. Lifetime body mass index and risk of oral cavity and oropharyngeal cancer by smoking and drinking habits. *British Journal of Cancer,* 89**,** 1667-1671.

178. NIXON, I. J., PALMER, F. L., LAKIN, P., KATTAN, M. M., LEE, N. Y. & GANLY, I. 2013. Pathologically Determined Tumor Volume vs Pathologic T

Stage in the Prediction of Outcome After Surgical Treatment of Oropharyngeal Squamous Cell Carcinoma. *JAMA Otolaryngol Head Neck Surg*.

179. OHNISHI, K., TOBITA, T., SINJO, K., TAKESHITA, A. & OHNO, R. 1998. Modulation of homeobox B6 and B9 genes expression in human leukemia cell lines during myelomonocytic differentiation. *Leuk Lymphoma,* 31**,** 599-608.

180. OKAMI, K., REED, A. L., CAIRNS, P., KOCH, W. M., WESTRA, W. H., WEHAGE, S., JEN, J. & SIDRANSKY, D. 1999. Cyclin D1 amplification is independent of p16 inactivation in head and neck squamous cell carcinoma. *Oncogene,* 18**,** 3541-5.

181. OKUYEMI, O. T., PICCIRILLO, J. F. & SPITZNAGEL, E. 2013. TNM staging compared to a new clinicopathological model in predicting oral tongue squamous cell carcinoma survival. *Head Neck.*

182. ONDREY, F. G., DONG, G., SUNWOO, J., CHEN, Z., WOLF, J. S., CROWL-BANCROFT, C. V., MUKAIDA, N. & VAN WAES, C. 1999. Constitutive activation of transcription factors NF-(kappa)B, AP-1, and NF-IL6 in human head and neck squamous cell carcinoma cell lines that express pro-inflammatory and pro-angiogenic cytokines. *Mol Carcinog,* 26**,** 119-29.

183. ONORATI, M., BINETTI, M., CONTI, L., CAMNASIO, S., CALABRESE, G., ALBIERI, I., DI FEBO, F., TOSELLI, M., BIELLA, G., MARTYNOGA, B., GUILLEMOT, F., CONSALEZ, G. G. & CATTANEO, E. 2011. Preservation of positional identity in fetus-derived neural stem (NS) cells from different mouse central nervous system compartments. *Cell Mol Life Sci,* 68**,** 1769-83.

184. OU, D. L., CHIEN, H. F., CHEN, C. L., LIN, T. C. & LIN, L. I. 2008. Role of Twist in head and neck carcinoma with lymph node metastasis. *Anticancer Res,* 28**,** 1355-9.

185. P, O. C., WONGKAJORNSILP, A., RHYS-EVANS, P. H. & ECCLES, S. A. 2004. Signaling pathways required for matrix metalloproteinase-9 induction by betacellulin in head-and-neck squamous carcinoma cells. *Int J Cancer,* 111**,** 174-83.

186. PAN, L., XIE, Y., BLACK, T. A., JONES, C. A., PRUITT, S. C. & GROSS, K. W. 2001. An Abd-B class HOX.PBX recognition sequence is required for expression from the mouse Ren-1c gene. *J Biol Chem,* 276**,** 32489-94.

187. PARK, N. J., ZHOU, H., ELASHOFF, D., HENSON, B. S., KASTRATOVIC, D. A., ABEMAYOR, E. & WONG, D. T. 2009. Salivary microRNA: discovery, characterization, and clinical utility for oral cancer detection. *Clin Cancer Res,* 15**,** 5473-7.

188. PARKIN, D. M. 2011. 11. Cancers attributable to infection in the UK in 2010. *Br J Cancer,* 105 Suppl 2**,** S49-56.

189. PARTRIDGE, M., EMILION, G., PATEROMICHELAKIS, S., PHILLIPS, E. & LANGDON, J. 1999. Location of candidate tumour suppressor gene loci at chromosomes 3p, 8p and 9p for oral squamous cell carcinomas. *Int J Cancer,* 83**,** 318-25.

190. PAUL, D., BRIDOUX, L., REZSOHAZY, R. & DONNAY, I. 2011. HOX genes are expressed in bovine and mouse oocytes and early embryos. *Mol Reprod Dev,* 78**,** 436-49.

191. PAVIA, M., PILEGGI, C., NOBILE, C. G. A. & ANGELILLO, I. F. 2006. Association between fruit and vegetable consumption and oral cancer: a meta-analysis of observational studies. *American Journal of Clinical Nutrition,* 83**,** 1126-1134.

192. PLOWRIGHT, L., HARRINGTON, K. J., PANDHA, H. S. & MORGAN, R. 2009. HOX transcription factors are potential therapeutic targets in non-small-cell lung cancer (targeting HOX genes in lung cancer). *Br J Cancer,* 100**,** 470-5.

193. POPOVIC, R., RIESBECK, L. E., VELU, C. S., CHAUBEY, A., ZHANG, J., ACHILLE, N. J., ERFURTH, F. E., EATON, K., LU, J., GRIMES, H. L., CHEN, J., ROWLEY, J. D. & ZELEZNIK-LE, N. J. 2009. Regulation of mir-196b by MLL and its overexpression by MLL fusions contributes to immortalization. *Blood,* 113**,** 3314-22.

194. PREVOT, D., VOELTZEL, T., BIROT, A. M., MOREL, A. P., ROSTAN, M. C., MAGAUD, J. P. & CORBO, L. 2000. The leukemia-associated protein Btg1 and the p53-regulated protein Btg2 interact with the homeoprotein Hoxb9 and enhance its transcriptional activation. *J Biol Chem,* 275**,** 147-53.

195. QIU, W., SCHONLEBEN, F., LI, X., HO, D. J., CLOSE, L. G., MANOLIDIS, S., BENNETT, B. P. & SU, G. H. 2006. PIK3CA mutations in head and neck squamous cell carcinoma. *Clin Cancer Res,* 12**,** 1441-6.

196. RAHMAN, M., SAKAMOTO, J. & FUKUI, T. 2003. Bidi smoking and oral cancer: a meta-analysis. *Int J Cancer,* 106**,** 600-4.

197. RAUTAVA, J., KUUSKOSKI, J., SYRJANEN, K., GRENMAN, R. & SYRJANEN, S. 2012. HPV genotypes and their prognostic significance in head and neck squamous cell carcinomas. *J Clin Virol,* 53**,** 116-20.

198. REED, A. L., CALIFANO, J., CAIRNS, P., WESTRA, W. H., JONES, R. M., KOCH, W., AHRENDT, S., EBY, Y., SEWELL, D., NAWROZ, H., BARTEK, J. & SIDRANSKY, D. 1996. High frequency of p16 (CDKN2/MTS-1/INK4A) inactivation in head and neck squamous cell carcinoma. *Cancer Res,* 56**,** 3630-3.

199. REHMAN, A. O. & WANG, C. Y. 2008. SDF-1alpha promotes invasion of head and neck squamous cell carcinoma by activating NF-kappaB. *J Biol Chem,* 283**,** 19888-94.

200. REINHART, B. J., SLACK, F. J., BASSON, M., PASQUINELLI, A. E., BETTINGER, J. C., ROUGVIE, A. E., HORVITZ, H. R. & RUVKUN, G. 2000. The 21-nucleotide let-7 RNA regulates developmental timing in Caenorhabditis elegans. *Nature,* 403**,** 901-6.

201. RINN, J. L., KERTESZ, M., WANG, J. K., SQUAZZO, S. L., XU, X., BRUGMANN, S. A., GOODNOUGH, L. H., HELMS, J. A., FARNHAM, P. J., SEGAL, E. & CHANG, H. Y. 2007. Functional demarcation of active and silent chromatin domains in human HOX loci by noncoding RNAs. *Cell,* 129**,** 1311-23.

202. ROCHE, D. D., LIU, K. J., HARLAND, R. M. & MONSORO-BURQ, A. H. 2009. Dazap2 is required for FGF-mediated posterior neural patterning, independent of Wnt and Cdx function. *Dev Biol,* 333**,** 26-36.

203. RODRIGUES, V. C., MOSS, S. M. & TUOMAINEN, H. 1998. Oral cancer in the UK: to screen or not to screen. *Oral Oncology,* 34**,** 454-465.

204. RODRIGUEZ, T., ALTIERI, A., CHATENOUD, L., GALLUS, S., BOSETTI, C., NEGRI, E., FRANCESCHI, S., LEVI, F., TALAMINI, R. & LA VECCHIA, C. 2004. Risk factors for oral and pharyngeal cancer in young adults. *Oral Oncol,* 40**,** 207-13.

205. SANKARANARAYANAN, R. 1990. Oral cancer in India: an epidemiologic and clinical review. *Oral Surg Oral Med Oral Pathol,* 69**,** 325-30.

206. SATYANARAYANA, L. & ASTHANA, S. 2008. Life time risk for development of ten major cancers in India and its trends over the years 1982 to 2000. *Indian J Med Sci,* 62**,** 35-44.

207. SCANLON, C. S., VAN TUBERGEN, E. A., INGLEHART, R. C. & D'SILVA, N. J. 2013. Biomarkers of epithelial-mesenchymal transition in squamous cell carcinoma. *J Dent Res,* 92**,** 114-21.

208. SCHEIFELE, C. & REICHART, P. A. 2003. Is there a natural limit of the transformation rate of oral leukoplakia? *Oral Oncology,* 39**,** 470-475.

209. SCHIMANSKI, C. C., FRERICHS, K., RAHMAN, F., BERGER, M., LANG, H., GALLE, P. R., MOEHLER, M. & GOCKEL, I. 2009. High miR-196a levels promote the oncogenic phenotype of colorectal cancer cells. *World J Gastroenterol,* 15**,** 2089-96.

210. SCHULTE, I., BATTY, E. M., POLE, J. C., BLOOD, K. A., MO, S., COOKE, S. L., NG, C., HOWE, K. L., CHIN, S. F., BRENTON, J. D., CALDAS, C., HOWARTH, K. D. & EDWARDS, P. A. 2012. Structural analysis of the genome of breast cancer cell line ZR-75-30 identifies twelve expressed fusion genes. *BMC Genomics,* 13**,** 719.

211. SCHUURING, E. 1995. The involvement of the chromosome 11q13 region in human malignancies: cyclin D1 and EMS1 are two new candidate oncogenes--a review. *Gene,* 159**,** 83-96.

212. SEKI, H., HAYASHIDA, T., JINNO, H., HIROSE, S., SAKATA, M., TAKAHASHI, M., MAHESWARAN, S., MUKAI, M. & KITAGAWA, Y. 2012. HOXB9 expression promoting tumor cell proliferation and angiogenesis is associated with clinical outcomes in breast cancer patients. *Ann Surg Oncol,* 19**,** 1831-40.

213. SEKI, S., FUJIWARA, M., MATSUURA, M., FUJITA, S., IKEDA, H., UMEDA, M., ASAHINA, I. & IKEDA, T. 2013. Prognostic Value of Podoplanin Expression in Oral Squamous Cell Carcinoma-A Regression Model Auxiliary to UICC Classification. *Pathol Oncol Res*.

214. SELBACH, M., SCHWANHAUSSER, B., THIERFELDER, N., FANG, Z., KHANIN, R. & RAJEWSKY, N. 2008. Widespread changes in protein synthesis induced by microRNAs. *Nature,* 455**,** 58-63.

215. SELCUKLU, S. D., DONOGHUE, M. T., REHMET, K., DE SOUZA GOMES, M., FORT, A., KOVVURU, P., MUNIYAPPA, M. K., KERIN, M. J., ENRIGHT, A. J. & SPILLANE, C. 2012. MicroRNA-9 inhibition of cell proliferation and identification of novel miR-9 targets by transcriptome profiling in breast cancer cells. *J Biol Chem,* 287**,** 29516-28.

216. SERRANO, M., HANNON, G. J. & BEACH, D. 1993. A new regulatory motif in cell-cycle control causing specific inhibition of cyclin D/CDK4. *Nature,* 366**,** 704-7.

217. SESSA, L., BREILING, A., LAVORGNA, G., SILVESTRI, L., CASARI, G. & ORLANDO, V. 2007. Noncoding RNA synthesis and loss of Polycomb group repression accompanies the colinear activation of the human HOXA cluster. *RNA,* 13**,** 223-39.

218. SHA, S., GU, Y., XU, B., HU, H., YANG, Y., KONG, X. & WU, K. 2013. Decreased expression of HOXB9 is related to poor overall survival in patients with gastric carcinoma. *Dig Liver Dis*.

219. SHAH, C. A., BEI, L., WANG, H., PLATANIAS, L. C. & EKLUND, E. A. 2012. HoxA10 protein regulates transcription of gene encoding fibroblast growth factor 2 (FGF2) in myeloid cells. *J Biol Chem,* 287**,** 18230-48.

220. SHAH, N. & SUKUMAR, S. 2010. The Hox genes and their roles in oncogenesis. *Nat Rev Cancer,* 10**,** 361-71.

221. SHAY, J. W., WRIGHT, W. E., BRASISKYTE, D. & VAN DER HAEGEN, B. A. 1993. E6 of human papillomavirus type 16 can overcome the M1 stage of

immortalization in human mammary epithelial cells but not in human fibroblasts. *Oncogene,* 8**,** 1407-13.

222. SHEN, W. F., MONTGOMERY, J. C., ROZENFELD, S., MOSKOW, J. J., LAWRENCE, H. J., BUCHBERG, A. M. & LARGMAN, C. 1997. AbdB-like Hox proteins stabilize DNA binding by the Meis1 homeodomain proteins. *Mol Cell Biol,* 17**,** 6448-58.

223. SHIOTSUGU, J., KATSUYAMA, Y., ARIMA, K., BAXTER, A., KOIDE, T., SONG, J., CHANDRARATNA, R. A. & BLUMBERG, B. 2004. Multiple points of interaction between retinoic acid and FGF signaling during embryonic axis formation. *Development,* 131**,** 2653-67.

224. SIBLEY, C. R., SEOW, Y., SAAYMAN, S., DIJKSTRA, K. K., EL ANDALOUSSI, S., WEINBERG, M. S. & WOOD, M. J. 2012. The biogenesis and characterization of mammalian microRNAs of mirtron origin. *Nucleic Acids Res,* 40**,** 438-48.

225. SLINGERLAND, J. & PAGANO, M. 2000. Regulation of the cdk inhibitor p27 and its deregulation in cancer. *J Cell Physiol,* 183**,** 10-7.

226. SMALL, S. & LEVINE, M. 1991. The initiation of pair-rule stripes in the Drosophila blastoderm. *Curr Opin Genet Dev,* 1**,** 255-60.

227. SMITH, A., TEKNOS, T. N. & PAN, Q. 2013. Epithelial to mesenchymal transition in head and neck squamous cell carcinoma. *Oral Oncol,* 49**,** 287-92.

228. SMITH, L. L., YEUNG, J., ZEISIG, B. B., POPOV, N., HUIJBERS, I., BARNES, J., WILSON, A. J., TASKESEN, E., DELWEL, R., GIL, J., VAN LOHUIZEN, M. & SO, C. W. 2011a. Functional crosstalk between Bmi1 and MLL/Hoxa9 axis in establishment of normal hematopoietic and leukemic stem cells. *Cell Stem Cell,* 8**,** 649-62.

229. SMITH, P. K., KROHN, R. I., HERMANSON, G. T., MALLIA, A. K., GARTNER, F. H., PROVENZANO, M. D., FUJIMOTO, E. K., GOEKE, N. M., OLSON, B. J. & KLENK, D. C. 1985. Measurement of protein using bicinchoninic acid. *Anal Biochem,* 150**,** 76-85.

230. SMITH, S. M., WUNDER, M. B., NORRIS, D. A. & SHELLMAN, Y. G. 2011b. A simple protocol for using a LDH-based cytotoxicity assay to assess the effects of death and growth inhibition at the same time. *PLoS One,* 6**,** e26908.

231. SOAMES, J. V. & SOUTHAM, J. C. 2005. *Oral pathology,* Oxford, Oxford University Press.

232. SOK, J. C., COPPELLI, F. M., THOMAS, S. M., LANGO, M. N., XI, S., HUNT, J. L., FREILINO, M. L., GRANER, M. W., WIKSTRAND, C. J., BIGNER, D. D., GOODING, W. E., FURNARI, F. B. & GRANDIS, J. R. 2006. Mutant epidermal growth factor receptor (EGFRvIII) contributes to head and neck cancer growth and resistance to EGFR targeting. *Clin Cancer Res,* 12**,** 5064-73.

233. SOSHNIKOVA, N. 2013. Hox genes regulation in vertebrates. *Dev Dyn*.

234. SOSHNIKOVA, N. & DUBOULE, D. 2009. Epigenetic temporal control of mouse Hox genes in vivo. *Science,* 324**,** 1320-3.

235. SQUARIZE, C. H., CASTILHO, R. M., ABRAHAO, A. C., MOLINOLO, A., LINGEN, M. W. & GUTKIND, J. S. 2013. PTEN deficiency contributes to the development and progression of head and neck cancer. *Neoplasia,* 15**,** 461-71.

236. STANTON, P., RICHARDS, S., REEVES, J., NIKOLIC, M., EDINGTON, K., CLARK, L., ROBERTSON, G., SOUTER, D., MITCHELL, R., HENDLER, F. J. & ET AL. 1994. Epidermal growth factor receptor expression by human squamous cell carcinomas of the head and neck, cell lines and xenografts. *Br J Cancer,* 70**,** 427-33.

237. SUEMORI, H. & NOGUCHI, S. 2000. Hox C cluster genes are dispensable for overall body plan of mouse embryonic development. *Dev Biol,* 220**,** 333-42.

238. SUN, M., LIU, X. H., LI, J. H., YANG, J. S., ZHANG, E. B., YIN, D. D., LIU, Z. L., ZHOU, J., DING, Y., LI, S. Q., WANG, Z. X., CAO, X. F. & DE, W. 2012. MiR-196a is upregulated in gastric cancer and promotes cell proliferation by downregulating p27(kip1). *Mol Cancer Ther,* 11**,** 842-52.

239. SUN, Q., ZHANG, J., CAO, W., WANG, X., XU, Q., YAN, M., WU, X. & CHEN, W. 2013. Dysregulated miR-363 affects head and neck cancer invasion and metastasis by targeting podoplanin. *Int J Biochem Cell Biol,* 45**,** 513-20.

240. SUN, W., GAYKALOVA, D. A., OCHS, M. F., MAMBO, E., ARNAOUTAKIS, D., LIU, Y., LOYO, M., AGRAWAL, N., HOWARD, J., LI, R., AHN, S., FERTIG, E., SIDRANSKY, D., HOUGHTON, J., BUDDAVARAPU, K., SANFORD, T., CHOUDHARY, A., DARDEN, W., ADAI, A., LATHAM, G., BISHOP, J., SHARMA, R., WESTRA, W. H., HENNESSEY, P., CHUNG, C. H. & CALIFANO, J. A. 2014. Activation of the NOTCH Pathway in Head and Neck Cancer. *Cancer Res,* 74**,** 1091-104.

241. SUNNY, L., YEOLE, B. B., HAKAMA, M., SHIRI, R., SASTRY, P. S., MATHEWS, S. & ADVANI, S. H. 2004. Oral cancers in Mumbai, India: a fifteen years perspective with respect to incidence trend and cumulative risk. *Asian Pac J Cancer Prev,* 5**,** 294-300.

242. TAKAHASHI, O., HAMADA, J., ABE, M., HATA, S., ASANO, T., TAKAHASHI, Y., TADA, M., MIYAMOTO, M., KONDO, S. & MORIUCHI, T. 2007. Dysregulated expression of HOX and ParaHOX genes in human esophageal squamous cell carcinoma. *Oncol Rep,* 17**,** 753-60.

243. TAKAMIZAWA, J., KONISHI, H., YANAGISAWA, K., TOMIDA, S., OSADA, H., ENDOH, H., HARANO, T., YATABE, Y., NAGINO, M.,

NIMURA, Y., MITSUDOMI, T. & TAKAHASHI, T. 2004. Reduced expression of the let-7 microRNAs in human lung cancers in association with shortened postoperative survival. *Cancer Res,* 64**,** 3753-6.

244. TANAKA, M., KITAJIMA, Y., EDAKUNI, G., SATO, S. & MIYAZAKI, K. 2002. Abnormal expression of E-cadherin and beta-catenin may be a molecular marker of submucosal invasion and lymph node metastasis in early gastric cancer. *Br J Surg,* 89**,** 236-44.

245. TANZER, A., AMEMIYA, C. T., KIM, C. B. & STADLER, P. F. 2005. Evolution of microRNAs located within Hox gene clusters. *J Exp Zool B Mol Dev Evol,* 304**,** 75-85.

246. THAKKER, N. & HUNTER, K. 2011. Tumours of the oral cavity. *Periodontol 2000,* 57**,** 7-9.

247. TIBERIO, C., BARBA, P., MAGLI, M. C., ARVELO, F., LE CHEVALIER, T., POUPON, M. F. & CILLO, C. 1994. HOX gene expression in human small-cell lung cancers xenografted into nude mice. *Int J Cancer,* 58**,** 608-15.

248. TSAI, K. W., LIAO, Y. L., WU, C. W., HU, L. Y., LI, S. C., CHAN, W. C., HO, M. R., LAI, C. H., KAO, H. W., FANG, W. L., HUANG, K. H. & LIN, W. C. 2012. Aberrant expression of miR-196a in gastric cancers and correlation with recurrence. *Genes Chromosomes Cancer,* 51**,** 394-401.

249. TUPLER, R., PERINI, G. & GREEN, M. R. 2001. Expressing the human genome. *Nature,* 409**,** 832-3.

250. VAN ROOIJ, E. & OLSON, E. N. 2007. MicroRNAs: powerful new regulators of heart disease and provocative therapeutic targets. *J Clin Invest,* 117**,** 2369-76.

251. VANWYK, C. W., STANDER, I., PADAYACHEE, A. & GROBLERRABIE, A. F. 1993. The Areca Nut Chewing Habit and Oral Squamous-Cell Carcinoma

in South-African Indians - a Retrospective Study. *South African Medical Journal,* 83**,** 425-429.

252. VERMORKEN, J. B., MESIA, R., RIVERA, F., REMENAR, E., KAWECKI, A., ROTTEY, S., ERFAN, J., ZABOLOTNYY, D., KIENZER, H. R., CUPISSOL, D., PEYRADE, F., BENASSO, M., VYNNYCHENKO, I., DE RAUCOURT, D., BOKEMEYER, C., SCHUELER, A., AMELLAL, N. & HITT, R. 2008. Platinum-based chemotherapy plus cetuximab in head and neck cancer. *N Engl J Med,* 359**,** 1116-27.

253. WALTER, V., YIN, X., WILKERSON, M. D., CABANSKI, C. R., ZHAO, N., DU, Y., ANG, M. K., HAYWARD, M. C., SALAZAR, A. H., HOADLEY, K. A., FRITCHIE, K., SAILEY, C. G., WEISSLER, M. C., SHOCKLEY, W. W., ZANATION, A. M., HACKMAN, T., THORNE, L. B., FUNKHOUSER, W. D., MULDREW, K. L., OLSHAN, A. F., RANDELL, S. H., WRIGHT, F. A., SHORES, C. G. & HAYES, D. N. 2013. Molecular subtypes in head and neck cancer exhibit distinct patterns of chromosomal gain and loss of canonical cancer genes. *PLoS One,* 8**,** e56823.

254. WANG, D., MULLER, S., AMIN, A. R., HUANG, D., SU, L., HU, Z., RAHMAN, M. A., NANNAPANENI, S., KOENIG, L., CHEN, Z., TIGHIOUART, M., SHIN, D. M. & CHEN, Z. G. 2012. The pivotal role of integrin beta1 in metastasis of head and neck squamous cell carcinoma. *Clin Cancer Res,* 18**,** 4589-99.

255. WANG, H., WANG, L., ERDJUMENT-BROMAGE, H., VIDAL, M., TEMPST, P., JONES, R. S. & ZHANG, Y. 2004. Role of histone H2A ubiquitination in Polycomb silencing. *Nature,* 431**,** 873-8.

256. WARNAKULASURIYA, S., KOVACEVIC, T., MADDEN, P., COUPLAND, V. H., SPERANDIO, M., ODELL, E. & MOLLER, H. 2011. Factors predicting

malignant transformation in oral potentially malignant disorders among patients accrued over a 10-year period in South East England. *J Oral Pathol Med*.

257. WARNAKULASURIYA, S., SUTHERLAND, G. & SCULLY, C. 2005. Tobacco, oral cancer, and treatment of dependence. *Oral Oncol,* 41**,** 244-60.

258. WHEATER, P. R., YOUNG, B. & HEATH, J. W. 2000. *Wheater's functional histology : a text and colour atlas,* Edinburgh, Churchill Livingstone.

259. WILHELMSEN, K. C., EGGLETON, K. & TEMIN, H. M. 1984. Nucleic acid sequences of the oncogene v-rel in reticuloendotheliosis virus strain T and its cellular homolog, the proto-oncogene c-rel. *J Virol,* 52**,** 172-82.

260. WOENCKHAUS, J., STEGER, K., WERNER, E., FENIC, I., GAMERDINGER, U., DREYER, T. & STAHL, U. 2002. Genomic gain of PIK3CA and increased expression of p110alpha are associated with progression of dysplasia into invasive squamous cell carcinoma. *J Pathol,* 198**,** 335-42.

261. WOLTERING, J. M. & DURSTON, A. J. 2008. MiR-10 represses HoxB1a and HoxB3a in zebrafish. *PLoS One,* 3**,** e1396.

262. WU, X., JOHANSEN, J. V. & HELIN, K. 2013. Fbxl10/Kdm2b recruits polycomb repressive complex 1 to CpG islands and regulates H2A ubiquitylation. *Mol Cell,* 49**,** 1134-46.

263. XU, B. & WELLIK, D. M. 2011. Axial Hox9 activity establishes the posterior field in the developing forelimb. *Proc Natl Acad Sci U S A,* 108**,** 4888-91.

264. YAMAGISHI, T., HIROSE, S. & KONDO, T. 2008. Secondary DNA structure formation for Hoxb9 promoter and identification of its specific binding protein. *Nucleic Acids Res,* 36**,** 1965-75.

265. YEKTA, S., SHIH, I. H. & BARTEL, D. P. 2004. MicroRNA-directed cleavage of HOXB8 mRNA. *Science,* 304**,** 594-6.

266. YEUDALL, W. A., TORRANCE, L. K., ELSEGOOD, K. A., SPEIGHT, P., SCULLY, C. & PRIME, S. S. 1993. Ras gene point mutation is a rare event in premalignant tissues and malignant cells and tissues from oral mucosal lesions. *Eur J Cancer B Oral Oncol,* 29B**,** 63-7.

267. YI, R., QIN, Y., MACARA, I. G. & CULLEN, B. R. 2003. Exportin-5 mediates the nuclear export of pre-microRNAs and short hairpin RNAs. *Genes Dev,* 17**,** 3011-6.

268. ZAAROOR-REGEV, D., DE BIE, P., SCHEFFNER, M., NOY, T., SHEMER, R., HELED, M., STEIN, I., PIKARSKY, E. & CIECHANOVER, A. 2010. Regulation of the polycomb protein Ring1B by self-ubiquitination or by E6-AP may have implications to the pathogenesis of Angelman syndrome. *Proc Natl Acad Sci U S A,* 107**,** 6788-93.

269. ZEISBERG, M. & NEILSON, E. G. 2009. Biomarkers for epithelial-mesenchymal transitions. *J Clin Invest,* 119**,** 1429-37.

270. ZHANG, H., KOLB, F. A., BRONDANI, V., BILLY, E. & FILIPOWICZ, W. 2002. Human Dicer preferentially cleaves dsRNAs at their termini without a requirement for ATP. *EMBO J,* 21**,** 5875-85.

271. ZHANG, Q., THOMAS, S. M., XI, S., SMITHGALL, T. E., SIEGFRIED, J. M., KAMENS, J., GOODING, W. E. & GRANDIS, J. R. 2004. SRC family kinases mediate epidermal growth factor receptor ligand cleavage, proliferation, and invasion of head and neck cancer cells. *Cancer Res,* 64**,** 6166-73.

272. ZINK, B. & PARO, R. 1989. In vivo binding pattern of a trans-regulator of homoeotic genes in Drosophila melanogaster. *Nature,* 337**,** 468-71.

273. National Cancer Institute. 2013. Head and Neck Cancer. [ONLINE] Available at: http://www.cancer.gov/cancertopics/factsheet/Sites-Types/head-and-neck. [Accessed 30 July 13].

274. Cancer Research UK. 2010. Cancer information. [ONLINE] Available at: http://www.cancerresearchuk.org/cancer-info/. [Accessed 31 July 2013].

Chapter 9: Appendix

Appendix 9.1

Name of Supplier	Location
Sigma Aldrich	Poole, UK
Applied Biosystems, Life Technologies	Paisley, UK
Invitrogen, Life Technologies	Paisley, UK
Ambion, Life Technologies	Paisley, UK
Grenier Bio-one	Stonehouse, UK
Nalgene	Matlock, UK
Sarstedt	Leicester, UK
Qiagen	Manchester, UK
Thermo Scientific	Hempstead, UK
CellPath	Newtown, UK
Starlab	Milton Keyes, UK
Fisher Scientific	Loughborough, UK
GE Healthcare	Hatfield, UK
Bio-Rad	Hempstead, UK
Abcam	Cambridge, UK
Promega	Southampton, UK
BD Biosciences	Oxford, UK
New England Biolabs (NEB)	Herts, UK
Bioline	London, UK
Agilent	Wokingham, UK
Qlucore	Lund, Sweden

Gibco, Life Technologies	Paisley, UK
Corning	Corning, USA
Olympus	Southend-on-Sea, UK
Roche	Welwyn Garden City, UK
Tecan	Reading, UK
Geneflow	Lichfield, UK

Appendix 9.2

HOX gene name	Product length (bp)	Primer sequence
HOXA1	153	F: 5’ CTGGCCCTGGCTACGTATAA 3’ R: 5’ TCCAACTTTCCCTGTTTTGG 3’
HOXB1	157	F: 5’ TTCAGCAGAACTCCGGCTAT 3’ R: 5’ CCTCCGTCTCCTTCTGATTG 3’
HOXD1	232	F: 5’ TTCAGCACCAAGCAACTGAC 3’ R: 5’ TAGTGGGGGTTGTTCCAGAG 3’
HOXA2	176	F: 5’ TTCAGCAAAATGCCCTCTCT 3’ R: 5’ TAGGCCAGCTCCACAGTTCT 3’
HOXB2	259	F: 5’ CTCCCAAAATCGCTCCATTA 3’ R: 5’ GAAAGGAGGAGGAGGAGGAA 3’
HOXA3	227	F: 5’ ACCTGTGATAGTGGGCTTGG 3’ R: 5’ ATACAGCCATTCCAGCAACC 3’
HOXB3	299	F: 5’ TATGGCCTCAACCACCTTTC 3’ R: 5’ AAGCCTGGGTACCACCTTCT 3’
HOXD3	176	F: 5’ CAGCCTCCTGGTCTGAACTC 3’ R: 5’ ATCCAGGGGAAGATCTGCTT 3’

HOXA4	271	F: 5’ CCCTGGATGAAGAAGATCCA 3’ R: 5’ AATTGGAGGATCGCATCTTG 3’
HOXB4	155	F: 5’ TCTTGGAGCTGGAGAAGGAA 3’ R: 5’ GTTGGGCAACTTGTGGTCTT 3’
HOXC4	276	F: 5’ CGCTCGAGGACAGCCTATAC 3’ R: 5’ GCTCTGGGAGTGGTCTTCAG 3’
HOXD4	173	F: 5’ TCAAATGTGCCATAGCAAGC 3’ R: 5’ TCCATAGGGCCCTCCTACTT 3’
HOXA5	193	F: 5’ CCGGAGAATGAAGTGGAAAA 3’ R: 5’ ACGAGAACAGGGCTTCTTCA 3’
HOXB5	189	F: 5’ AAGGCCTGGTCTGGGAGTAT 3’ R: 5’ GCATCCACTCGCTCACTACA 3’
HOXC5	268	F: 5’ CAGTTACACGCGCTACCAGA 3’ R: 5’ AGAGAGGAAAGGCGAAAAGG 3’
HOXA6	158	F: 5’ AAAGCACTCCATGACGAAGG 3’ R: 5’ TCCTTCTCCAGCTCCAGTGT 3’
HOXB6	184	F: 5’ ATTTCCTTCTGGCCCTCACT 3’ R: 5’ GGAAGGTGGAGTTCACGAAA 3’
HOXC6	190	F: 5’ AAGAGGAAAAGCGGGAAGAG 3’

		R: 5’ GGTCCACGTTTGACTCCCTA 3’
HOXA7	285	F: 5’ TGGTGTAAATCTGGGGGTGT 3’ R: 5’ TCTGATAAAGGGGGCTGTTG 3’
HOXB7	249	F: 5’ CAGCCTCAAGTTCGGTTTTC 3’ R: 5’ CGGAGAGGTTCTGCTCAAAG 3’
HOXB8	265	F: 5’ GTAGGCTTCAGCTGGGACTG 3’ R: 5’ GGGAGCCTTTGCTTAAATCC 3’
HOXC8	150	F: 5’ CTCAGGCTACCAGCAGAACC 3’ R: 5’ TTGGCGGAGGATTTACAGTC 3’
HOXD8	290	F: 5’ TCAAATGTTTCCGTGGATGA 3’ R: 5’ GCTCTTGGGCTTCCTTTTTC 3’
HOXA9	203	F: 5’ AATAACCCAGCAGCCAACTG 3’ R: 5’ ATTTTCATCCTGCGGTTCTG 3’
HOXB9	198	F: 5’ TAATCAAAGACCCGGCTACG 3’ R: 5’ CTACGGTCCCTGGTGAGGTA 3’
HOXC9	190	F: 5’ AGACGCTGGAACTGGAGAAG 3’ R: 5’ AGGCTGGGTAGGGTTTAGGA 3’
HOXD9	236	F: 5’ TCCCCCATGTTTCTGAAAAG 3’ R: 5’ GGGCTCCTCTAAGCCTCACT 3’

HOXA10	159	F: 5’ ACACTGGAGCTGGAGAAGGA 3’ R: 5’ GATCCGGTTTTCTCGATTCA 3’
HOXC10	289	F: 5’ CGCCTGGAGATTAGCAAGAC 3’ R: 5’ GGTCCCTTGGAAGGAGAGTC 3’
HOXD10	154	F: 5’ GCTCCTTCACCACCAACATT 3’ R: 5’ AAATATCCAGGGACGGGAAC 3’
HOXA11	279	F: 5’ CGCTGCCCCTATACCAAGTA 3’ R: 5’ GTCAAGGGCAAAATCTGCAT 3’
HOXC11	186	F: 5’ CGGAACAGCTACTCCTCCTG 3’ R: 5’ CAGGACGCTGTTCTTGTTGA 3’
HOXD11	253	F: 5’ GGGGCTACGCTCCCTACTAC 3’ R: 5’ GCTGCCTCGTAGAACTGGTC 3’
HOXC12	180	F: 5’ CAAGCCCTATTCGAAGTTGC 3’ R: 5’ GCTTGCTCCCTCAACAGAAG 3’
HOXD12	201	F: 5’ CGCTTCCCCCTATCTCCTAC 3’ R: 5’ CTTCGGGCGCATAGAACTTA 3’
HOXA13	176	F: 5’ GGATATCAGCCACGACGAAT 3’ R: 5’ ATTATCTGGGCAAAGCAACG 3’
HOXB13	234	F: 5’ CTTGGATGGAGCCAAGGATA 3’

		R: 5’ CCGCCTCCAAAGTAACCATA 3’
HOXC13	170	F: 5’ GTGGAAATCCAAGGAGGACA 3’ R: 5’ TTGTTGAGGGACCCACTCTC 3’
HOXD13	265	F: 5’ GGGGATGTGGCTCTAAATCA 3’ R: 5’ AACCTGGACCACATCAGGAG 3’
β-actin	182	F: 5’ ATGTACCCTGGCATTGCCGAC 3’ R: 5’ GACTCGTCATACTCCTGCTTG 3’

Appendix 9.3

List of variable genes from microarray:

Variable genes Down-regulated in Group 2 compared to Group 1 based on Qlucore Omics analysis				
SMOX	GSK3B	LPXN	ASPSCR1	GJC2
METRNL	NSUN5	UNC119B	CLEC11A	SLC36A4
GGTA1	BBS7	CARKD	EEF1A2	FLYWCH1
TUBB4	PDCD2L	SNX11	LARP6	PANX2
MDK	CD33	TMEM222	ARFRP1	MKRN9P
SLC26A11	DHRS3	PRH2	DNLZ	
FICD	TMEM39B	DRAM1	CTAGE5	
PLEKHO2	ZDHHC23	BBS1	EVI5L	
DBP	PRR22	SLC1A4	DUS1L	
MANBAL	ProSAPiP1	ITPKC	LIMS2	
DNTTIP1	DNAJB6	IL2RB	SPPL3	
FAM38A	DIRAS1	STAC	PSG5	
MOV10L1	TIMP3	ADAMTS14	RHBDD3	
CSN2	CLN8	PER3	FOXS1	
CTSH	MON1A	DHRSX	CBR1	
B4GALT2	NUDT14	SAMD4A	BAI1	
C16orf48	FUK	FMNL1	EIF2B3	
FJX1	SLC25A42	TBC1D20	ABCC3	
VPS37B	JUP	LOXL4	SBNO2	
BTNL3	RFX2	CA5A	SH3D20	
MUS81	ACBD6	TMEM132B	FAM83G	
CBS	GTF2IRD2	YDJC	CCDC57	
POPDC2	BTG2	ZNF425	NUDCD3	
STX1A	LOC84856	CT45A5	MGP	
OPLAH	SLC38A7	DOM3Z	ERCC1	
DNAH1	SIRT7	MBD6	CNTLN	
PSEN1	DOCK6	HSBP1L1	EFEMP2	
USP31	TRAPPC9	PRKAA2	TPRA1	
NSFL1C	CRYM	DGKQ	SLC6A9	
EIF4EBP1	MAFG	DFNA5	FAM43A	
STX5	MAOB	C6orf170	ABI3BP	

Variable genes up-regulated in Group 2 compared to Group 1 based on Qlucore Omics analysis			
CASC5	C5orf23	FOXO3	SAA2
S100A7	HSPA1L	SDC3	MAPK11
APLN	KIF20B	ZNF254	C19orf38
ARID4A	HOXC8	TM2D1	TMPO

RLF	ANKRD53	GCNT1	E2F6
ACP2	SPG7	EHMT1	HTA
DDC	ZNF273	DENND4C	ZNF782
C7orf34	ANKRD37	C9orf102	GBX2
MAMDC2	IFIT5	FLJ20464	CRLS1
IWS1	OSGEPL1	HOXC6	
CCDC21	ANKRD36BP2	AACSP1	
HP	RAB12	RPGRIP1L	
CEP135	DCLRE1B	TMEM144	
IFI44	SAA3P	MYH16	
ZNF572	ZNF708	PLOD2	
C14orf147	CCDC132	BLOC1S3	
KDM1B	ADD3	PLEKHA2	
CTRC	HAUS6	PIKFYVE	
SKIL	CENPF	TFAP2A	
SLC35D1	SMC5	CFH	
ANKRD5	ZCCHC2	WHSC1L1	
ZAK	C17orf105	FANCA	
PAPOLA	RPL7	OR5A2	
DPPA2	LDHA	C20orf165	
ZFHX4	RBMX	IL1R1	
S100A8	AK4	BNIP3L	
ERRFI1	RFC3	RN5-8S1	
ESAM	ANKRD36	TLE6	
NUP37	VSTM2B	PPP1R14A	
TWF1	SLC9A5	ANKRD20A2	
NFYB	AURKAPS1	CRHR1	

The unannotated genes have not been mentioned in these tables.

Appendix 9.4

Gene symbol	B16 transfected v/s control	p-value	Absolute fold change	D19 transfected v/s control	p-value	Absolute fold change
KRTAP6-2	up	0.029	1.813	down	0.006	2.497
FBXW2	down	0.049	1.134	up	0.048	1.051
BMP7	down	0.021	2.062	up	0.028	2.522
AKAP9	up	0.007	1.131	down	0.013	1.108
AIFM2	down	0.017	2.552	up	0.010	2.363
IFITM10	down	0.042	1.158	up	0.028	1.330
PDPN	down	0.044	1.200	up	0.023	1.090
DIRC2	up	0.021	1.110	down	0.019	1.108
C6orf154	down	0.024	1.145	up	0.041	1.189
UNG	down	0.002	1.133	up	0.048	1.168
ZNF470	down	0.037	2.364	up	0.016	1.534
WDFY3	up	0.043	1.117	down	0.032	1.141
TPM1	down	0.045	1.169	up	0.006	1.188
FMNL3	down	0.045	1.152	up	0.043	1.093
KCNH5	down	0.005	2.052	down	0.039	1.653

Gene symbol	OKF4 transfected v/s control	p-value	Absolute fold change
KRTAP6-2	up	1.373	1.373
FBXW2	up	1.126	1.126
BMP7	down	3.155	-3.155
AKAP9	up	1.429	1.429
AIFM2	down	2.823	-2.823
IFITM10	up	1.266	1.266
PDPN	down	1.123	-1.123
DIRC2	up	1.116	1.116
C6orf154	down	1.054	-1.054
UNG	up	1.101	1.101
ZNF470	down	1.086	-1.086
WDFY3	up	1.325	1.325
TPM1	down	1.033	-1.033
FMNL3	down	1.230	-1.230
KCNH5	down	1.237	-1.237

Appendix 9.5

Variance values for genes in Table 6.3. NC, negative control; AM, anti-miR-196a; PM, pre-miR-196a.

Gene symbol	B16 NC 1	B16 NC 2	B16 NC 3	B16 AM 1	B16 AM 2	B16 AM 3	D19 NC 1	D19 NC 2
CASC5	1.715	1.855	1.967	1.988	2.241	2.108	-0.593	-0.685
S100A7	-0.277	0.022	-0.091	0.020	-0.091	0.075	-0.465	-0.546
APLN	-0.153	0.100	-0.276	0.062	0.697	0.715	-0.702	-0.807
DDC	-0.103	-0.347	-0.376	-0.108	-0.299	0.034	2.215	1.943
MAMDC2	-3.686	-3.953	-3.943	-3.413	-2.521	-2.898	0.318	0.328
IFI44	-2.433	-2.576	-2.577	-2.494	-2.266	-2.401	0.585	0.807
CTRC	-0.380	-0.863	0.029	-0.029	-0.106	0.149	-1.148	-1.035
SKIL	0.631	0.573	0.531	0.773	0.721	0.677	-1.427	-1.606
ZFHX4	-0.287	0.037	-0.052	-0.002	0.002	-0.173	1.002	1.195
S100A8	-0.450	-0.324	-0.523	0.136	0.610	0.606	-0.861	-0.230
C5orf23	2.163	2.235	2.227	2.417	2.480	2.363	-0.370	-0.080
HSPA1L	-1.554	-1.785	-1.782	-1.544	-1.147	-0.634	0.592	0.330
KIF20B	1.330	1.318	1.388	1.810	1.812	1.758	-1.204	-0.865
HOXC8	0.272	0.443	0.326	0.629	0.762	0.505	-0.200	-0.643

ANKRD36BP2	-1.369	-1.415	-1.293	-1.208	-1.254	-1.311	1.141	1.165
SAA3P	-0.569	-0.708	-0.693	0.266	-0.133	-0.130	0.025	-0.041
LOC202181	0.496	1.186	1.343	1.217	0.998	1.467	-1.282	-1.452
RFC3	1.918	1.898	1.979	2.093	2.240	2.123	-0.858	-1.046
ANKRD36	-0.979	-1.153	-0.932	-1.017	-1.000	-0.920	0.997	1.040
AURKAPS1	1.125	1.209	1.385	1.502	1.503	1.562	-1.383	-1.125

Gene symbol	D19 NC 3	B16 AM 1	B16 AM 2	B16 AM 3	OKF4 NC 1	OKF4 NC 2	OKF4 PM 1	OKF4 PM 2
CASC5	-0.653	-0.589	-0.531	-0.375	-0.029	0.097	-0.027	0.027
S100A7	-0.269	0.036	-0.050	-0.020	9.392	9.483	9.346	9.435
APLN	-0.436	-0.335	-0.062	-0.486	4.380	4.436	4.358	4.318
DDC	2.225	2.367	2.587	2.370	-0.034	0.452	-0.209	-0.130
MAMDC2	0.240	0.308	0.329	0.700	0.200	0.287	-0.200	-0.353
IFI44	0.732	0.947	0.969	0.867	-0.011	0.011	-0.068	0.025

CTRC	-0.260	0.115	0.309	-0.144	3.023	3.007	3.002	2.497
SKIL	-1.501	-1.579	-1.365	-1.349	0.114	0.049	-0.154	-0.049
ZFHX4	1.182	1.304	1.332	1.500	-0.954	-0.713	-1.307	-1.280
S100A8	-0.057	-0.049	-0.089	0.049	9.617	9.753	9.623	9.592
C5orf23	-0.060	-0.050	0.050	0.206	-2.552	-2.184	-2.484	-2.547
HSPA1L	0.599	0.856	1.074	1.269	-0.111	0.650	-0.854	0.111
KIF20B	-0.897	-0.680	-0.856	-0.690	-0.037	0.074	-0.171	0.037
HOXC8	-0.275	-0.097	0.097	0.180	-2.926	-2.797	-3.056	-2.979
ANKRD36BP2	1.285	1.186	1.293	1.363	0.094	0.314	-0.094	-0.117
SAA3P	-0.220	0.309	-0.025	0.162	8.064	8.355	8.026	8.152
LOC202181	-1.486	0.432	-0.613	-0.737	-0.078	0.078	-0.507	-0.629
RFC3	-0.858	-0.619	-0.828	-0.586	0.039	-0.002	0.002	-0.084
ANKRD36	1.163	1.226	1.278	1.357	0.157	0.161	-0.157	-0.269
AURKAPS1	-1.096	-0.943	-1.003	-0.970	0.052	-0.099	0.052	-0.052